Intracellular transport and protein processing in a non-viral transfection model

vorgelegt von
Diplom-Ingenieur
Sean-Patrick Riechers

von der Fakultät III – Prozesswissenschaften
der Technischen Universität Berlin
zur Erlangung des akademischen Grades
Doktor der Ingenieurwissenschaften
-Dr.-Ing.-

genehmigte Dissertation

Promotionsausschuss:

Vorsitzender: Prof. Dr. rer. nat. Roland Lauster
Gutachter: Dekan Univ.-Prof. Dipl.-Ing. Dr. Ulf Stahl
Gutachter: Prof. Dr. rer. nat. Christine Lang

Tag der wissenschaftlichen Aussprache:
08. Oktober 2007

Berlin 2007
D 83

Um klar zu sehen, genügt oft ein

Wechsel der Blickrichtung

(*Antoine de Saint-Exupéry*)

Danksagung

Diese Arbeit wurde im Zeitraum von Mai 2003 bis Mai 2007 im Fachgebiet Mikrobiologie und Genetik des Instituts für Biotechnologie der TU Berlin erstellt.

Ganz herzlich möchte ich Frau Prof. Dr. Christine Lang danken für ihr unermüdliches Engagement um die Finanzierung dieser Arbeit, der Überlassung des Themas der Arbeit und der Betreuung derselben neben ihren zahlreichen anderen Verpflichtungen. Ausdrücklich möchte ich ihr dafür danken, dass ich bei meiner Arbeit in ihrer Arbeitsgruppe viele eigene Ideen verwirklichen und verfolgen konnte.

Prof. Dr. Ulf Stahl danke ich dafür, dass er es mir ermöglicht hat diese Arbeit in seinem Fachgebiet zu realisieren. Außerdem danke ich Prof. Dr. Ulf Stahl für sein Vertrauen in meine Tätigkeiten während meiner Promotion und die Begutachtung dieser Arbeit.

Ich danke außerdem Prof. Dr. Roland Lauster für seine Bereitschaft den Vorsitz des Promotionsausschusses zu übernehmen.

Mein besonderer Dank gilt den Mitarbeitern der AG Lang, die mich durch viele fachliche Diskussionen innerhalb, aber auch außerhalb der AG Seminare unterstützten, bei denen ich aber auch in anderen Belangen auf ein offenes Ohr zählen konnte. Vielen Dank dafür an Birgit Baumann, Thomas Lautz, Andreas Raab, Eva Graf und ganz besonders an Dr. Cristina Martín Granados, auf die ich in jeder Situation bauen konnte und mit der ich stets während der Arbeit und auch privat viel lachen konnte.

Vielen Dank auch an Anna Lewandowski für ihre exzellente Mitarbeit als Praktikantin bei der Reproduktion meiner Daten. Jatuporn Ngoengkam (Takk) hat mich, wie es Anna auch getan hat, bei der Bearbeitung von Mutanten unterstützt, die zur Untermauerung der in dieser Arbeit präsentierten Daten dienten. Dafür danke ich beiden sehr. Dr. Birgit Neukamm danke ich für die wichtigen und sehr fundierten Vorarbeiten im Rahmen ihrer Promotion. Auf ihrer Dissertation fußt die hier vorliegende Arbeit. Außerdem danke ich Eva Graf für die Fortführung der Untersuchungen basierend auf den Erkenntnissen meiner Arbeit.

Vielen Dank auch an Rita Waggad, auf deren Organisation in der „Medienküche“, und auf deren Vorräte man sich immer verlassen konnte, wenn mal ein Zentrifugenbecher fehlte. Sie war in vielen Dingen eine große Unterstützung.

Vielen Dank auch an Conny Luban dafür, dass sie immer schnell und zuverlässig zur Stelle war, wenn ich mal wieder eine weitere Mutante aus der Sammlung der BY4741-Mutanten haben wollte.

Danke auch an alle anderen Mitarbeiter des Fachgebietes, die sich an den Diskussionen in den Fachgebietsseminaren bezüglich dieser Arbeit beteiligt haben.

Vielen Dank auch an Roslin Bensmann für das Lesen dieser Arbeit in Bezug auf die englische Sprache.

Ich möchte auch ganz herzlich denjenigen danken mit denen ich in Projekten zusammen arbeiten konnte, die diese Arbeit nicht inhaltlich betreffen. Durch diese Zusammenarbeiten wurde es mir möglich parallel diese Arbeit verwirklichen zu können. Diesbezüglich danke ich für die sehr nette Zusammenarbeit mit Dr. Till Hornbogen und PD Dr. Rainer Zocher in einem Projekt eine fungale Enniatin Synthetase betreffend. Ebenfalls danke ich sehr der RiNA GmbH und hier insbesondere Dr. Jörn Glökler, PD Dr. Reinhard Geßner (Charité), Dr. Wolfgang Stiege und Doreen Meschkat für die nette Zusammenarbeit und die sehr anregenden und fruchtbaren Diskussionen in einem Projekt, welches sich mit der Selektion von Aptameren beschäftigte. Im Besonderen in dem erst genannten Projekt bedanke ich mich ganz besonders für die nette Zusammenarbeit und die große Unterstützung von Birgit Baumann, ohne die das alles zeitlich und vom Aufwand her nicht zu schaffen gewesen wäre.

Im Rahmen der Zusammenarbeit mit Dr. Till Hornbogen konnte, unter meiner direkten Betreuung, eine Studienarbeit und eine Diplomarbeit erstellt werden, von Dinusha Weinert-Sepalage und von Kristin Ebert. Dafür möchte ich Kristin und Dinusha danken, da durch ihre Arbeiten weitere Einblicke in die heterologe Expression von Domänen der Enniatin Synthetase gewonnen wurden.

Zuletzt, aber ganz besonders, möchte ich meiner Familie danken, und da speziell meinen Eltern Dr. Heinz-Hermann und Annegret E. Riechers und meinem Bruder Dominik A. Riechers, für die stete und unermüdliche Unterstützung während meiner Promotion. Vielen Dank auch für die Unterstützung meiner Freunde insbesondere in Form einer netten Ablenkung von der Arbeit, um danach wieder mit geschärfterem Blick an die Dinge meiner Promotion heranzugehen.

Contents

List of abbreviations

Abbreviations of amino acids and nucleic acids:

http://www.chem.qmul.ac.uk/iupac/misc/naabb.html

SI-units:

http://www.chemie.fu-berlin.de/chemistry/general/

Abbreviations of yeast genes and proteins (SGD):

http://www.yeastgenome.org/

Abbreviations of human genes and proteins:

http://source.stanford.edu/cgi-bin/source/sourceSearch or

http://www.expasy.org/sprot/

AAV	adeno-associated virus
α-GalA	α-galactosidase A
ALP	alkaline phosphatase
AP-2	adapter protein complex-2
AP3	adapter protein complex 3
API	vacuolar aminopeptidase
α-Syn	α-synuclein
ATP	adenosine tri-phosphate
AV	adenovirus
β-APP	β-amyloid peptide precursor
bp	base pairs
BRIa	a bone marrow protein receptor
BRII	a bone marrow protein receptor
CHO	Chinese hamster ovary
COPI	coat protomer I
COPII	coat protomer II
CPY	carboxypeptidase Y (Prc1p)
CVT	cytosol to vacuole targeting
DEAE	diethylaminoethyl
DMRIE	N-[1-(2,3-dimyristyloxy)propyl]-N,N-dimethyl-N-(2-hydroxy-ethyl) ammonium bromide

DMRIE-C	DMRIE + cholesterol (1:1)
DMSO	dimethyl sulfoxide
DNA	deoxyribonucleic acid
DOPE	dioleoyl phosphatidyl ethanolamine
DOPC	dioleoyl phosphatidyl choline
DOTMA	N-(1-2,3-dioleyloxypropyl)-N,N,N-triethylammonium
EDTA	ethylenediaminetetraacetic acid
EGF	epidermal growth factor
EMA	ethidium bromide monoazide
ER	endoplasmic reticulum
ESCRT	endosomal sorting complex required for transport (protein complex)
EUROFANII	European functional analysis network II
EUROSCARF	European *Saccharomyces cerevisiae* archive for functional analysis
Fig.	Figure
FM4-64	fluorescent molecule 4-64
FPF-g-PEI	folate-poly(ethylene glycol)-folate-grafted-PEI
FRET	fluorescence resonance energy transfer
GFP	green fluorescent protein
GM1	ganglioside M1
GPI	glycosylphosphatidylinositol
HAP1	Huntingtin associated protein 1
Hepes	4-(2-Hydroxyethyl)piperazine-1-ethanesulfonic acid
HIP1	Huntingtin interacting protein 1
HIP1R	HIP1 related protein
HIV	human immunodeficiency virus
HOPS	homotypic vacuole fusion and vacuole protein sorting (protein complex)
HPLC	high performance liquid chromatography
HSV	herpes simplex virus
IL-2	Interleukin 2
LB	Luria Bertani (medium)

LDLR	low density lipoprotein receptor
LY-CH	Lucifer Yellow CH
M	molar
MMLV	Moloney murine leukaemia virus
MVB	multi vesicular body
NP-C	Niemann-Pick type C
NVJ	nucleus-vacuole junction
PAS	preautophagosomal body
PCR	polymerase chain reaction
PEI	polyethylene imine
PLD	phospholipase D
PLL	poly-L-lysine
PMN	piecemeal microautophagy of the nucleus
PP1	protein phosphatase 1
PrA	proteinase A (Pep4p)
PrB	proteinase B (Prb1p)
PtdIns(4,5)P_2	phosphatidyl-inositol-(4,5)-bisphosphate
PVC	pre-vacuolar compartment
RAVE	regulator of the H^+-ATPase of the vacuolar and endosomal membranes (protein complex)
RNA	ribonucleic acid
RNAi	RNA interference
RV	retrovirus
SAINT-2	some transfection enhancing substance
SDS	sodium dodecyl sulphate
SGD	*Saccharomyces* genome database
SV40	simian virus 40
Tab.	Table
TAE	Tris acetate-EDTA (buffer)
Taq	*Thermus aquaticus* (DNA-polymerase of)
TβRII	TGF (transforming growth factor)-β receptor type II
TE	Tris-EDTA (buffer)
TfR	Transferrin (Tf) receptor

TGFβ	transforming growthfactor β
TGN	*trans* Golgi network
Tris	Tris(hydroxymethyl)aminomethane
Trition X-100	4-(1,1,3,3-Tetramethylbutyl)phenyl-polyethylene glycol
Tween 20	Polyethylene glycol sorbitan monolaurate
vps	vacuolar protein sorting
VSV	vesicular stomatitis virus
WASp	Wiskott-Aldrich syndrome protein
WIP	WASp-interacting protein
WSLP	water-soluble lipopolymer
YE	yeast extract (medium)
YPD	yeast extract peptone dextran (medium)

Index of figures

Index of tables

1 Introduction

1.1 Intracellular membrane transport processes

Intracellular membrane transport is involved in many processes important for cellular functioning. The endocytosis process is needed to acquire nutrients from the cell exterior, especially to take up macromolecules or even larger structures by different endocytic uptake mechanisms including phagocytosis. Phagocytosis can be observed in specific cell types in higher mammalian eukaryotes such as macrophages or other phagocytes (reviewed in: Aderem and Underhill, 1999). Even unicellular organisms such as the algae *Ochromonas malhamensis* are phagocytosis competent (Stoltze et al, 1969). Macromolecules are often been taken up via receptor mediated endocytosis as in the case of albumin which is taken up, for example, via the transforming growth factor (TGF)-β receptor type II (TβRII) e.g. in epithelial cells of higher eukaryotes (Siddiqui et al, 2004). However, albumin also binds to other cell surface proteins. Transcytosis of albumin through lens epithelial cells seems to be mediated by clathrin and caveolin-1 dependent endocytosis (Sabah et al, 2007).
After receptor binding of specific target surfaces, receptor mediated endocytosis begins. This process plays a role in signal transduction and adaptation to the signal after a while, as seen in the case of the insulin receptor and its clathrin mediated endocytosis (Ceresa et al, 1998; Su et al, 2006). In higher eukaryotes, endo- and exocytosis are also involved in signal submission between neighbouring neurons over the synaptic cleft. Secretory vesicles harbouring neurotransmitters fuse to the pre-synaptic membrane after the influx of Ca^{2+}-ions into the pre-synapses due to an electric signal. Neurotransmitters submit the signal to the post-synaptic cell by binding to corresponding receptors. After this, to render the pre-synaptic cell competent again for the next signal, excess membrane and secretory vesicle proteins have to be recovered. Three types of endocytosis at pre-synapses are known: clathrin mediated endocytosis, bulk retrieval of large portions of the plasma membrane, and the “kiss and run” mechanism where vesicles do not fully collapse into the pre-synaptic membrane and are recovered very rapidly (reviewed in: Royle and Lagnado, 2003). The receptor mediated uptake of specific cofactors such as iron atoms via transferrin which binds to the transferrin-receptor also requires endocytosis

(Karin and Mintz, 1981). Intracellular transport is needed to recycle molecules such as some receptors, like the transferrin receptor, for example, back to the cell surface in mammalian cells. This can be used for directed drug delivery purposes (reviewed in: Qian et al, 2002). Receptors are sorted between intracellular compartments such as the CPY receptor Pep1p (Vps10p) in yeast between the *trans* Golgi network (TGN) and the late endosome (Cereghino et al, 1995). This shows that intracellular membrane transport is important to localize proteins correctly.

Further on, the cell uses intracellular transport to adapt to changed conditions e.g. under stress conditions. Chitosomes are some kind of early endosomes storing chitin synthases Chs1p and Chs3p. Chitin synthases stored in chitosomes, are transported to the cell surface when yeast cells are exposed to shear stress. This is done to strengthen the cell wall by synthesising additional cell wall chitin (Ziman et al, 1996; Ziman et al, 1998; Valdivia and Schekman, 2003).

Autophagy is up-regulated in order to react to nitrogen starvation conditions in yeast and also higher cells. The cell uses autophagy to recycle parts of the nucleus or whole organelles as mitochondria which are no longer needed (Roberts et al, 2003; Onodera and Ohsumi, 2005). Autophagy is also involved in cellular suicide, described in detail for higher eukaryotes (reviewed in: Gozuacik and Kimchi, 2007). This process is known as apoptosis.

1.1.1 Endocytic uptake

The first step in endocytosis is the uptake step. Endocytosis has been studied extensively, starting with phagocytosis, since the late fourties/early fifties of the 20th century, but there have been even older publications from the 19th century describing phagocytic events (DeBruyne, 1897). Phagocytosis is responsible taking up large solid particles into the cell and is restricted to specialized cells such as macropinocytosis is also. Macro- and micropinocytosis (under 150 nm vesicle size) is needed to take up extracellular fluid and macromolecules. Clathrin coated vesicles in yeast were discovered in 1984 (Mueller and Branton, 1984) eight years after the discovery of clathrin and its structural abilities in pig brain, bullock medulla and brain and mouse lymphoma cells (Pearse, 1976). In the late seventies of the last century, endocytosis via clathrin coated pits was described in experiments in which the concentration to punctuated structures of α2-macroglobulin, insulin and epidermal growth factor (EGF) at the surface of Swiss 3T3-4 cells was observed (Maxfield et al,

1978). EGF, α2-macroglobulin and insulin bind to specific surface receptors. In yeast, finger like plasma membrane invaginations, but not clathrin coated pits as in mammals have been observed (Mulholland et al, 1994).
The endocytic uptake step is described in detail in the following chapters in the form of its initiation followed by clathrin mediated endocytosis, caveolae and lipid rafts.

1.1.1.1 Eisosomes

From later studies in yeast, we know about earlier organization structures temporally prior to coated pits. These structures are named eisosomes due to their stability and immobility (Walther et al, 2006). The 20-45 eisosomes of the cell consist of nearly equimolar amounts of Pil1p and Lsp1p in 2,000-5,000 molecule complexes. In addition, plasma membrane protein Sur7p localizes to eisosomes and is known to interact with additional endocytic effectors. Eisosomes play a role in protein and lipid endocytosis. This was observed in experiments monitoring FM4-64 and Hxt2p-GFP and Ste3p uptake. However, eisosome mediated endocytic uptake does not seem to be the only type of endocytic uptake. Actin patch formation is an important step in endocytosis in eisosome mediated upake, but actin patches containing Abp1p and Sla2p also form at eisosome unrelated sites of the cell. The eisosome independency of actin patches, and the observation that endocytosis is only reduced in *pil1*, *lsp1* or *pil1 lsp1* cells, are indications that eisosome mediated uptake is only one of several uptake mechanisms.

1.1.1.2 Clathrin mediated endocytosis

Clathrin mediated endocytosis is an important uptake mechanism in yeast and mammals. It is known that clathrin mediated endocytosis in yeast is not the only type of endocytic uptake, as can be seen in the *chc1* mutant deleted for the clathrin heavy chain. In this *chc1* mutant, α-factor internalization is reduced by only 50% (Tan et al, 1993). A reduction of internalization was also observed in *clc1* cells, deleted for the clathrin light chain (Chu et al, 1996). The endocytosis defect can be suppressed in *chc1* cells by overexpression of the clathrin light chain (Newpher et al, 2006). It is predicted that Clc1p increases the turnover rate of Sla2p cortical patches. It is assumed that Sla2p is some kind of anchor between the vesicle coat and the actin polymerization machinery which provides the force needed for internalization

(Newpher and Lemmon, 2006; Kaksonen et al, 2003). Overexpression of *CLC1* does not affect defects in transport departing from the TGN (Huang et al, 1997) where clathrin mediated budding is also important. In yeast, clathrin and Ede1p localize to endocytic sites as the first proteins (Newpher et al, 2005). Pan1p is the yeast homolog to mammalian Eps15 which is known to localize to edges of clathrin coated pits and interacts with AP-2 adaptor complex (van Delft et al, 1997; Wendland and Emr, 1998). Epsin interacts with Eps15 also and is responsible, for example, for receptor mediated internalization of transferrin (Tf) or epidermal growth factor (EGF) (Chen et al, 1998). Epsin homologs have also been identified in yeast and are named Ent1p and Ent2p. They are known to interact with Pan1p. Both yeast and mammalian epsins are known to be required for actin cytosceletal organization and function. Furthermore, it is known that yeast homologs are required for actin cortical patch localization and endocytic internalization (Wendland et al, 1999).

1.1.1.3 Uptake signals and ubiquitination

The endocytic uptake of proteins from the plasma membrane normally is regulated. In some publications they have investigated the binding of tyrosine based internalisation signals of membrane proteins directly to the µ2 subunit of AP-2 adapter complex in mammalian cells (Ohno et al, 1995). Yeast has homologs for mammalian AP-2 proteins (Newpher and Lemmon, 2006; Kaksonen et al, 2003), but tyrosin based signals in yeast are known as retention signals for TGN localized proteins (Wilcox et al, 1992). This does not exclude that a tyrosine based signal could possibly function as a signal for endocytic internalisation for retention to the Golgi via the endocytic pathway. Another internalization signal in mammalian cells is a di-leucine motif (Hunziker and Fumey, 1994; Pond et al, 1995). In contrast, a di-leucine motif in yeast is known to be a sorting signal from the TGN to the vacuole (Vowels and Payne, 1998). The PEST-like sequence SINNDAKSS of the Ste2p receptor and the NPFXD signal of the receptor Ste3p are known examples of internalization signals in yeast (Rohrer et al, 1993; Tan et al, 1996). For rapid internalisation of Ste2p, for example, ubiquitination of the SINNDAKSS lysine residue is needed (Hicke and Riezman, 1996). Ubc4p and Ubc5p are involved in this process. In contrast to poly-ubiquitinated cytoplasmic proteins (Lys48) which are degraded in proteasomes (Varadan et al, 2004; Reviewed in: Hochstrasser et al, 1999), plasma membrane protein internalisation is commonly regulated by mono-ubiquitination (Polo et al,

2002). Ubiquitination is induced by ligand binding, which at first leads to hyper-phosphorylation of normally mono-phosporylated neighbouring serine residues of the lysine residue of the SINNDAKSS motif (Reneke et al, 1988). In some specific cases, as described for the uracil permease Fur4p, it is known that Fur4p needs poly-ubiquitin chains for proper internalization as proteasome degraded cytoplasmic proteins (Galan et al, 1996). In the case of Fur4p, ubiquitination is performed by Rsp5p and not by Ubc4p and Ubc5p. In addition, ubiquitin is bound to the membrane protein via the ε-amino group of K63 of ubiquitin (Galan and Haguenauer-Tsapis, 1997). An example in higher eukaryotes, that ubiquitination is important for the internalization of the growth hormone receptor, are Chinese hamster ovary (CHO) cells (Strous et al, 1996). Ubiquitination might be involved in sorting to the early endocytic pathway and it is not only a signal for sorting of membrane proteins into the lumen of the multi vesicular body (MVB) for later degradation in the vacuole. Variants of normally internal Ste6p with defects in ubiquitination, and due to that mislocalization to the plasma membrane, can be observed again inside the cell in a mutant inactivated for Ypt6p (Krsmanović et al, 2005). Ypt6p is important for recycling plasma membrane proteins via early endosome and TGN.

1.1.1.4 The role of actin, myosin and dynamin in endocytic internalization

It is commonly accepted that actin in yeast plays a role in endocytic internalization. In cells lacking Sla2p accumulation of immobile cortical patches containing Sla1p, Pan1p, Las17p, clathrin, and epsin adaptors with wide actin comet tails was observed (Newpher et al, 2005, Gourlay et al, 2003). The immobile patches in *sla2* cells are unable to develop to endocytic pits. This indicates that Sla2p is a regulator to promote maturation of early patches to later stages in invagination. The mammalian homolog of Sla2p is HIP1R which interacts with Huntingtin. HIP1R is known to be associated with clathrin coated pits and actin-rich membrane ruffles as also seen in yeast (Engqvist-Goldstein et al, 1999). This means that according to current knowledge, the involvement of actin function in endocytic internalisation is also well accepted for mammals (reviewed in: Engqvist-Goldstein and Drubin, 2003). However, the question as to how clathrin and actin functions are correlated to each other remains unanswered. Proteins known to be correlated to endocytic internalisation partly or often fully co-localise with punctuate cortical actin patches in yeast. Warren et al (2002) described different kinds of patches with different protein

compositions and motile properties. Later, it became clear that these different cortical actin patch types are different maturation states during endocytic invagination. The first step involves early proteins such as Arp2/3 complex activators, endocytic adaptors and scaffolds assembling in a non-motile plasma membrane complex (Kaksonen et al, 2003). This complex harbours Sla1p, Sla2p, Pan1p and Las17p. In a later step, actin (Act1p), Abp1p, Arc15p and the Arp2/3 complex bind to the early patch. The Arp2/3 complex consists of Arp2p, Arp3p, Arc15p, Arc18p, Arc19p, Arc35p and Arc40p (reviewed in: Welch, 1999). Sla1p, Sla2p and Pan1p subsequently disappear from the plasma membrane. The pit now only harbours Abp1p and Arc15p. Till this stage has been reached, only slow movement can be observed and, after splitting the complex, movement accelerates. It can be assumed that movement in the early slow phase is due to actin polymerisation invaginating the plasma membrane followed by contraction of the vesicle neck. Actin filament assembly is dependent on nucleation by Arp2/3 complex. Actin, cofilin (Cof1p) and Abp1p can be detected at finger-like plasma membrane invaginations by immuno electron microscopy (Mulholland et al, 1994). Arp2/3 complex can be activated by three activators: Las17p, Pan1p and Abp1p. It might be that the internalization process is guided by these (Kaksonen et al, 2003). Las17p, which has the longest lifetime, is the first activator in the early complex. Pan1p is also an early component, but during disappearance of the complex from the cortex Las17p is no longer present. Thus Pan1p might be responsible for vesicle release. Pan1p complex also contains End3p. Abp1p is present in the complex at a later stage and it is assumed that it has a fine-tuning role in this step. When Abp1p is present in the complex, the recruitment of actin to the patch is at its maximum. The membrane fusion or vesicle scission is proposed to be done by the unconventional class I myosin Myo5p (Jonsdottir and Li, 2004). Myo5p is recruited by actin assembly and Vrp1p, a Las17p interacting protein. Myp5p activates the Arp2/3 complex also as Las17p, Pan1p and Abp1p do. The largest association of Myo5p with cortical patches was observed when Arp2/3 complex movement accelerates. *In vitro* Myo5p induces cytosol- and Arp2/3 complex-dependent actin polymerization (Idrisi et al, 2002). Cof1p is also involved in this process. Apart from Myo5p, a second unconventional class I myosin Myo3p is involved in receptor mediated endocytosis (Geli and Riezman, 1996). At the end of the early slow phase of invagination, the early proteins Pan1p and Sla1p are disassembled, most likely due to phosphorylation by Prk1p and Ark1p kinases

(Kaksonen et al, 2003). Phosphorylated forms of Pan1p and Sla1p cannot interact after being phosphorylized by Prk1p (Zeng et al, 2001) and Ark1p, which co-localizes with actin patches. This is furthermore dependent on the presence of Abp1p (Cope et al, 1999). Defects in Ark1p kinase activity leads to accumulation of actin clumps and endocytic vesicles (Cope et al, 1999). Other proteins are important for endocytic internalization additionally, such as fimbrin (Sac6p), calmodulin (Cmd1p), Rvs161p, Rvs167p, Cap1p, Cap2p and actin related protein Arp2p (Kübler and Riezman, 1993; Kübler et al, 1994; Kaksonen et al, 2005; Moreau et al, 1997). Dewar et al (2002) discovered two additional cortical components linking actin cytoskeleton and endocytosis: Ysc84p and Lsb5p. The interesting point is that they discovered that single deletions of *YSC84* or *LSB5* do not lead to a dramatic phenotype where a double deletion is lethal. This indicates that there might be overlapping pathways of actin dependent endocytosis. After internalization, endocytic vesicles move towards early endosomes on actin cables (≈85%) (Toshima et al, 2006). At the same time, early endosomes move towards the endocytic sites and are also associated to actin cables in ≈89% of all cases (Toshima et al, 2006). Endosomes in wild type cells move with a velocity of approximately 213.46±139.47 nms^{-1}. Endosome speed is greatly reduced when actin cable turnover is inhibited. Formins Bni1p and Bnr1p also seem to be relevant, due to their role in actin cable assembly. Las17p mediated actin polymerization and type V myosins Myo2p and Myo4p do not affect early endosome motility. Myo2p and Myo4p are known to be relevant for transport of secretory vesicles at actin cables for example (reviewed in: Bretscher, 2003).

Dynamin in mammalian cells is also required for endocytic uptake and it is assumed that it pinches off vesicles from the plasma membrane (reviewed in: Hinshaw and Schmid, 1995). There are three homologs of the mammalian dynamin in yeast, named Mgm1p, Dnm1p and Vps1p. Mgm1p is localized to mitochondria (Shepard and Yaffe, 1999). Dnm1p is indicated to be involved in late endocytosis and mitochondrial morphology (Gammie et al, 1995; Sesaki and Jensen, 1999) and Vps1p is required for export from the *trans* Golgi network (TGN) towards the endosomal system. Vps1p is involved in actin cytoskeleton organization via its interaction with Sla1p (Nothwehr et al, 1995, Yu and Cai, 2004). Interestingly, Sla1p is known to be an early endocytic factor involved in completion of internalization together with Abp1p (Newpher and Lemmon, 2006; Kaksonen et al, 2003) and it is known to interact with the cytosolic tail of endocytic receptor Ste2p (Howard et al,

2002; Kaksonen et al, 2003). It is currently not known whether Vps1p is involved in endocytic internalization, as dynamin in mammals. The endocytic defect might not be predominant due to redundancy of this internalisation type depending on Vps1p. Some papers suggest that there might be more than one internalization pathway in yeast (Tan et al, 1993; Heese-Peck et al, 2002; Munn et al, 1999; Pichler and Riezman, 2004 (review)).

1.1.1.5 Caveolae

Clathrin mediated endocytosis in mammalian cells is not the only type of endocytic internalization. There are many publications about caveolae mediated endocytosis which does not require clathrin in mammals. Furthermore, there are numerous publications about controversially discussed lipid rafts and their involvement in endocytosis in mammals and yeast. Caveolae are flask shaped plasma membrane invaginations which do not require clathrin as a scaffold and can be found in many cell types of higher eukaryotes, particularly in endothelial cells but never in lymphocytes. One major protein component found to be located at caveolae is the cholesterol-binding protein, caveolin (Kurzchalia and Parton, 1999). Caveolin-1, 2 and 3 are the main components of caveolae and caveolin-1 has two isoforms, α and β (Rothberg et al, 1992; Scherer et al, 1996; Tang et al, 1996). Caveolin-1 is responsible for organizing cholesterol and saturated lipids within the invaginations (Schlegel et al, 2000). Proteins located at caveolae are also found in lipid rafts. Dynamin is localized near to caveolae at their neck (Henley et al, 1998; Oh et al, 1998). Several kinds of cargo are sorted via caveolae mediated and other non-clathrin mediated internalization pathways which are not as well described as caveolae mediated internalization. Furthermore, caveolae are involved in signal transduction of receptors such as tyrosine kinase receptor, serine-threonine receptor or bone marrow protein receptors BRIa and BRII (Nohe et al, 2005). BRIa and BRII directly interact with the isoforms of caveolin-1, followed by initiation of the Smad signalling cascade after ligand binding. Interleukin 2 receptor (IL-2), for example, is taken up in the absence of clathrin mediated internalization (Lamaze et al, 2001). Furthermore, when caveolae mediated internalization is not possible, as in lymphocytes, IL-2 is still taken up into the cell (Lamaze et al, 2001) by a RhoA (small GTPase) dependent mechanism. As lymphocytes do not express caveolin or exhibit caveolae there is evidence of other non-clathrin mediated uptake mechanisms apart

from caveolae mediated endocytosis. Kirkham et al (2005) describes non-clathrin coated caveolin unrelated early endocytic compartments. There are clathrin independent Cdc42 (small GTPase) regulated pinocytic events involved in the recycling of glycosyl-phosphatidyl-inositol (GPI)-anchored proteins (Sabharanjak et al, 2002). Observations made in both publications (Kirkham et al, 2005; Sabharanjak et al, 2002) are independent of dynamin function which is needed for clathrin and caveolin mediated endocytosis. Glebov et al (2005) discovered a third uptake pathway, apart from clathrin and caveolin mediated uptake, namely the uptake mediated by flotillin-1 (reggie-2). They demonstated that flotillin-1 can be detected at the plasma membrane and specific endocytic intermediates in punctuated structures. Flotillin-1 is present even in lysosomal membranes (Liu et al, 2005). GPI-anchored proteins are internalized via these structures. These internalization sites harbouring flotillin-1 do not contain caveolin-1 or clathrin. Flotillins (reggie-1 and reggie-2) are evolutionary highly conserved and homologs have been found even in fungi and bacteria, but not in *Saccharomyces cerevisiae* (Rivera-Milla et al, 2006). The SV40 virus particle uses caveolae mediated uptake to subsequently deliver to the endoplasmatic reticulum (ER) (reviewed in: Norkin, 1999). After the uptake of SV40 into the cell, it is delivered to intracellular organelles which are different to early endosomes usually harbouring the TfR. Apart from SV40, caveolin is also present in these different compartments and as a result of this, these compartments have been named caveosomes. Caveosomes are very stable in contrast to early endosomes which harbour TfR (Pelkmans et al, 2001). Caveolae are very stable and immobile, as eisosomes are in yeast too, (Thomsen et al, 2002) and overexpression of caveolin-1 inhibits endocytic uptake of gp60 receptor for albumin in endothelial cells (Minshall et al, 2000). This indicates that in this case the amount of dynamin is too low for efficient uptake of the receptor from more caveolae than normal, or there is some kind of regulatory process such as phosphorylation which is needed for budding from the plasma membrane (Parton et al, 1994). Some receptors are known to be taken up via more than one pathway, such as the transforming growth factor β (TGFβ) receptor which is taken up via clathrin mediated and caveolin mediated endocytosis (Di Guglielmo et al, 2003; Razani et al, 2001). Clathrin mediated uptake of the TGFβ receptor leads to signalling where caveolin mediated uptake is associated with receptor turnover. Another prominent cargo, the cholera toxin B subunit, seems to be taken up into the cell via caveolae mediated internalization

(Orlandi and Fishman, 1998). The cholera toxin B subunit binds to GM1, a glycosphingolipid which is located to caveolae and lipid rafts (Parton, 1994). The cholera toxin B subunit is also taken up in a flotillin-1 dependent pathway (Glebov et al, 2006). Furthermore, cholera toxin B subunit bound to GM1 was detected in clathrin coated pits (Tran et al, 1987). This might be due to differences in membrane composition in clathrin coated pits, in comparison to other membrane regions.

1.1.1.6 Lipid rafts

Lipid rafts are membrane microdomains consisting of cholesterol, glycosphigolipids, sphingomyelin and lipid raft dependent GPI anchored proteins. Composition differs according to their localisation in the cell (reviewed in Pike, 2004).

The major drawback of most publications about lipid rafts is that the data are based on experiments where lipid rafts are isolated from cells with the help of detergents, which is how they are defined. That means that these experiments present an *in vitro* situation to envisage what takes place *in vivo*. It might be possible that, due to detergent treatment, the composition of lipid rafts is forced to develop into the form we detect them and does not actually represent the situation in a living cell. This is supported by observations that lipid raft composition is strongly dependent on the detergent used (Schuck et al, 2003). This means that one cannot talk about some kind of compartment or static definable region of the plasma membrane in a cell when considering lipid rafts, as described in most papers. *In vivo* research of lipid rafts is problematic, but there are FRET (fluorescence resonance energy transfer) measurements between GPI anchored proteins and lipid anchored proteins on the inner site of the plasma membrane supporting an *in vivo* existence model for lipid rafts (Zacharias et al, 2002; Varma and Mayor, 1998; Reviewed in: Simons and Ikonen, 1997). Furthermore, local membrane viscosity of rafts and non-raft regions have been measured (Pralle et al, 2000). The most interesting point is that proteins known to be internalized independent from clathrin are present in lipid rafts. Proteins which need clathrin to be taken up cannot be detected in lipid rafts, as observed for the low density lipoprotein receptor (LDLR) for example (Nichols and Lippincott-Schwartz et al, 2001). It has also been observed that when cholesterol is depleted from the plasma membrane, numerous molecules reported to be internalized via clathrin independent pathways are no longer taken up (Nichols and Lippincott-Schwartz et al, 2001 (review); Lamaze et al, 2001; Sabharanjak et al, 2002). In addition, when depletion of cholesterol from the plasma membrane is too strong,

clathrin mediated endocytosis is also inhibited (Rodal et al, 1999; Subtil et al, 1999). These data indicate that there are clathrin independent internalization pathways which are more dependent on specific lipid compositions of the plasma membrane than in clathrin mediated uptake. This is supported by the cholesterol binding ability of caveolin-1 (Murata et al, 1995; Kurzchalia and Parton, 1999). The observation that this binding ability is resistant to detergents leads to the suggestion that caveolae represent a type of lipid raft (reviewed in: Harder and Simons, 1997).

Finally, there is a model suggesting that lipid raft proteins are only surrounded by raft lipids floating in the membrane, with the shell preventing them from detergent extraction (reviewed in: Anderson and Jacobson, 2002).

Moreover, lipids in yeast are important for membrane transport. For example, the seven yeast *OSH* genes are responsible for intracellular sterol distribution and lipid composition of the plasma membrane, and this is needed for endocytosis (Beh and Rine, 2004). Fragmented vacuoles in mutants of these genes have also been observed. Comparable phenotypes are present in *erg2* and *arv1* mutants. Yeast *OSH* genes are homologs of the mammalian oxysterol-binding protein OSBP. Lipid rafts in yeast similar to those described for mammalian cells have also been identified. For example, plasma membrane ATPase Pma1p already associates with lipid rafts during its transport through the Golgi, or even earlier (Lee et al, 2002; Wang and Chang, 2002). Without raft components, Pma1p is mis-targeted to the vacuole indicating the relevance of raft components for sorting processes. Very long chain fatty acids (C26) in sphingolipids or glycerophospholipids are crucial in this process (Gaigg et al, 2005; Gaigg et al, 2006). Furthermore, Gas1p, Hsp30p and Nce2p are also localized to lipid rafts during secretory transport (Bagnat et al, 2000). There has also been research on mammalian cells where it was described that secretory transport and proper targeting is dependent on cholesterol and sphingolipids (Wang et al, 2000; Reviewed in: Salaün et al, 2004). Similar to the mammalian plasma membrane, yeast plasma membrane also contains lipid rafts (Bagnat et al, 2000). Yeast uracil permease Fur4p localizes to lipid rafts in the plasma membrane. After Fur4p is endocytosed it seems to be transferred to non-lipid raft fractions of the membrane, maybe due to altered membrane composition in endosomes (Dupré and Haguenauer-Tsapis, 2003; Hearn et al, 2003). Furthermore, yeast homologs Inp52p and Inp53p of the mammalian 5-phosphatase synaptojanin localize to plasma membrane lipid rafts in resting cells. During hyper-osmotic shift they co-localize with

actin patches for local de-phosphorylation of phosphatidyl-inositol-(4,5)-bisphosphate (PtdIns(4,5)P_2) and thereby actin re-arrangement (Ooms et al, 2000). Enzymes modifying phosphatidyl-inositol-phosphates are also involved in regulating other transport steps in endocytosis (e.g.: Odorizzi et al, 1998). Endocytosis in yeast, including that of Ste2p, is dependent on sterols and sphingolipids (Zanolari et al, 2000; Heese-Peck et al, 2002; Munn et al, 1999; Pichler and Riezman, 2004 (review)). Finally, the *in vivo* existence of lipid rafts is highly probable.

1.1.2 Intracellular transport (A brief summary)

Transport processes in the Golgi, between the Golgi and the endosomal/vacuolar system, in the endosomal/vacuolar system and the cytosol to vacuole targeting (CVT)/autophagy pathway are briefly summarized here. Endocytosis has been studied intensively. Yeast uses the clathrin dependent internalization pathway (Baggett and Wendland, 2001 (review)) as described in chapter 1.1.1 in detail. In addition, cells are able to internalize the receptor bound α-factor at a level of 36–50% of the wild-type in the absence of the clathrin component Chc1p (Tan et al, 1993; Payne et al, 1987), indicating that yeast also possesses a clathrin-independent internalization pathway. It is known that transport between the TGN and endosomes is also clathrin dependent. Correct sorting of the vacuolar carboxypeptidase Y (CPY) to the vacuole in *chc1* mutant was explained later by the recycling of the mislocalized CPY-receptor Pep1p (Vps10p) via the plasma membrane into endosomes (Deloche and Schekman, 2002). Newly synthetized proteins directed to the endosomal/vacuolar system or the cell surface are sorted through the Golgi coming from the endoplasmatic reticulum (ER). Retrograde transport processes from the Golgi back to the ER and *intra*-Golgi transport are COPI dependent and not clathrin mediated (reviewed in: McMahon and Mills, 2004), where anterograde transport from the ER to the Golgi is dependent on COPII. Clathrin dependent endocytic internalisation seems to be dependent on actin, in both mammalian (Yarar et al, 2005) and yeast cells. After internalization, the vesicles are uncoated by the auxin homolog Swa2p (Pishvaee et al, 2000) before they fuse to early endosomal membranes, as described for mammalian cells (Aschenbrenner et al, 2004). Clathrin also seems to be involved in budding events in endocytosis in later compartments (McMahon and Mills, 2004). Proteins coming from the TGN are sorted into the early endosomal compartment, such as the Golgi resident protease Kex2p. The yeast mutant deleted for the F-box protein Rcy1p accumulates Ste2p, Lucifer Yellow (LY-

CH) and FM4-64 in enlarged early endosomes at sites of apical growth (Wiederkehr et al, 2000) and such endosomes also enrich the yeast furin homolog Kex2p (Chen et al, 2005). The next compartment after the early endosome on the way to the vacuole is the late endosome, also described as the prelysosomal or prevacuolar compartment (PVC) (Gerrard et al, 2000[b]; Singer-Krüger et al, 1995) or the multi vesicular body (MVB) (Odorizzi et al, 2003). Many proteins are sorted via this compartment. Proteins using the CPY sorting pathway from the TGN towards the PVC/MVB and the endocytosed material meet here on their way to the vacuole (Bryant et al, 1998). Important proteins for vacuolar function such as proteinase A (PrA) (Cooper and Stevens, 1996), which is involved in the processing of several vacuolar hydrolases (Jones et al, 1982), are sorted via this CPY-sorting pathway. It has been described that some COPI components in mammalian cells localize to endosomes, indicating additional involvement in endosomal transport (Whitney et al, 1995). Experiments with the vesicular stomatitis virus (VSV) and the delivery of endogenous cargo proteins of late endosomes and the lysosome in Chinese hamster ovary (CHO) cells indicated that COPI mediated transport is also involved in transport from early to late endosomes and MVB biogenesis (Daro et al, 1997; Gu et al, 1997). Subsequently, it was demonstrated for yeast that Snc1p v-SNARE protein recycling is impaired in some COPI mutants (Robinson et al, 2006). Later it became clear that COPI components in yeast are also important for MVB function. Sorting defects and a class E like vps defect was observed in mutants of COPIb (Sec27p, Sec28p, Sec33p) which fulfils clathrin like functions. This was not observed for COPIf (Sec21p, Sec26p, Ret2p, Ret3p) mutants (Gabriely et al, 2007). COPIb is associated with Vps27p as a component of the ESCRTI complex and typical vps class E protein.
Non-functional V-ATPase (endosomal/vacuolar acidification) correlates with reduced endocytic transport (Bowers et al, 2000; Brett et al, 2005; Klionsky et al, 1992). Acidification also influences protein activities as well as ionic composition of the endocytic system as described for Kex2p whose activity is dependent on K^+-ion concentration (Rockwell and Fuller, 2002).
In addition to the CPY sorting pathway, the ALP–pathway, named for its most prominent cargo, the alkaline phosphatase, has been described. Material is directly transported via this route to the vacuole from the TGN, bypassing the late endosome (Darsow et al, 2001; Panek et al, 1997). A prominent group of proteins involved in export from the PVC/MVB is encoded by class E vps genes. Deletion mutants for vps

class E genes exhibit an enlarged late endosome which accumulates vacuolar proteins. In addition, proteins derived from the plasma membrane which are normally recycled via the late endosome or are designated to be degraded in the vacuole, are accumulated in class E compartments (Babst et al, 1997; Bowers et al, 2004; Piper et al, 1995). Export from the late endosome, both in the retrograde transport direction to the Golgi and early endosomes as well as in the anterograde transport direction towards the vacuole, is strongly inhibited in class E vps deletion mutants. This results in nearly vacuolar conditions in the class E compartment (Finken-Eigen et al, 1997; Pieper et al, 1995; Raymond et al, 1992; Rieder et al, 1996). The mutants are furthermore incompetent at budding ubiquitinated membrane proteins into the lumen of the late endosome for degradation in the vacuole (Babst et al, 1997; Bowers et al, 2004; Piper et al, 1995).

Finally, proteins are transported via the cytosol to vacuole targeting (CVT)/autophagy pathway. Atg19p is a receptor for the vacuolar aminopeptidase (API) which is translated at free ribosomes. API, which is bound to Atg19p clusters, and is taken up into the vacuole via CVT (Leber et al, 2001; Scott et al, 2001). Under starvation conditions, API, which is bound to Atg19p locates to preautophagosomal bodies (PAS) and is transported into the vacuole by autophagy (Shintani et al, 2002; Suzuki et al, 2002). In addition, also under starvation conditions the cells recycle mitochondria by autophagy and also show piecemeal microautophagy of the nucleus (PMN) (Pan et al, 2000; Roberts et al, 2003) by nucleus-vacuole junctions (NVJ).

1.2 Yeast as a model for human diseases related to the intracellular transport system

Many human diseases are related to defects in intracellular transport processes (reviewed in: Aridor and Hannan, 2000; Aridor and Hannan, 2002). The yeast *Saccharomyces cerevisiae* is a well known model organism for the study of such processes (Shaw et al, 2001) and therefore yeast is a model organism to study human diseases, based on intracellular transport also. Yeast is used to get novel insights in these diseases on molecular level.

1.2.1 Yeast as a model to study neurodegenerative disorders

Huntington´s disease is a neurodegenerative disorder where the patient's neurons die in selected areas of the brain. This leads to motor deficiencies, called chorea,

coordination deficiencies, deficiencies of mental abilities and changes in personality. In Huntington disease patients, the N-terminus of the ubiquitous expressed protein Huntingtin is expansed in the poly-glutamine stretch (Duyao et al, 1993). Some proteins interact with Huntingtin: for example Huntingtin-associated protein 1 (HAP1), Huntingtin-interacting protein 1 (HIP1) or Hip1-related protein (HIP1R). The yeast homolog of HIP1R is Sla2p. Sla2p is known to be associated with clathrin coated and actin-rich membrane ruffles as also seen in human cells (Engqvist-Goldstein et al, 1999). HIP1 and HIP1R in human cells bind to the clathrin light chain influencing clathrin assembly and actin distribution (Chen and Brodsky, 2005; Legendre-Guillemin et al, 2005). HAP1 is known to interact with the Hrs protein in human cells (Li et al, 2002). Hrs is the human homolog to the yeast class E vps protein Vps27p. Defects in Vps27p leads to enlarged late endosomes, named class E compartments (Finken-Eigen et al, 1997; Piper et al, 1995). Defects in HAP1 expression affect the size of endocytic compartments in affected cells too. Finally, yeast is a suitable model to study aspects of Huntington´s disease.

Alzheimer´s disease is a neurodegenerative disease. First symptoms are a progressive loss of memory. In later stages in the disease there is progressive cognitive deterioration, patients´ activities in daily life decline and they develop neurospastic symptoms or behavioral changes. Intellectual impairment extends caused by neuronal loss or atrophy in both the temporoparietal cortex and the frontal cortex. They display aphasia, apraxia, agnosia, and they lose the abilities of decision-making and planning. The processing of the β-amyloid peptide precursor (APP) in human cells is involved in Alzheimer´s disease. The secretases β and γ process β-APP, resulting in Aβ peptides causing Alzheimer´s disease in cerebal amyloid cells (reviewed in: Haas and Selkoe, 1993; Haas et al, 1995). A third secretase α cleaves the Aβ peptides so that the peptide is no longer membrane bound. When β-APP is expressed in yeast cells deleted for the genes *SEC1* and *SEC7* and due to that, inhibited in export competence from the Golgi, β-APP is processed as described for processing by mammalian α-secretases. In yeast, GPI-anchored aspartyl proteases Yap3p and Mkc7p are involved in β-APP processing which was observed before β-APP processing proteases in mammals were discovered (Zhang et al, 1997; Zhang et al, 1994). Finally, yeast is a suitable model to study aspects of Alzheimer´s disease.

Parkinson´s disease is a neurodegenerative disorder of the central nervous system. Initial symptoms are decreased stimulation of the motor cortex by the basal ganglia due to malfunctions in the dopamineric neurons of the brain. After a while, patients develop higher level cognitive dysfunction and subtle language problems, and finally the patients are impaired in motor skills and speech muscle rigidity, and have tremors, bradykinesia, and in extreme cases akinesia. α-synuclein (αSyn) plays a significant role in Parkinson´s disease. αSyn in mammalian cells is localized at the nucleus, cytosol and membranes in the brain and interacts with vesicles and a variety of proteins (reviewed in: Lücking and Brice, 2000). In diseased brains αSyn is found in large cytoplasmic inclusions. Quality control of protein mis-folding plays a role in the development of Parkinson´s disease. When αSyn is expressed in yeast it localizes to the plasma membrane and, in smaller amounts, to the cytoplasm (Outeiro and Lindquist, 2003). αSyn also accumulates in cytoplasmic inclusions in concentrations which are too high in yeast. Defective αSyn in yeast leads to altered cellular distribution of the protein, as is already known from early-onset familial Parkinson´s disease. In one case, cytoplasmic distribution of the protein disappears. When wild-type αSyn is expressed in yeast cells, the cells accumulate high amounts of lipids, in contrast to expression of Parkinson related mutated forms. It has also been postulated by *in vitro* experiments with human phospholipase D (PLD) that it is inhibited by αSyn (Jenco et al, 1998). This could be confirmed for yeast PLD using deletion mutants for *SEC14* and *CKI1* (Outeiro and Lindquist, 2003), known to be related to yeast PLD (Bankaitis et al, 1990). Finally, binding of αSyn to vesicles, as in mammals, and vesicle transport alterations have been confirmed for the yeast model (Outeiro and Lindquist, 2003). FM4-64 distribution after its uptake was affected in cells expressing αSyn.

Additionally, glutathione depletion plays a significant role in degenerative processes as is the case for Parkinson´s disease, for example (reviewed in: Schulz et al, 2000), maybe due to effects on late endosome/vacuolar function (Perrone et al, 2005), in comparison to observations concerning αSyn effects on membrane transport (Outeiro and Lindquist, 2003). Yeast is a model to test the effect of glutathione homeostasis and might also give new insights into Parkinson´s disease (Perrone et al, 2005). Finally, yeast is a suitable model to study aspects of Parkinson´s disease.

1.2.2 Yeast as a model to study immune deficiency disorders

Wiskott-Aldrich syndrome is a recessive immune deficiency disorder. The protein which causes the disease when it is defect (WASp) is located on the X chromosome. The disease is characterized by draining ears, eczematous dermatitis, bloody diarrhoea, impaired cellular and humoral immunity and thrombocytopenia (Aldrich et al, 1954; Cooper et al, 1968). T cells in patients show delayed hypersensitivity to stimuli and the number of platelets is also reduced (Ochs et al, 1980; Marone et al, 1986). Lymphocytes of WAS patients show cytosceletal abnormalities and defects in actin re-organization in addition to reduced numbers of microvilli (Gallego et al, 1997). The yeast homolog of the human WASp is Las17p which is known to be important for actin patch assembly and actin polymerisation as an activator of the Arp2/3 complex (Kaksonen et al, 2003). Madania et al (1999) discovered that Las17p interacts with the Arp2/3 complex, actin, verprolin (Vrp1p), Rvs167p and others. In addition, human WASp interacts with the corresponding Arp2/3 complex (Machesky and Insall, 1998). Furthermore, the yeast homolog Vrp1p of the human WASp-interacting protein (WIP) which is essential for endocytosis, has also been discovered (Naqvi et al, 1998). WIP is a chaperone for WASp (de la Fuente et al, 2007). Vrp1p interacts with Las17p and Myo5p (Naqvi et al, 1998; Anderson et al, 1998). Defects in a *vrp1* mutant are suppressed by an additional deletion of *BBC1* (*MTI1*) (Mochida et al, 2002). This suggests an antagonist role between Vrp1p and Bbc1p in Myo5p recruitment to the actin patch. Yeast is a suitable model to study aspects of Wiskott-Aldich-Syndrome.

1.2.3 Yeast as a model to study lysosomal storage disorders

Batten disease is a lysosomal storage disorder belonging to the group of neuronal ceroid lipofuscinosis. There are several forms of Batten disease based on dysfunctions of different genes, summarized under CLN-genes. Batten disease is subdivided according to age of onset: infantile (Santavuori-Haltia disease), late infantile (Jansky-Bielschowsky disease), juvenile (Batten disease), adult form (Kuf´s and Paruy´s disease) and others (Finnish late infantile Batten disease, variant late infantile Batten disease, Turkish late infantile Batten disease and Nothern epilepsy) (reviewed in: Wisniewski et al, 1992). Symptons are declining mental abilities, intractable seizures, progressive loss of sight and motor skills and patients commonly die prematurely. Lipoprotein pigments in Batten disease patients can be found in

brain, eye, skin and muscle cells in green-yellow particles in cells lysosomes. In the juvenile form it is known that the major component of these particles is the subunit c of the mitochondrial ATP synthase. In yeast there is an ortholog of the human CLN3 protein, the protein Yhc3p (Chattopadhyay et al, 2003). In an *yhc3* mutant, expression of Btn2p is up-regulated and Btn2p seems to interact with Yif1p, an ER/Golgi resident protein. Yif1p is mis-localized to the vacuole in *btn2* mutant cells. Btn2p interacts with Rhb1p, also known to be mis-localized in *btn2* cells. Btn1p, Btn2p and Ist2p are probably involved in ion- and amino acid homeostasis (Kim et al, 2005). Rhb1p is a regulator of plasma membrane arg/lys permease Can1p and arg/lys levels are lower in *btn1* mutant cells than in the wild type (Kim et al, 2003). As all these observations are made in yeast, it is a good model to study aspects of Batten disease.

Cystinosis and some cases of inherited renal Fanconi syndrome are caused by defects of the *CTNS* gene, coding for cystinosin. There are three allelic clinical forms of the autosomal recessive disorder cystinosis. In the infantile form, renal tibulopathy, retinal blindness, hypo-thyroidism, diabetes mellitus, swallowing difficulties and neurological deterioration have been observed (reviewed in: Kalatzis and Antiqnac, 2002). In the juvenile form, glomerular renal damage and photophobia is predominant. In the third form, only mild photophobia is shown by the patient. Cystinosin is involved in lysosomal export of cystein. There is a functional homolog of the human cystinosin in *S. cerevisiae* called Ers1p (Kalatzis et al, 2001, Gao et al, 2005). Multicopy suppressors of the *ers1* phenotype were discovered in a yeast based screen. Meh1p was shown to be involved in regulating the Ers1p function (Gao et al, 2005). Loss of Meh1p results in defects in vacuolar acidification (Gao et al, 2005). In addtion cytinosin function is dependent on compartimental pH-value too (Kalatzis et al, 2001). Gao et al further demonstrated that Gtr1p is an interacting protein of Meh1p and all three proteins associate with vacuolar membranes. Yeast is a suitable model to study aspects of Cystinosis.

Niemann-Pick type C (NP-C) disease is a neurodegenerative disorder caused by accumulation of cholesterol, phospholipids, glycosphingolipids and glycoproteins in the lysosome (reviewed in: Sturley et al, 2004; Sun et al, 2001). Cholesterol is derived from low density lipoprotein particles taken up into the cell (Liscum et al, 1989). It is a progressive fatal, autosomal recessive neurodegenerative disorder with heterogeneous age of onset (Sun et al, 2001). The yeast ortholog of the human NP-

C gene (NPC1) is the NP-C related gene *NCR1*. Ncr1p is a transmembrane glycoprotein that can be found in yeast vacuoles. Mutant cells defect for Ncr1p are resistant to inhibitors of sphingolipid biosynthesis and the ether lipid drug edelfosine (Malathi et al, 2004; Berger et al, 2005). Ncr1p seems to be responsible for recycling sphingolipids to internal membranes (Malathi et al, 2004). It is presumed that the accumulation of sterols in mammalian lysosomes is a secondary result of sphingolipid accumulation in the lysosome. Ncr1p does not have a relevant function in known endocytic pathways in yeast (Zhang et al, 2004). A homolog of a second protein involved in Niemann-Pick type C disease has also been discovered in yeast, namely Npc2p homologous to human NPC2 (Berger et al, 2005[b]). It was demonstrated that yeast Npc2p reverts the accumulation of unesterified cholesterol and GM1 in NPC2 (-/-) fibroblasts. Finally, yeast is a suitable model to study aspects of NP-C disease.

1.2.4 Yeast as a model to study ion transporter defects

Menkes disease is a disorder linked to the X-chromosome (reviewed in: Vulpe and Packman, 1995). Copper export from some cell types in Menkes patients is deficient and copper is accumulated in these tissues, particularly in intestinal mucosa and the kidneys (Prins et al, 1979). This results in failure of copper transport to other tissues, so the phenotype in Menkes disease is mainly based on systemic copper insufficiency (Voskoboinik et al, 2001). Patients display pili torti, hypopigmentation, growth and skeletal defects, arterial aneurysms, hypothermia, seizures and progressive degeneration of the central nervous system with early fatal outcome.

Wilson disease is an autosomal recessive disorder (reviewed in: Vulpe and Packman, 1995). As with Menkes disease, copper export from some tissues in Wilson disease is defective, resulting in chronic liver disease in Wilson patients and pathologies in the brain, kidneys and eyes. Phenotypes of Wilson disease are mainly caused by toxic effects of accumulating copper in specific tissues. Wilson disease patients exhibit progressive neurological symptoms such as behavioural disturbances, dysarthria and movement disorders. Furthermore, Wilson patients have chronic liver disease with cirrhosis, renal tubular dysfunctions and pigmented corneal rings. The onset of the disease is varied, but neurologic defects are seldom found in the case of an early onset. Menkes and Wilson disease is caused by deficiencies of specific P-type ATPases. Menkes disease is often correlated to defects in the MNK

gene or ATP7A gene, whereas the WND gene is defect in Wilson disease (Chelly et al, 1993; Mercer et al, 1993; Vulpe et al, 1993; Tanzi et al, 1993; Petrukhin et al, 1993; Bull et al, 1993; Reviewed in: Silver et al, 1993; Bull and Cox, 1994). Menkes disease protein ATP7A, which is re-internalized via its di-leucine signal, is taken up clathrin and caveolin independently, but is dependent on Rac1 (Cobbold et al, 2003).

A structural and functional homolog of the mammalian P-type ATPases has been discovered in yeast, namely Ccc2p (Fu et al, 1995). *ccc2* mutants are deficient in delivering copper ions to copper binding sites of Fet3p outside the cytosol (Yuan et al, 1995). This indicates that the *ccc2* mutant is defective for copper export into the secretory pathway, as has also been observed in mammalian cells affected by Menkes and Wilson disease. Mutant *ccc2* is a proper model to further study Menkes and Wilson disease. Yuan et al (1997) wrote that Ccc2p-dependent copper export is restricted to a late- or post-Golgi compartment.

Malignant infantile osteopetrosis, one of three forms of the Alberts-Schonberg disease, is a heterogeneous autosomal recessive disorder with fatal outcome when untreated. Bone metabolism in osteopetrosis is affected. Osteopetrosis patients have hematological difficulties, including anemia, thrombocytopenia and granulocytopenia. When the cranial nerves are compressed in osteopetrosis patients due to build-up of bone tissue, patients became blind and deaf. Other symptoms include pathological fractures and infections. Malignant infantile osteopetrosis patients have defects in the ATP6i subunit of the lysosomal proton pumping ATPase (Frattini et al, 2000). ATP6i is evolutionally strongly conserved. The *Saccharomyces cerevisiae* homolog is the V0 subunit component Vph1p of the yeast vacuolar proton transporting ATPase (Sobacchi et al, 2001). Even the region around the disease inducing “Costa Rica mis-sense mutations”, which causes abnormal transcripts and in most cases severe translation defects of the mRNA in the patient, is well conserved on a protein sequence level. Concluding that, yeast is a suitable model to study molecular aspects of osteopetrosis.

Dent´s disease, also called inherited Fanconi syndrome, is a renal disorder linked to the X-chromosome. Dent´s patients display low-molecular-weight proteinuria, aminoaciduria, hyperphosphaturia, and hypercalciuria, which results in kidney stones and nephrocalcinosis (Wrong et al, 1994). The disease is caused by defects in the CLCN5 gene coding for the ClC-5 chloride channel protein (Lloyd et al, 1996). ClC-5 is known to co-localize with the lysosomal proton transporting ATPase (Günther et al,

1998) and the disease is caused by defects in endocytosis, caused by a lack of endosomal chloride conductance. Thus, yeast as model for endocytosis and the lysosomal/vacuolar proton transporting ATPase (Shaw et al, 2001; Reviewed in: Finbow and Harrison, 1997) might be also a suitable for research on Dent´s disease.

1.2.5 Yeast can be used to cure human diseases

Fabry disease is a recessive glycolipid storage disorder linked to the X-chromosome. In Fabry disease, α-galactosidase A (α-GalA) is deficient. Patients develop painful neuropathy and renal, cardiovascular and cerebrovascular dysfunctions (reviewed in: Breunig and Wanner, 2003). The enzyme α-GalA hydrolyses ceramide trihexoside accumulated in Fabry lysosomes. Enzyme replacement therapy is used to cure Fabry disease. For this kind of therapy, α-GalA is expressed heterologously in N-glycosylation outer chain deficient *Saccharomyces cerevisiae* (Chiba et al, 2002). The α-GalA is subsequently treated with bacterial α-mannosidase, so that Man-6-P residues on the surface of α-GalA are exposed. This is necessary for an efficient uptake by Man-6-P specific receptors in the patient. An alternative expression in *Pichia pastoris* has not been successful due to immune response reactions against *P. pastoris* glycosylation (Vinogradov et al, 2000).

1.3 Gene therapy

The term “gene therapy” summarizes a variety of methods, both viral and non-viral, whose aim is to cure monogenic hereditary diseases or cancer by means of exchanging deficient genes, or specifically introducing suicide genes into cells affected by the disease, e.g. cancer cells (reviewed in: Tiberghien, 1994). Additionally, there are approaches in gene therapy against infectious diseases in which restriction enzymes, ribozymes, or the RNAi mechanism is used to cut out a retrovirus out of the genome of an infected cell, or inhibit the expression of viral genes, such as by combatting the human immunodeficiency virus (HIV) (Sakuma et al, 2007; Banerjea et al, 2004; Delgado and Regueiro, 2005). In gene therapy, most test treatment studies in patients used viral gene therapeutic approaches largely because viral systems are much more efficient in comparison to non-viral ones.

1.3.1 Transduction

In viral transfections, also named transductions, most vector constructs are based on retroviruses (RNA virus), adenoviruses (dsDNA virus), adeno-associated virus (ssDNA virus) and herpes simplex virus (DNA virus) (reviewed in: Robbins and Ghivizzani, 1998). Retrovirus (RV) vectors have the advantage that they integrate into the genome and are thus stable over a long period. However, they require mitotic cells for integration and due to that for a transduction success. An exception is the lentivirus subgroup which does not need mitotic events for infections. The HI virus belongs to the lentivirus subgroup. Most RV vectors used in clinical approaches have been based on the Moloney murine leukaemia virus (MMLV). Adenovirus (AV) vectors can infect both dividing and non-dividing cells, but expression is not very stable using AV vectors. Cells infected by an adenoviral construct are easily recognized by the immune system, resulting in an immune response and loss of expression soon after infection, e.g in mouse (Yang et al, 1995). Additionally, a humoral immune response has also been observed when using AV constructs (Mack et al, 1997). Adeno-associated virus (AAV) vectors infect both dividing and non-dividing cells such as adenoviral vectors and AAV stabilly integrates into the genome in chromosome 19 in humans. However, the amount of DNA delivered by an AAV vector construct is strictly limited, and needs a helper virus to be successful (AV or herpes simplex virus (HSV)). Furthermore, the integration ability of the AAV vector has been lost in many constructs. HSV constructs can deliver large amounts of DNA, but this vector is highly cytotoxic, only resulting in short term expressions of a maximum of one week. Finally, rarely used viral vectors are plus-stranded RNA viridae as polio or hepatitis A derived vectors, or combinations of human papilloma virus (HPV) or sindbis virus derived vectors with additional helper virus constructs.

The problem in most viral gene therapy studies has been that in several cases patients have developed cancer, even in an *ex vivo* application, most probably as a result of the viral gene therapy approach (Hacein-Bey-Abina et al, 2003). This leads to the pressing need to enhance the efficiency of non-viral gene therapeutic approaches for following clinical applications.

1.3.2 Transfection

Non-viral transfection has not, till date, been efficient enough for realistic gene therapeutic approaches. Many non-viral transfection methods developed in recent

years have been based on endocytosis of the vector construct, followed by its liberation from the endocytic/lysosomal system. The problem is that barriers reducing the efficiency of these methods are insufficiently understood. Methods known to implicate endocytic uptake of the transfection construct are:

- Calcium phosphate based transfection:

This procedure seems to require endocytic uptake. Experiments to optimize calcium phosphate based transfection efficiency in bovine chromaffin cells showed that efficiency of the transfection rises when calcium phosphate solutions become turbid (Wilson et al, 1995). These authors demonstrated that, apart from other factors, a pH-value of 6.95 and the buffer itself used for calcium phosphate-DNA precipitate formation were important factors for transfection efficiency. The observation that larger particles enhance rather than lower transfection efficiency indicates that endocytosis is involved in the transfection procedure. Additionally, it was later published that calcium phosphate based transfection efficiency was optimal after an initial 24 hour culture of primary fetal rat hepatocytes before precipitate incubation for 20 hours during transfection (Hilliard et al, 1996). These observations are comparable to observations made for endocytosis based yeast transfection procedure (Neukamm et al, 2002). Furthermore, it has been demonstrated that the calcium phosphate based transfection procedure is enhanced by the addition of inhibitors of autophagic-lysosomal function (Ege et al, 1984). Finally, it was demonstrated by Batard et al (2001) that in calcium phosphate based transfection procedure, fluorescence of the PNA-fluorescein labelled plasmid DNA decreases after approximately 1 hour of incubation. As fluorescein fluorescence is dependent on the pH-value, this indicates an uptake of the labelled plasmid in compartments with a low pH-value in the cell and an endosomal or lysosomal accumulation of the labelled DNA.

- Nanoparticle based transfection

This process is mediated by endocytosis. With fluorescent latex particles of different sizes in murine melanoma B16-F10 cells, it has been demonstrated that these particles are taken up via endocytosis (Rejman et al, 2004). Non-phagocytic cells as B16 cells can internalize particles smaller than 1 µm. The authors demonstrated that

even the internalization pathway used, and intracellular routing, is dependent on particle size. Clathrin mediated internalization is involved in the uptake of particles below 200 nm, whereas larger particles are taken up caveolin dependent, exclusively. In rabbit conjunctival epithelial cells (RCEC), poly(dl-lactide-co-glycolide (PLGA) nanoparticles are taken up via caveolin independent and clathrin independent pathways, but are taken up also partly via clathrin dependent endocytosis (Qaddoumi et al, 2003).

- DEAE (diethylaminoethyl)-dextran based transfection

This process also seems to be endocytosis related. Mack et al (1998) published that expression of the probe protein luciferase in human macrophages is at its maximum after 24 hours, using DEAE-dextran method. This indicates time consuming endocytic uptake of the vector construct before entering the cytosol.

- Polyethylene imine (PEI) based transfection

This method also seems to involve endocytosis. PEI is a cationic polymer that can be complexed with DNA. Using fluorescence microscopy it was found out that these complexes associate with the plasma membrane and are subsequently taken up via endocytosis (Bieber et al, 2002). PEI-DNA complexes accumulate in cells lysosomes and are liberated via small local membrane damages. PEI protects DNA from DNase 1 and 2 mediated degradation (Godbey et al, 2000). The amount of PEI-DNA complexes in the cytosol is low, but stable PEI-DNA complexes move from endocytosis site to nuclear entry without obstacles (Bieber et al, 2002; Godbey et al, 2000). How the liberation from the lysosomes is carried out is not clarified completely till date. Boussif et al (1995) postulated a proton sponge mechanism where PEI´s nitrogen atoms were protonated during uptake. The protonation of PEI results in an increase of chloride anions which are co-transported to endosomes and the lysosome. The accumulation of chloride anions in these compartments leads to an increase of the osmotic pressure and rupture of the compartments harbouring protonated PEI-DNA complexes. Thus PEI is a DNA condensing and endosomal disruption agent due to its protonation when pH-value decreases (Coll et al, 1999, Bragonzi et al, 1999). PEI can be optimized for its transfection efficiency in specific cells by modification. Folate-poly(ethylene glycol)-folate-grafted-PEI (FPF-g-PEI) showed increased transfection efficiency in cancer cells in comparison to PEI (Benns

et al, 2002). Furthermore, modification of PEI with integrin-binding peptide resulted in enhancement of transfection efficiency in HeLa (integrin expressing epithelial carcinoma cells) and MRC5 (fibroblasts) cells, indicating involvement of integrins in its uptake (Erbacher et al, 1999; Kunath et al, 2003). As this construct shares these properties with AV´s, they are named synthetic virus-like particles. Branched PEI constructs were also conjugated to cholesterol and designated water-soluble lipopolymer (WSLP). This leads to enhanced transfection efficiency compared to PEI based transfection in CT-26 (colon adenocarcinoma) and 293 T (human embryonic kidney) cells (Han et al, 2001), which is also true for Jurkat cells (Wang et al, 2002). Finally, transferrin (Tf) was coupled to polyethylene glycol (PEG)-PEI constructs for successful optimization of transfection efficiency in TfR rich K562 cells and the A/J mouse model injected with Neuro2a blastoma cells (Kursa et al, 2003). In the systemic model, tumor growth was substantially reduced due to a transfection using a Tf-PEG-PEI based method with a TNFα (tumor necrosis factor α) carrying vector. Coupling PNA (peptide nucleic acid) to Tf for RNAi mediated knock down of an antibiotic resistance in combination with PEI based transfection procedure was successful too (Liang et al, 2000).

- poly-L-lysine (PLL)-DNA complex based transfection

In PLL-DNA complex mediated transfection, the complex also seems to be taken up via endocytosis as PEI-DNA complex. PLL-DNA complexes are less stable against DNase 1 degradation of the DNA in comparison with PEI-DNA complexes (Godbey et al, 2000). PLL-DNA complexes merge with the lysosome during transfection. Finally, transfection efficiency in glycosylated PLL-DNA based receptor mediated tranfection protocols using human hepatoma cells (HepG2) can be enhanced by the addition of chloroquine, which is predicted to lower the endosomal-lysosomal pH-value during transfection (Midoux et al, 1993).

- Cell penetrating peptide based transfection

These peptides as antennapedia, TAT-peptide, transportan and polyarginine deliver molecules taken up via endocytosis. Liberation from endocytic compartments by peptide mediated delivery seems to be based on lipid raft mediated and not clathrin mediated endocytosis (Jones et al, 2005). Uptake was at its maximum after 1-3 hours, depending on the cell type (HeLa, A549, CHO). Loss of cellular energy and

low temperature significantly decreases the internalization of a protein complexed with cell penetrating peptides (Säälik et al, 2004; Richard et al, 2003), indicating that endocytosis is involved in the delivery mechanism. Ionic interactions are involved in endocytosis dependent uptake of the TAT-peptide (reviewed in: Vives, 2003). The TAT peptide is taken up via clathrin mediated endocytosis and involves heparan sulphate receptors and others (Richard et al, 2005).

- Liposome based transfection

Transfection mediated by liposomes implicates an endosomal uptake of the construct (reviewed in: Harashima et al, 2001). There is a broad range of components used for the cationic lipid-mediated gene transfer, such as DOPE (dioleoyl phosphatidyl ethanolamine), CHEMS (cholesterylhemisuccinate), DOPC (dioleoyl phosphatidyl choline), vectamidine (3-tetradecylamino-N-tert-butyl-N´-tetradecyl-propionamidine), lipofectin (1:1 of N-(1-2,3-dioleyloxypropyl)-N,N,N-triethylammonium (DOTMA) and DOPE) or [3] DMRIE-C (1:1 of N-[1-(2,3-dimyristyloxy)propyl]-N,N-dimethyl-N-(2-hydroxy-ethyl) ammonium bromide (DMRIE) and cholesterol) and many more (Tachibana et al, 1998; Hui et al, 1996). Most publications indicate an endocytic uptake of these liposomes consisting of cationic lipids. It has been observed in HepG2 and CHO cells that liposome-cell mixing is efficiently disturbed at 4°C; thus lipid mixing is dependent on temperature and also addition of monensin inhibited lipid mixing (Wrobel and Collins, 1995). Furthermore, it was observed that transfection efficiency greatly depends on the size of cationic liposomes, indicating that endocytosis is the cause for uptake of these constructs (Kawaura et al, 1998). Vesicles larger than 1.4 µm are inappropriate for transfection purposes. In addition, Nakanishi and Noguchi (2001) described the involvement of endocytosis and liberation from endosomes as well as the involvement of microtubules, in the intracellular dynamics in transfection procedures with liposomes.

Internalisation of SAINT-2/DOPE lipoplexes is reduced by 80% when cholesterol is depleted from the plasma membrane of COS7 cells (Zuhorn et al, 2002). Additionally, lipoplexes co-localize with transferrin into early endocytic compartments, and the uptake is dependent on potassium. Uptake is also inhibited by overexpression of deficient Eps15. This means that lipoplexes are taken up by a clathrin dependent uptake mechanism. Finally, Johnson et al (1999) showed that the internalization of plasmid DNA in a lipofectin transfection procedure in human head and neck FaDu

squamous carcinoma cells increases from hour one to hour three in the transfection experiment.

In summary, the consequence of the observations concerning non-viral transfection procedures is that endocytosis of the vector and its liberation from the endosomal/lysosomal system are crucial in most important methods of non-viral transfection and that the vector is not directly transferred over the plasma membrane in these methods.

2 Subject description

In most clinical studies on gene therapy, viral vectors have been used as viral gene therapy is highly efficient. High efficiency is necessary for most applications of gene therapy. Less efficient gene therapeutic approaches would be of minor interest, for example, in suicide gene vector based therapy as defence therapy against cancer. A major disadvantage for the use of viral vectors is that they involve a high risk for the patient.

2.1 Viral versus non-viral transfection

In several studies with retrovirus based vectors, a significant group of patients acquired severe diseases as a side effect; often this was leukaemia (Strauss and Costanzi-Strauss, 2007; Haviernik and Bunting, 2004). These side effects are normally caused by non-directed integration into the genome at critical locations in respect to cancer development. In addition, studies using other viral systems such as adenovirus based vectors often resulted in the death of the patient, as seen in the case of Jesse Gelsinger who died from an immune response after being injected with an adenoviral gene therapy vector (Teichler Zallen, 2000). In comparison to viral vectors in gene therapy, the use of non-viral vectors does not seem to involve such a high risk factor, however, they have also been much less efficient till date. Several non-viral transfection procedures use endocytosis to take up the vector into the cell (See chapter 1.3). A known bottle neck for endocytosis mediated non-viral gene therapy is the efficiency of uptake of the vector into a living cell without degradation during transfection procedure. Further problems are the liberation of the endocytosed DNA from endocytic/lysosomal compartments, the transport of the vector to the nucleus, the import into the nucleus and the integration into the genome, preferable at a defined location. There are two possible approaches to optimize a process such as transfection, a non-systematic screening or a systematic approach based on logic advisements.

In an earlier study at the Department of Microbiology and Genetics at the TU Berlin, substances were screened in an effort to find those which would enhance non-viral transfection (Neukamm et al, 2006). In this study, several substances –mainly licensed drugs- were screened using the yeast model system for transfection enhancing properties. Positive drugs were then verified successfully as transfection

enhancers in DEAE-dextran based transfection experiments in a mammalian cell line (HepG2: human hepatic carcinoma). As yeast has been established as a model organism to study endocytosis (Shaw et al, 2001), it is possible to use *Saccharomyces cerevisiae* as a model for endocytosis based non-viral transfection. It was shown by Neukamm et al (2002) that the yeast transfection assay is based on endocytosis. In this assay, osmotic pressure is applied to yeast cells using 1 M sucrose. In this solution, the cells take up DNA via endocytosis. Afterwards the cells are exposed to an osmotic shift with a factor of 4 and in consequence endocytosed DNA is released into the cytosol. DNA import across the cell plasma membrane is not involved in this method, as shown by Neukamm et al (2002); for example by using sorbit instead of sucrose. Sorbit leads to the same osmotic pressure as sucrose, but does not deliver energy to the cell needed for endocytosis. Endocytosis is an evolutionary conserved process, thus results obtained in yeast can be transferred to mammalian cells in most cases.

2.2 Aim of the thesis

The research carried out as part of this thesis aims at using a systematic approach utilizing the established yeast transfection system to optimize non-viral transfection. That is, to select specific protein targets to optimize transfection based on logic advisements. The best way to optimize a process is to know how the process works in detail. Keeping this in mind, this thesis concentrates on a more detailed understanding of the endocytic uptake of non-viral DNA, the conditions for the DNA in compartments where it accumulates, and its liberation from intracellular compartments harbouring the DNA. Mutants from the EUROSCARF yeast deletion mutant collection (Winzler et al, 1999) are used, which were selected by logical means. The study consists of the following subtopics:

- Selecting typical mutations for specific transport steps in endocytosis to find out which step, or steps, in endocytosis is or are the main bottlenecks in endocytosis based transfection. Based on this, it will be proposed how transfection efficiency can be enhanced by transport inhibition and at which step this has to be realized.
- Studying intra-compartmental conditions in the endocytic/vacuolar compartments in respect to degradation. It was shown in previous studies that deletion of the major processing vacuolar protease PrA enhances transfection efficiency (Neukamm et

al, 2002). This indicated that processing proteases, or maybe also other hydrolases in the endocytic/vacuolar system, affect transfection efficiency. Studies in higher eukaryotes show that there is some indication that the presence of lysosomal DNases lowers transfection efficiency (Howell et al, 2003). Furthermore, it is important to investigate the influence of the pH-value and ion composition of the endosomes and the vacuole on transfection efficiency as enzymatic activities of proteins involved in degradation are dependent on these factors.

- Inhibition of intercompartimental transport pathways between the Golgi and the endosomal pathway. Proteins involved in degradation of endocytosed material are sorted to the endosomes and the vacuole, predominantly via the secretory pathway, followed by sorting steps at intersections between the *trans*-Golgi-network and endosomes/vacuole. In addition, proteins involved in transport processes at endosomes and the vacuole are sorted this way. The presence of these proteins affects the transport of endocytosed vector construct. Intercompartimental transport pathways between the Golgi and the endosomal pathway will be tested in this thesis for their influence on transfection efficiency.
- Checking cytosol to vacuole targeting (CVT)/autophagy pathway. Endocytic/vacuolar proteins predominantly use the sorting pathway via the Golgi, but there are also proteins, and even whole organelles such as mitochondria, which are sorted to the vacuole using the CVT and autophagy pathway. This means that CVT/autophagy pathways will be tested in this thesis for their influence on transfection efficiency.
- Dissecting proteolytic protein processing and glycosylation of cell wall proteins at the Golgi. These processes are important for the structure and function of the cell wall. The structure and function of the cell wall probably affects proximity of the vector to the plasma membrane, due to influences of cell surface charge, for example. This might influence uptake efficiency of the vector. It is important to access how differences in cell wall composition influence transfection efficiency before judging results obtained with different mutants in which cell wall composition might also be affected. This is important for the transfer of these results to mammalian cells, as these cells do not have cell walls as fungi have.
- Interrupting processing of other proteins. Transfection efficiency could also be enhanced by defects in Golgi processing of non-cell wall proteins. Several endosomal/vacuolar proteins are sorted to their target location via the Golgi and are

processed by proteolytic cleavage and/or by glycosylation at the Golgi. This indicates that it is important to investigate proteins involved in Golgi sorting and processing also due to that.

This thesis will reveal target protein information which can be used to develop a strategy to optimize non-viral transfection in mammalian cells. The aim will be to subsequently use specific known inhibitors for those proteins identified to suppress high transfection efficiencies afterwards in mammalian transfection approaches. In the case where no specific inhibitor can be found, the process will be much easier and comprise much less financial risk if one is able to screen or to construct an inhibitor for a known target as opposed to having to do screening experiments with a substance library against a spectrum of targets and conditions.

3 Material and Methods

3.1 Material

3.1.1 Primers and Plasmids

Primers were designed by hand, using rules of Innis and Gelfand (1990). All primers were purchased from metabion (Martinsried, D)

Tab. 3.1: Primers to check deletion mutants used in this work. Mutants are listed in alphabetical order. Sequence information to construct primers is taken from the *Saccharomyces* Genome Database (http://db.yeastgenome.org/cgi-bin/seqTools)

mutant	primer	sequence (5´→3´)
kanMX1	G1for	ACA TGG CAA AGG TAG C
	G2rev	TCA CTC GCA TCA ACC A
BY4741 *apl5*	apl5ctrlfor	CAG TTG TAC ACC GAA TGG
	apl5ctrlrev	CCA GAT ATT CTG CTT CCC
BY4741 *arf1*	arf1ctrlfor	CGA GGT GGC TTG TAT TTG
	arf1ctrlrev	GCA GGG GTG CTG TAA AAC
BY4741 *atg19*	atg19ctrlfor	GCG TTC CAT TTG AGA AGC
	atg19ctrlrev	GTT CTA TCA TTC TGC GGG
BY4741 *chs3*	chs3ctrlfor	GTC AGC ACT ATT TGG AGC
	chs3ctrlrev	GCG TTC TTT CCT CTC TCC
BY4741 *cis3*	cis3ctrlfor	CCC GAA CGG GAT TAT TTC
	cis3ctrlrev	CAG CCA AGT AAG CGA TGG
BY4741 *cwp2*	cwp2ctrlfor	GAT TGC TTT TCC CAC GCC
	cwp2ctrlrev	CGC CTA TGT TTT TCA CGC
BY4741 *exg1*	exg1ctrlfor	GAT GTG GGG TAA GAA TGG
	exg1ctrlrev	CGA CAC AAC CAG AAT CCC
BY4741 *hsp150*	hsp150ctrlfor	CAA TCT CAC TGC TTT GCC
	hsp150ctrlrev	CTA CTA CTA CCG CTA CCC
BY4741 *kex1*	kex1ctrlfor	CTC TCG TCT CAA CAA AGC
	kex1ctrlrev	GTA GCG AAA CAG CAA AGG
BY4741 *kex2*	kex2ctrlfor	GGA ACT ATC CTG CCA TCG
	kex2ctrlrev	GTG CCT CTC TAC AAA ACC
BY4741 *lap4*	lap4ctrlfor	GAC GAA GGC AAC ACA TTC
	lap4ctrlrev	GCA GAA AGG CGA AAA GGG
BY4741 *mnn1*	mnn1ctrlfor	CAT CCC ACT TTT CGA ACC
	mnn1ctrlrev	GAA TTT TAC CCA GCA CGC
BY4741 *mnn9*	mnn9ctrlfor	CAA GCA CAA GCA CAA ACC
	mnn9ctrlrev	GAT ACA GCC TAC GGT AGG
BY4741 *nhx1*	nhx1ctrlfor	GAC TTG TTT GAC GGA AGC
	nhx1ctrlrev	AGA GAA AAG TGC TCT CCG
BY4741 *och1*	och1ctrlfor	GCT GGA TTA CAC AAG ACC
	och1ctrlrev	CGC TAT CAA CCA TCA ACC
BY4741 *pep4*	pep4ctrlfor	TGT AAC CCG TCT TAT GCC
	pep4ctrlrev	GGG AGT TAC TTC TAG TGG
BY4741 *pir1*	pir1ctrlfor	CTT TTG TCC CCT CTT GGC
	pir1ctrlrev	GCA TCC GAT TTC AAT CCC
BY4741 *pir3*	pir3ctrlfor	CAA CAA CGG GAT GAT AGG
	pir3ctrlrev	CTA CAT TGC CGT TAT CGC
BY4741 *pmc1*	pmc1ctrlfor	CAA ATA GTA TCA GCC CCC
	pmc1ctrlrev	ACT TGG GCA TCT TCT AGG
BY4741 *pmr1*	pmr1ctrlfor	CTG CTT CAT CAT TTG CCC
	pmr1ctrlrev	GAG CGA TAC ACC AAT AGC

to be continued on the next page

continuation of Tab. 3.1

mutant	primer	sequence (5´→3´)
BY4741 *pmt2*	pmt2ctrlfor	CCT GTA TTT GCG TCT GCC
	pmt2ctrlrev	CAA CGA GCG AAT AAC ACG
BY4741 *prb1*	prb1ctrlfor	GCA CAA GCA AGC AAA CAG
	prb1ctrlrev	CGA GAC GCC TAA GGA AAG
BY4741 *rav1*	rav1ctrlfor	CCT CCA AAC TGC TTT GGG
	rav1ctrlrev	GGG AGA GTT TGT AGA ACC
BY4741 *rcy1*	rcy1ctrlfor	CCA GTT TGT ACT CTT CGC
	rcy1ctrlrev	GCT CTT CCT TTC GTT GGC
BY4741 *ste13*	ste13ctrlfor	GGC TTA GAG GCG AAA AGG
	ste13ctrlrev	CGA AGA TGT CGT TGA CGC
BY4741 *stv1*	stv1ctrlfor	CTA CAT GCT ACC CAT TGC
	stv1ctrlrev	TCG TTT TGG TCG CAT TCC
BY4741 *tlg2*	tlg2ctrlfor	GCT TTC CGT TAC CGT CTC
	tlg2ctrlrev	CCG CAC AGA AAT CCT TCG
BY4741 *vac8*	vac8ctrlfor	GTG TAA CAA ACA GCG AGG
	vac8ctrlrev	CTA CGG AAC AAA GAC AGC
BY4741 *vam6*	vam6ctrlfor	CCT TCC AAC CTT AGT TGG
	vam6ctrlrev	GAT GGG CAG TAA AAC TCC
BY4741 *vcx1*	vcx1ctrlfor	GCT ATC AGT TTG GAG AGG
	vcx1ctrlrev	CTG CAC CAG CAT TTT TCG
BY4741 *vph1*	vph1ctrlfor	TCC TAA TGA GAG GCA ACG
	vph1ctrlrev	CTG CGG TAA AAA TCT GGC
BY4741 *vps1*	vps1ctrlfor	CCA GTT CCT TCC TCT CTC
	vps1ctrlrev	CGC ATT CTT GGT TGT TGG
BY4741 *vps4*	vps4ctrlfor	GGG TTG GCA TTG AAG ATC
	vps4ctrlrev	GAA GAG CAA CGT CAA AGC
BY4741 *vps13*	vps13ctrlfor	GTA AGC AAC TGG AAG ACG
	vps13ctrlrev	GAG TCA ATT AGC CAA CGG
BY4741 *vps17*	vps17ctrlfor	CGA TTT GTC CTC CAA TCC
	vps17ctrlrev	TGG CTT TCT GGC AAA TGG
BY4741 v*ps21*	vps21ctrlfor	GGC ATT TGG AGA CTA TCG
	vps21ctrlrev	CAC TGA AGA TGA TGC TGG
BY4741 *vps27*	vps27ctrlfor	CGG AGC CTA CCT TTT AGC
	vps27ctrlrev	TCG TGT GGT TAG ACA ACG
BY4741 *vps33*	vps33ctrlfor	GCT ACA GAA TCG GGT ATC
	vps33ctrlrev	GTG ACG AAA ACA GCC TTC
BY4741 *vps45*	vps45ctrlfor	CGG ATG CGT ATT TGT TGG
	vps45ctrlrev	TCC ATG AGG AGA ATA CCC
BY4741 *ypt6*	ypt6ctrlfor	GTG GTA AGA TGA AGC CTC
	ypt6ctrlrev	GAT GCG GAT GAC GAA GAC
BY4741 *yvc1*	yvc1ctrlfor	GCT ACT TGG GCT GTT TCG
	yvc1ctrlrev	GCA AGA AGG TGG GGA AAG

As a control for a positive PCR reaction plasmid pUCP29 was used together with primers M13for and M13rev (metabion, Martinsried, D):

M13for: 5´-TGT TTT CCC AGT CAC GAC GTT G-3´
M13rev: 5´-CAG GAA ACA GCT ATG ACC-3´

The protocol for the PCR control reactions of the deletion mutants will be described later.

For the uptake assay for linear DNA two fluorescein labelled primers were used (metabion, Martinsried, D).

5´ Fluo Probe: 5´-Fluo-CGA CAC TAC GGC ATC GGC TAC GGC AGA GGC TAC CTA G-3´
Fluo Probe 3´: 5´-GTA GCC TCT GCC GTA GCC GAT GCCGTA GTG TCG CCG G-Fluo-3´

Synthetic sequences were designed, keeping in mind to get a sequence with a high GC content, not predicted to form intra-sequential hairpins, and forming a di-fluorescein labelled probe after annealing of both strands with an unlabelled overhanging end compatible to itself to form a tetra-fluorescein labelled and protected probe after a final T4-ligase reaction.

As a non-viral vector for yeast transfections 2-μm shuttle plasmid pFL1 (7,769 bp) was used (Botstein et al, 1979). The vector has a replication origin for *Escherichia coli* and a β-lactamase gene for selection in the bacterial host. This part of the vector derives from the plasmid pBR322. On the other part we find 2-μm DNA as replication origin, and the *Saccharomyces cerevisiae URA3* gene for selection in *S. cerevisiae*.

3.1.2 Mutants

Saccharomyces cerevisiae mutants used in this study are derivatives of the EUROFAN II mutant BY4741 (*MATa; his3Δ1; leu2Δ0; met15Δ0; ura3Δ0*) (Brachmann et al, 1998) and are listed in the following table (EUROFANII: http://web.uni-frankfurt.de/fb15/mikro/euroscarf/). The BY4741 mutant is referred to as a wild-type mutant further on.

Tab. 3.2: Mutants used in this study with the systematic names, aliases and human homologues of the deleted genes. Mutants are listed in alphabetical order. Information is taken from *Saccharomyces* Genome Database (http://www.yeastgenome.org/)

mutant	systematic gene name	alias gene names	homolog in *H. sapiens*	source
BY4741	-	-	-	EUROFANII
BY4741 *apl5*	*YPL195W*	*YKS4*	AP3D1	EUROFANII
BY4741 *arf1*	*YDL192W*	-	ARF1	EUROFANII
BY4741 *atg19*	*YOL082W*	*CVT19*	-	EUROFANII
BY4741 *chs3*	*YBR023C*	*CAL1, CSD2, DIT101, KTI2*	HAS3	EUROFANII
BY4741 *cis3*	*YJL158C*	*CCW11, PIR4, CCW5*	-	EUROFANII
BY4741 *cwp2*	*YKL096W-A*	*LPR1, YKL097W-A*	-	EUROFANII
BY4741 *exg1*	*YLR300W*	*BGL1*	-	EUROFANII
BY4741 *hsp150*	*YJL159W*	*CCW7, ORE1, PIR2*	-	EUROFANII
BY4741 *kex1*	*YGL203C*	-	CTSA, artificial?	EUROFANII
BY4741 *kex2*	*YNL238W*	*QDS1, VMA45, SRB1*	PCSK7 (PC7), FURIN	EUROFANII
BY4741 *lap4*	*YKL103C*	*APE1, YSC1, API*	DNPEP	EUROFANII
BY4741 *mnn1*	*YER001W*	-	-	EUROFANII
BY4741 *mnn9*	*YPL050C*	-	-	EUROFANII
BY4741 *nhx1*	*YDR456W*	*VPS44, NHA2*	SL9A6	EUROFANII
BY4741 *och1*	*YGL038C*	*NGD29, LDB12*	-	EUROFANII
BY4741 *pep4*	*YPL154C*	*PHO9, PRA1*	CATD	EUROFANII
BY4741 *pir1*	*YKL164C*	*CCW6*	-	EUROFANII
BY4741 *pir3*	*YKL163W*	*CCW8*	-	EUROFANII
BY4741 *pmc1*	*YGL006W*	-	ATP2B3, PMCA1a	EUROFANII
BY4741 *pmr1*	*YGL167C*	*BSD1, LDB1, SSC1*	ATP2C1	EUROFANII
BY4741 *pmt2*	*YAL023C*	*FUN25*	POMT2	EUROFANII
BY4741 *prb1*	*YEL060C*	*CVT1*	PCSK9	EUROFANII
BY4741 *rav1*	*YJR033C*	*SOI3*	DMXL1	EUROFANII
BY4741 *rcy1*	*YJL204C*	-	-	EUROFANII
BY4741 *ste13*	*YOR219C*	*YCI1*	DPP4	EUROFANII
BY4741 *stv1*	*YMR054W*	-	ATP6V0A1	EUROFANII
BY4741 *tlg2*	*YOL018C*	-	NPEPL1, artificial?	EUROFANII
BY4741 *vac8*	*YEL013W*	*YEB3*	ARMC3	EUROFANII
BY4741 *vam6*	*YDL077C*	*CVT4, VPL18, VPL22, VPS39*	VPS39	EUROFANII
BY4741 *vcx1*	*YDL128W*	*HUM1, MNR1*	-	EUROFANII
BY4741 *vph1*	*YOR270C*	-	ATP6V0A1	EUROFANII
BY4741 *vps1*	*YKR001C*	*GRD1, LAM1, SPO15, VPL1, VPT26*	DNM1L	EUROFANII
BY4741 *vps4*	*YPR173C*	*CSC1, END13, GRD13, VPL4, VPT10, DID6*	VPS4B	EUROFANII
BY4741 *vps13*	*YLL040C*	*SOI1, VPT2*	VPS13A	EUROFANII
BY4741 *vps17*	*YOR132W*	*PEP21*	-	EUROFANII
BY4741 *vps21*	*YOR089C*	*VPS12, VPT12, YPT21, YPT51*	RAB5A	EUROFANII
BY4741 *vps27*	*YNR006W*	*GRD11, SSV17, VPL23, VPL27, VPT27, DID7*	HGS	EUROFANII
BY4741 *vps33*	*YLR396C*	*CLS14, MET27, PEP14, SLP1, VAM5, VPL25, VPT33*	VPS33A	EUROFANII
BY4741 *vps45*	*YGL095C*	*STT10, VPL28*	VPS45A	EUROFANII
BY4741 *yil064w*	*YIL064W*	-	NP_997719.2	EUROFANII
BY4741 *ypt6*	*YLR262C*	-	RAB6B	EUROFANII
BY4741 *yvc1*	*YOR087W*	*YOR088W*	-	EUROFANII

Escherichia coli SF8 (*recBC, lop11, tonA1, thr1, leuB6, thy1, lacY1, supE44, hsm$^-$, hsr$^-$*) was used as a host for plasmid pFL1.

3.1.3 Media

YPD medium was used for all pre and main cultures of *S. cerevisiae* cultivations (20 gl^{-1} typtone, 20 gl^{-1} glucose*H_2O, 10 gl^{-1} yeast extract). Glucose was autoclaved separately and added to the medium under sterile conditions afterwards in order to reduce formation of Maillard products, which could possibly influence experimental results.
YE medium was chosen (20 gl^{-1} glucose*H_2O, 5 gl^{-1} yeast extract, adjusted to pH 6.3 using NaOH, 15 gl^{-1} agar agar) as non selective solid medium for *S. cerevisiae*.
WMIX medium (Neukamm et al, 2002) was used under selective conditions for *S. cerevisiae* BY4741 mutant and its derivatives (20 gl^{-1} glucose*H_2O, 10 gl^{-1} sodium L-glutamate, 0.075 gl^{-1} meso-inositol, 0.25 gl^{-1} $MgCl_2$*$6H_2O$, 0.1 gl^{-1} $CaCl_2$*$2H_2O$, 0.55 gl^{-1} $MgSO_4$*$7H_2O$, 20 mM potassium-phosphate buffer pH 6.5, 1.5% agar agar, trace elements and vitamins as described for WMVIII) (Lang and Looman, 1995), supplemented with 1 gl^{-1} casamino acids, 100 mgl^{-1} L-histidine*HCl*H_2O, 80 mgl^{-1} L-methionine and 40 mgl^{-1} L-leucin.

Luria Bertani (LB) medium was used for cultivation of *E. coli* cells (10 gl^{-1} tryptone, 5 gl^{-1} yeast extract, 10 gl^{-1} NaCl, adjusted to pH 7.4 using NaOH) supplemented with 100 gl^{-1} ampicillin for plasmid selection.

Tab. 3.3: Compounds used for media preparation. If it is available, p. A. quality was chosen.

constituent	manufacturer
agar agar	Serva, Heidelberg, D
ampicillin	Boehringer Mannheim, Mannheim, D
Bacto casamino acids	BD, Le Pont de Claix, F
$CaCl_2$*$2H_2O$	Merck, Darmstadt, D
glucose*H_2O	Carl Roth, Karlsruhe, D
L-histidine*HCl*H_2O	Merck, Darmstadt, D
L-leucin	Carl Roth, Karlsruhe, D
L-methionine	Carl Roth, Karlsruhe, D
meso-inositol	Carl Roth, Karlsruhe, D
$MgCl_2$*$6H_2O$	Merck, Darmstadt, D
$MgSO_4$*$7H_2O$	Merck, Darmstadt, D
NaCl	Merck, Darmstadt, D
NaOH	Merck, Darmstadt, D
sodium L-glutamate*H_2O	Merck, Darmstadt, D
tryptone LP0042	Oxoid, Basingstroke, UK
yeast extract Ohly KAT	DHW, Hamburg, D

3.1.4 Buffers and Solutions

a) For media preparation:

25x potassium phosphate buffer	solution a: 0.5 M KH_2PO_4 solution b: 0.5 M K_2HPO_4 mix both solutions to pH 6.5
250x vitamin solution	2.5 gl^{-1} nicotinic acid, 6.25 gl^{-1} pyridoxine, 2.5 gl^{-1} thiamine, 0.625 gl^{-1} biotin, 12.5 gl^{-1} calcium phantothenate
250x trace element solution	0.4375 gl^{-1} $ZnSO_4$*$7H_2O$, 0.125 gl^{-1} $FeSO_4$*$7H_2O$, 0.025 gl^{-1} $CuSO_4$*$5H_2O$, 0.025 gl^{-1} $MnCl_2$*$4H_2O$, 0.025 gl^{-1} Na_2MoO_4, dissolved in 10 mM EDTA

b) For assays:

washing solution LY-CH assay	50 mM sodium succinate, 10 mM sodium azide, pH 5, for experiments under transfection conditions add 1 M sucrose
buffered YPD for quinacrine-HCl assay (standard conditions)	YPD buffered to pH 7.6 using 100 mM Hepes
buffered sucrose quinacrine-HCl assay (transfection conditions)	1 M sucrose buffered to pH 7.6 using 100 mM Hepes
washing solution quinacrine assay	100 mM Hepes, 20 gl^{-1} glucose, pH 7.6, for experiments under transfection conditions add 1 M sucrose
10x TAE buffer	400 mM Tris, 200mM sodium acetate, 20 mM EDTA, adjust to pH 8.3 using glacial acetic acid
DNA-stopper solution	600 gl^{-1} sucrose, 20 mM EDTA, 0.25 gl^{-1} bromophenol blue
lysis buffer for genomic yeast DNA preparation	20 gl^{-1} Triton X-100, 10 gl^{-1} SDS, 100 mM NaCl, 10 mM Tris, 1mM EDTA, pH 8
TE buffer	10 mM Tris, 1 mM EDTA, pH 8
4x PCR buffer	dilute 10x PCR buffer (160 mM $(NH_4)_2SO_4$, 670 mM Tris HCl (pH8.8), 1 gl^{-1} Tween 20) 1:2.5 and $MgCl_2$ solution (50mM) 1:8.3 together in HPLC (PCR) water

Tab. 3.4: Additional compounds used for buffers and solutions. Furthermore, other compounds needed for the experiments. If it is available, p. A. quality was chosen.

constituent	manufacturer
1-butanole	Merck, Darmstadt, D
2-propanole	neolab, Heidelberg, D
10x PCR buffer	Rapidozym, Berlin, D
10x T4 ligase buffer	Boehringer Mannheim, Mannheim, D
≥99.8% ethanol	Carl Roth, Karlsruhe, D
agarose	Genaxxon, Biberach, D
ammonium acetate	neolab, Heidelberg, D
D (+)-biotin	Carl Roth, Karlsruhe, D
bromophenol blue	Germed, Sebnitz, DDR
calcium D-phantothenate	Fluka, Buchs, CH
chloroform	neolab, Heidelberg, D
$CuSO_4*5H_2O$	Merck, Darmstadt, D
DMSO	Sigma-Aldrich, Steinheim, D
EDTA	Sigma, Steinheim, D
ethidium bromide	Boehringer Mannheim, Mannheim, D
ethidium bromide monoazide	Sigma, Steinheim, D
$FeSO_4*7H_2O$	Merck, Darmstadt, D
FM4-64	Sigma-Aldrich, Steinheim, D
GeneRuler DNA Ladder Mix	Fermentas, St. Leon-Rot, D
glacial acetic acid	Carl Roth, Karlsruhe, D
glass beads	Carl Roth, Karlsruhe, D
glycerol	Carl Roth, Karlsruhe, D
Hepes	Serva, Heidelberg, D
*Hin*dIII	Fermentas, St. Leon-Rot, D
isoamyl alcohol	Merck, Darmstadt, D
KH_2PO_4	Merck, Darmstadt, D
K_2HPO_4	Merck, Darmstadt, D
λ-DNA	New England BioLabs, Ipswich, MA, USA
Lucifer Yellow-CH	Sigma, Steinheim, D
$MgCl_2$ solution	Rapidozym, Berlin, D
$MnCl_2*4H_2O$	Riedel de Haen, Seelze, D
$Na_2MoO_4*2H_2O$	Merck, Darmstadt, D
nail polish	Rival de Loop, Berlin, D
nicotinic acid	Merck, Darmstadt, D
poly-L-lysine HBr	Sigma, Steinheim, D
pyridoxine HCl	Serva, Heidelberg, D
quinacrine HCL	Fluka, Buchs, CH
RNAseA	Qiagen, Hilden, D
SDS	MP Biomedicals, Eschwege, D
sodium acetate trihydrate	Carl Roth, Karlsruhe, D
sodium azide	Sigma, St. Louis, MO, USA
sodium succinate	Sigma, St. Louis, MO, USA
sucrose	Serva, Heidelberg, D
T4 ligase	Boehringer Mannheim, Mannheim, D
thiamine HCl	Sigma, Steinheim, D
Tris	Carl Roth, Karlsruhe, D
Tris saturated phenol	Biomol, Hamburg, D
Triton X-100	Carl Roth, Karlsruhe, D
$ZnSO_4*7H_2O$	Merck, Darmstadt, D

3.2 Culture conditions

All yeast cells used for any experimental approach were spread on YE agar plates from -80°C glycerol stock and were grown between 4 to 8 days at 28°C, prior to the preparatory culture in liquid medium. A single colony was used to inoculate 20 ml of YPD in a 100 ml Erlenmeyer flask and reciprocally shaken with a velocity of 120 rpm at 28°C for 48 hours. Main cultures were inoculated with an appropriate volume of preparatory culture to obtain a cell density of 5 to $9*10^7$ cells per ml, after an incubation time of 16 to 18 hours. Main cultures were grown in 100 ml YPD in 500 ml Erlenmeyer flasks at 28°C with reciprocal shaking at 120 rpm for the experiments in this work. YE medium agar plates were used for non-selective conditions in transfection experiments; selective medium used was WMIX minimal medium with agar (Neukamm et al, 2002) which was developed further from WMVIII minimal medium (Lang and Looman, 1995), supplemented with casaminoacids, histidine, methionine and leucin as described above. Any Erlenmeyer flask, Schott flask or graduated cylinder used for yeast cultivation, cultivation preparation or media preparation was washed with distilled water prior to usage or autoclaving to exclude additional effects on transfection by ion contamination.

E. coli cells were grown on LB medium with 100 mgl^{-1} ampicillin at 37°C with 160 rpm reciprocal shaking. The preparatory culture was inoculated using 50 µl of the -80°C glycerol stock in 20 ml of medium in a 100 ml Erlenmeyer flask and was grown for 8 hours. Five 2 l Erlenmeyer flasks with 500 ml medium each were inoculated with 750 µl of preparatory culture for the main culture for plasmid purification and cells were grown for 16 hours.

3.2.1 Determination of the cell concentration

The cell concentration of yeast main cultures was determined using a Thoma chamber with a Leitz microscope of the type Ortholux (Leica, Wetzlar, D). The magnification was 562.5x (12.5x ocular, 45x objective). Samples were diluted ten times and cells of four large squares in diagonal were counted. The average value of two determinations was used for cell concentration determination by the following eqation.

$$cc = \frac{DF \cdot X_{av}}{64 \cdot V_{ss}} \qquad \text{(eq. 3.1)}$$

cc	cell concentration in [$cellsml^{-1}$]
DF	dilution factor
X_{av}	average cell number of four large squares in [cells]
64	four large squares equal 64 small squares
V_{ss}	volume of a small square in [ml]: here $2.5 \cdot 10^{-7}$ ml (side length: 50 µm; height: 100 µm)

3.2.2 Determination of the optical density

The optical density was determined with an appropriate dilution of the sample at a wavelength of 600 nm using a $Uvikon_{XS}$ photometer (BioTek, Bad Friedrichshall, D) with the LabPower Junior software (BioTek, Bad Friedrichshall, D) and disposable semi-micro cuvettes (ratiolab, Dreieich-Buchschlag, D). Samples were measured in the linear range of the calibration curve between OD_{600} 0.4 and 0.8 against medium in the same dilution as the sample.

3.3 Plasmid purification

Plasmid pFL1 was purified from *E. coli* SF8 using the Plasmid purification Mega Kit (Qiagen, Hilden, D) as recommended by the manufacturer. 7.5 g cells were harvested for each purification. After purification, plasmid DNA was resolved in 500 µl distilled sterile water for at least 24 hours at 4°C. It is important to use distilled water to resolve the DNA as it is possible that transfection efficiency is influenced by components of the TE buffer. Plasmid solution was transferred to a fresh 1.5 ml reaction tube (Greiner Bio-One, Frickenhausen, D) afterwards. Plasmid concentration and purity were determined. Plasmid DNA was also checked on a 1% agarose gel, dyed by incubating in an ethidium bromide TAE bath for 15 minutes and visualized using a UV light transilluminator with camera and documentation software from Intas (Göttingen, D). λ-DNA resticted with *Hin*dIII was used as a molecular weight marker.

3.3.1 Determination of plasmid purity and concentration

DNA solution from the plasmid purification was diluted by factors of 50 and 100 in distilled water for determination of plasmid DNA concentration and purity. Precision silica glass cuvettes (Hellma, Müllheim, D) were used for absorption measurement at wavelengths of 260 nm, 280 nm and 310 nm using a Uvikon$_{XS}$ photometer with the LabPower Junior software. Both samples were measured against distilled water. DNA concentration was determined with the following equation.

$$c_{DNA} = [(OD_{260,X} - OD_{260,0}) - (OD_{310,X} - OD_{310,0})] \cdot DF \cdot F_{dsDNA} \quad \text{(eq. 3.2)}$$

c_{DNA}	plasmid DNA concentration in [µgml^{-1}]
$index_{number}$	measuring wavelength in [nm]
$index_X$	value for the sample to be determined
$index_0$	value for water sample
DF	dilution factor
F_{dsDNA}	Factor for double stranded DNA: 50 µgml^{-1}

DNA purity was determined by the following equation and should be between 1.5 and 2.

$$P_{DNA} = \frac{(OD_{260,X} - OD_{260,0}) - (OD_{310,X} - OD_{310,0})}{(OD_{280,X} - OD_{280,0}) - (OD_{310,X} - OD_{310,0})} \quad \text{(eq. 3.3)}$$

P_{DNA}	purity of the plasmid DNA in [-]
$index_{number}$	measuring wavelength in [nm]
$index_X$	value for the sample to be determined
$index_0$	value for water sample

3.4 Purification of genomic DNA from *Saccharomyces cerevisiae*

Cells from a -80°C glycerol stock were spread on YE agar plates. After 4-8 days, a single colony was used to inoculate 20 ml YPD medium in a 100 ml Erlenmeyer flask and was grown for 36 hours at 28°C under 120 rpm reciprocal shaking. Cells corresponding to a OD_{600} of 160 units were harvested by centrifugation at 8,850 x g for 5 minutes in 15 ml Greiner tubes (Greiner Bio-One, Frickenhausen, D) using a Heraeus Biofuge primo R centrifuge (Thermo, Walthem, MA, USA) and a #7590 rotor (Thermo, Walthem, MA, USA). Cells were resuspended in 1 ml distilled water, transferred to a 2 ml reaction tube (Eppendorf, Hamburg, D) and centrifuged for 5 minutes at 9,700 x g using a #7593 rotor (Thermo, Walthem, MA, USA). The pellet was resuspended in 200 µl lysis buffer and 0.3 g of 0.45-0.5 mm glass beads, 100 µl Tris saturated phenol and 100 µl chloroform/isoamyl

alcohol (24:1) was added. The suspension was vortexed for four minutes. 600 µl TE buffer was added and the suspension centrifuged for 5 minutes at 9700 x g. The upper watery phase was transferred to a new reaction tube and 1 ml ≥99.8% ethanol was added to precipitate the DNA, followed by a centrifugation step at 9700 x g for 10 minutes. The pellet was resuspended in 400 µl TE buffer and incubated with 3 µl RNAse A at 37°C for 5 minutes. 10 µl of 5 M ammonium acetate and 1 ml ethanol was added followed by a centrifugation at 9,700 x g for 10 minutes. The pellet was washed once again in 1 ml of 70% ethanol and was resuspended in 50 µl distilled water after drying at room temperature for 10 minutes. Genomic DNA was checked on a 1% agarose gel as described for plasmid purification.

3.5 Deletion mutant check

To verify the EUROFANII deletion mutants used for this work, genomic DNA of each mutant was used as a template for a check PCR. Genomic DNA preparations were diluted by a factor of 10. For each PCR, a master mix was prepared including PCR buffer, dNTPs, polymerase and PCR water. The PCR reaction was carried out in a 20 µl scale in 8-tube PCR reaction strips (Brand, Wertheim, D) using a Mastercycler gradient (Eppendorf, Hamburg, D). The composition of a sample and the PCR program used is described in table 3.5. PCR samples were centrifuged for a few seconds using a butterfly rotor table centrifuge (Carl Roth, Karlsruhe, D) prior to putting samples in the cycler. Primers used were constructed in a way that in each case one oligonucleotide primes inside the deletion cassette in the kanamycin resistance gene and the other one outside the deletion cassette in the flanking regions to the deletion. Each deletion mutant was checked twice using two independent primer pairs. Primer pairs prime at each two ends of the deletion cassette in two independent PCR reactions. A negative control was performed for each mutant using an oligonucleotide as second primer, priming somewhere else in the genome but not flanking the site of the deletion. PCR products were checked on a 1% agarose gel. GeneRuler DNA Ladder Mix was used as a molecular weight marker. Plasmid pUCP29 was used as a PCR positive control with the primers M13for and M13rev.

Tab. 3.5: a) Composition of one sample of the check PCR reaction. b) PCR program of the check PCR.

a)

component	volume (for 1 sample)	concentration (in sample)	manufacturer
HPLC (PCR) water	11.82 µl	-	Merck, Darmstadt, D
4x PCR buffer	5.00 µl	1x	Rapidozym, Berlin, D
dNTPs	1.60 µl	325 µM each	Rapidozym, Berlin, D
Taq DNA polmerase	0.08 µl	10 mU	Rapidozym, Berlin, D
primer for	0.50 µl	250 nM	metabion, Martinsried, D
primer rev	0.50 µl	250 nM	metabion, Martinsried, D
template DNA	0.50 µl	1/400	-

b)

temperature	duration	
94°C	4 minutes	
94°C	0.25 minutes	↰ 40x
50°C	0.75 minutes	
72°C	2.5 minutes	
4°C	∞	

3.6 Transfection of yeast cells

A modified protocol of Neukamm et al (2002) was used for yeast transfection. Briefly, *Saccharomyces cerevisiae* cultures were grown as recommended in chapter 3.2. 1 x 10^9 cells were harvested for each sample by centrifugation at 3,500 x g for 8 minutes at 4°C in 50 ml Greiner tubes (Greiner Bio-One, Frickenhausen, D) using a Heraeus Biofuge primo R centrifuge and a #7590 rotor. Cells were washed twice in 17 ml sterile distilled water for 30 minutes at 4°C each to make the cells competent for transfection by swelling. Centrifugation for 5 minutes at 3,500 x g and 4°C was part of the incubation time and cells were transferred to 15 ml Greiner tubes after the first washing step. Then, cells were resuspended in 1 M sucrose (pH 4). Plasmid DNA was added to the cells at a concentration of 15 $\mu g ml^{-1}$. The experiments were performed in a 1 ml scale in 15 ml Greiner tubes. The tubes were not closed completely, so that overpressure could not be formed in the tubes during incubation time, which might influence transfection efficiency due to pressure drop when the tubes were reopened. After 22 hours of incubation at 28°C, two times 10 µl of the cell suspension were taken from each sample for double determination of the number of surviving cells. Then, cells were harvested by centrifugation at 3,500 x g for 3 minutes at room temperature. The supernatant was discarded excluding a residuum of 150 µl including the cell pellet. Cells were exposed to a hypotonic shift by adding three volumes of sterile distilled water to the remaining sucrose/cell suspension (fig. 3.1).

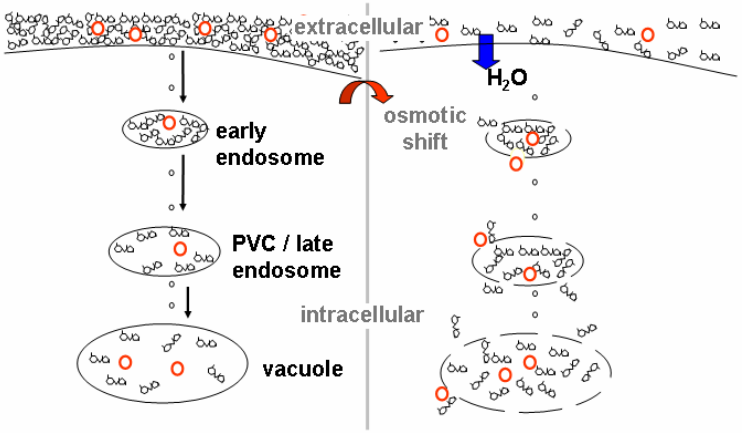

Fig. 3.1: Transfection assay. Plasmid DNA is endocytosed during 22 hours of incubation at 28°C under hyperosmotic pressure in 1 M sucrose solution (small bicircular drawings). Cells were exposed to a hypotonic shift by adding three volumes of sterile distilled water and due to the osmotic shift the plasmid DNA (red circles) will be liberated.

After this, three aliquots of 200 µl were spread on selective WMIX medium agar plates. After a three-step dilution in 250 mM sucrose solution of the samples taken prior to the centrifugation step after the incubation step at 28°C, cells of each sample were spread on non-selective YE medium agar plates in duplicate to calculate the transfection rate as transfectants per surviving cell. Transfection rates of the deletion mutants were divided by the transfection rate of the wild-type mutant, resulting in a factor.

3.6.1 Determination of pH dependency of the transfection method

In transfection experiments designed to determine the influence of the pH-value on transfection, the 1 M sucrose solution was adjusted to pH 4, pH 5, pH 7.5 and pH 9.5, respectively, with NaOH. In addition, for comparison of these samples 1 M sucrose solution was used, buffered with 100 mM Hepes to the same pH values and also adjusted with NaOH. Hepes is a zwitterionic buffering substance also used for cell culture media to keep the pH value constant (Medzon and Gedies, 1971).

3.7 Microscopy assays

3.7.1 Quinacrine mustard staining assay

Quinacrine staining was performed following a method modified from Perzov et al (2002). Cultivation of the cells followed the procedure described for yeast transfection. When the cells reached a concentration of 5 to 9 x 10^7 cells per ml, cells were harvested as described for the transfection procedure. 3 x 10^7 cells were resuspended in 90 µl YPD buffered with 100 mM Hepes to pH 7.6. To simulate transfection conditions, additional samples were washed in distilled water as described for the transfection method and resuspended in 100 µl of 1 M sucrose. Cells in sucrose were incubated for 22 hours at 28°C. After that, cells were harvested and re-suspended in 90 µl of fresh 1.1 M sucrose, buffered with 100 mM Hepes to pH 7.6. 10 µl of quinacrine stock were added to the cells, both in buffered YPD and in buffered sucrose at a final concentration of 200 µM. All steps after the dye was added were performed in the dark. After incubating cells with quinacrine for 10 minutes at 30°C, cells were harvested by centrifugation at 5000 rpm and 4°C using a Mikrorapid/K centrifuge (Hettich, Tuttlingen, D) with a Nr. 1395 rotor (Hettich, Tuttlingen, D). After that cells were handled on crushed ice further on to conserve cellular status at the time point of harvesting the cells. Cells were washed three times with 1 ml of quinacrine washing buffer using the same centrifugation conditions as for harvesting the cells.

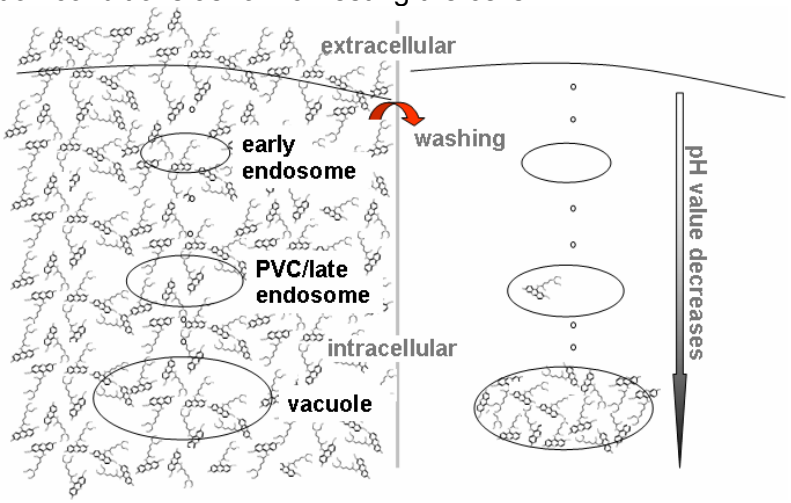

Fig. 3.2: Quinacrine staining assay. Quinacrine permeates membranes under basic pH conditions only. Cells were dyed in Hepes buffered staining solution at pH values of pH 7.6. After staining, cells were washed at pH 7.6. After accumulation in the acidic compartments, quinacrine remains there only because it does not cross membranes at acidic pH-values only.

Cells were resuspended in 50 µl washing buffer and 10 µl of cell suspension was used for fluorescence and phase-contrast imaging using poly-L-lysine HBr coated microscopic slides (Menzel, Braunschweig, D) (poly-L-lysine solution: 1 $mgml^{-1}$). Cover glasses (VWR, Darmstadt, D) were fixed using nail polish. Photos were taken with an Axioskop (Zeiss, Jena, D) using a C4000 Zoom digital camera (Olympus, Tokyo, J) with a C3040-ADU adapter (Olympus, Tokyo, J) and the Argus X1 software, version 2.2.8 (biostep, Jahnsdorf, D). Identical manual settings were used for all samples, and pictures were taken immediately after exposure to UV-light to reduce bleaching effects. Manual settings were as follows:

UV imaging:	hardware:	filter cube 09 (Zeiss, Jena, D), λ_{ex} = 450-490 nm, beam splitter: 510 nm, $\lambda_{em} \geq$ 515 nm,
	software:	white balance: Fluoreszenzlampe (fluorescence lamp), sensitivity: ISO100, zoom: 19.5 mm, aperture: 2.8, exposure time: 5,000 ms, resolution: 3,200x2,400 pixels, file format: tiff

phase contrast: hardware: conversion filter 3,200/5,500 K (Zeiss, Jena, D) (conversion artificial light to daylight), voltage (halogen lamp): 7.5 V
software: white balance: Glühlampe (light bulb), sensitivity: ISO100, zoom: 19.5 mm, aperture: 4, exposure time: 167 ms, resolution: 3,200x2,400 pixels, file format: tiff

Quinacrine fluorescence is constant over a broad pH range:

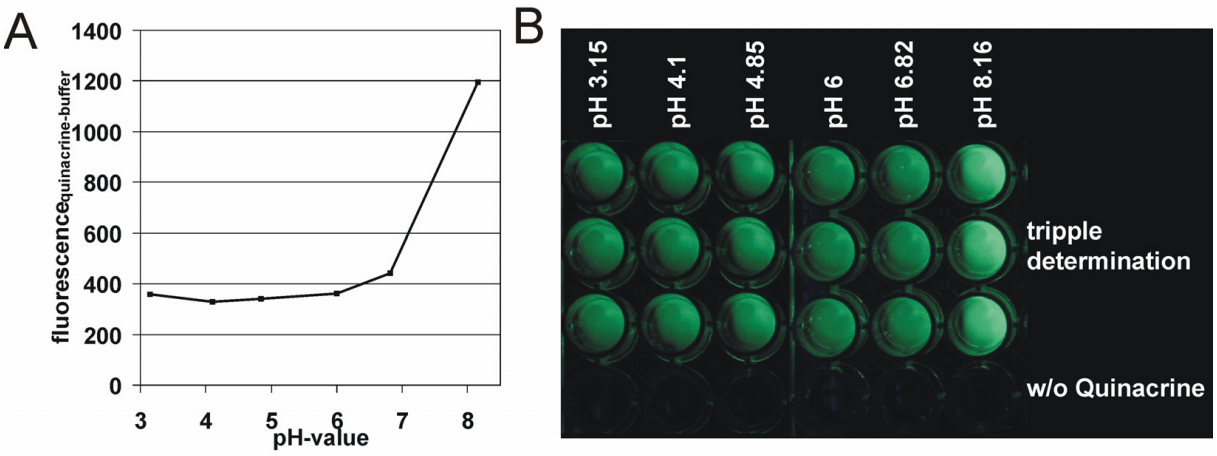

Fig. 3.3: Quinacrine fluorescence in correlation to the pH value. A: Quinacrine fluorescence was determined in 100 mM Hepes solution, using a CytoFluor 2350 fluorescence measurement system (Millipore, Schwalbach, D) with an exitation wavelength of λ_{ex} = 360 nm and an emission wavelength of λ_{em} = 530 nm. B: The same samples in a 96 well plate (Greiner Bio-One, Frickenhausen, D), visualized by orthogonal UV radiation.

3.7.2 Lucifer Yellow-CH accumulation assay

Lucifer Yellow CH (LY-CH) accumulation assay was performed as described earlier by Dulic et al (1991) with the following modifications: cells were grown, harvested and prepared for staining as described for quinacrine staining. After that, cells were resuspended in 90 µl YE medium or 1 M sucrose solution. 10 µl of a 40 $mgml^{-1}$ Lucifer Yellow stock was added immediately. All steps after the dye was added were performed in the dark. Cells were incubated for 22 hours at 28°C, followed by washing three times in 1 ml of ice cold LY-CH washing buffer as described for washing steps in the quinacrine staining assay. Finally the cells were resuspended in 50 µl LY-CH washing buffer. Visualisation and documentation followed the procedure described for quinacrine staining.

3.7.3 FM4-64 staining assay

A procedure modified from Vida and Emr (1995), was used to visualize vacuolar and endosomal membranes. Briefly, cells were grown, harvested and prepared for staining as described for quinacrine staining. After that, cells were resuspended in 90 µl YE medium or 1 M sucrose solution. 10 µl of FM4-64 stock (FM4-64 ≡ SynaptoRed C2), diluted in YE or 1 M sucrose from a 16 mM stock in DMSO, was added immediately to a final concentration of 80 µM. All steps after the dye was added were performed in the dark. Cells were incubated with the dye for 10 minutes at 30°C. Cells were harvested, resuspended in 100 µl fresh YE medium or 1 M sucrose and incubated for 22 hours at 28°C. Finally, the cells were harvested as described for the cells in the quinacrine staining assay and resuspended in 50 µl YE medium or 1 M sucrose solution. Visualisation and documentation followed the procedure described for quinacrine staining exept for the exposure time under UV imaging conditions. Exposure time under UV imaging conditions was 10,000 ms for the FM4-64 stainings.

3.7.4 Uptake assay for fluorescein labelled linear DNA

a) Preparation of the fluorescein labelled probe:
Primers 5´Fluo Probe and Fluo Probe3´ were ligated at equimolar concentrations of 200 μM by heating to 90°C for a few seconds followed by an annealing step at room temperature for 5 minutes. After that, 2.6 μl 10 x T4 ligase buffer and 1.3 μl T4 ligase (1 $U\mu l^{-1}$) were added to 22 μl of the annealed primers. The ligation took place at 19°C overnight.

b) Endocytosis assay with the linear fluorescein labelled probe:
Cells were grown, harvested, prepared for staining and stained as described for FM4-64 staining assay. The final FM4-64 concentration was 20 μM, because low fluorescence intensity was expected for the fluorescein labelled probe in correlation to FM4-64. When cells were harvested after 10 minutes incubation time during FM4-64 staining, cells were resuspended in 30 μl fluorescein labelled probe previously diluted by a factor of 10 in YE medium or in 1.1 M sucrose, respectively. This means there is a theoretical concentration of 20 μM FM4-64 and of 80 μM fluorescein molecules (20 μM fluorescein labelled probe). Cells were incubated in the dark for 22 h, harvested and visualized as described for LY-CH staining assay.

3.7.5 Uptake assay for ethidium bromide monoazide labelled plasmid

a) Preparation of the ethidium bromide monoazide labelled plasmid:
Plasmid pFL1 was used for labelling purposes. Labelling was performed as described by Tseng et al (1996) with some modifications. Briefly, due to the plasmid size of 7,769 bp there are 7769 spaces between the base paires. Assuming that one ethidium bromide monoazide (EMA) molecule intercalates in any space, EMA was added to a small molar excess in correlation to the spaces between the base pairs (1.129 EMA per internucleotide space). Thus, 37.6 nM pFL1 and 330 μM EMA were solved in TE buffer for labelling approach. This leads to 178.07 μgml^{-1} pFL1 (MW 4,734,775.6) and 138.7 μgml^{-1} EMA (MW 420.31). EMA was previously solved in an ethanol stock solution at 33 mM. 10 μl of EMA stock solution was added to 990 μl the plasmid solution in TE in a 2 ml reaction tube in the dark and EMA was allowed to intercalate for 15 minutes on crushed ice. After that, 1 ml of this solution was placed in an open 1.5 ml reaction tube on crushed ice under the halogen light source of a Leitz microscope of the type Ortholux with a 12 V / 50 W halogen light lamp (OBI, Wermelskirchen, D) in a distance of 1 cm for 30 minutes at maximum voltage of the light source. Non-bound EMA was extracted from the EMA labelled plasmid solution several times using 1 ml 1-butanole until the organic phase remained colourless. The organic and aqueous phase separation was forced by centrifugation with 100 x g for 1 minute at 4°C using a Heraeus Biofuge primo R centrifuge and a #7593 rotor. After that, 1 ml 2-propanole was added to the labelled plasmid solution to precipitate the construct with 22,000 x g for 15 minutes at 4°C. The pellet was washed using 70% ethanol and was recentrifuged with 22,000 x g for 10 minutes at 4°C. The pellet was resolved in 100 μl sterile distilled water.

b) Endocytosis assay with the ethidium bromide monoazide labelled plasmid:
Cells were grown, harvested, prepared for staining as described for the LY-CH staining assay. After that, cells were resuspended in 30 μl EMA labelled plasmid probe previously diluted by a factor of 5 in YE medium or in 1.25 M sucrose, respectively. This means that there is a theoretical concentration of 75.2 nM pFL1 (356.14 μgml^{-1}) and of 660 μM EMA molecules. After that, cells were incubated in the dark for 22 h, harvested and visualized as described for LY-CH staining assay.

4 Results

4.1 The influence of endocytic pathway mutations on transfection

To find bottle necks of endocytosis mediated non-viral transfection in mammalians, defined deletion stains of the well known endocytosis model organism *Saccharomyces cerevisiae* were used (Shaw et al, 2001). The first parameter analysed for all tested deletion mutants was the transfection efficiency determined by a modified method of Neukamm et al (2002). Transfection was assayed using 15 $\mu g ml^{-1}$ of the 2-μm plasmid, pFL1 selecting for *URA3* prototroph cells; transfection efficiency was calculated in relation to the mutant BY4741 (wild-type mutant).
Three different staining assays were applied (Fig. 4.1) in order to understand what takes place in endocytosis in the cells deleted for specific genes in correlation to the wild-type stain under standard conditions (in YE medium) and transfection conditions (in 1 M sucrose). (I) Intraendosomal/vacuolar pH-conditions were determined by

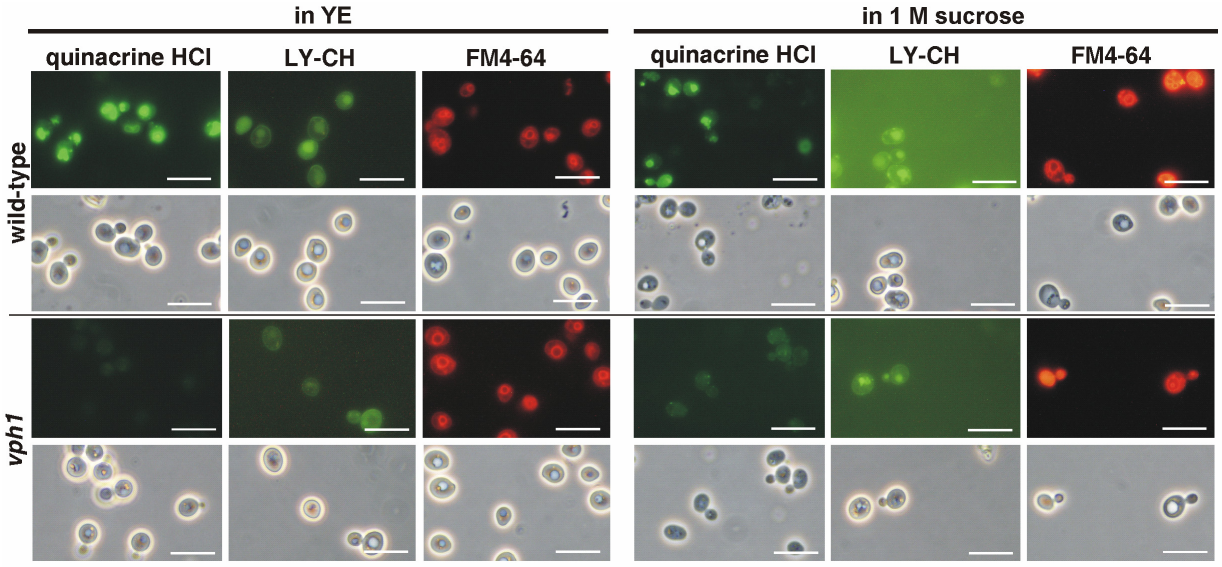

Fig. 4.1: Common phenotypes and differences in acidification and intracellular transport in YE and 1 M sucrose. Vacuolar acidification after 22 hours was visualized using quinacrine-HCl staining. Quinacrine HCl accumulates in acidic compartments. Lucifer Yellow CH and FM4-64 were used to study endocytic uptake and membrane dynamics after 22 hours. Pictures of representative cells from one of at least two independent experiments were taken with FITC-fluorescence optics (quinacrine and LY-CH) or rhodamine optics (FM4-64) (upper panels), and with phase-contrast optics (lower panels) as described in “Materials and Methods”. The bar represents 10 μm.

quinacrine staining using a modified method of Perzov et al (2002). (II) Lucifer Yellow (LY-CH) (Dulic et al, 1991; altered) accumulation and (III) membrane dynamics (FM4-

64) (Vida and Emr, 1995; altered) were also analyzed, demonstrating differences in accumulation of the dyes in deletion mutants in correlation to the wild type. Cells were analysed after 22 hours of incubation with the endocytic marker dyes LY-CH and FM4-64. Cells were incubated in quinacrine HCl staining assay for 22 hours prior to staining to determine intraendosomal/vacuolar pH-conditions. In cells stained in 1 M sucrose, more compartments near the plasma membrane are stained than in cells in YE (Fig. 4.1), but differences of the mutant in comparison to the wild-type mutant are highly comparable in both solutions. In quinacrine staining in both solutions, the accumulation of quinacrine in intracellular compartments of mutant *vph1* is reduced in comparison to the wild type. LY-CH accumulation in the mutant *vph1* is weaker than in wild-type endosomes and the vacuole in both solutions. In FM4-64 staining experiments, it may be that diffuse staining near the vacuole is weakly higher in the *vph1* mutant in both solutions, but this difference between the wild type and the mutant is not very significant. YE based stainings only are shown further on, due to the comparability of results obtained in both solutions for interpretation of the mutant phenotype in any tested mutant.

4.1.1 The early endocytic pathway

Mutants *rcy1*, *yil064w* and *rav1* were tested as mutants defect in the early endocytic pathway. Wild-type acidification of the vacuole was observed in the mutant deleted for the F-box protein Rcy1p, involved in early endocytosis (Wiederkehr et al, 2000). The mutant accumulates LY-CH in small compartments near the plasma membrane, predominantly near sites of polarized growth (Fig. 4.2 C). The vacuolar accumulation of LY-CH is reduced in comparison to the wild type. The *rcy1* mutant in transfection experiments (Fig. 4.2 A) exhibits reduced transfection efficiency in comparison to the wild type. Reduced vacuolar accumulation of LY-CH in mutant *rcy1* was described previously for a shorter incubation time (Wiederkehr et al, 2000). This phenotype is indicated to be stable to experimental conditions.

In mutant *yil064w* previously described to be defect for a putative methyltransferase (Katz et al, 2003), the transfection efficiency was reduced as in *rcy1* mutant (Fig. 4.2 A). In addition, acidification, LY-CH accumulation and membrane dynamics turned out to be comparable to mutant *rcy1* (Fig. 4.2 C). In some cells, accumulation of LY-CH in compartments near the vacuole was observed and in all cells LY-CH accumulation to the vacuole was weaker than in *rcy1* cells. All these observations for

yil064w in correlation to *rcy1* could be made exclusively in the case when the cells of *yil064w* were in very late logarithmic phase when harvested from the main culture for transfection and staining experiments.

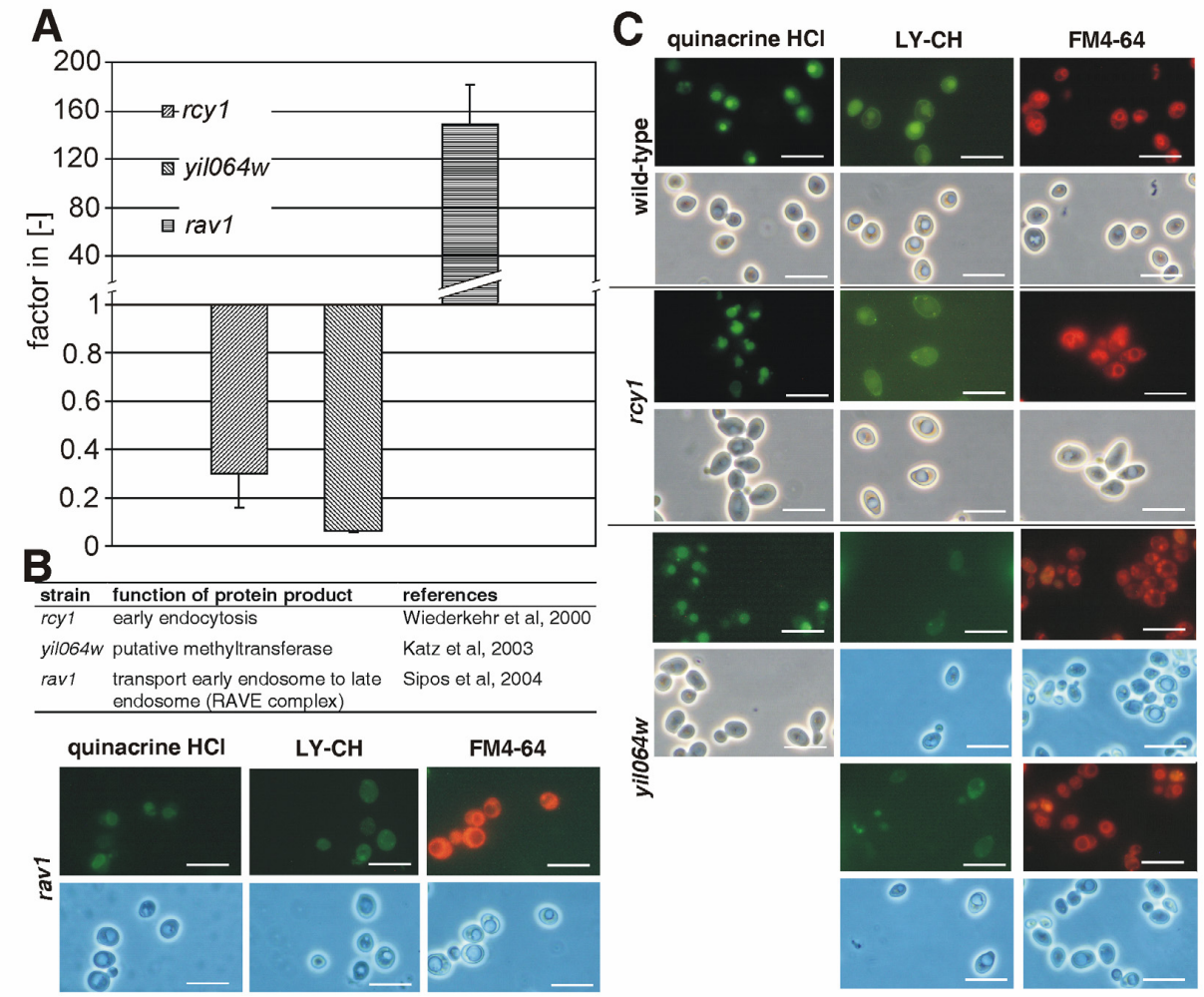

Fig. 4.2: Mutants defective for early endocytosis. (A) Transfection efficiency of mutants deleted for genes coding proteins important in the early endocytic pathway. Transfection was performed as described in “Materials and Methods”. All values are given as a factor in relation to the transfection rate of the wild-type mutant (BY4741). The mean values (± s.d.) of the factors were calculated from at least three independent experiments. (B) Description of the deletion mutants used. (C) Impact of specific gene deletions of the early endocytic pathway on vacuolar acidification, Lucifer Yellow (LY-CH) accumulation and membrane dynamics in BY4741 background in YE. Vacuolar acidification after 22 hours was visualized using quinacrine-HCl staining. Quinacrine HCl accumulates in acidic compartments. Lucifer Yellow CH and FM4-64 were used to study endocytic uptake and plasma membrane dynamics after 22 hours. Photos of representative cells from one of at least two independent experiments were taken with FITC-fluorescence optics (quinacrine and LY-CH) or rhodamine optics (FM4-64) (upper panels), and with phase-contrast optics (lower panels) as described in “Materials and Methods”. The bar represents 10 μm.

These results turned out to be highly reproducible in three independent experiments. Wild-type transfection efficiencies were observed for *yil064w* cells in earlier growth phases.

In single experiments with mutants defect for steps in actin metabolism, indicated that these defects negatively influence transfection efficiency (data not shown). Mutant *aip1* was tested as an actin cortical patch component involved in actin depolymerization. Additionally, a transfection experiment was performed with the *twf1* mutant. Twf1p is an actin monomer sequestering protein found at sites of actin filament assembly. In mutants defect for proteins which only localize to actin patches during hyperosmotic stress, as in the case of Inp52p or Inp53p, transfection efficiency either remains as observed for the wild type or is weakly reduced. Inp51p or Inp52p are also known to be involved in endocytosis. Please note that these results are based on a single experiment each.

In mutant *rav1*, in contrast to mutants *rcy1* and *yil064w*, transfection efficiency was significantly enhanced by a factor of approximately 150 (Fig. 4.2 A). Rav1p is part of the RAVE complex (Smardon et al, 2002, Seol et al, 2001) and known to be involved in the transport between the early endosome and the MVB (multivesicular body)/late endosome. In *rav1* cells, a significant reduction in vacuolar acidification and LY-CH accumulation was observed (Fig. 4.2 C). LY-CH accumulates predominantly in compartments also near the plasma membrane in *rav1* mutant and a diffuse background staining could be observed in LY-CH and FM4-64 stainings possibly representing vesicle like structures in the cytoplasm.

4.1.2 Import into the late endosome via the early endosome

Vps21p is involved the fusion process of early endosome derived vesicles to the MVB/late endosome. *VPS21* encodes for the yeast homolog of the human Rab5b protein, a GTPase involved in a step of endocytosis after Rcy1p (Gerrard et al, 2000[b]; Singer-Krüger et al, 1995). *VPS45* encodes for a Sec1/Munc-18 protein homologous to the human Vps45a protein (Cowles et al, 1994; Tellam et al,1997) and acts in the same protein complex as Vps21p in protein sorting from the trans Golgi network (TGN) to the prevacuolar compartment (PVC)/MVB/late endosome (Burd et al, 1997; Tall et al, 1999). Transfection efficiencies in the mutants deleted for *VPS21* and *VPS45*, are enhanced by a factor of approximately 10 (Fig. 4.3 A). Neukamm et al (2002) previously described this effect on transfection in a different mutant background for *VPS21* deletion. Mutant *vps8* deleted for a protein interacting with Vps21p (Horazdovsky et al, 1996) presents a transfection efficiency enhanced by a factor of approximately 10 in a single experiment (data not shown). Vacuoles are

not acidified in mutants *vps21* and *vps45*, whereas some small acidic compartments are visible near the vacuole (Fig. 4.3 C). LY-CH accumulates in small non-vacuolar compartments also near the plasma membrane; these are present in higher numbers than in the wild type. Stronger membrane accumulation was observed with FM4-64 staining in *vps21* and *vps45* cells in comparison to the wild type as seen in mutant *rav1* also. Such vesicle accumulations have been described earlier (Cowles et al, 1994; Gerrard et al, 2000).

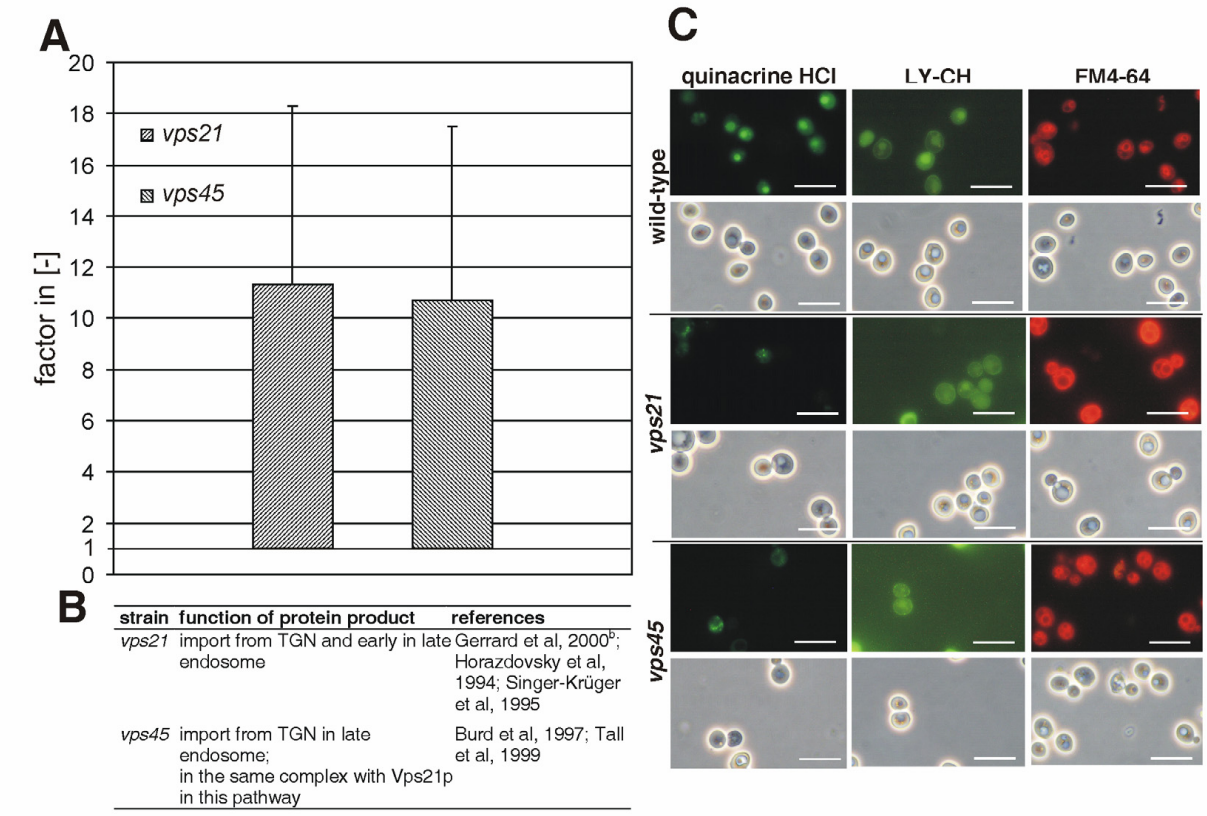

strain	function of protein product	references
vps21	import from TGN and early in late endosome	Gerrard et al, 2000[b]; Horazdovsky et al, 1994; Singer-Krüger et al, 1995
vps45	import from TGN in late endosome; in the same complex with Vps21p in this pathway	Burd et al, 1997; Tall et al, 1999

Fig. 4.3: Mutants defective for import into the MVB/late endosome. (A) Transfection efficiency of mutants deleted for genes coding for proteins important in import into the MVB/late endosome. Transfection was performed as described in “Materials and Methods”. All values are given as a factor in relation to the transfection rate of the wild-type mutant (BY4741). The mean values (± s.d.) of the factors were calculated from at least three independent experiments. (B) Description of the deletion mutants used. (C) Impact of specific gene deletions involved in import into the MVB/late endosome on vacuolar acidification, Lucifer Yellow (LY-CH) accumulation and membrane dynamics in BY4741 background in YE. Vacuolar acidification after 22 hours was visualized using quinacrine-HCl staining. Quinacrine HCl accumulates in acidic compartments. Lucifer Yellow CH and FM4-64 were used to study endocytic uptake and plasma membrane dynamics after 22 hours. Photos of representative cells from one of at least two independent experiments were taken with FITC-fluorescence optics (quinacrine and LY-CH) or rhodamine optics (FM4-64) (upper panels), and with phase-contrast optics (lower panels) as described in “Materials and Methods”. The bar represents 10 μm.

4.1.3 The vps class E phenotype

Mutants presenting a class E vps defect which results in an enlarged late endosome, such as in *vps27* and *vps4*, do not exhibit a transfection behaviour different to the wild type (Fig. 4.4 A). Class E mutants *stp22* and *vps36* were tested in single experiments, also with comparable results (data not shown). Reduced vacuolar acidification and large acidified structures near the vacuolar membrane are observed in class E deletion mutants *vps27* and *vps4* (Fig. 4.4 C). These mutants are deleted for proteins which are involved in export steps from late endosomes (Finken-Eigen et al, 1997; Piper et al, 1995) and are part of the ESCRT complex (Bilodeau et al, 2003;

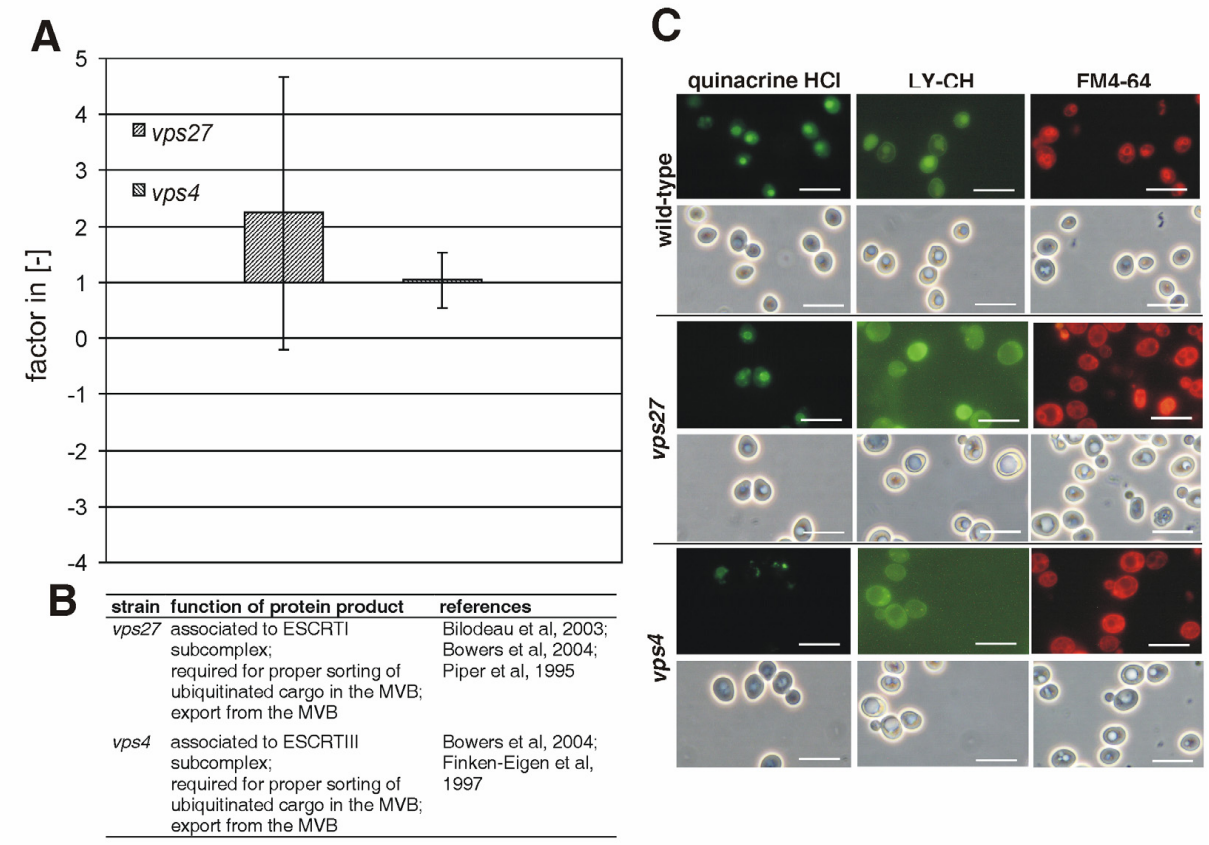

B

strain	function of protein product	references
vps27	associated to ESCRTI subcomplex; required for proper sorting of ubiquitinated cargo in the MVB; export from the MVB	Bilodeau et al, 2003; Bowers et al, 2004; Piper et al, 1995
vps4	associated to ESCRTIII subcomplex; required for proper sorting of ubiquitinated cargo in the MVB; export from the MVB	Bowers et al, 2004; Finken-Eigen et al, 1997

Fig. 4.4: The vps class E phenotype. (A) Transfection efficiency of vps class E deletion mutants. Transfection was performed as described in “Materials and Methods”. All values are given as a factor in relation to the transfection rate of the wild-type mutant (BY4741). The mean values (± s.d.) of the factors were calculated from at least three independent experiments. (B) Description of the deletion mutants used. (C) Impact of specific gene deletions involved in export from the late endosome on vacuolar acidification, Lucifer Yellow (LY-CH) accumulation and membrane dynamics in BY4741 background in YE. Vacuolar acidification after 22 hours was visualized using quinacrine-HCl staining. Quinacrine HCl accumulates in acidic compartments. Lucifer Yellow CH and FM4-64 were used to study endocytic uptake and plasma membrane dynamics after 22 hours. Photos of representative cells from one of at least two independent experiments were taken with FITC-fluorescence optics (quinacrine and LY-CH) or rhodamine optics (FM4-64) (upper panels), and with phase-contrast optics (lower panels) as described in “Materials and Methods”. The bar represents 10 μm.

Bowers et al, 2004). Vps27p is a homolog of the human Hgs, and *VPS4* encodes an AAA-type ATPase homologous to human Vps4a. No accumulation of LY-CH and FM4-64 is observed in the vacuole, indicating a very strong transport inhibition between the class E compartment and the vacuole. Large compartments near the vacuole are visualized using LY-CH or FM4-64, presumably representing class E compartments (Babst et al, 1997; Bowers et al, 2004; Piper et al, 1995).

4.1.4 Import into the vacuole

The HOPS complex (Seals et al, 2000; Ungermann et al, 2000) and the vps class C complex (Peterson et al, 2001; Rieder and Emr, 1997) are responsible for the fusion step of MVB/late endosome derived membranes to the vacuole. Mutant transfection efficiency in the *vam6* mutant deleted for a protein, which is part of the HOPS complex, is enhanced by a factor of approximately 15 (Fig. 4.5 A). Vam6p is involved in vacuolar fusion and fusion of late endosomes to vacuolar membranes (Nakamura et al, 1997; Wada et al, 1992) and it harbours acidified fragments spread all over the cell (Fig. 4.5 C). Some non-near plasma membrane fragments in the cells accumulate LY-CH and FM4-64 more strongly than other fragments. The phenotype of cells harbouring a fragmented vacuole was earlier named vps class B phenotype (Banta et al, 1988; Raymond et al, 1992).

In mutant *vps33,* the transfection efficiency is as in the wild type (Fig. 4.5 A). Mutant *vps33* presents a vps class C phenotype (Peterson et al, 2001; Seals et al, 2000) which means that *vps33* cells do not have any vacuole. Staining experiments in *vps33* mutant deleted for a protein of the vps class C complex, result in diffuse background staining of the cytoplasm in all three methods used (Fig. 4.5 C). This background staining might represent membrane structures that are not able to fuse to a vacuole. Vps33p is involved in transport from the TGN to MVB/late endosomes also (Subramanian et al, 2004; Peterson and Emr, 2001).

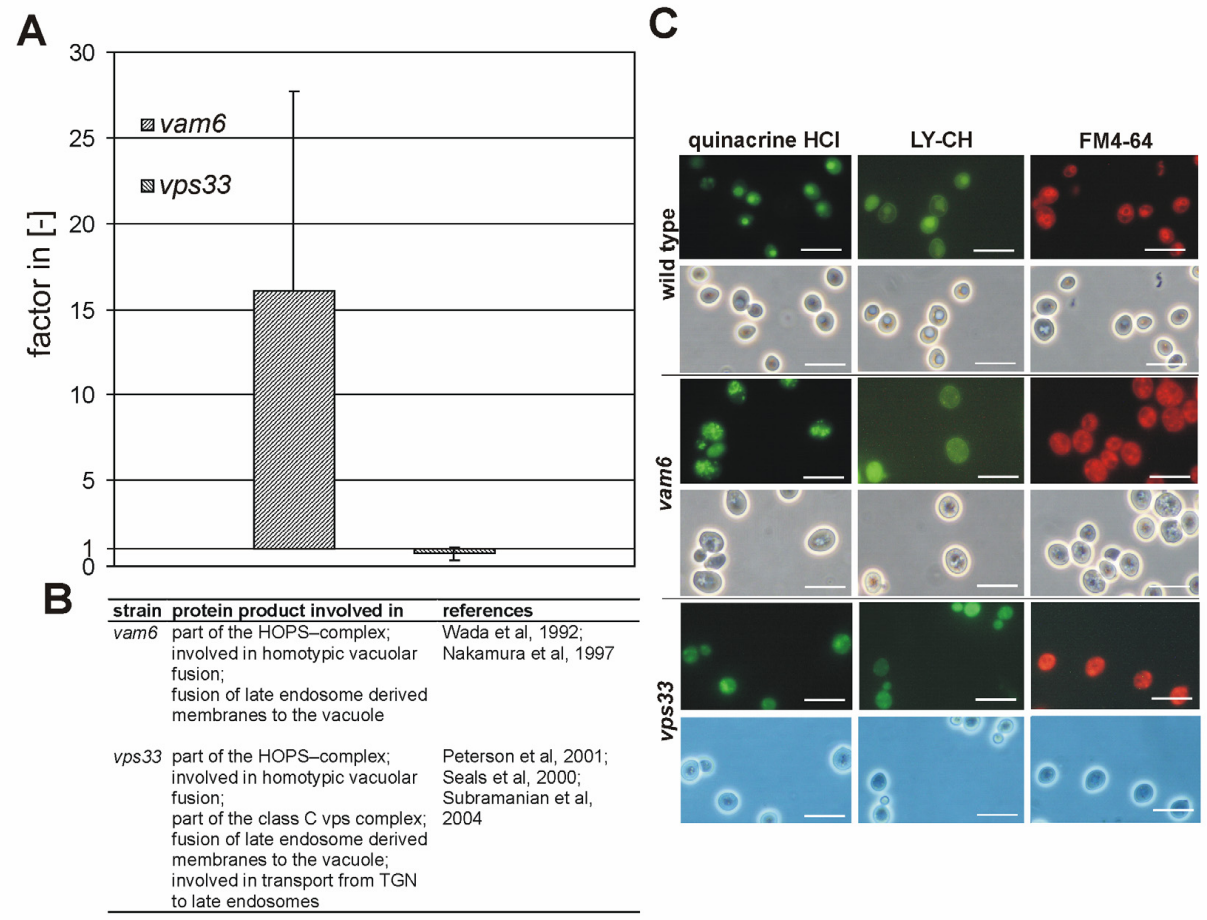

B

strain	protein product involved in	references
vam6	part of the HOPS–complex; involved in homotypic vacuolar fusion; fusion of late endosome derived membranes to the vacuole	Wada et al, 1992; Nakamura et al, 1997
vps33	part of the HOPS–complex; involved in homotypic vacuolar fusion; part of the class C vps complex; fusion of late endosome derived membranes to the vacuole; involved in transport from TGN to late endosomes	Peterson et al, 2001; Seals et al, 2000; Subramanian et al, 2004

Fig. 4.5: Mutants defective for import into the vacuole and homotypic vacuolar fusion. (A) Transfection efficiency of deletion mutants involved in import into the vacuole and homotypic vacuolar fusion. Transfection was performed as described in “Materials and Methods”. All values are given as a factor in relation to the transfection rate of the wild-type mutant (BY4741). The mean values (± s.d.) of the factors were calculated from at least three independent experiments. Despite the high error bars for *vam6* mutant, the effect could be seen in any single experiment, and the high error seems to be due to inhomogeneous distribution of endocytosed material and vacoular ATPase in fragmented membrane structures. (B) Description of the deletion mutants used. (C) Impact of specific gene deletions involved in import into the vacuole and homotypic vacuolar fusion on vacuolar acidification, Lucifer Yellow (LY-CH) accumulation and membrane dynamics in BY4741 background in YE. Vacuolar acidification after 22 hours was visualized using quinacrine-HCl staining. Quinacrine HCl accumulates in acidic compartments. Lucifer Yellow CH and FM4-64 were used to study endocytic uptake and plasma membrane dynamics after 22 hours. Photos of representative cells from one of at least two independent experiments were taken with FITC-fluorescence optics (quinacrine and LY-CH) or rhodamine optics (FM4-64) (upper panels), and with phase-contrast optics (lower panels) as described in “Materials and Methods”. The bar represents 10 μm.

4.1.5 Visualization of endocytic DNA accumulation for specific endocytosis defect mutants

To verify data collected from LY-CH and FM4-64 stainings in relation to the effect on transfection efficiency on a more direct way, experiments with fluorescence labelled DNA constructs were performed. YE was used as a medium in a first experiment with a fluorescein labelled linear DNA construct (Fig. 4.6) for an endocytic uptake assay.

No significant differences could be observed between wild type and mutants in YE. This could be due to the high pH-value in YE, which circumvents appropriate proximity of the negatively charged DNA to the also negatively charged plasma membrane. The observation that only very low amount of DNA was taken up under these conditions matched the result that transfection under these conditions does not work either.

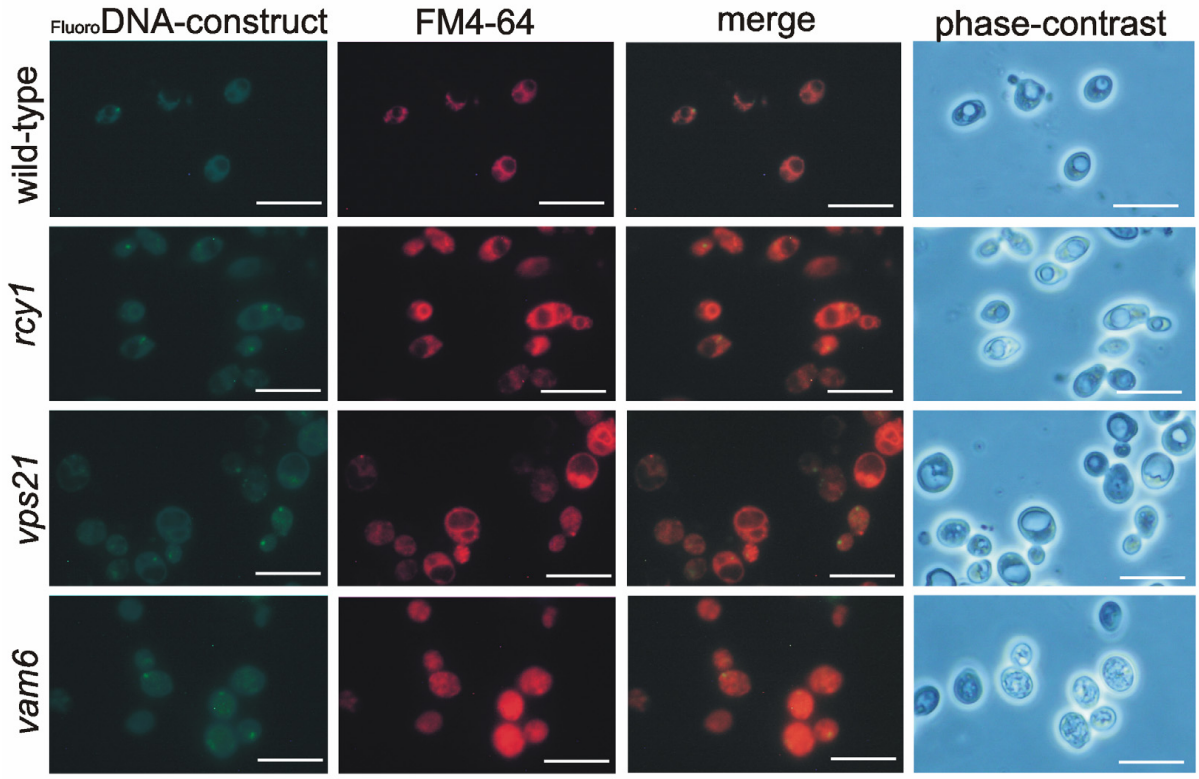

Fig. 4.6: Endocytosis of fluorescein labelled linear DNA in different deletion mutants in YE. The relatively high pH value during incubation in comparison to transfection conditions seems to be inappropriate for uptake of nucleic acid constructs. Fluorescein labelled linear DNA construct is visualized in the first column with FITC-fluorescence optics. Parallel FM4-64 staining is shown in the second column using rhodamine optics as described in “Materials and Methods”. Pictures in the third column are merged and represent both, accumulation of the fluorescein labelled DNA construct and membrane dynamics. Phase-contrast pictures can be seen in the fourth column. The bar represents 10 μm.

The experiment was repeated in 1 M sucrose instead of YE to test endocytic uptake of fluorescein labelled DNA construct as in transfection experiments (Fig. 4.7). Under these conditions significant differences were observed. Fluorescein labelled linear DNA accumulated predominantly in non vacuolar compartments near the vacuole in the wild-type mutant. Vacuolar accumulation was weak, but a stronger vacuolar accumulation of the construct can not be excluded, as fluorescein fluorescence intensity is reduced at low pH values. As a result, these data represent preliminary

information that should be confirmed and extended using another fluorescence label in additional experiments.

However, what still could be seen with the fluorescein labelled linear DNA was that in the *rcy1* mutant the construct accumulates predominantly in distinct compartments near the plasma membrane in contrast to the wild type, as also previously seen for LY-CH accumulation. In *vps21* mutant as seen for LY-CH staining, the fluorescein labelled DNA accumulates in compartments also near the vacuole with a stronger signal than in the wild type. Fluorescein labelled DNA accumulates in distinct compartments all over the cell in mutant *vam6*. In this mutant, the fluorescence signal per cell is much stronger than in the wild type or in both other mutants tested. In comparison to quinacrine data from previous experiments, a weaker acidification of all these compartments is unlikely, so that a stronger endocytic uptake is probable in this mutant. In some compartments, the correlation between fluorescein signal and

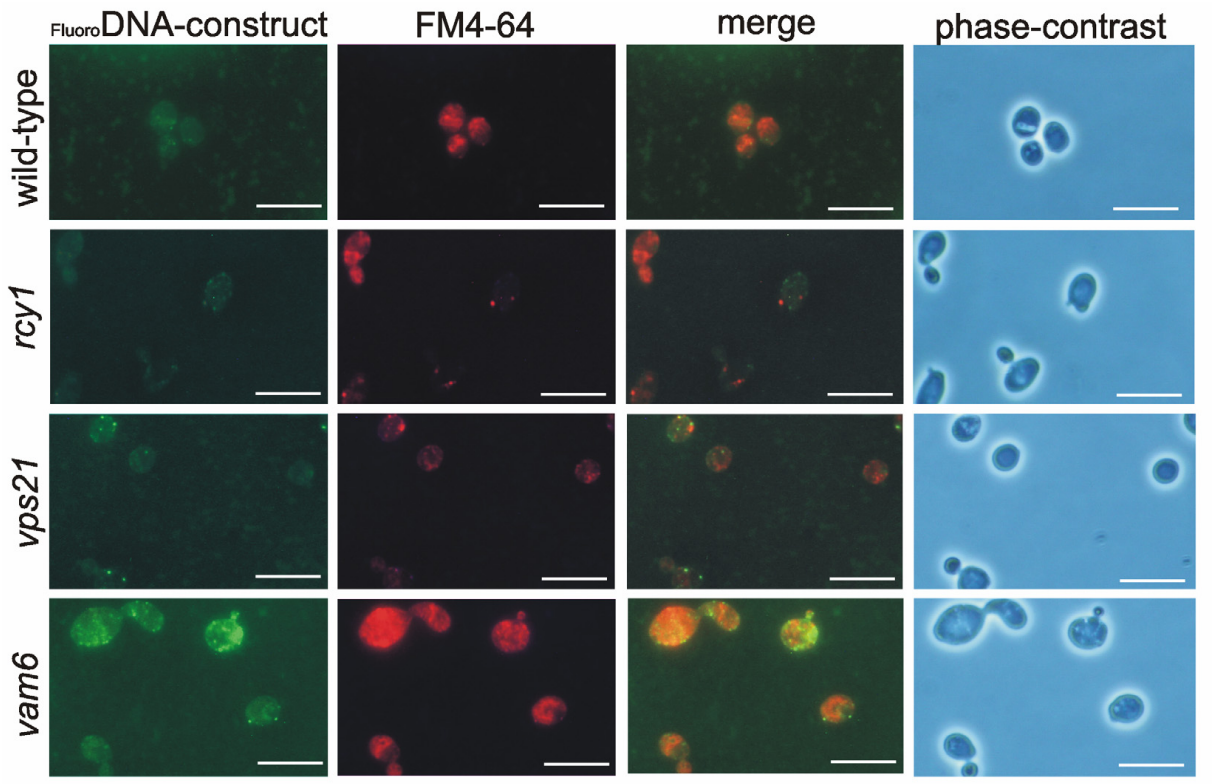

Fig. 4.7: Endocytosis of fluorescein labelled linear DNA in different deletion mutants in 1 M sucrose. As for LY-CH stainings, for accumulation of endocytosed fluorescein labelled DNA construct in 1 M sucrose accumulation in plasma membrane near compartments could also be observed. Fluorescein labelled linear DNA construct is visualized with FITC-fluorescence optics in the first column. Parallel FM4-64 staining is shown in the second column using rhodamine optics as described in “Materials and Methods”. Pictures in the third column are merged and represent both accumulation of the fluorescein labelled DNA construct and membrane dynamics. Phase-contrast pictures can be seen in the fourth column. The bar represents 10 μm.

FM4-64 signal is different to other compartments, so that it seems likely that there are different conditions in different compartments as regards pH-value and/or degradation potential as regards the DNA which was taken up.

Finally, ethidium bromide monoazide (EMA) labelled plasmid DNA (pFL1) was tested in an endocytic uptake assay in YE and 1 M sucrose (Fig. 4.8). EMA labelled pFL1 was taken up into distinct non-vacuolar compartments in the wild type and mutant strains in YE but not in 1 M sucrose. Nearly no labelled DNA was taken up in 1 M sucrose under transfection conditions. The different mutants tested in YE could be distinguished from the wild-type mutant. In *rcy1* mutant, EMA labelled pFL1 accumulates in compartments at sites of polarized growth. In *vps21* mutant there are compartments stained near the vacuole, predominantly. Accumulation of the construct in compartments which are spread all over the cell could be observed in *vam6* mutant. No distinct compartments harbouring EMA labelled plasmid DNA could

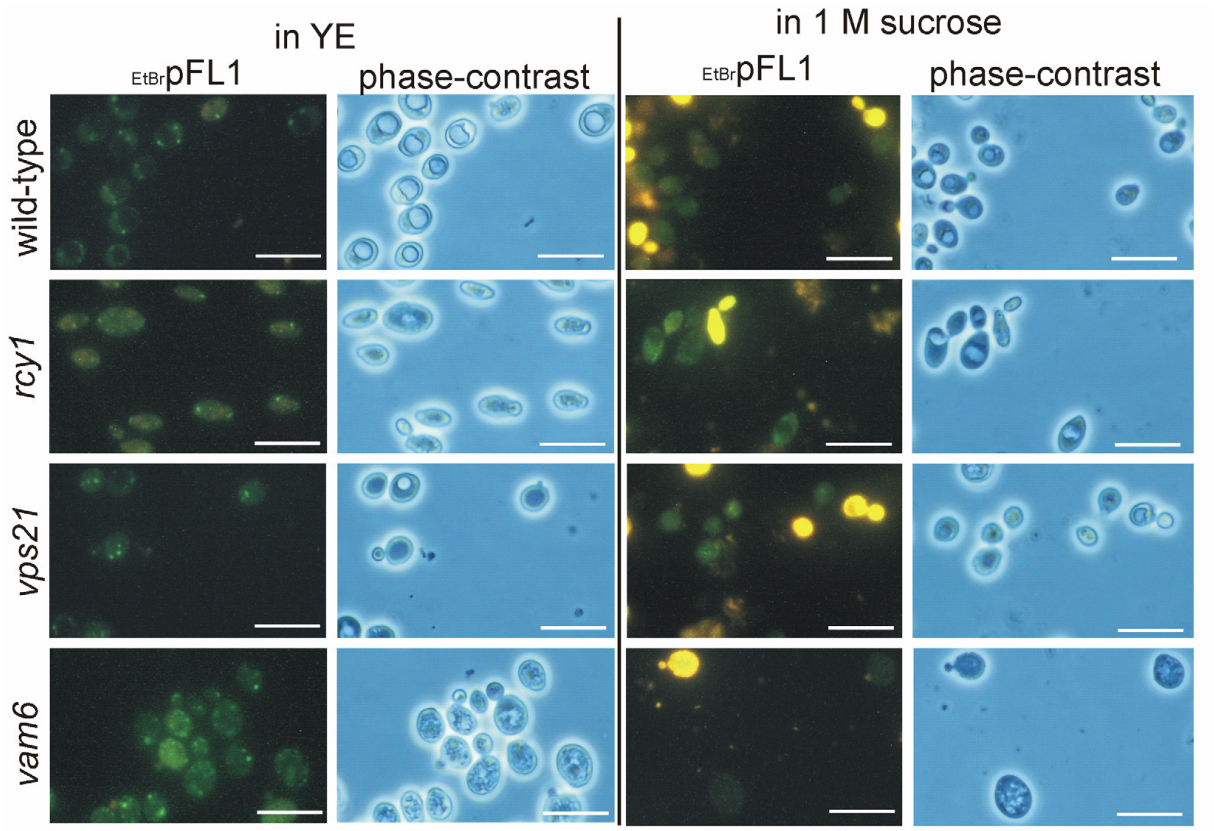

Fig. 4.8: Endocytosis of ethidium bromide monoazide (EMA) labelled plasmid DNA (pFL1) in different deletion mutants in YE and 1 M sucrose. As for LY-CH stainings, for accumulation of endocytosed EMA labelled plasmid DNA in YE accumulation in distinct compartments could also be observed, but the labelled plasmid DNA could not be determined in the vacuole in contrast to LY-CH. In *rcy1* mutant the labelled plasmid DNA could be observed in compartments near the plasma membrane at sites of polar growth. EMA labelled plasmid DNA is visualized with FITC-fluorescence optics in the first and third column. Phase-contrast pictures can be seen in the second and fourth column. The bar represents 10 μm.

be visualized in 1 M sucrose in all mutants. These results for the staining experiments in YE and 1 M sucrose might be due to the strongly altered surface charge of the EMA labelled plasmid DNA molecule in comparison to the fluorescein labelled linear DNA construct. However, the method seems to be inappropriate to visualize endoyctic DNA uptake on a realistic way due to strong alteration of the molecular charge by ligation of too many EMA molecules to the plasmid DNA. The method might be usable after titrating molarities between DNA and EMA.

4.2 The influence of transport pathways between the Golgi and the endocytic/vacuolar system on transfection

Many proteins known to be involved in endocytic transport (Bryant and Stevens, 1998) and endocytic/vacuolar processing and degradation (Klionsky et al, 1990) are also known to be sorted via the secretory pathway to the endosomes and the vacuole. Due to this, it seems likely that deleting genes affecting transport between the TGN and the endosomal/vacuolar system also affect transfection efficiency.

4.2.1 Transport between the *trans* Golgi network and the early endosome

The first connection between the TGN and the endosomal/vacuolar system is the transport pathway between the TGN and the early endosome. Genes *YPT6* and *TLG2* are involved in retrograde transport from the endosomes to the TGN (Siniossoglou and Pelham, 2001; Lewis et al, 2000). Mutant *ypt6* is affected in transport from the endosomes to the Golgi and in *intra*-Golgi transport (Siniossoglou and Pelham, 2001; Luo and Gallwitz, 2003), whereas *tlg2* mutant is defect in transport from early endosomes to the TGN only (Lewis et al, 2000). In both mutants, a transfection efficiency was observed which is enhanced only weak in comparison to the wild type (Fig. 4.9 A). Further on, defects in LY-CH accumulation were observed in some cells, but LY-CH accumulated in near plasma membrane compartments only in these cells (Fig. 4.9 C), comparible to an early endocytic defect.

Mutant *vps1* is defect for budding vesicles from the TGN, as a dynamine homolog, and is also defect for correct actin cytoskeleton organization and peroxisome biogenesis (Ekena et al, 1993; Nothwehr et al, 1995, Nothwehr et al, 1996, Yu and Cai, 2004). The transfection efficiency in the *vps1* mutant was enhanced more strongly than in mutants *ypt6* and *tgl2*, by a factor of approximately 2.6 (Fig. 4.9 A).

Acidification and LY-CH accumulation was reduced in larger structures but a weak backround staining was observed, probably representing vesicles (Fig. 4.9 C). This indicates that inhibiting transport of endosomal/vacuolar derived proteins affect endocytic functions, and this also results in a partial effect on transfection efficiency in addition to possible defects in degradation.

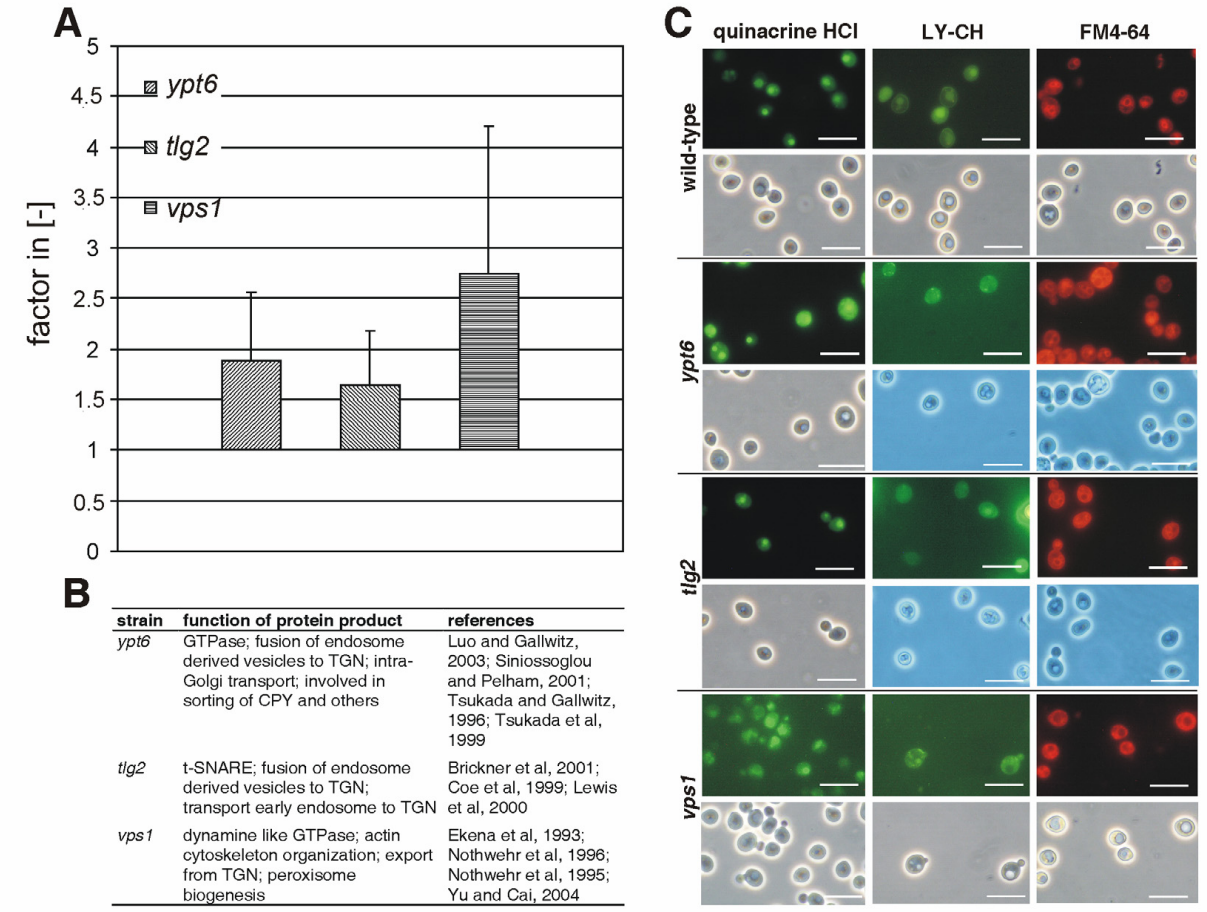

B

strain	function of protein product	references
ypt6	GTPase; fusion of endosome derived vesicles to TGN; intra-Golgi transport; involved in sorting of CPY and others	Luo and Gallwitz, 2003; Siniossoglou and Pelham, 2001; Tsukada and Gallwitz, 1996; Tsukada et al, 1999
tlg2	t-SNARE; fusion of endosome derived vesicles to TGN; transport early endosome to TGN	Brickner et al, 2001; Coe et al, 1999; Lewis et al, 2000
vps1	dynamine like GTPase; actin cytoskeleton organization; export from TGN; peroxisome biogenesis	Ekena et al, 1993; Nothwehr et al, 1996; Nothwehr et al, 1995; Yu and Cai, 2004

Fig. 4.9: Mutants defective for transport between the TGN and the early endosome. (A) Transfection efficiency of mutants deleted for genes coding for proteins important in transport between the TGN and the early endosome. Transfection was performed as described in “Materials and Methods”. All values are given as a factor in relation to the transfection rate of the wild-type mutant (BY4741). The mean values (± s.d.) of the factors were calculated from at least three independent experiments. (B) Description of the deletion mutants used. (C) Impact of specific gene deletions involved in early endosome–TGN sorting on vacuolar acidification, Lucifer Yellow (LY-CH) accumulation and membrane dynamics in BY4741 background in YE. Vacuolar acidification after 22 hours was visualized using quinacrine-HCl staining. Quinacrine HCl accumulates in acidic compartments. Lucifer Yellow CH and FM4-64 were used to study endocytic uptake and plasma membrane dynamics after 22 hours. Photos of representative cells from one of at least two independent experiments were taken with FITC-fluorescence optics (quinacrine and LY-CH) or rhodamine optics (FM4-64) (upper panels), and with phase-contrast optics (lower panels) as described in “Materials and Methods”. The bar represents 10 μm.

4.2.2 Transport between the *trans* Golgi network and the late endosome

The absence of Vps13p involved in transport from endosomes to the TGN does not significantly affect transfection efficiency (Fig. 4.10 A). A slight positive effect on transfection efficiency was observed in a mutant deleted for the gene encoding for the retromer complex protein Vps17p (Horazdovsky et al, 1997; Köhrer and Emr, 1993). Transfection efficiency in the *vps17* mutant is enhanced by a factor of approximately 2 (Fig. 4.10 A). Effects on acidification, LY-CH accumulation or membrane dynamics are negligible in both mutants (Fig. 4.10 C).

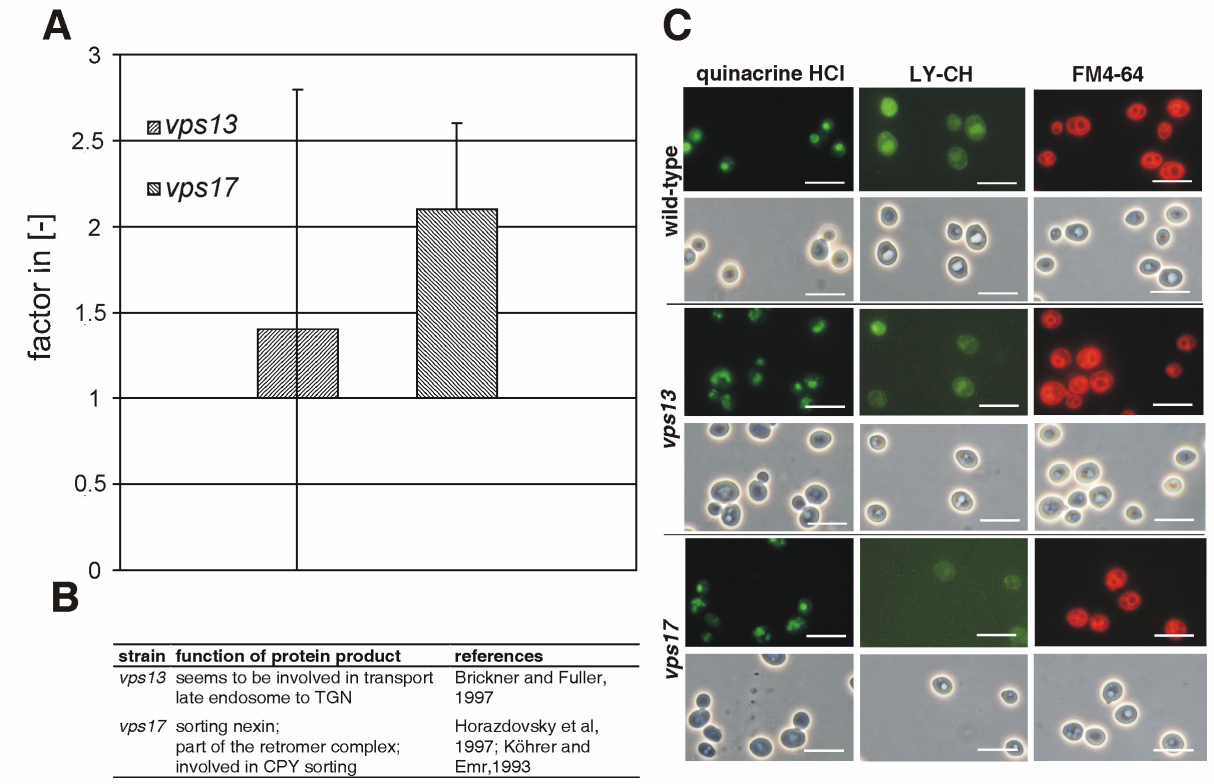

strain	function of protein product	references
vps13	seems to be involved in transport late endosome to TGN	Brickner and Fuller, 1997
vps17	sorting nexin; part of the retromer complex; involved in CPY sorting	Horazdovsky et al, 1997; Köhrer and Emr,1993

Fig. 4.10: Mutants defective for transport between the TGN and the MVB/late endosome. (A) Transfection efficiency of mutants deleted for genes coding for proteins important in transport between the TGN and the MVB/late endosome. Transfection was performed as described in “Materials and Methods”. All values are given as a factor in relation to the transfection rate of the wild-type mutant (BY4741). The mean values (± s.d.) of the factors were calculated from at least three independent experiments. (B) Description of the deletion mutants used. (C) Impact of specific gene deletions involved in MVB/late endosome–TGN sorting on vacuolar acidification, Lucifer Yellow (LY-CH) accumulation and membrane dynamics in BY4741 background in YE. Vacuolar acidification after 22 hours was visualized using quinacrine-HCl staining. Quinacrine HCl accumulates in acidic compartments. Lucifer Yellow CH and FM4-64 were used to study endocytic uptake and plasma membrane dynamics after 22 hours. Photos of representative cells from one of at least two independent experiments were taken with FITC-fluorescence optics (quinacrine and LY-CH) or rhodamine optics (FM4-64) (upper panels), and with phase-contrast optics (lower panels) as described in “Materials and Methods”. The bar represents 10 μm.

4.2.3 Transport between the *trans* Golgi network and the vacuole

A strong effect on transfection efficiency in mutants defect for a transport step beween TGN and the endosomal/vacuolar system was observed by interrupting the ALP sorting pathway which bypasses the late endosome and sorts cargo directly from the TGN to the vacuole. Deletion of *APL5*, coding for a protein homologous to the human Ap3d1 results in a 16 fold enhancement of transfection efficiency (Fig. 4.11 A). No significant differences in the mutant *apl5* in comparison with the wild type were detected in quinacrine, LY-CH and FM4-64 stainings, indicating that the effect on transfection efficiency might be due to transport defects of processing and degrading enzymes via the ALP pathway only.

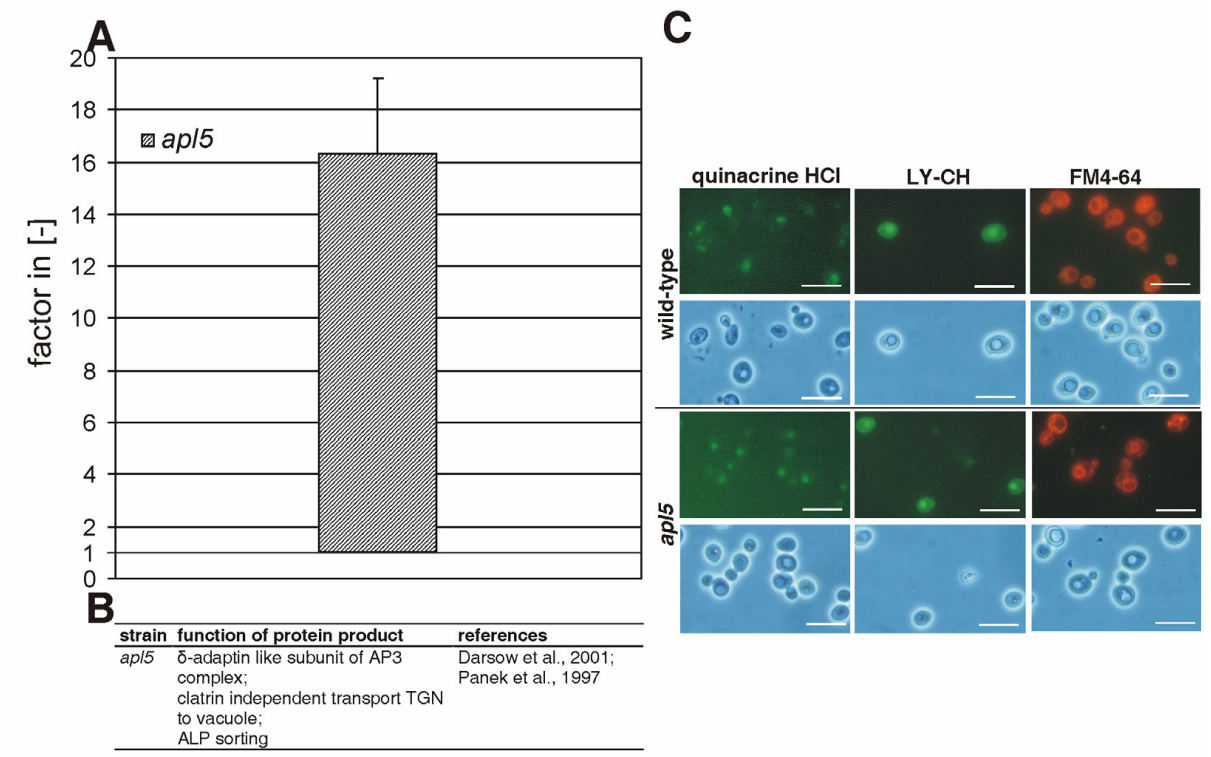

strain	function of protein product	references
apl5	δ-adaptin like subunit of AP3 complex; clatrin independent transport TGN to vacuole; ALP sorting	Darsow et al., 2001; Panek et al., 1997

Fig. 4.11: Mutant defective for transport between the TGN and the vacuole using the ALP-pathway. (A) Transfection efficiency of a mutant deleted for a subunit of the AP3-complex, responsible for transport between the TGN and the vacuole. Transfection was performed as described in "Materials and Methods". The value is given as a factor in relation to the transfection rate of the wild-type mutant (BY4741). The mean value (± s.d.) of the factor is calculated from three independent experiments. (B) Description of the deletion mutant used. (C) Impact of the specific gene deletion on vacuolar acidification, Lucifer Yellow (LY-CH) accumulation and membrane dynamics in BY4741 background in YE. Vacuolar acidification after 22 hours was visualized using quinacrine-HCl staining. Quinacrine HCl accumulates in acidic compartments. Lucifer Yellow CH and FM4-64 were used to study endocytic uptake and plasma membrane dynamics after 22 hours. Photos of representative cells from one of two independent experiments were taken with FITC-fluorescence optics (quinacrine and LY-CH) or rhodamine optics (FM4-64) (upper panels), and with phase-contrast optics (lower panels) as described in "Materials and Methods". The bar represents 10 μm.

4.3 The influence of *intra*-Golgi transport on transfection

A mutant which results in a more general effect on transport between the Golgi and the endosomal/vacuolar system was selected for transfection efficiency analysis. COP mediated transport between the endoplasmatic reticulum (ER) and the *cis* Golgi is defect in mutant *arf1*, however *intra*-Golgi transport and clathrin mediated export from the Golgi is also affected (Dell´Angelica et al, 2000; Gall et al, 2002; Gillingham et al, 2004; Ooi et al, 1998; Szaler et al, 2000; Trautwein et al, 2006; Yahara et al, 2001; Zhdankina et al, 2001). A strong positive effect on transfection efficiency is present in the mutant deleted for Arf1p, resulting in a factor of approximately 80 (Fig. 4.12 A). This indicates that there are additional transport mechanisms between the

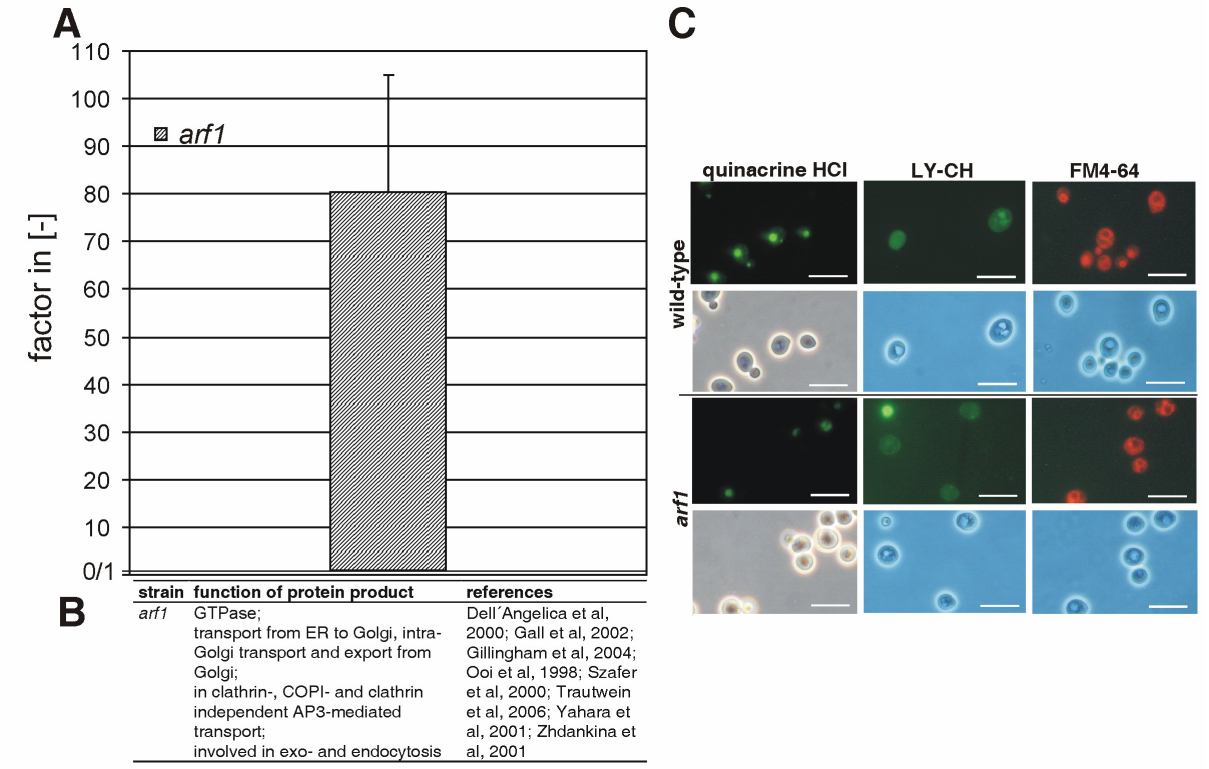

strain	function of protein product	references
arf1	GTPase; transport from ER to Golgi, intra-Golgi transport and export from Golgi; in clathrin-, COPI- and clathrin independent AP3-mediated transport; involved in exo- and endocytosis	Dell´Angelica et al, 2000; Gall et al, 2002; Gillingham et al, 2004; Ooi et al, 1998; Szafer et al, 2000; Trautwein et al, 2006; Yahara et al, 2001; Zhdankina et al, 2001

Fig. 4.12: Mutant defective for *intra*-Golgi transport. (A) Transfection efficiency of a mutant deleted for a protein important for COP- mediated transport between ER and Golgi, *intra*-Golgi transport and clathrin-mediated and AP3-mediated export from the Golgi. Transfection was performed as described in “Materials and Methods”. The value is given as a factor in relation to the transfection rate of the wild-type mutant (BY4741). The mean value (± s.d.) of the factor is calculated from three independent experiments. (B) Description of the deletion mutant used. (C) Impact of the specific gene deletion on vacuolar acidification, Lucifer Yellow (LY-CH) accumulation and membrane dynamics in BY4741 background in YE. Vacuolar acidification after 22 hours was visualized using quinacrine-HCl staining. Quinacrine HCl accumulates in acidic compartments. Lucifer Yellow CH and FM4-64 were used to study endocytic uptake and plasma membrane dynamics after 22 hours. Photos of representative cells from one of two independent experiments were taken with FITC-fluorescence optics (quinacrine and LY-CH) or rhodamine optics (FM4-64) (upper panels), and with phase-contrast optics (lower panels) as described in “Materials and Methods”. The bar represents 10 μm.

TGN and the endosomal/vacuolar system which influence transfection efficiency and may show an additive effect. Defects in endosomal/vacuolar acidification were detected in fluorescence staining experiments resulting in a weaker quinacrine signal, but only a very weak defect in LY-CH accumulation was observed (Fig. 4.12 C). This indicates that the major factor affecting transfection efficiency is due to transport inhibition of degrading enzymes to the endosomal/vacuolar system.

4.4 The influence of the cytoplasm to vacuole targeting and autophagy pathways on transfection

Deletion of *VAC8* positively affects transfection. Transfection efficiency is enhanced by a factor of approximately 8 (Fig. 4.13 A). Deletion of *ATG19* did not result in relevant influence on transfection efficiency. Deletion of *LAP4*, coding for API, known to be sorted by Atg19p, results in the same transfection behaviour (data not shown). Acidification and endocytic transport is not influenced in mutants defective for genes involved in CVT/autophagy (Fig. 4.13 C).

The enhanced transfection efficiency in mutant *vac8* might be due to reduced import of DNA degrading proteins to the vacuole by autophagy.

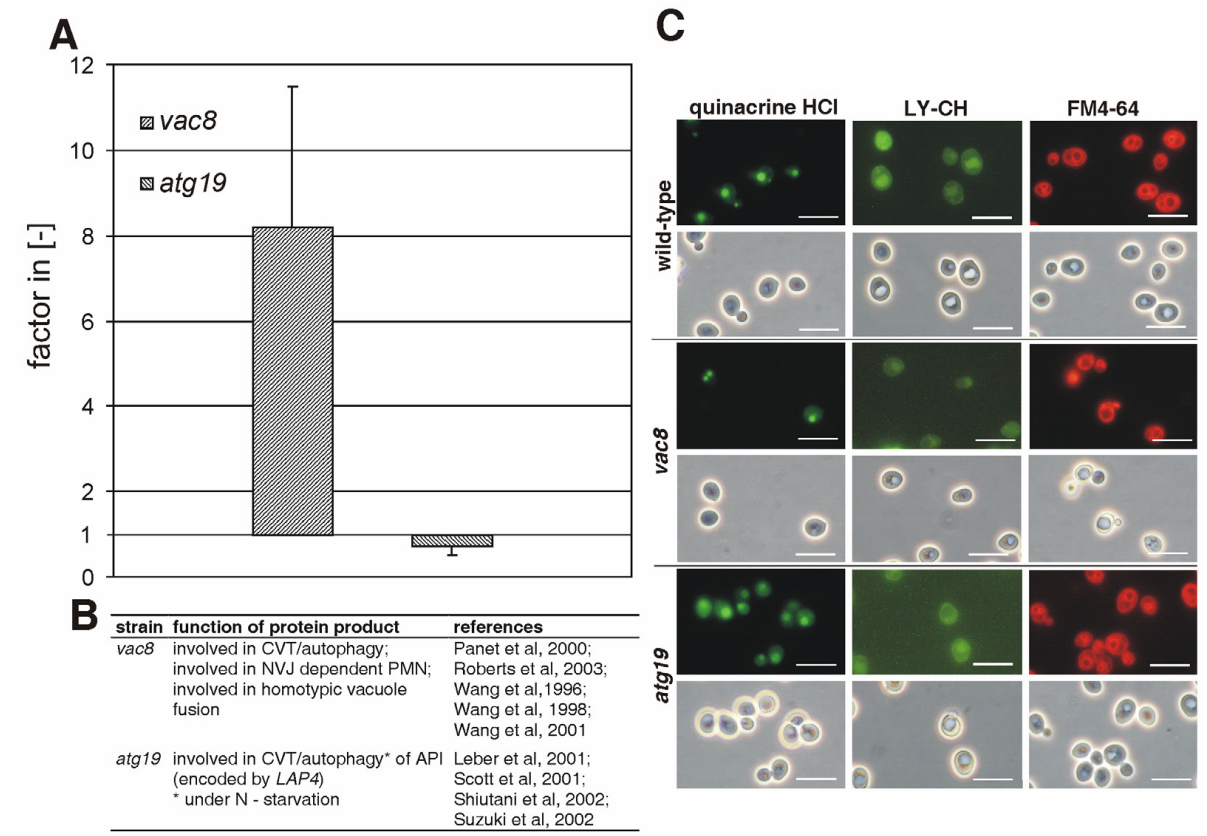

strain	function of protein product	references
vac8	involved in CVT/autophagy; involved in NVJ dependent PMN; involved in homotypic vacuole fusion	Panet et al, 2000; Roberts et al, 2003; Wang et al,1996; Wang et al, 1998; Wang et al, 2001
atg19	involved in CVT/autophagy* of API (encoded by *LAP4*) * under N - starvation	Leber et al, 2001; Scott et al, 2001; Shiutani et al, 2002; Suzuki et al, 2002

Fig. 4.13: Mutants defective for CVT and autophagy. (A) Transfection efficiency of mutants deleted for genes coding for proteins important in CVT and autophagy. Transfection was performed as described in “Materials and Methods”. All values are given as a factor in relation to the transfection rate of the wild-type mutant (BY4741). The mean values (± s.d.) of the factors were calculated from at least three independent experiments. (B) Description of the deletion mutants used. (C) Impact of specific gene deletions involved in CVT and autophagy on vacuolar acidification, Lucifer Yellow (LY-CH) accumulation and membrane dynamics in BY4741 background in YE. Vacuolar acidification after 22 hours was visualized using quinacrine-HCl staining. Quinacrine HCl accumulates in acidic compartments. Lucifer Yellow CH and FM4-64 were used to study endocytic uptake and plasma membrane dynamics after 22 hours. Photos of representative cells from one of at least two independent experiments were taken with FITC-fluorescence optics (quinacrine and LY-CH) or rhodamine optics (FM4-64) (upper panels), and with phase-contrast optics (lower panels) as described in “Materials and Methods”. The bar represents 10 μm.

4.5 The influence of the endosomal/vacuolar pH value and ion homeostasis on transfection

Activity and functionality of proteins is dependent on the pH-value and concentration of other ions.

4.5.1 The vacuolar ATPase

Mutants deleted for *STV1* and *VPH1*, respectively, were chosen to determine the influence of the activity of the V-ATPase in correlation to its localization on transfection. Stv1p is present in the V0 subunit of the V-ATPase in endosomes and

Golgi, whereas Vph1p is an isoform to Stv1p present in the vacuole (Manolson et al, 1994; Perzov et al, 2002). Both Stv1p and Vph1p are homologous to the human *ATP6V0A1* protein. Transfection efficiency in the *stv1* mutant is enhanced by a factor of 17, whereas an 11.5 fold enhancement could be observedin the *vph1* mutant (Fig. 4.14 A).

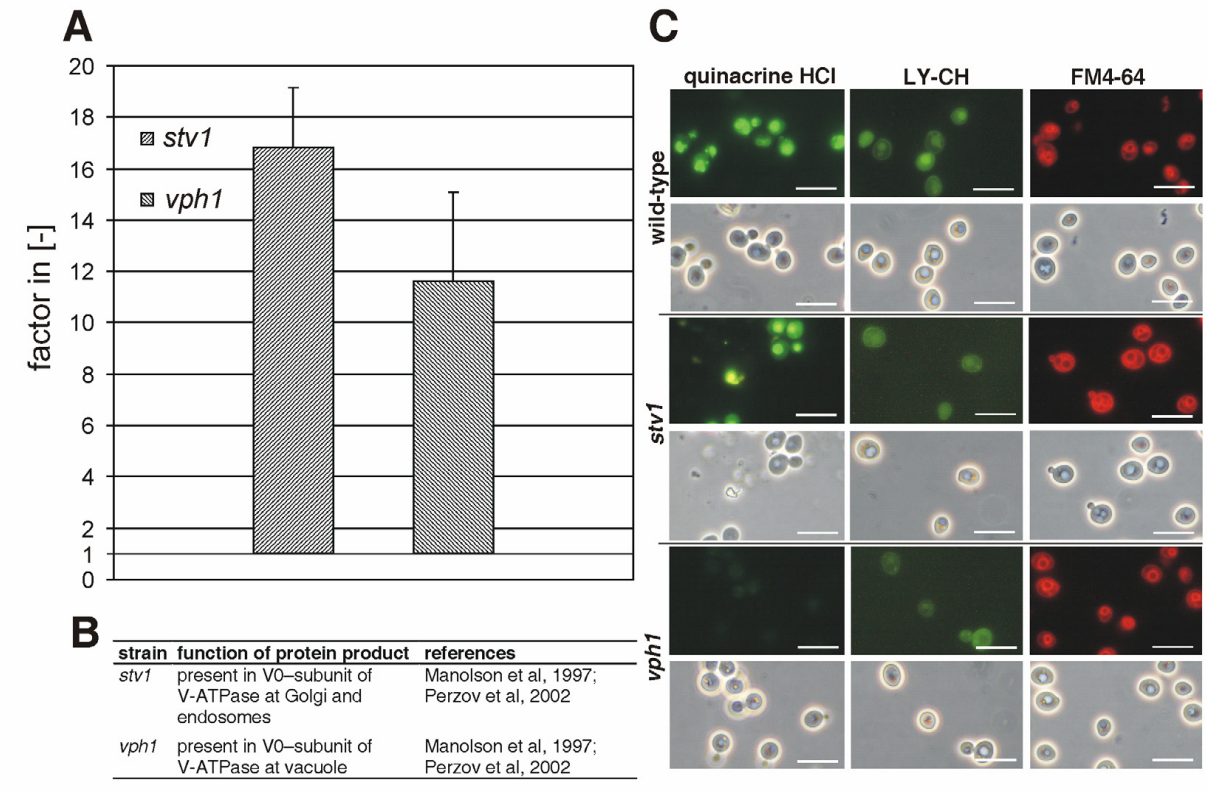

B

strain	function of protein product	references
stv1	present in V0–subunit of V-ATPase at Golgi and endosomes	Manolson et al, 1997; Perzov et al, 2002
vph1	present in V0–subunit of V-ATPase at vacuole	Manolson et al, 1997; Perzov et al, 2002

Fig. 4.14: Mutants defective for acidification of the Golgi and the endosomal/vacuolar system. (A) Transfection efficiency of mutants deleted for genes coding for proteins of the V0 subunit of the vacuolar ATPase. Transfection was performed as described in “Materials and Methods”. All values are given as a factor in relation to the transfection rate of the wild-type mutant (BY4741). The mean values (± s.d.) of the factors were calculated from at least three independent experiments. (B) Description of the deletion mutants used. (C) Impact of specific gene deletions involved in Golgi and endosomal or vacuolar acidification on endosomal/vacuolar acidification, Lucifer Yellow (LY-CH) accumulation and membrane dynamics in BY4741 background in YE. Vacuolar acidification after 22 hours was visualized using quinacrine-HCl staining. Quinacrine HCl accumulates in acidic compartments. Lucifer Yellow CH and FM4-64 were used to study endocytic uptake and plasma membrane dynamics after 22 hours. Photos of representative cells from one of at least two independent experiments were taken with FITC-fluorescence optics (quinacrine and LY-CH) or rhodamine optics (FM4-64) (upper panels), and with phase-contrast optics (lower panels) as described in “Materials and Methods”. The bar represents 10 μm.

This suggests correlations between the endosomal/vacuolar pH-value, endocytic/vacuolar transport and transfection efficiency.

The *stv1* mutant exhibits a slightly enhanced accumulation of quinacrine in vacuoles, suggesting a slightly lower pH-value in comparison to the wild type (Fig. 4.14 C).

Vacuoles are not acidified in the *vph1* mutant. The *vph1* mutant shows reduced LY-CH accumulation and slightly higher FM4-64 accumulation in vacuolar membranes than the wild type. LY-CH accumulation is also slightly reduced in the *stv1* mutant, whereas FM4-64 accumulates more efficiently in non-vacuolar membranes.
These observations indicate that non-wild-type endosomal/vacuolar acidification correlates with enhanced transfection efficiency due to secondary transport defects.

4.5.2 Endosomal/vacuolar ion homeostasis

It was observed that $Na^+(K^+)/H^+$ ion homeostasis affects transfection efficiency, which was deduced by deleting the gene *NHX1*, encoding for a member of the NHE family of Na^+/H^+ exchangers. Transfection efficiency is enhanced by a factor of approximately 5 in the mutant deleted for *NHX1* (Fig. 4.15 A). Ca^{2+} accumulation in the vacuole does not seem to influence transfection efficiency, as deduced from unchanged transfection behaviour in the deletion mutants *vcx1* and *pmc1*. Even reducing Ca^{2+} release from the vacuole during osmotic shift in transfection does not affect transfection efficiency. This was tested by deleting *YVC1*, a vacuolar cation channel known to be involved in Ca^{2+} release from the vacuole during osmotic shift. This indicates that vacuolar Ca^{2+} homeostasis is irrelevant for transfection efficiency. The transfection efficiency of mutants *vph1* and *vcx1*, in comparison, and the results of quinacrine staining in *vcx1* mutant (Fig. 4.15 C) show that the effect on vacuolar pH–value is negligible in mutant *vcx1* under transfection conditions. Results of staining experiments in all mutants tested in this chapter did not show significant differences to the wild type.

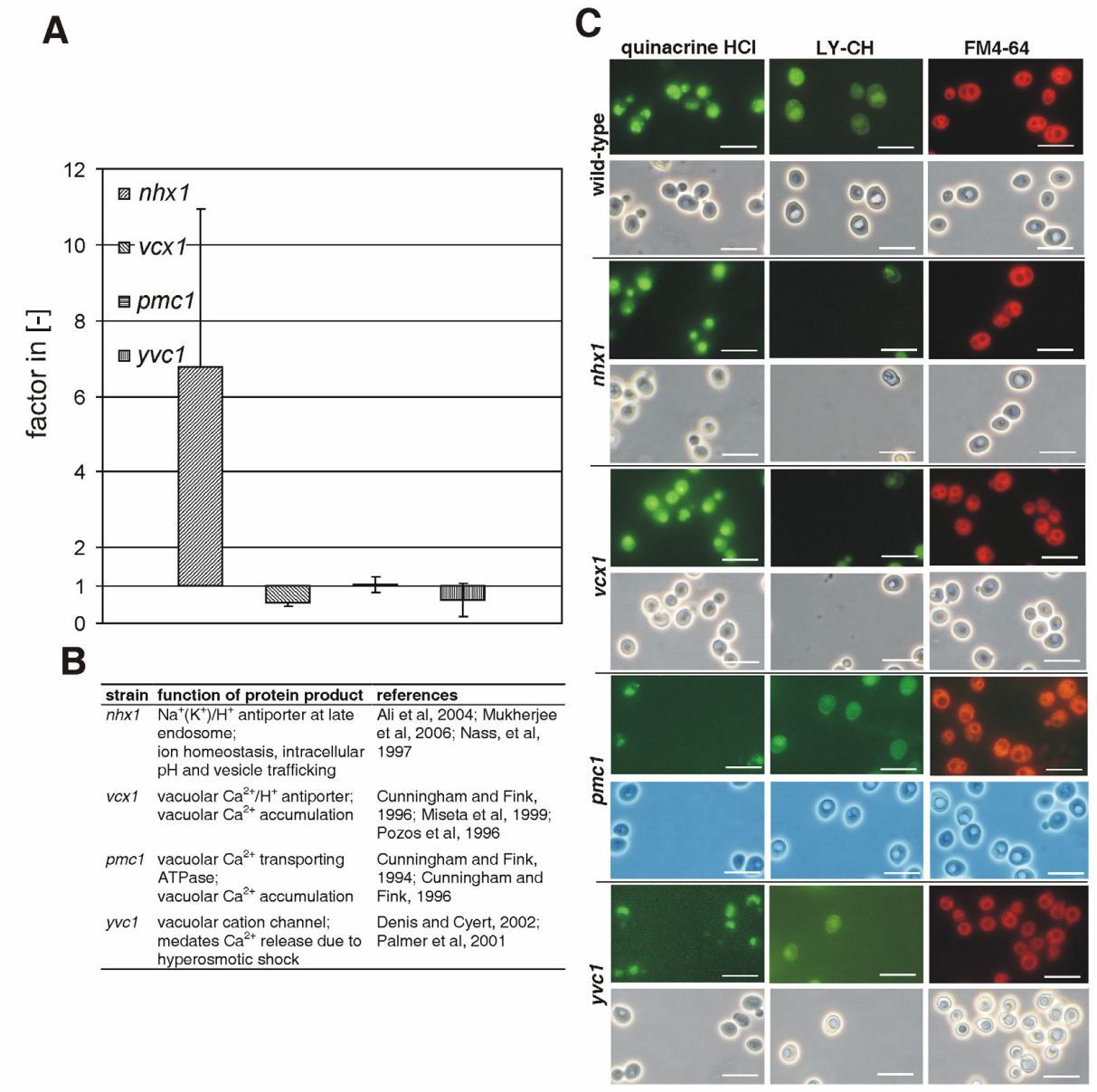

strain	function of protein product	references
nhx1	$Na^+(K^+)/H^+$ antiporter at late endosome; ion homeostasis, intracellular pH and vesicle trafficking	Ali et al, 2004; Mukherjee et al, 2006; Nass, et al, 1997
vcx1	vacuolar Ca^{2+}/H^+ antiporter; vacuolar Ca^{2+} accumulation	Cunningham and Fink, 1996; Miseta et al, 1999; Pozos et al, 1996
pmc1	vacuolar Ca^{2+} transporting ATPase; vacuolar Ca^{2+} accumulation	Cunningham and Fink, 1994; Cunningham and Fink, 1996
yvc1	vacuolar cation channel; medates Ca^{2+} release due to hyperosmotic shock	Denis and Cyert, 2002; Palmer et al, 2001

Fig. 4.15: Mutants defective for endosomal/vacuolar ion homeostasis. (A) Transfection efficiency of mutants deleted for genes coding for ion transporters of the MVB/late endosome and the vacuole. Transfection was performed as described in “Materials and Methods”. All values are given as a factor in relation to the transfection rate of the wild-type mutant (BY4741). The mean values (± s.d.) of the factors were calculated from at least three independent experiments. (B) Description of the deletion mutants used. (C) Impact of specific gene deletions involved in endosomal/vacuolar ion homeostasis on vacuolar acidification, Lucifer Yellow (LY-CH) accumulation and membrane dynamics in BY4741 background in YE. Vacuolar acidification after 22 hours was visualized using quinacrine-HCl staining. Quinacrine HCl accumulates in acidic compartments. Lucifer Yellow CH and FM4-64 were used to study endocytic uptake and plasma membrane dynamics after 22 hours. Photos of representative cells from one of at least two independent experiments were taken with FITC-fluorescence optics (quinacrine and LY-CH) or rhodamine optics (FM4-64) (upper panels), and with phase-contrast optics (lower panels) as described in “Materials and Methods”. The bar represents 10 μm.

4.5.3 Transport defects and pH-value

Endoytic transport is dependent on the pH-value present in endocytic compartments under standard growth conditions (Bowers et al, 2000; Brett et al, 2005; Klionsky et al, 1992). In addition, in experiments in this thesis, performed in 1 M sucrose, transport defects in correlation to defects in acidification of endocytic/vacuolar compartments could be confirmed. This explains the positive effects on transfection efficiency. Mutants *stv1* and *vph1*, for example, exhibit transport defects in correlation to acidification defects (Fig. 4.14 C). This, in consequence, will lead to enhanced accumulation of endocytosed DNA in non-vacuolar compartments, as also seen, for example, in the *vps21* mutant which exhibits accumulation of membranes similar to *stv1* mutant (seen for FM4-64 staining) (Figs. 4.3 and 4.7). Furthermore, mutants *rav1* and *vps45,* for example, exhibit reduced acidification and endocytic accumulation of LY-CH in the vacuole in combination with an enhanced transfection efficiency, indicating an pH-value mediated transport defect. (Figs. 4.2 and 4.3).

4.5.4 Extracellular pH value

The pH-value of endocytic compartments and vacuole influences transfection efficiency (See chapters 4.5.1 and 4.5.3). Transfection experiments were performed using different extracellular pH-values with and without buffering to elucidate whether transfection efficiency is also dependent on extracellular pH.

Using non-buffered transfection solutions adjusted to different pH-values, no significant effect on transfection in the wild type or in either of the deletion mutants *stv1* and *vph1* was observed (Fig. 4.16). Transfection rates in samples with a starting pH-value of pH 9.5-10 were reduced in each mutant. After 22 hours of incubation, the extracellular pH was decreased to pH 4–5 in all samples. The transfection rates under buffered conditions were very low at pH 5 and were zero for higher pH values in all mutants tested (data not shown).

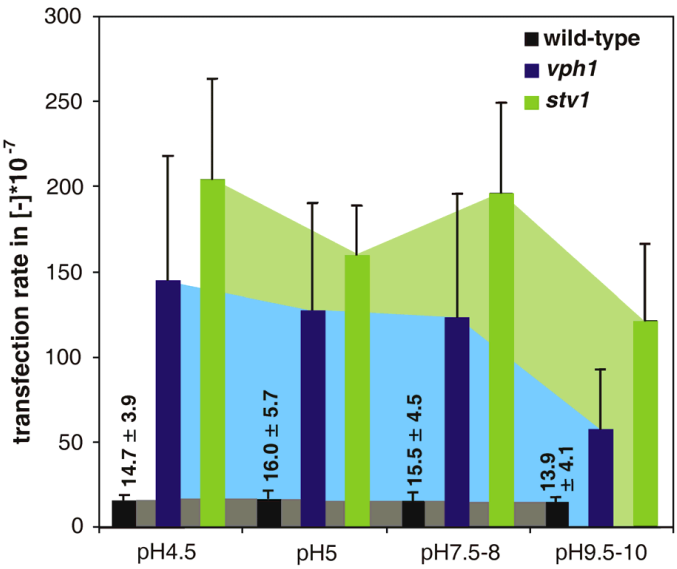

Fig. 4.16: Influence of the extracellular pH-value on transfection efficiency. Transfection rates in mutants BY4741, BY4741 *stv1* and BY4741 *vph1* in relation to the pH-value of the non-buffered transfection solution. A high pH value of the transfection solution negatively influences the transfection rate and cannot mimic a defect in *STV1* or *VPH1*. Using transfection solutions buffered to high pH-values with 100 mM Hepes results in transfection rates of zero when the pH-value is higher than pH 5 (data not shown). The mean values (± s.d.) of the factors were calculated from at least three independent experiments.

The pH–value did not change during incubation in buffered transfection solutions with a starting pH of pH 4.5 and pH 5. Samples starting at a pH value of pH 7.5–8 or pH 9.5–10 were acidified to pH 5–5.5 or pH 7–7.5, respectively. This suggests that the starting extracellular pH value does not influence transfection efficiency in unbuffered transfection solutions. The transfection rate is zero when the transfection solutions are buffered to higher pH–values, which indicates that the extracellular solution has to be acidified before efficient uptake of DNA is possible, maybe due to less strong ionization of the DNA.

4.6 The influence of proteolytic protein processing on transfection

Proteins involved in endocytosis and endocytic/vacuolar degradation are often required to be protolyticaly processed.

4.6.1 Vacuolar processing proteases and other vacuolar proteins

Deletion of the gene encoding for the important vacuolar processing protease PrA in the *pep4* mutant only demonstrates a minor influence on transfection efficiency,

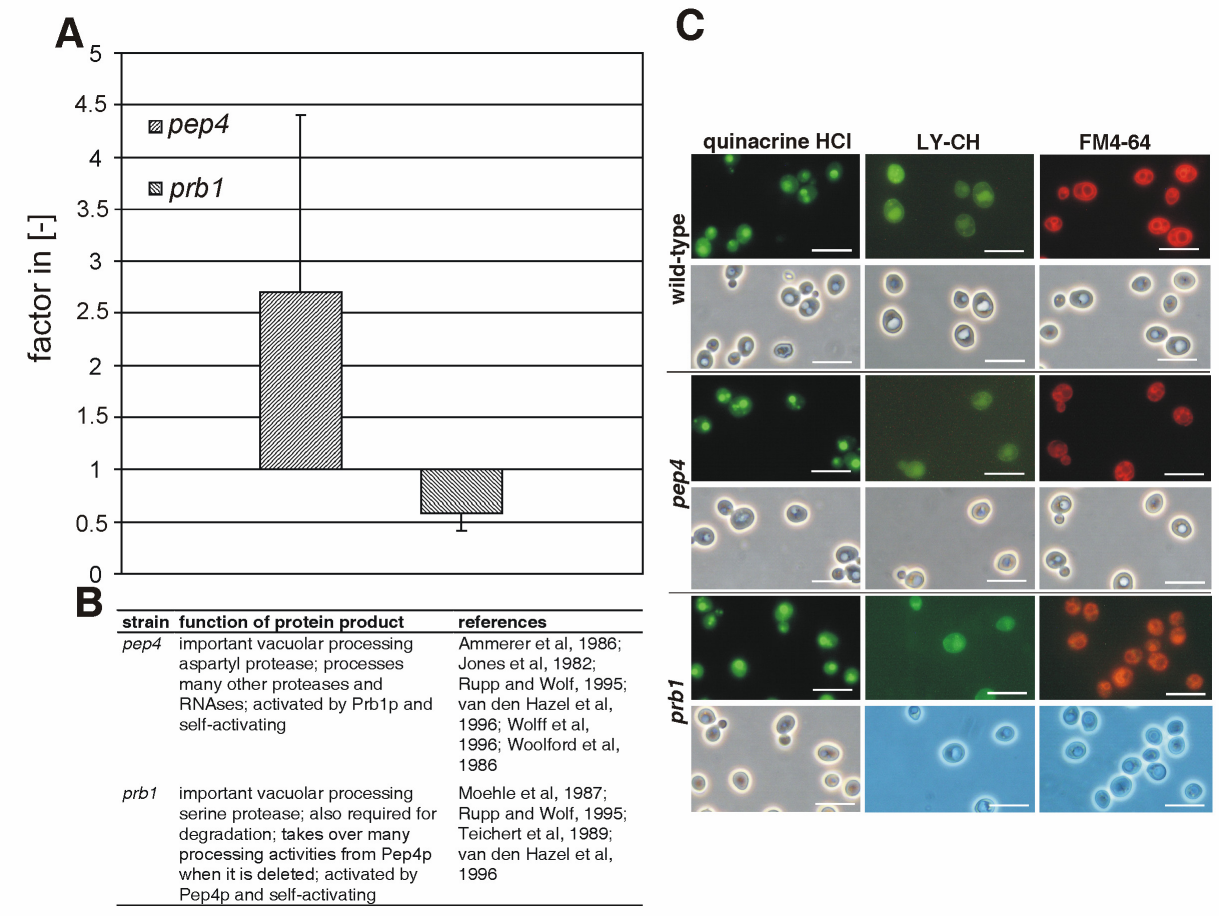

B

strain	function of protein product	references
pep4	important vacuolar processing aspartyl protease; processes many other proteases and RNAses; activated by Prb1p and self-activating	Ammerer et al, 1986; Jones et al, 1982; Rupp and Wolf, 1995; van den Hazel et al, 1996; Wolff et al, 1996; Woolford et al, 1986
prb1	important vacuolar processing serine protease; also required for degradation; takes over many processing activities from Pep4p when it is deleted; activated by Pep4p and self-activating	Moehle et al, 1987; Rupp and Wolf, 1995; Teichert et al, 1989; van den Hazel et al, 1996

Fig. 4.17: Mutants defective for vacuolar protein processing. (A) Transfection efficiency of mutants deleted for genes coding for proteases PrA (Pep4p) and PrB (Prb1p). Transfection was performed as described in “Materials and Methods”. All values are given as a factor in relation to the transfection rate of the wild-type mutant (BY4741). The mean values (± s.d.) of the factors were calculated from at least three independent experiments. (B) Description of the deletion mutants used. (C) Impact of specific gene deletions involved in vacuolar protein processing on vacuolar acidification, Lucifer Yellow (LY-CH) accumulation and membrane dynamics in BY4741 background in YE. Vacuolar acidification after 22 hours was visualized using quinacrine-HCl staining. Quinacrine HCl accumulates in acidic compartments. Lucifer Yellow CH and FM4-64 were used to study endocytic uptake and plasma membrane dynamics after 22 hours. Photos of representative cells from one of at least two independent experiments were taken with FITC-fluorescence optics (quinacrine and LY-CH) or rhodamine optics (FM4-64) (upper panels), and with phase-contrast optics (lower panels) as described in “Materials and Methods”. The bar represents 10 μm.

resulting in an enhancement factor of 2-3 (Fig. 4.17 A). This result had been reported previously for the *pep4* mutation in a different mutant background (Neukamm et al, 2002). In contrast, deletion of *PRB1* encoding for PrB resulted in a weak negative effect on transfection efficiency. PrB, like PrA, is an important vacuolar processing protease. PrB and PrA activate each other and are also self activating (Jones, 2002;

Jones et al, 1982; Zubenko et al, 1983). All other vacuolar proteases tested, Ape3p, Cps1p, Dap2p, Lap4p, and Prc1p, did not show any influence on transfection efficiency (data not shown). Staining experiments with quinacrine, LY-CH and FM4-64 did not show significant changes in comparison to the wild type for any deletion mutant described in this chapter (data partly shown in Fig. 4.17 C).

4.6.2 Golgi resident processing proteases

Many proteins of the endocytic/vacuolar system are sorted via the secretory pathway. Some of these proteins are known to be processed proteolytical in the secretory pathway. CPY or PrA, for example, are known to be proteolytical processed during their passage through the Golgi (Kato et al, 2006). Nhx1p which is located to the MVB/late endosome is predicted to be proteolytical processed in the secretory pathway (Wells and Rao, 2001). Due to that, proteases of the Golgi became interesting for transfection efficiency tests of mutants deleted for these proteins.

Deletion mutants *kex1*, *kex2* and *ste13*, deleted for proteins involved in α-factor processing and in the case of Kex2p and Kex1p also killer toxin processing (Julius et al, 1984; Dmochowska et al, 1987; Fuller et al, 1989), were tested in transfection assays. The mutant deleted for *KEX2* showed an enhanced transfection efficiency when late logarithmic cells were used for transfection experiments. Wild-type transfection efficiencies are observed in *kex1* and *ste13* mutants (Fig. 4.18 A). Endocytic/vacuolar compartments in mutant *kex2* seem to be more strongly acidified than in the wild type (Fig. 4.18 C). In addition, transport defects were observed. Vacuoles are stained weaker in LY-CH staining and stronger background staining can be seen in the FM4-64 staining experiment. This may represent accumulating vesicles as seen in mutant *vps21* or *stv1* previously. Mutants *kex1* and *ste13* do not exhibit significantly different staining patterns from the wild type in quinacrine, LY-CH and FM4-64 stainings.

Mutant *pmr1* is deleted for the important Ca^{2+}-importing ATPase of the Golgi (Antebi and Fink, 1992; Mandal et al, 2003; Vashist et al, 2002). Transfection efficiency in this mutant is enhanced even more strongly than in mutant *kex2* (Fig. 4.18 A). Kex2p activity is known to be Ca^{2+}-dependent (Fuller et al, 1989), which might partly explain the positive effect of the deletion of *PMR1* on transfection efficiency. Acidification seems to be stronger than in the wild type in *pmr1* mutant, as in *kex2* mutant, and

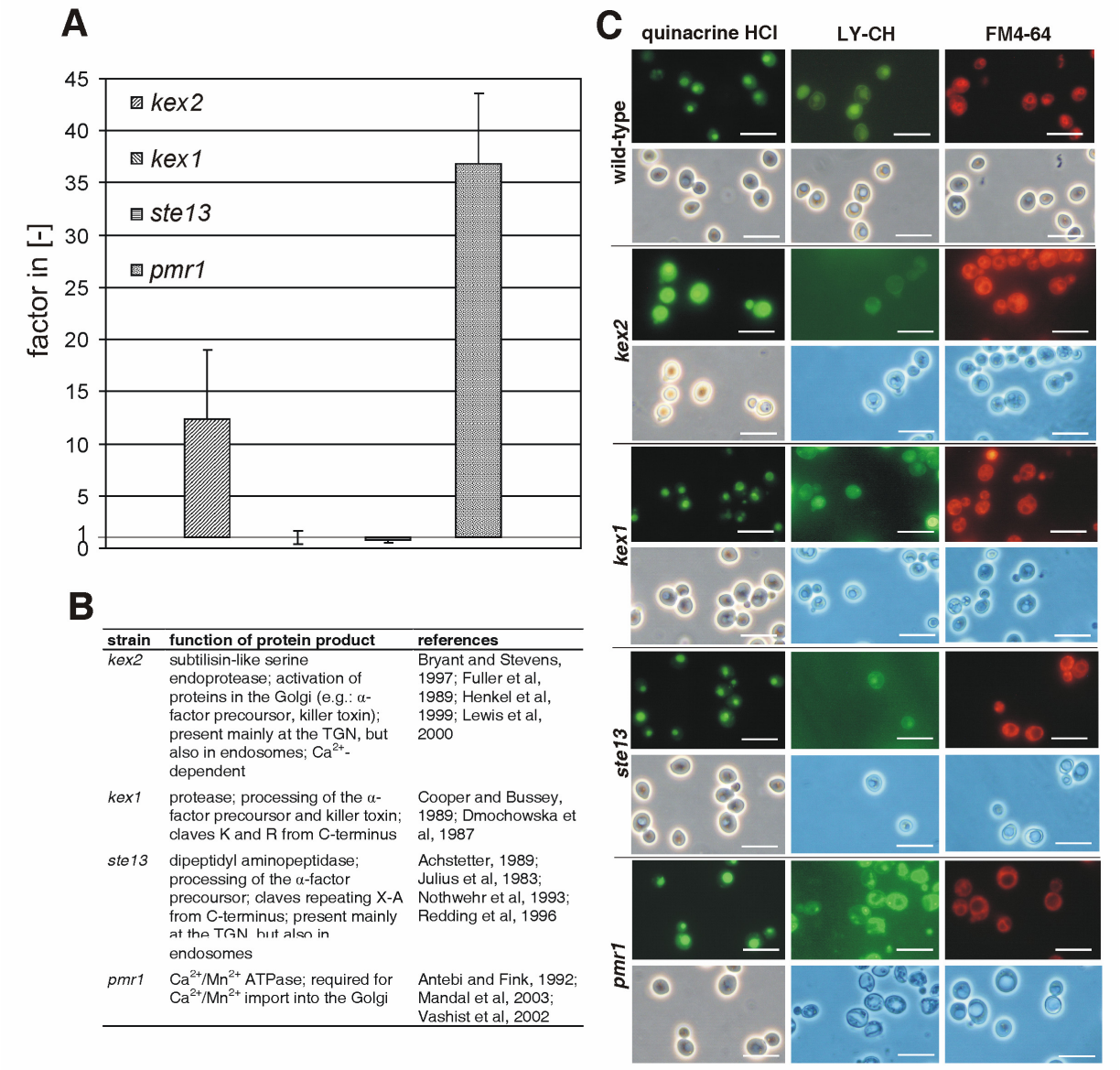

strain	function of protein product	references
kex2	subtilisin-like serine endoprotease; activation of proteins in the Golgi (e.g.: α-factor precoursor, killer toxin); present mainly at the TGN, but also in endosomes; Ca^{2+}-dependent	Bryant and Stevens, 1997; Fuller et al, 1989; Henkel et al, 1999; Lewis et al, 2000
kex1	protease; processing of the α-factor precoursor and killer toxin; claves K and R from C-terminus	Cooper and Bussey, 1989; Dmochowska et al, 1987
ste13	dipeptidyl aminopeptidase; processing of the α-factor precoursor; claves repeating X-A from C-terminus; present mainly at the TGN, but also in endosomes	Achstetter, 1989; Julius et al, 1983; Nothwehr et al, 1993; Redding et al, 1996
pmr1	Ca^{2+}/Mn^{2+} ATPase; required for Ca^{2+}/Mn^{2+} import into the Golgi	Antebi and Fink, 1992; Mandal et al, 2003; Vashist et al, 2002

Fig. 4.18: Mutants defective for Golgi proteolytic protein processing. (A) Transfection efficiency of mutants deleted for genes coding for Golgi proteases predominantly known to be involved in processing of the α-factor. Transfection was performed as described in "Materials and Methods". All values are given as a factor in relation to the transfection rate of the wild-type mutant (BY4741). The mean values (± s.d.) of the factors were calculated from at least three independent experiments. (B) Description of the deletion mutants used. (C) Impact of specific gene deletions involved in Golgi proteolytic protein processing on vacuolar acidification, Lucifer Yellow (LY-CH) accumulation and membrane dynamics in BY4741 background in YE. Vacuolar acidification after 22 hours was visualized using quinacrine-HCl staining. Quinacrine HCl accumulates in acidic compartments. Lucifer Yellow CH and FM4-64 were used to study endocytic uptake and plasma membrane dynamics after 22 hours. Photos of representative cells from one of at least two independent experiments were taken with FITC-fluorescence optics (quinacrine and LY-CH) or rhodamine optics (FM4-64) (upper panels), and with phase-contrast optics (lower panels) as described in "Materials and Methods". The bar represents 10 μm.

endocytic transport to the vacuole is reduced where accumulation of LY-CH and FM4-64 in the cytoplasm is enhanced, maybe representing accumulating vesicles (Fig. 4.18 C).

4.6.3 Known targets of Kex2p processing

To understand the positive effect of the deletion of *KEX2* on transfection efficiency, deletion mutants of known substrates of Kex2p were tested for effects on transfection efficiency. These deletion mutants included *exg1* (major cell wall exo-1,3-β-glucanase) and some other cell wall protein mutants (mutants *pir1*, *hsp150*, *pir3* and *cis3*). In mutant *pir1* a weak positive and in mutant *hsp150* a weak negative effect on transfection efficiency was observed. However, these effects cannot explain the effect on transfection efficiency of the deletion of *KEX2* (Fig. 4.19 A). No significant differences to the wild type could be seen in quinacrine, LY-CH and FM4-64 stainings for mutants *exg1*, *pir1*, *hsp150*, *pir3* and *cis3* (Fig. 4.19 C).

Only one mutant tested in this thesis, *och1*, might partly explain the effect on transfection efficiency in mutant *kex2*. It is predicted that Och1p is processed by Kex2p (Fig. 4.20) and the deletion of *OCH1* also leads to an enhanced transfection efficiency. Och1p is involved in N-type glycosylation at the Golgi (Harris and Waters, 1996; Munro, 2001; Nakayama et al, 1992).

See following page for:

Fig. 4.19: Proteins processed by the Golgi protease Kex2p. (A) Transfection efficiency of mutants deleted for genes coding for proteins known to be processed by Kex2p. Transfection was performed as described in “Materials and Methods”. All values are given as a factor in relation to the transfection rate of the wild-type mutant (BY4741). The mean values (± s.d.) of the factors were calculated from at least three independent experiments. (B) Description of the deletion mutants used. (C) Impact of deleting genes encoding for Kex2p processed proteins on vacuolar acidification, Lucifer Yellow (LY-CH) accumulation and membrane dynamics in BY4741 background in YE. Vacuolar acidification after 22 hours was visualized using quinacrine-HCl staining. Quinacrine HCl accumulates in acidic compartments. Lucifer Yellow CH and FM4-64 were used to study endocytic uptake and plasma membrane dynamics after 22 hours. Photos of representative cells from one of at least two independent experiments were taken with FITC-fluorescence optics (quinacrine and LY-CH) or rhodamine optics (FM4-64) (upper panels), and with phase-contrast optics (lower panels) as described in “Materials and Methods”. The bar represents 10 μm.

Fig. 4.19: See previous page for legend

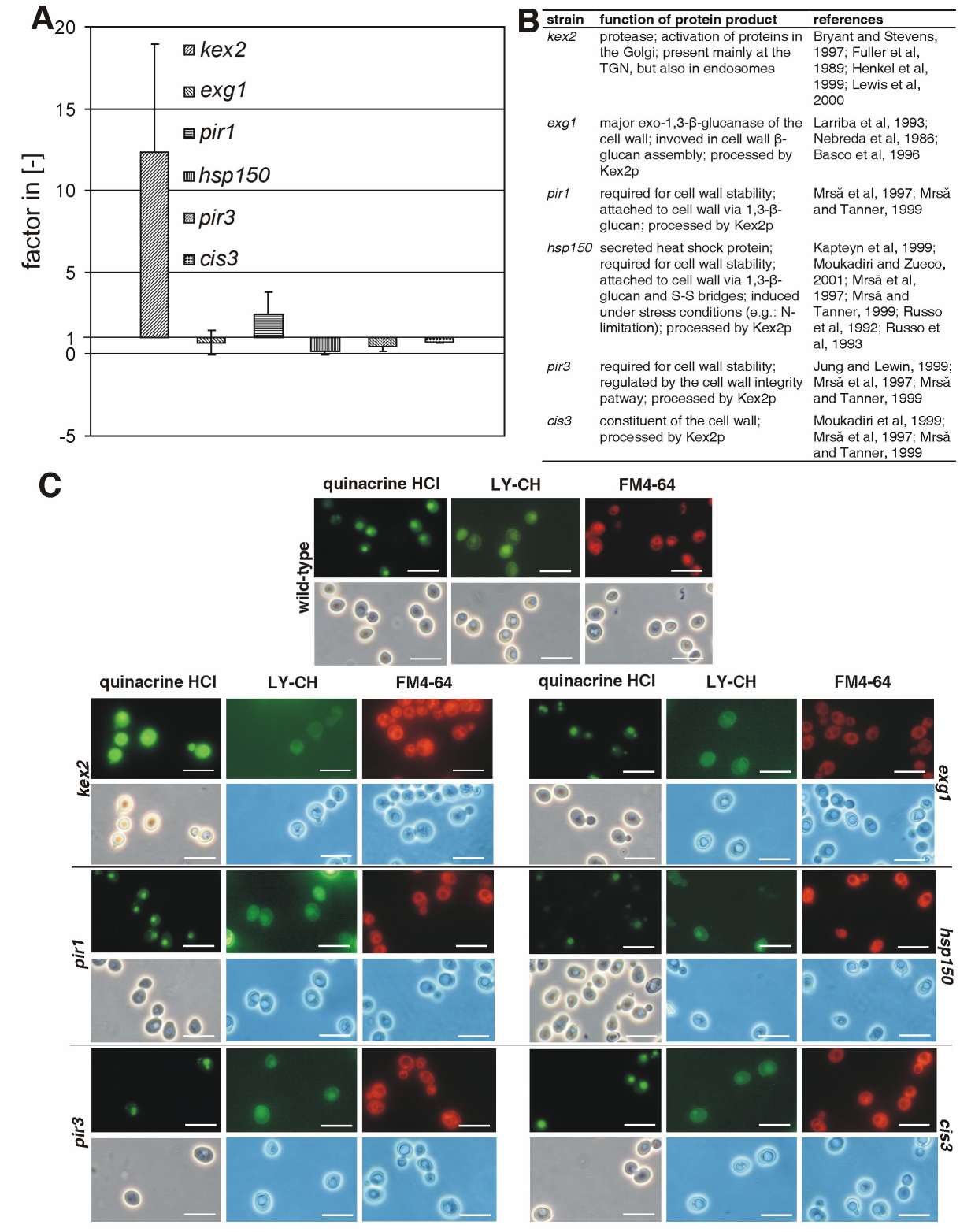

Fig. 4.20: See following page for legend

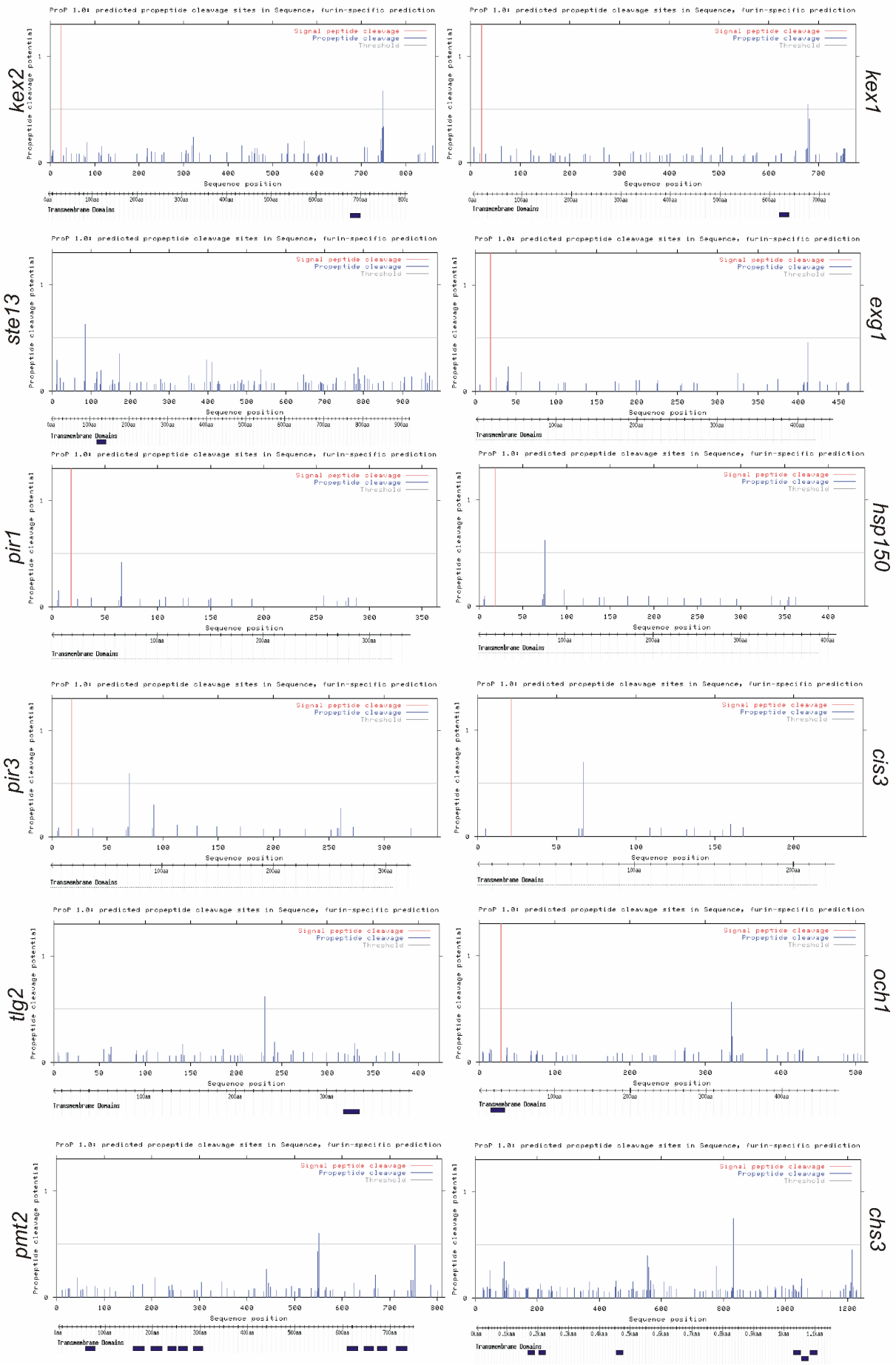

See previous page for:

Fig. 4.20: Prediction of processing sites of Kex2p in proteins deleted in mutants tested in this thesis. Prediction was performed using the ProP 1.0 server which predicts Furin and PC (protein convertase) specific cleavage sites (http://www.cbs.dtu.dk/services/ProP/) (Duckert et al, 2004). Trans membrane domains were predicted using the TMHMM 2.0 server (http://www.cbs.dtu.dk/services/TMHMM-2.0/). All other predictions, which are not shown, were negative for Kex2p cleavage site prediction or are not sorted via the Golgi. The only mutant deleted for a protein, predicted to be cleaved by Kex2p and which additionally also represents an enhanced transfection efficiency is BY4741 *och1*.

4.6.4 Intracellular localization of the "*kex2*-effect"

A major proportion of Kex2p is located at the TGN in the wild type mutant, however Kex2p can also be found in endosomes as it is sorted between endosomes and TGN, most likely via a circular route (Tsukada and Gallwitz, 1996; Luo and Chang, 1997; Brickner and Fuller, 1997; Sipos et al, 2004; Chen et al, 2005; Blanchette et al, 2004). Based on this location of Kex2p to different intracellular compartments, it was interesting to try to correlate the effect of losing Kex2p in a specific compartment in the *kex2* mutant to the effect on transfection efficiency. Different deletion mutants known to be involved in transporting Kex2p between endosomes and TGN were used to enrich Kex2p or reduce Kex2p amount to specific compartments.

The first group of deletion mutants were those known to be involved in export of Kex2p from the TGN (*ypt6*, *tgl2*), or in Kex2p retention to the TGN and defect in TGN export processes (*vps1*). A negligible positive effect on transfection efficiency was observed here. This effect is not sufficient to explain the effect of deleting *KEX2* (Fig. 4.21 A). Some of Kex2p in mutants *ypt6*, *tgl2* and *vps1* is sorted to the vacuole via the plasma membrane, or even reduced in amount and mislocated (Tsukada and Gallwitz, 1996; Panek et al, 2000; Wilsbach and Payne, 1993; Nothwehr et al, 1995). Accumulation of LY-CH in very early endosomal compartments in some *ypt6* mutant cells could be observed (Fig. 4.21 C). Acidification in *ypt6* mutant and all other phenotypes tested by staining in mutants *tgl2* and *vps1* are not significantly affected in comparison to the wild type.

In the *rav1* mutant which is known to be involved in the transport of Kex2p from early to late endosomes (Sipos et al, 2004), Kex2p will be accumulated in early endosomes together with endocytosed DNA in transfection. In transfection in a *rav1* background, a strong positive effect on transfection efficiency could be seen which is even higher than in the *kex2* mutant (Fig. 4.21 A). Furthermore, acidification of intracellular compartments in mutant *rav1* seems to be reduced and transport of LY-

Fig. 4.21: See following page for legend

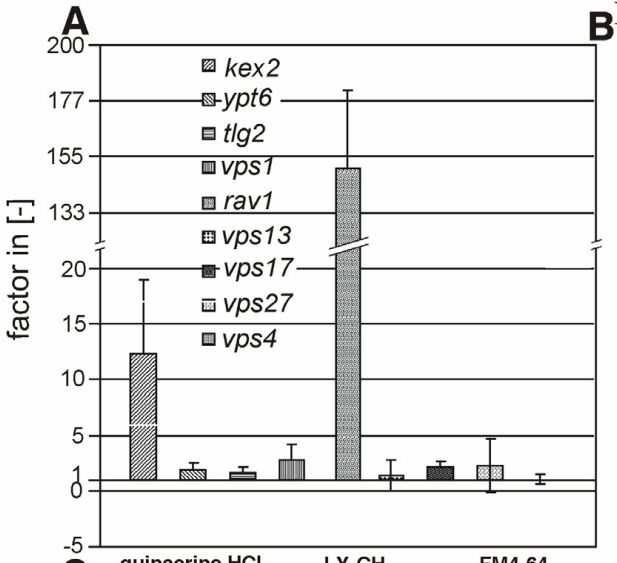

B

strain	function of protein product	references
kex2	protease; activation of proteins in the Golgi; present mainly at the TGN, but also in endosomes	Bryant and Stevens, 1997; Fuller et al, 1989; Henkel et al, 1999; Lewis et al, 2000
ypt6	GTPase; fusion of endosome derived vesicles to TGN; intra-Golgi transport; involved in CPY sorting; Kex2p activity and sorting is affected	Luo and Gallwitz, 2003; Siniossoglou and Pelham, 2001; Tsukada and Gallwitz, 1996; Tsukada et al, 1999
tlg2	t-SNARE; fusion of endosome derived vesicles to TGN; transport early endosome TGN; Kex2p transport	Brickner et al, 2001; Coe et al, 1999; Lewis et al, 2000
vps1	dynamine like GTPase; actin cytoskeleton organization; Golgi retention of Kex2p	Ekena et al, 1993; Nothwehr et al, 1996; Nothwehr et al, 1995; Yu and Cai, 2004
rav1	transport early endosome to late endosome (RAVE complex); Kex2p transport	Sipos et al, 2004
vps13	seems to be involved in transport late endosome to TGN; involved in cycling of Vps10p (CPY sorting) and Kex2p between endosomes and TGN	Brickner and Fuller, 1997
vps17	sorting nexin; part of the retromer complex; involved in CPY sorting	Horazdovsky et al, 1997; Köhrer and Emr, 1993
vps27	associated to ESCRTI subcomplex; required for proper sorting of ubiquitinated cargo in the MVB; export from the MVB; 90% reduced Kex2p amount in class E strains; Kex2p digested in class E compartment	Bilodeau et al, 2003; Bowers et al, 2004; Piper et al, 1995; Celeghino et al, 1995
vps4	associated to ESCRTIII subcomplex; required for proper sorting of ubiquitinated cargo in the MVB; export from the MVB; 90% reduced Kex2p amount in class E strains; Kex2p digested in class E compartment	Bowers et al, 2004; Finken-Eigen et al, 1997; Celeghino et al, 1995

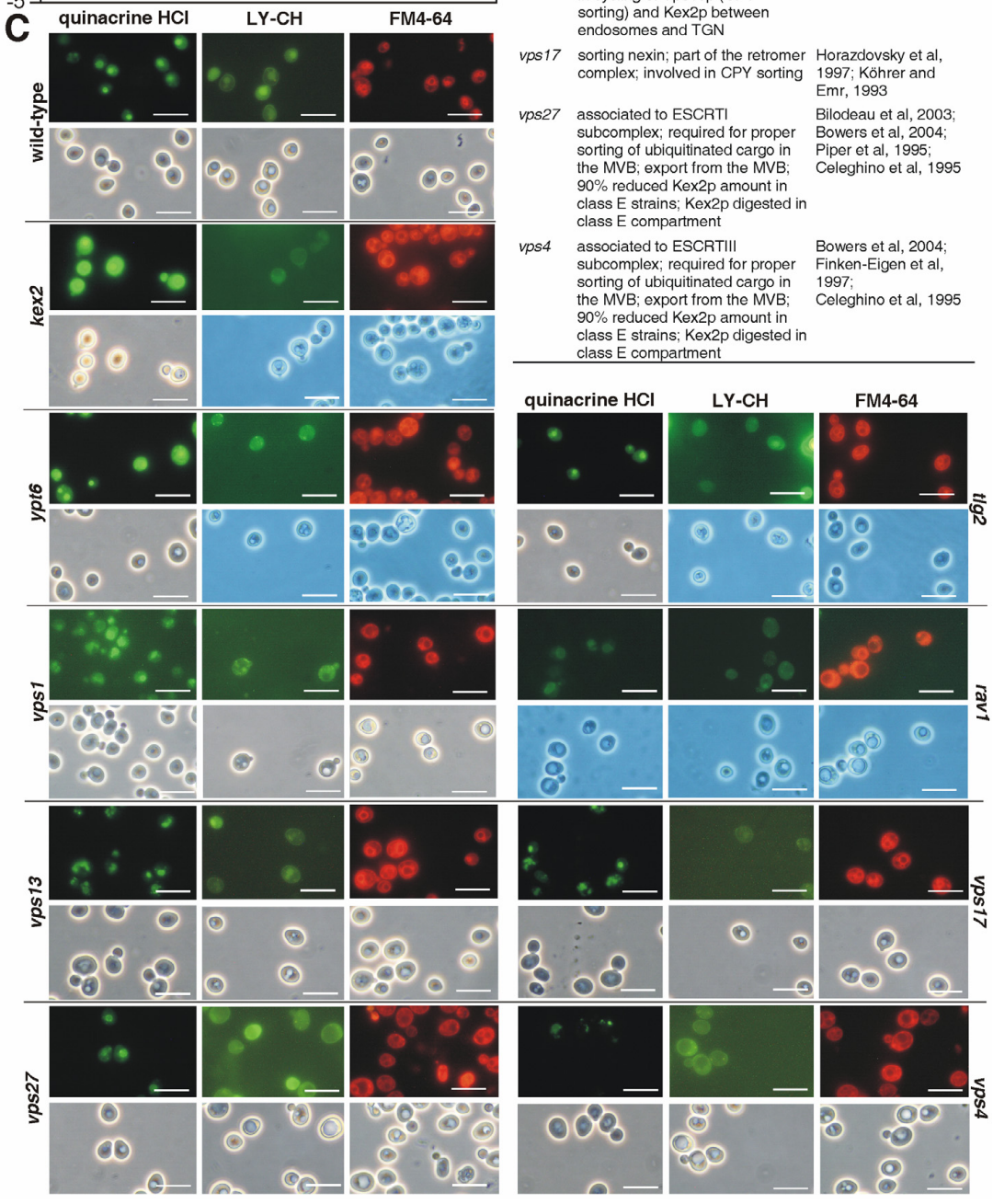

See previous page for:

Fig. 4.21: Localization of the effect of the *KEX2* deletion. (A) Transfection efficiency of mutants known to be involved in transport of Kex2p. Transfection was performed as described in "Materials and Methods". All values are given as a factor in relation to the transfection rate of the wild-type mutant (BY4741). The mean values (± s.d.) of the factors were calculated from at least three independent experiments. (B) Description of the deletion mutants used. (C) Impact of deleting genes encoding for proteins known to be involved in Kex2p transport on vacuolar acidification, Lucifer Yellow (LY-CH) accumulation and membrane dynamics in BY4741 background in YE. Vacuolar acidification after 22 hours was visualized using quinacrine-HCl staining. Quinacrine HCl accumulates in acidic compartments. Lucifer Yellow CH and FM4-64 were used to study endocytic uptake and plasma membrane dynamics after 22 hours. Photos of representative cells from one of at least two independent experiments were taken with FITC-fluorescence optics (quinacrine and LY-CH) or rhodamine optics (FM4-64) (upper panels), and with phase-contrast optics (lower panels) as described in "Materials and Methods". The bar represents 10 μm.

CH is inhibited before entering the vacuole. In FM4-64 staining a background staining was observed, probably represeng an accumulation of vesicles (Fig. 4.21 C).

Mutant *vps13* is known to be defect for retrograde transport of Kex2p from late endosomes to the TGN, so that part of Kex2p ends up in the vacuole for degradation (Brickner and Fuller, 1997). Vps17p is also involved in transport between the late endosome and TGN (Horazdovsky et al, 1997; Köhrer and Emr, 1992). The transfection efficiencies in both mutants do not explain the effect of deleting *KEX2* on transfection efficiency (Fig. 4.21 A). Effects on acidification, LY-CH accumulation or membrane dynamics are negligible in both mutants (Fig. 4.21 C).

In class E vps deletion mutants such as *vps4* and *vps27*, the Kex2p amount is reduced up to 90% (65% for *vps27*) and Kex2p which accumulates in the class E compartment is degraded there (Cereghino et al, 1995; Panek et al, 2000). Transfection efficiency in mutants *vps4* and *vps27* is comparible to transfection efficiency in the wild type (Fig 4.21 A). Reduced vacuolar acidification and large acidified structures near the vacuolar membrane are observed in class E deletion mutants *vps27* and *vps4* (Fig. 4.21 C). No accumulation of LY-CH and FM4-64 in the vacuole can be observed. Large compartments near the vacuole can be visualized using LY-CH or FM4-64, presumably representing class E compartments (Babst et al, 1997; Bowers et al, 2004; Piper et al, 1995).

These data indicate that the effect of deleting *KEX2* on transfection efficiency is a result of loss of Kex2p at the TGN.

4.7 The influence of protein glycosylation on transfection

Activities and functionality of proteins is dependent on wild-type glycosylation of these proteins and defects in higher eukaryotes lead to severe disease phenotypes (Dürr et al, 1998; Dempski and Imperiali, 2002; Helenius and Aebi, 2004). Resuming that, proteins involved in glycosylation are indicated to be an adequate target for influencing transfection efficiencies.

4.7.1 N-type and O-type glycosylation

There are two types of glycosylation in eukaryotic cells: O-type glycosylation at the carbonyl group of the peptide backbone at threonine or serine residues of proteins in the secretory pathway (Strahl-Bolsinger et al, 1999; Herscovics and Orlean, 1993) and N-type glycosylation at the amino group of the peptide backbone at asparagine (Asn) residues in a sequence triplet Asn-Xaa-Thr(Ser) of proteins in the secretory pathway (Welply et al, 1983; Knauer and Lehle, 1999; Silberstein and Gilmore, 1996) where Xaa could be any amino acid except proline (Herscovics and Orlean, 1993; Kukuruzinska et al, 1987; Yan and Lennarz, 2005; Munro, 2001).

Transfection efficiency is enhanced by a factor of 5.5 in mutant *och1* where the first N-type glycosylation step after entering the *cis*-Golgi is interrupted (Gaynor et al, 1994; Harris and Waters, 1996), (Fig. 4.22 A). In a deletion mutant defective for a later step in N-type glycosylation (mutant *mnn1*), transfection efficiency is as in the wild type. Transfection efficiency was as in the wild type in a single experiment in mutant *gnt1*, deleted for an N-acetylglucosamyltransferase involved in modification of N-linked glycans (data not shown). Enhanced acidification of the vacuole in *och1* mutant was observed in comparison to the wild type (Fig. 4.22 C). In addition, enhanced background staining in the cytoplasm in some cells was observed, maybe representing acidified smaller compartments in the cell. This background staining was also visible in *och1* for LY-CH and FM4-64 stainings. In LY-CH staining the vacuole often remains unstained, and in some cells the vacuole is fragmented in this mutant. In *mnn1*, acidification, endocytic uptake and membrane dynamics are as in the wild type.

A comparable phenotype to the phenotype in deletion mutant *och1*, described above, can also be detected in mutant *pmr1* defect for Ca^{2+} and Mn^{2+}-import into the Golgi (Fig. 4.22).

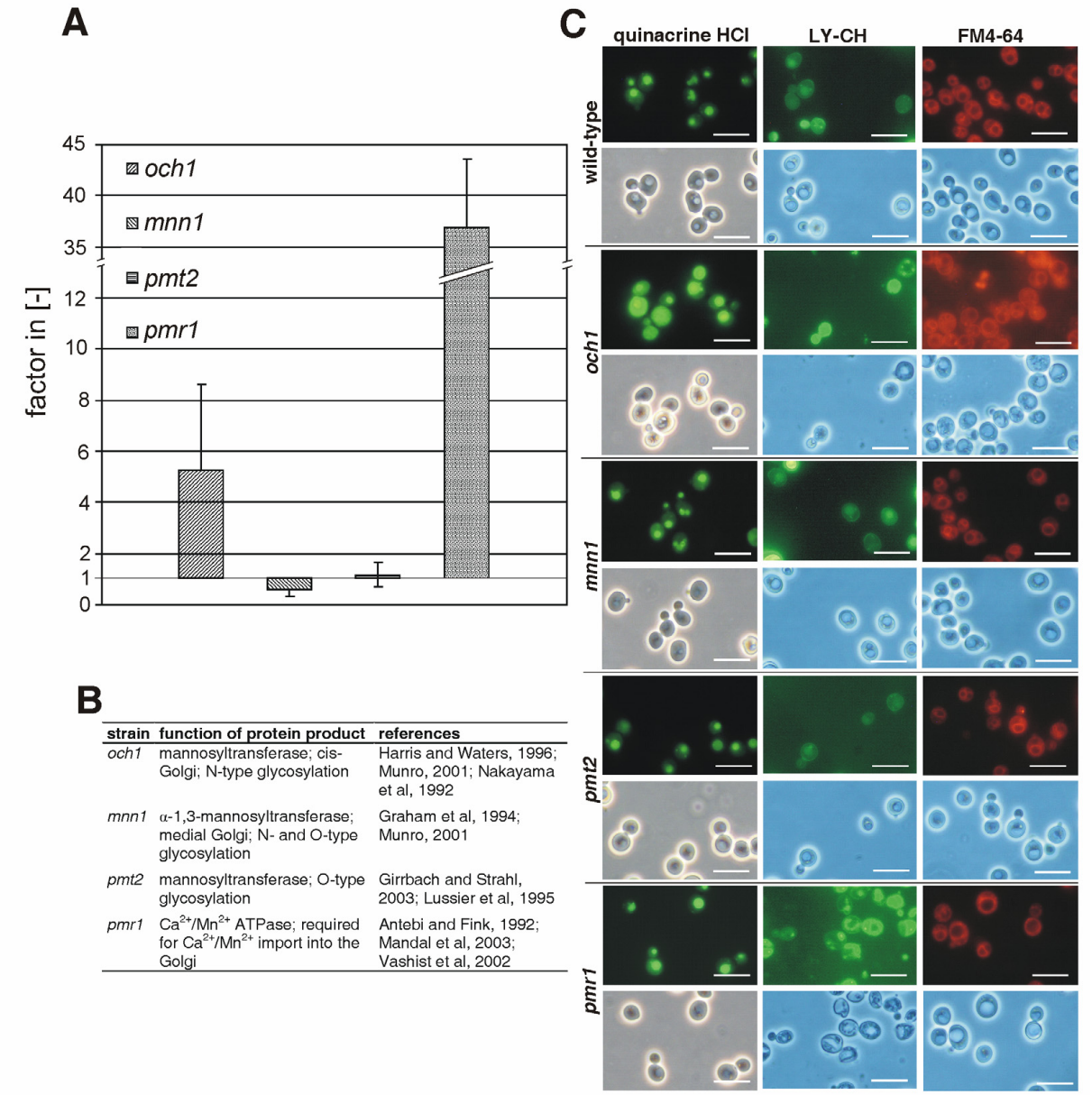

strain	function of protein product	references
och1	mannosyltransferase; cis-Golgi; N-type glycosylation	Harris and Waters, 1996; Munro, 2001; Nakayama et al, 1992
mnn1	α-1,3-mannosyltransferase; medial Golgi; N- and O-type glycosylation	Graham et al, 1994; Munro, 2001
pmt2	mannosyltransferase; O-type glycosylation	Girrbach and Strahl, 2003; Lussier et al, 1995
pmr1	Ca^{2+}/Mn^{2+} ATPase; required for Ca^{2+}/Mn^{2+} import into the Golgi	Antebi and Fink, 1992; Mandal et al, 2003; Vashist et al, 2002

Fig. 4.22: Mutants involved in glycosylation. (A) Transfection efficiency of mutants deleted for genes coding for proteins involved in N-glycosylation (*och1*, *mnn1*) and O-glycosylation (*pmt2*). Transfection was performed as described in "Materials and Methods". All values are given as a factor in relation to the transfection rate of the wild-type mutant (BY4741). The mean values (± s.d.) of the factors were calculated from at least three independent experiments. (B) Description of the deletion mutants used. (C) Impact of deleting genes encoding for proteins involved in glycosylation on vacuolar acidification, Lucifer Yellow (LY-CH) accumulation and membrane dynamics in BY4741 background in YE. Vacuolar acidification after 22 hours was visualized using quinacrine-HCl staining. Quinacrine HCl accumulates in acidic compartments. Lucifer Yellow CH and FM4-64 were used to study endocytic uptake and plasma membrane dynamics after 22 hours. Photos of representative cells from one of at least two independent experiments were taken with FITC-fluorescence optics (quinacrine and LY-CH) or rhodamine optics (FM4-64) (upper panels), and with phase-contrast optics (lower panels) as described in "Materials and Methods". The bar represents 10 μm.

Golgi glycosylation is suggested to be Ca^{2+} and known to be Mn^{2+} dependent (Antebi and Fink, 1992; Dürr et al, 1998; Munro, 2001). Och1p localization might be Ca^{2+}-dependent (Dürr et al, 1998) which might partly explain the positive effect of the

deletion of *PMR1* on transfection efficiency. In the *pmr1* mutant, as in the *och1* mutant, acidification seems to be stronger than in the wild type and endocytic transport to the vacuole is reduced where accumulation of LY-CH and FM4-64 in the cytoplasm is enhanced, maybe representing accumulating vesicles (Fig. 4.22 C).
In mutant *pmt2*, as a representative for defects in O-type glycosylation, transfection efficiency is as in the wild type mutant (Fig. 4.22 A). None of the staining procedures in this mutant showed significant differences to the wild-type phenotype (Fig. 4.22 C).

4.7.2 Outer-chain glycosylation

Due to enhanced transfection efficiency in mutant *och1*, it was interesting to know what the reason was for this effect on transfection efficiency. The first idea was that, maybe as a result of the altered cell wall properties, DNA was taken up more efficiently in mutant *och1*. This was tested with deletion mutants known to be deleted for proteins located to the cell wall in the wild type and having an outer-chain N-type glycosylation. Protein sequences were used to predict N-type glycosylation sites at SGD (http://www.yeastgenome.org/) using a licensed version of the Wisconsin Sequence Analysis Package® from the Genetics Computer Group (Fig. 4.23). The program used is called PeptideStructure.

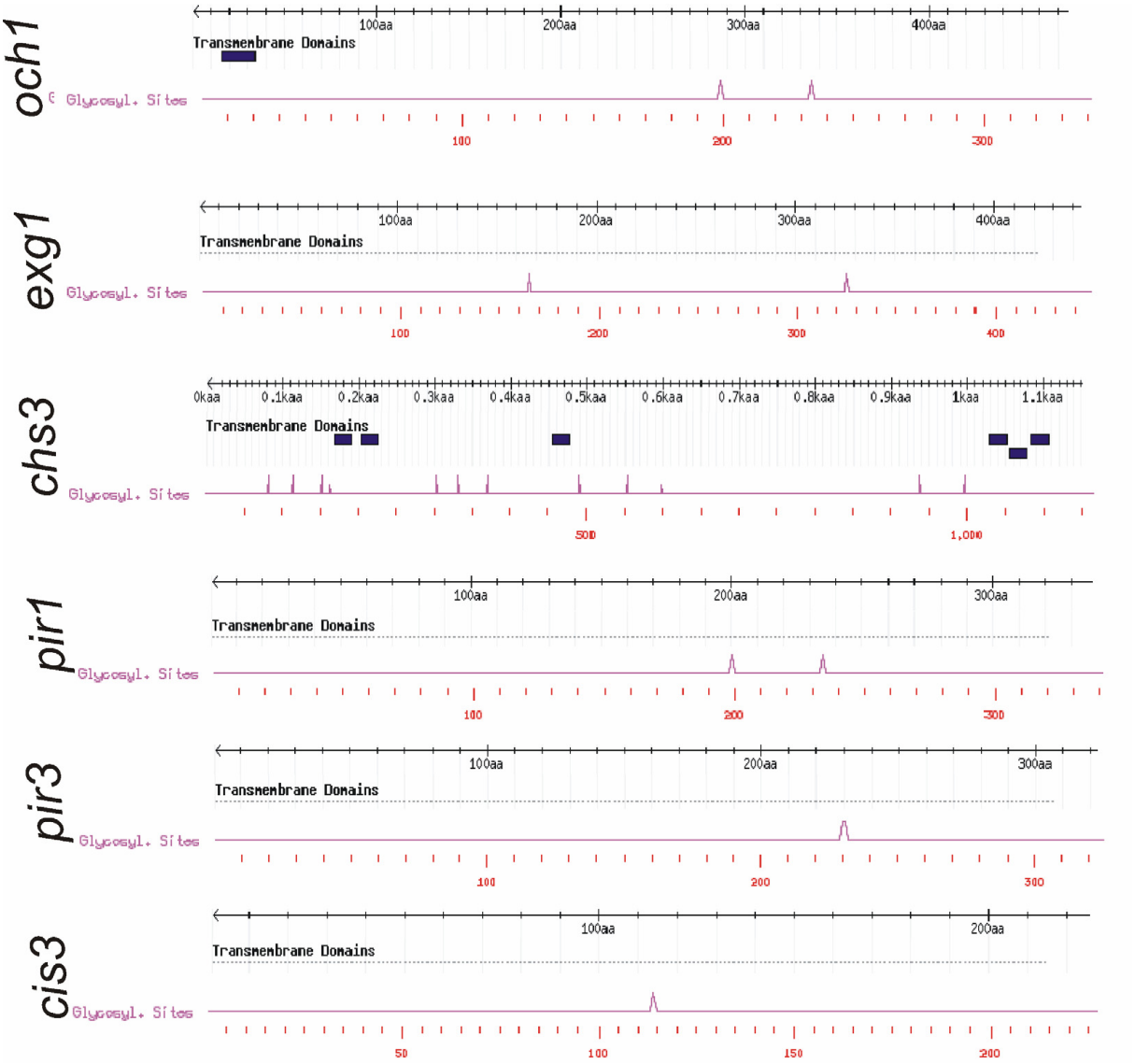

Fig. 4.23: Prediction of N-glycosylation sites in proteins deleted in mutants tested in this thesis I. Prediction was performed at SGD (http://www.yeastgenome.org/) using a licensed version of the Wisconsin Sequence Analysis Package® from the Genetics Computer Group. The program used is called PeptideStructure. Trans membrane domains were predicted using the TMHMM 2.0 server (http://www.cbs.dtu.dk/services/TMHMM-2.0/). All other predictions, which are not shown, were negative for N-type glycosylation prediction or are not sorted via the Golgi. Prediction of outer chain N-glycosylation of proteins, known to be sorted to the cell wall and tested with the transfection assay.

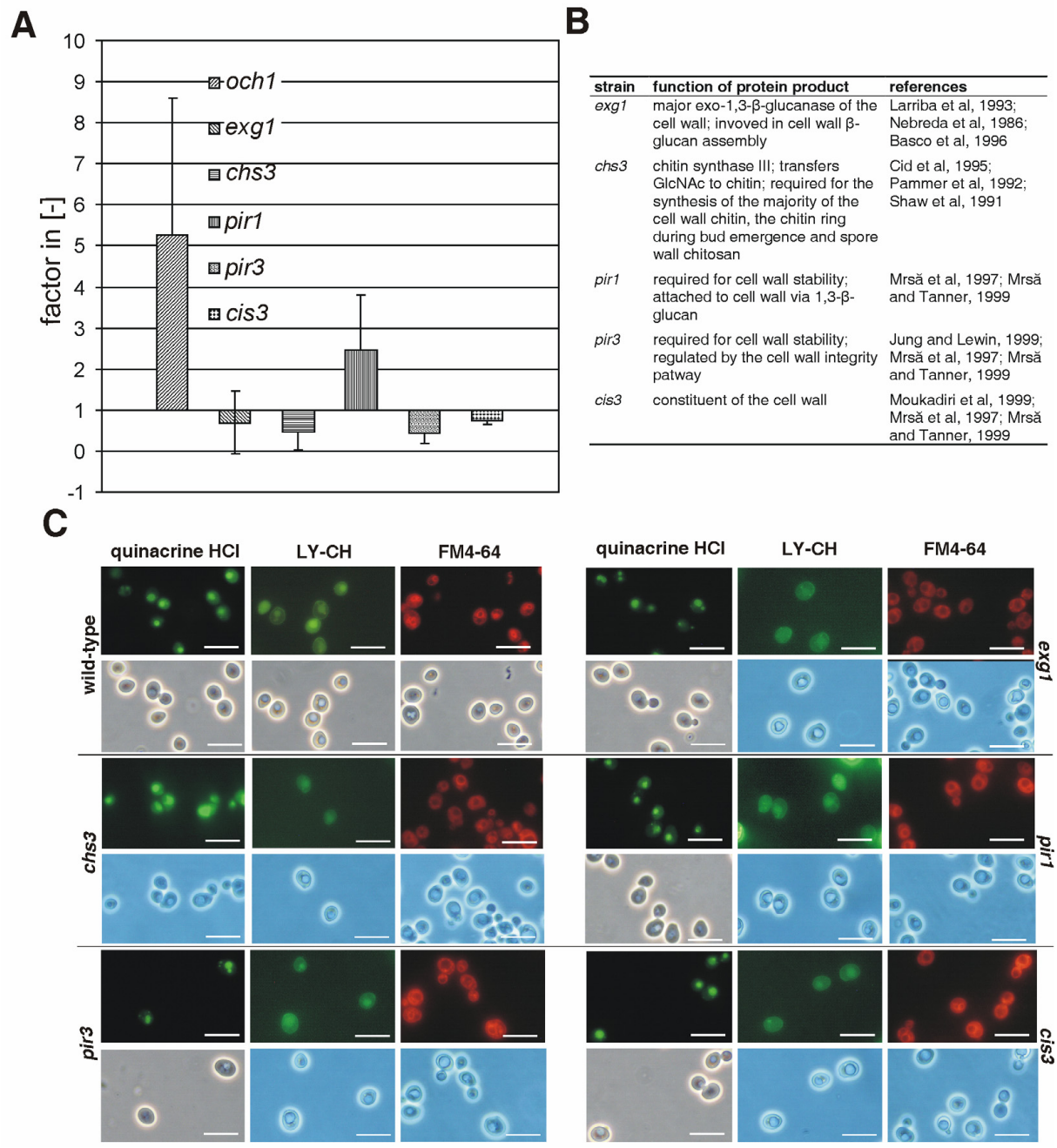

strain	function of protein product	references
exg1	major exo-1,3-β-glucanase of the cell wall; invoved in cell wall β-glucan assembly	Larriba et al, 1993; Nebreda et al, 1986; Basco et al, 1996
chs3	chitin synthase III; transfers GlcNAc to chitin; required for the synthesis of the majority of the cell wall chitin, the chitin ring during bud emergence and spore wall chitosan	Cid et al, 1995; Pammer et al, 1992; Shaw et al, 1991
pir1	required for cell wall stability; attached to cell wall via 1,3-β-glucan	Mrsă et al, 1997; Mrsă and Tanner, 1999
pir3	required for cell wall stability; regulated by the cell wall integrity patway	Jung and Lewin, 1999; Mrsă et al, 1997; Mrsă and Tanner, 1999
cis3	constituent of the cell wall	Moukadiri et al, 1999; Mrsă et al, 1997; Mrsă and Tanner, 1999

Fig. 4.24: Proteins predicted to be outer chain N-glycosylated and determined not to enhance transfection efficiency in absence. (A) Transfection efficiency of mutants deleted for genes coding for proteins predicted to be outer chain N-glycosylated and determined not to enhance transfection efficiency in absence. Transfection was performed as described in “Materials and Methods”. All values are given as a factor in relation to the transfection rate of the wild-type mutant (BY4741). The mean values (± s.d.) of the factors were calculated from at least three independent experiments. (B) Description of the deletion mutants used. (C) Impact of deleting genes encoding for proteins predicted to be outer chain N-glycosylated and determined not to enhance transfection efficiency in absence on vacuolar acidification, Lucifer Yellow (LY-CH) accumulation and membrane dynamics in BY4741 background in YE. Vacuolar acidification after 22 hours was visualized using quinacrine-HCl staining. Quinacrine HCl accumulates in acidic compartments. Lucifer Yellow CH and FM4-64 were used to study endocytic uptake and plasma membrane dynamics after 22 hours. Photos of representative cells from one of at least two independent experiments were taken with FITC-fluorescence optics (quinacrine and LY-CH) or rhodamine optics (FM4-64) (upper panels), and with phase-contrast optics (lower panels) as described in “Materials and Methods”. The bar represents 10 μm.

Not a single deletion mutant tested and predicted to be N-type glycosylated showed an effect on transfection efficiency, which might explain the effect of deleting *OCH1* on transfection (Fig. 4.24 A). The mutants tested were *exg1* which is involved in cell wall glucan layer assembly (Larriba et al, 1993; Nebreda et al, 1986; Basco et al, 1996), *chs3* which is required for the synthesis of the majority of cell wall chitin and mutants *pir1*, *pir3* and *cis3* which are deleted for structural cell wall proteins. Only in deletion mutant *pir1* transfection efficiency is slightly enhanced, but it is not as high as in mutant *och1*. A weak LY-CH transport defect was observed in mutant *exg1*. In all the other staining experiments in this and any further mutant tested lead to results comparible to the wild type and not to *och1* mutant (Fig. 4.24 C).

4.7.3 Core type glycosylation

Proteins directed to intracellular compartments via the secretory pathway are often N-type glycosylated. These proteins are only core-type glycosylated, which means that oligosaccharide residues are smaller (Munro, 2001) in the mature protein than in outer-chain glycosylated proteins. Maybe the effect of the deletion of *och1* on transfection efficiency can be explained by defects in core-type glycosylation, and as a result of that by influences on activities and functionalities of core-type glycosylated proteins.

The first group of proteins tested consisted of those which are located at the Golgi or the endosomal/vacuolar system and predicted to be core-type glycosylated by PeptideStructure program at SGD (http://www.yeastgenome.org/). These were Och1p, Mnn1p, Pmr1p, Stv1p, Vph1p, Nhx1p and Kex2p (Fig. 4.25).

Deletion of *PMR1* leads to enhanced transfection efficiency. Acidification was enhanced, as with mutant *och1*; transport defects were also detected (Fig. 4.26). Och1p activity is dependent on Mn^{2+}- and Ca^{2+}-ions, imported to the Golgi by Pmr1p (Antebi and Fink, 1992; Dürr et al, 1998; Munro, 2001). Defects in the V0-subunit of the V-ATPase in mutants *stv1* and *vph1* resulted in enhanced transfection efficiency. Acidification is enhanced and transport defects were detected in *stv1*, as is the case with the *och1* mutant but were less prominent than in the *och1* background. Kex2p is core-type glycosylated and the corresponding deletion mutant presents enhanced transfection efficiency and a comparable effect on acidification as *och1* mutant.

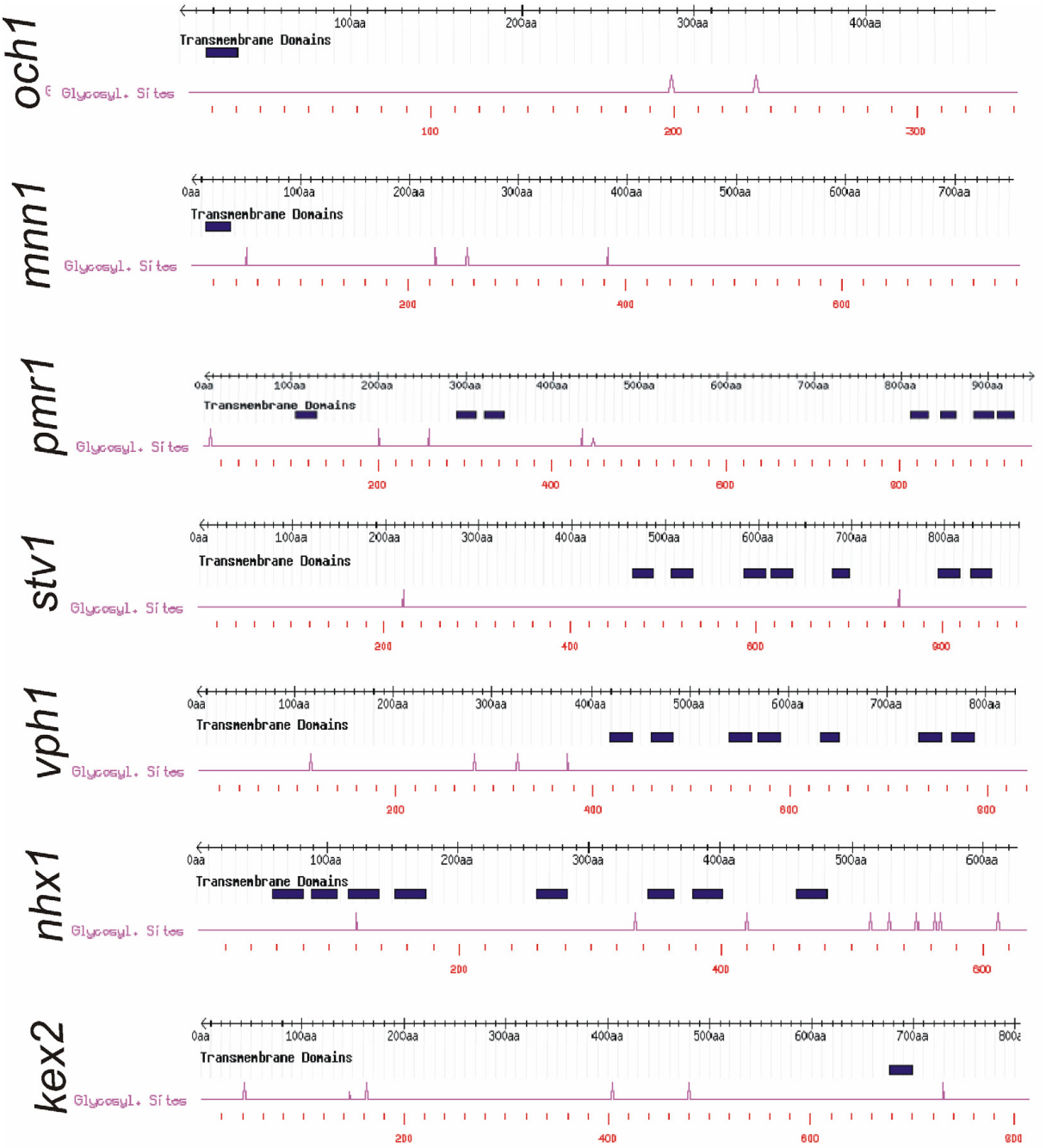

Fig. 4.25: Prediction of N-glycosylation sites in proteins deleted in mutants tested in this thesis II. Prediction was performed at SGD (http://www.yeastgenome.org/) using a licensed version of the Wisconsin Sequence Analysis Package® from the Genetics Computer Group. The program used is called PeptideStructure. Trans membrane domains were predicted using the TMHMM 2.0 server (http://www.cbs.dtu.dk/services/TMHMM-2.0/). Prediction of core-type N-glycosylation of proteins, known to be sorted to the Golgi or endosomal/vacuolar system via the secretory pathway and determined to enhace transfection eficiecy in absence.

As is the case with Och1p, Kex2p is also Ca^{2+}- dependent (Fuller et al, 1989). Transport defects are visible in *kex2* mutant, as is the case with the *och1* mutant, but in the *kex2* mutant the background staining is less predominant. Kex2p and Och1p activities seem to influence acidification of endosomal/vacuolar compartments and are regulated by Pmr1p activity.

Deletion of *NHX1* results in enhanced transfection efficiency (Fig. 4.26 A). Nhx1p is known to be core-type N-glycosylated (Wells and Rao, 2001). Nhx1p is relevant for import of K^+-ions to the late endosome (Ali et al, 2004; Mukherjee et al, 2006; Nass et al, 1997). Kex2p activity is K^+-ion dependent (Rockwell and Fuller, 2002) and Kex2p is sorted between TGN and endosomes (Tsukada and Gallwitz, 1996; Luo and Chang, 1997; Brickner and Fuller, 1997; Sipos et al, 2004; Chen et al, 2005; Blanchette et al, 2004). Acidification and endocytic transport in *nhx1* seem to be comparable to the wild type after 22 hours of incubation during staining procedures (Fig. 4.26 C).

The second group of proteins located at the Golgi or the endosomal/vacuolar system and predicted to be core-type glycosylated by the PeptideStructure program at SGD consists of Och1p, Mnn1p, Pmt2p, Tlg2p, Vcx1p, Pmc1p, Yvc1p, Kex1p and Ste13p (Fig. 4.27).

See following page for:

Fig. 4.26: Proteins predicted to be core-type N-glycosylated and determined to enhance transfection efficiency in absence. (A) Transfection efficiency of mutants deleted for genes coding for proteins predicted to be core-type N-glycosylated and determined to enhance transfection efficiency in absence. Transfection was performed as described in “Materials and Methods”. All values are given as a factor in relation to the transfection rate of the wild-type mutant (BY4741). The mean values (± s.d.) of the factors were calculated from at least three independent experiments. (B) Description of the deletion mutants used. (C) Impact of deleting genes encoding for proteins predicted to be core-type N-glycosylated and determined to enhance transfection efficiency in absence on vacuolar acidification, Lucifer Yellow (LY-CH) accumulation and membrane dynamics in BY4741 background in YE. Vacuolar acidification after 22 hours was visualized using quinacrine-HCl staining. Quinacrine HCl accumulates in acidic compartments. Lucifer Yellow CH and FM4-64 were used to study endocytic uptake and plasma membrane dynamics after 22 hours. Photos of representative cells from one of at least two independent experiments were taken with FITC-fluorescence optics (quinacrine and LY-CH) or rhodamine optics (FM4-64) (upper panels), and with phase-contrast optics (lower panels) as described in “Materials and Methods”. The bar represents 10 μm.

Fig. 4.26: See previous page for legend

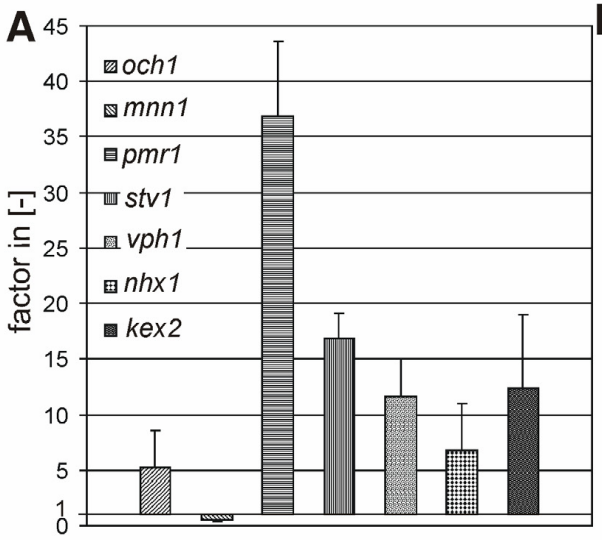

B

strain	function of protein product	references
och1	mannosyltransferase; cis-Golgi; N-type glycosylation	Harris and Waters, 1996; Munro, 2001; Nakayama et al, 1992
mnn1	α-1,3-mannosyltransferase; medial Golgi; N- and O-type glycosylation	Graham et al, 1994; Munro, 2001
pmr1	Ca^{2+}/Mn^{2+} ATPase; required for Ca^{2+}/Mn^{2+} import into the Golgi	Antebi and Fink, 1992; Mandal et al, 2003; Vashist et al, 2002
stv1	present in V0–subunit of V-ATPase at Golgi and endosomes	Manolson et al, 1997; Perzov et al, 2002
vph1	present in V0–subunit of V-ATPase at vacuole	Manolson et al, 1997; Perzov et al, 2002
nhx1	$Na^{+}(K^{+})/H^{+}$ antiporter at late endosome; ion homeostasis, intracellular pH and vesicle trafficking	Ali et al, 2004; Mukherjee et al, 2006; Nass, et al, 1997
kex2	subtilisin-like serine endoprotease; activation of proteins in the Golgi (e.g.: α-factor precoursor, killer toxin); present mainly at the TGN, but also in endosomes; Ca^{2+}-dependent	Bryant and Stevens, 1997; Fuller et al, 1989; Henkel et al, 1999; Lewis et al, 2000

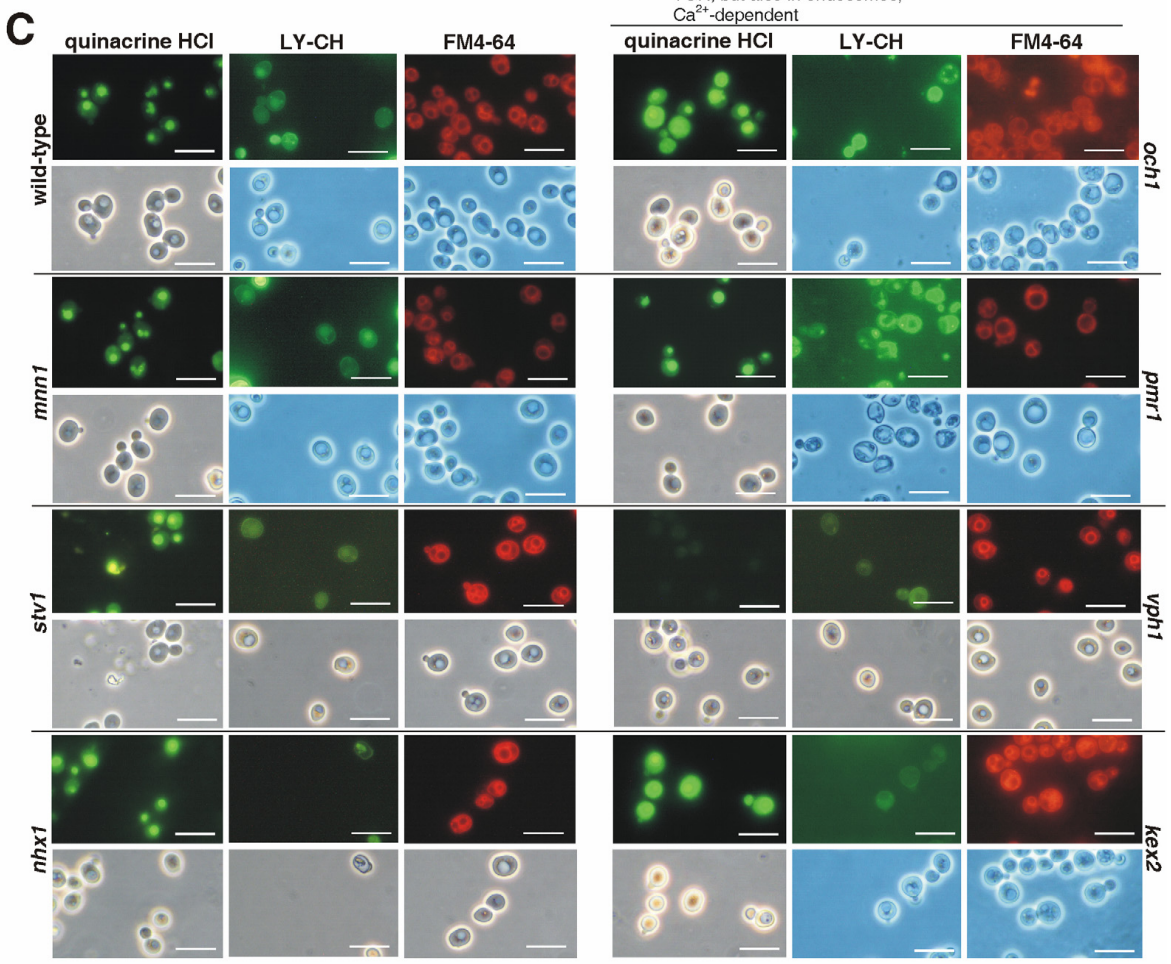

Fig. 4.27: See following page for legend

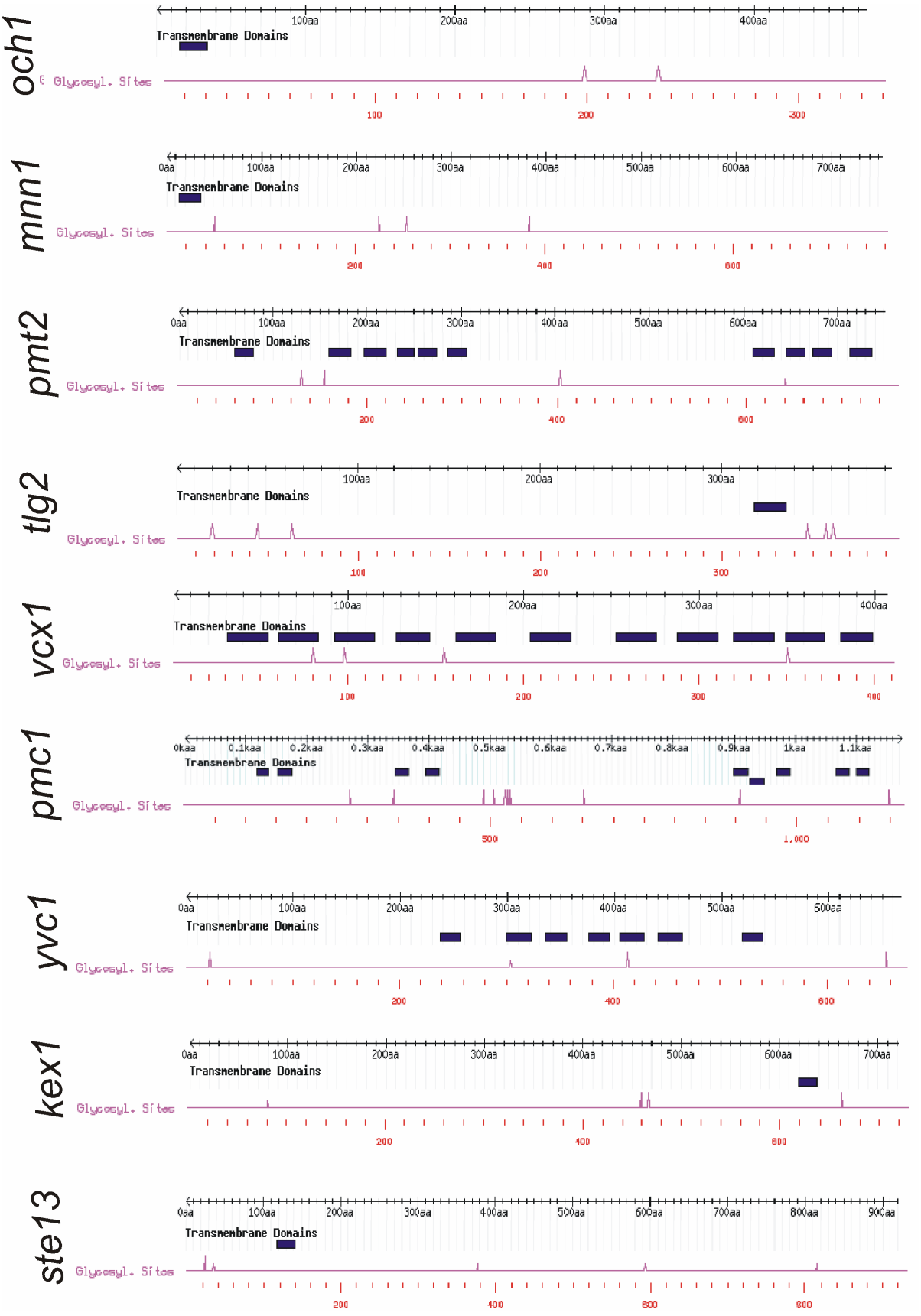

See previous page for:

Fig. 4.27: Prediction of N-glycosylation sites in proteins deleted in mutants tested in this thesis III. Prediction was performed at SGD (http://www.yeastgenome.org/) using a licensed version of the Wisconsin Sequence Analysis Package® from the Genetics Computer Group. The program used is called PeptideStructure. Trans membrane domains were predicted using the TMHMM 2.0 server (http://www.cbs.dtu.dk/services/TMHMM-2.0/). Prediction of core-type N-glycosylation of proteins, known to be sorted to the Golgi or endosomal/vacuolar system via the secretory pathway and determined not to enhace transfection eficiecy in absence.

No significant effect on transfection efficiency could be observed in the deletion mutants *mnn1*, *tlg2*, *vcx1*, *pmc1*, *yvc1*, *kex1*, and *ste13*. This indicates that a defect in core-type glycosylation is not a sufficient condition to affect transfection efficiency (Fig. 4.28 A). Acidification, endocytic transport and transport dynamic phenotypes are not significantly different to phenotypes observed in the wild type (Fig. 4.28 C).

See following page for:

Fig. 4.28: Proteins predicted to be core-type N-glycosylated and determined not to enhance transfection efficiency in absence. (A) Transfection efficiency of mutants deleted for genes coding for proteins predicted to be core-type N-glycosylated and determined not to enhance transfection efficiency in absence. Transfection was performed as described in “Materials and Methods”. All values are given as a factor in relation to the transfection rate of the wild-type mutant (BY4741). The mean values (± s.d.) of the factors were calculated from at least three independent experiments. (B) Description of the deletion mutants used. (C) Impact of deleting genes encoding for proteins predicted to be core-type N-glycosylated and determined not to enhance transfection efficiency in absence on vacuolar acidification, Lucifer Yellow (LY-CH) accumulation and membrane dynamics in BY4741 background in YE. Vacuolar acidification after 22 hours was visualized using quinacrine-HCl staining. Quinacrine HCl accumulates in acidic compartments. Lucifer Yellow CH and FM4-64 were used to study endocytic uptake and plasma membrane dynamics after 22 hours. Photos of representative cells from one of at least two independent experiments were taken with FITC-fluorescence optics (quinacrine and LY-CH) or rhodamine optics (FM4-64) (upper panels), and with phase-contrast optics (lower panels) as described in “Materials and Methods”. The bar represents 10 μm.

Fig. 4.28: See previous page for legend

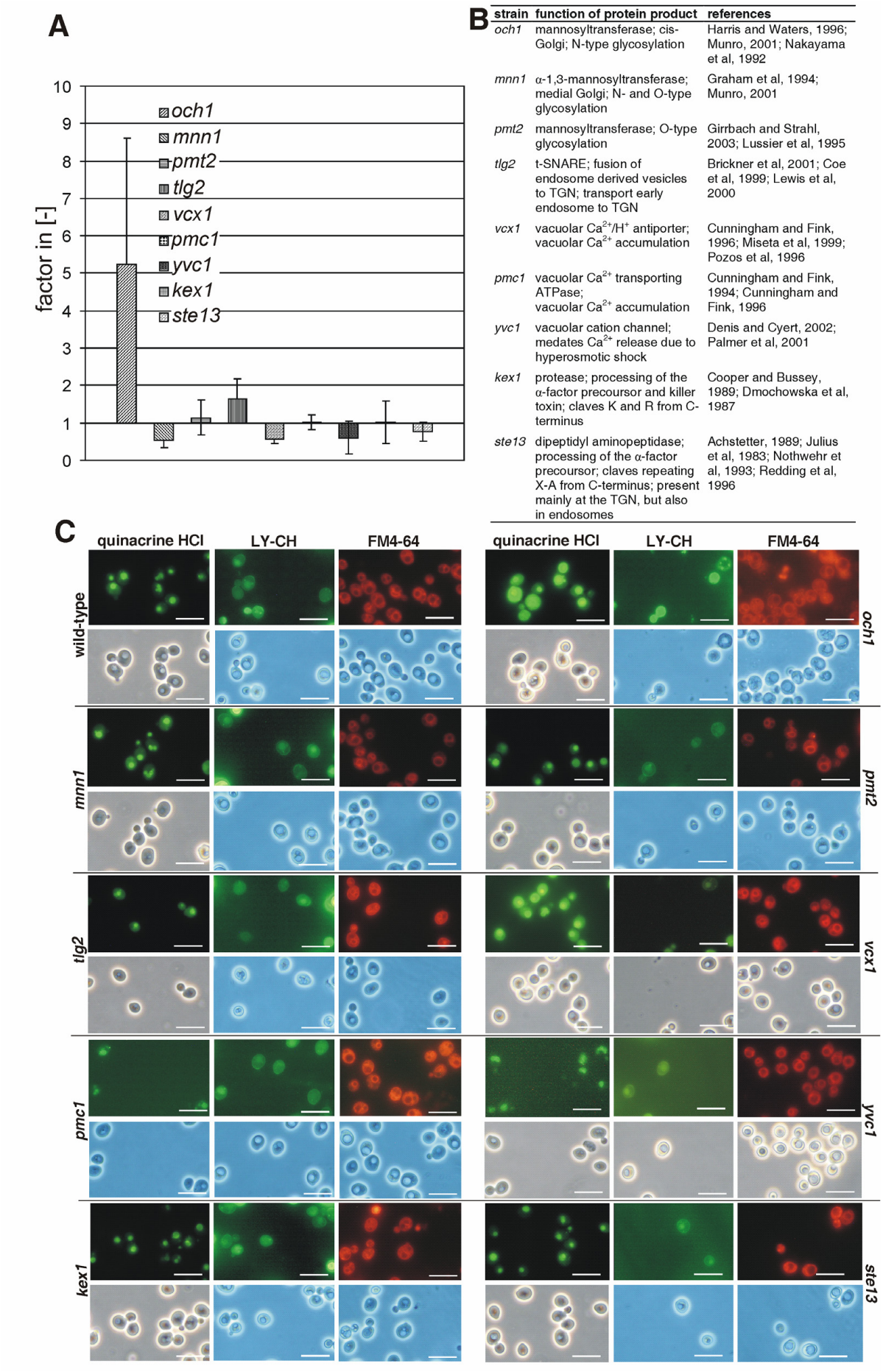

strain	function of protein product	references
och1	mannosyltransferase; cis-Golgi; N-type glycosylation	Harris and Waters, 1996; Munro, 2001; Nakayama et al, 1992
mnn1	α-1,3-mannosyltransferase; medial Golgi; N- and O-type glycosylation	Graham et al, 1994; Munro, 2001
pmt2	mannosyltransferase; O-type glycosylation	Girrbach and Strahl, 2003; Lussier et al, 1995
tlg2	t-SNARE; fusion of endosome derived vesicles to TGN; transport early endosome to TGN	Brickner et al, 2001; Coe et al, 1999; Lewis et al, 2000
vcx1	vacuolar Ca^{2+}/H^{+} antiporter; vacuolar Ca^{2+} accumulation	Cunningham and Fink, 1996; Miseta et al, 1999; Pozos et al, 1996
pmc1	vacuolar Ca^{2+} transporting ATPase; vacuolar Ca^{2+} accumulation	Cunningham and Fink, 1994; Cunningham and Fink, 1996
yvc1	vacuolar cation channel; medates Ca^{2+} release due to hyperosmotic shock	Denis and Cyert, 2002; Palmer et al, 2001
kex1	protease; processing of the α-factor precoursor and killer toxin; claves K and R from C-terminus	Cooper and Bussey, 1989; Dmochowska et al, 1987
ste13	dipeptidyl aminopeptidase; processing of the α-factor precoursor; claves repeating X-A from C-terminus; present mainly at the TGN, but also in endosomes	Achstetter, 1989; Julius et al, 1983; Nothwehr et al, 1993; Redding et al, 1996

4.7.4 Cell wall proteins

Transfection efficiency might also be affected by the composition and structure of the cell wall. Different surface charges, for example, could either reduce or enhance proximity of plasmid DNA to the cell surface under transfection conditions. Several cell wall mutants were tested in order to test the influence of cell surface structure and constitution on transfection efficiency.

The yeast cell wall consists of a β-glucan layer, cell wall chitin and proteins (Klis et al, 2006; Smits et al, 2001). Three deletion mutants, representing the major influencing factors for each subcomponent of the cell wall, were used in transfection. Mutant *exg1* is deleted for the major cell wall β-1,3-glucanase, important in cell wall glucan assembly. *chs3* is deleted for chitin synthase III, responsible for the synthesis of the majority of cell wall chitin, and *cwp2* is deleted for the major cell wall protein in *S. cerevisiae* (1,590,000 molecules per cell; http://www.yeastgenome.org). Transfection efficiency is decreased significantly in comparison to the wild type for all three mutants. Reduced endocytic accumulation of LY-CH was observed in mutant *cwp2* (Fig. 4.29). This indicates that changes in the cell wall, which reduce the proximity of plasmid DNA to the cell surface, which is needed for endocytic uptake, weakly reduce transfection efficiency.

See following page for:

Fig. 4.29: Mutants deleted for cell wall proteins. (A) Transfection efficiency of mutants deleted for genes coding for proteins which are important for cell wall structure. Transfection was performed as described in “Materials and Methods”. All values are given as a factor in relation to the transfection rate of the wild-type mutant (BY4741). The mean values (± s.d.) of the factors were calculated from at least three independent experiments. (B) Description of the deletion mutants used. (C) Impact of deleting genes encoding for proteins which are important for cell wall structure on vacuolar acidification, Lucifer Yellow (LY-CH) accumulation and membrane dynamics in BY4741 background in YE. Vacuolar acidification after 22 hours was visualized using quinacrine-HCl staining. Quinacrine HCl accumulates in acidic compartments. Lucifer Yellow CH and FM4-64 were used to study endocytic uptake and plasma membrane dynamics after 22 hours. Photos of representative cells from one of at least two independent experiments were taken with FITC-fluorescence optics (quinacrine and LY-CH) or rhodamine optics (FM4-64) (upper panels), and with phase-contrast optics (lower panels) as described in “Materials and Methods. The bar represents 10 μm.

Fig. 4.29: See previous page for legend

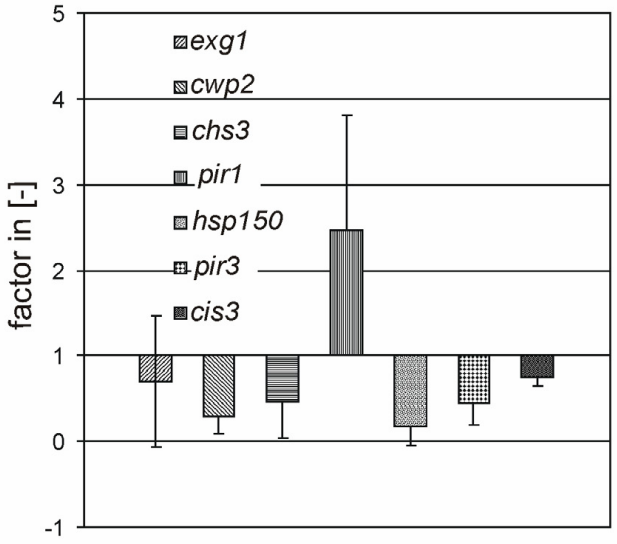

B

strain	function of protein product	references
exg1	major exo-1,3-β-glucanase of the cell wall; invoved in cell wall β-glucan assembly	Larriba et al, 1993; Nebreda et al, 1986; Basco et al, 1996
cwp2	major constituent of the cell wall; covalently linked mannoprotein; sabilizes the cell wall; involved in low pH resistance; GPI anchored	Skrzypek et al, 1997; van der Vaart et al, 1995
chs3	chitin synthase III; transfers GlcNAc to chitin; required for the synthesis of the majority of the cell wall chitin, the chitin ring during bud emergence and spore wall chitosan	Cid et al, 1995; Pammer et al, 1992; Shaw et al, 1991
pir1	required for cell wall stability; attached to cell wall via 1,3-β-glucan	Mrsă et al, 1997; Mrsă and Tanner, 1999
hsp150	secreted heat shock protein; required for cell wall stability; attached to cell wall via 1,3-β-glucan and S-S bridges; induced under stress conditions (e.g.: N-limitation)	Kapteyn et al, 1999; Moukadiri and Zueco, 2001; Mrsă et al, 1997; Mrsă and Tanner, 1999; Russo et al, 1992; Russo et al, 1993
pir3	required for cell wall stability; regulated by the cell wall integrity patway	Jung and Lewin, 1999; Mrsă et al, 1997; Mrsă and Tanner, 1999
cis3	constituent of the cell wall	Moukadiri et al, 1999; Mrsă et al, 1997; Mrsă and Tanner, 1999

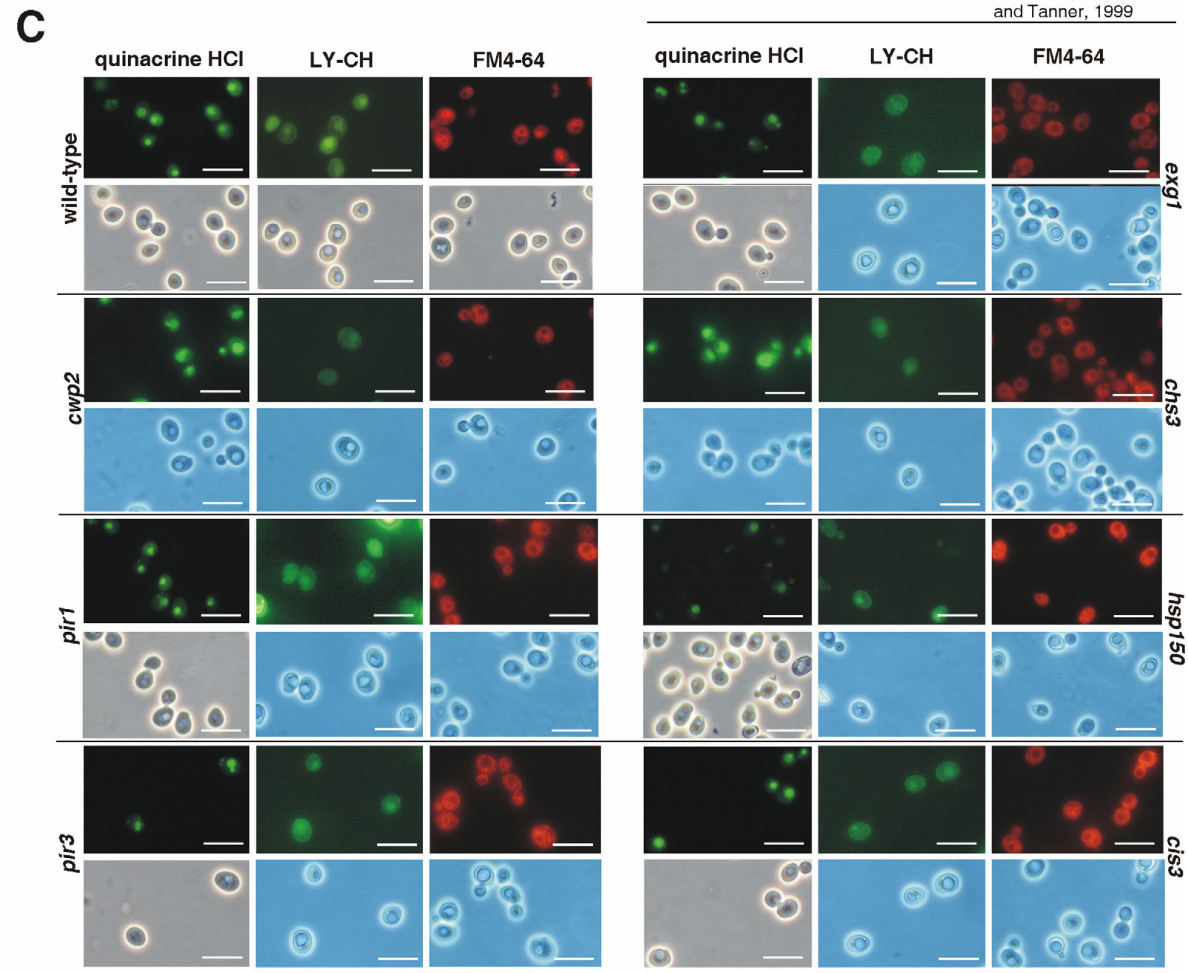

Reduced transfection efficiency was also observed for mutants *hsp150*, *pir3* and *cis3*, whereas the reduction of transfection efficiency in mutant *cis3* as in *exg1* is negligible (Fig. 4.29 A). A weak enhanced transfection efficiency was detected in mutant *pir1*. No significant differences to the wild type could be observed for mutants *exg1*, *pir1*, *hsp150*, *pir3* and *cis3* with quinacrine, LY-CH and FM4-64 stainings (Fig. 4.29 C). Proteins Pir1p, Hsp150p, Pir3p and Cis3p are constituents of the cell wall and proteolytical processed by Kex2p (Moukadiri et al, 1999; Mrsă et al, 1997; Mrsă and Tanner, 1999; Castillo et al, 2003). Cell wall proteins and enzymes or proteins affecting cell wall maintenance such as Egt2p, Fks1p, Flc2p, Gas4p, Gsc2p, Kre6p, Rot2p, Scw4p, Slt2p, Tip1p, Ypk2p, Yea4, Yps1 and Yps3 were tested in single experiments with comparable results as regards their influence on transfection efficiency (data not shown). Transfection efficiencies were neither significantly enhanced in comparison to the wild type nor decreased as in the first three examples of this chapter for these deletion mutants.

Summarizing these results, it seems that the cell wall for transfection efficiency is only of minor relevance.

5 Discussion

In this study yeast was used as a model to analyse endocytic uptake, transport and liberation of endocytosed DNA. Furthermore, the influence of endosomal/vacuolar pH-value, ion composition and hydrolase composition on DNA delivery was studied. The study revealed that there are two direct influences which are important to enhance transfection efficiency: the localization where endocytosed DNA accumulates during transfection and the degradation of the DNA at that place.

5.1 Transfection efficiency in correlation to localization of endocytosed DNA

Transfection efficiency is lower than under wild-type conditions when transport of endocytosed DNA is inhibited at a very early stage, as shown for mutants *rcy1* and *yil064w* (Fig. 5.1 A, B (a)). In these mutants, endocytosed material is predominantly accumulated in early endosomes, as seen with the LY-CH and FM4-64 experiments.
The level of transfection efficiency is as in the wild type when endocytosed DNA is located to the PVC/MVB as demonstrated by mutants *vps27* and *vps4* which are representatives for class E vps mutants (Fig. 5.1 A, C). This kind of mutation leads to the accumulation of any material which enters the class E compartment in there, due to a highly effective export defect from this compartment (Finken-Eigen et al, 1997; Piper et al, 1995).
Positive effects on transfection efficiency were observed in the mutants *rav1*, *vps21* and *vam6* (Fig. 5.1 A, B, E). Rav1p, being part of the RAVE complex (Smardon et al, 2002, Seol et al, 2001), is involved in transport between the early endosome and the PVC/MVB; Vps21p is a GTPase important in the fusion process of vesicles from the early endosome to the PVC/MVB (Gerrard et al, 2000[b]; Horazdovsky et al, 1994; Singer-Krüger et al, 1995), whereas Vam6p is part of the HOPS-complex and is involved in homotypic vacuolar fusion and fusion of PVC/MVB derived membranes to vacuolar membranes (Nakamura et al, 1997; Wada et al, 1992). In all these mutants, a diffuse background staining in LY-CH and FM4-64 experiments was observed at different stringencies. This background staining confirmed expectations that vesicles will accumulate in mutants *rav1*, *vps21* and *vam6*.
These observations allow the conclusion that the later in endocytic delivery endocytosed DNA accumulates, the more positive the effect on transfection efficiency. Class E vps-mutants are an exception to this rule. What is even more

important is that transfection efficiency is strongly enhanced when endocytosed DNA accumulates in vesicular compartments instead of endosomes or the vacuole.

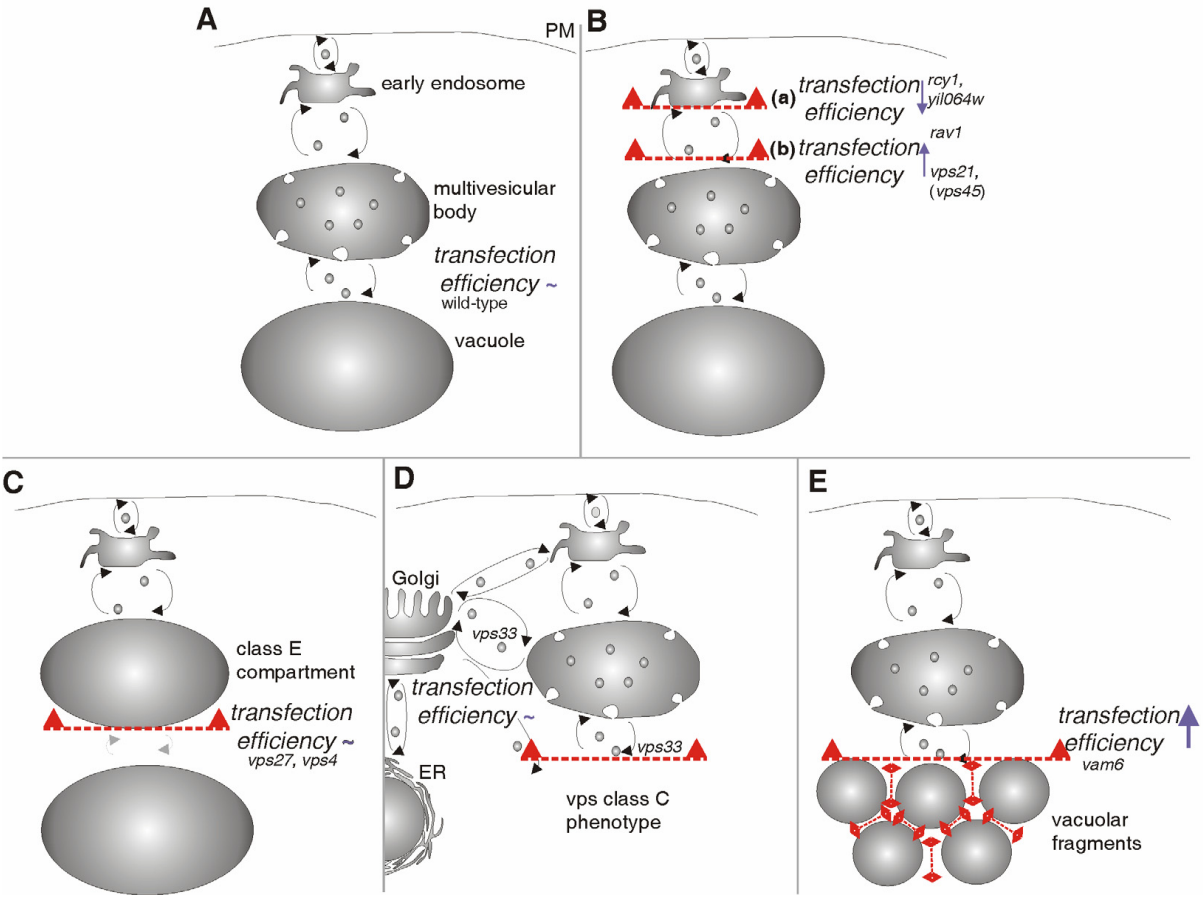

Fig. 5.1: Resuming model concerning transfection efficiency in correlation to membrane transport. Interrupting endocytic transport at different steps influences the transfection efficiency differently. The broken line with triangles represents the accumulation of endocytosed DNA. A: BY4741; B: (a) BY4741 *rcy1*, BY4741 *yil064w*; (b) BY4741 *rav1*, BY4741 *vps21*, BY4741 *vps45*; C: BY4741 *vps27*, BY4741 *vps4*; D: BY4741 *vps33*; E: BY4741 *vam6*, PM: plasma membrane.

5.2 Transfection efficiency in correlation to endocytic/vacuolar degradation

During endocytosis, extracellular material is taken up into the cell for nutrition purposes. Signal transduction in receptor mediated endocytosis involves endocytosis too. Macromolecules and larger structures are taken up by endocytic uptake especially in higher eukaryotes. Autophagy is involved in supplying the cell with nutrients under starvation conditions. Autophagocytosed material and endocytosed material will be degraded during endocytosis and in the vacuole/lysosome (Steinman et al, 1983; Onodera and Ohsumi, 2005; Mizushima et al, 2002; Nair and Klionsky,

2005). Hydrolases in the endocytic/vacuolar system are responsible for these degradation processes and might negatively affect transfection efficiency.

5.2.1 Endocytic/vacuolar DNases

First targets when considering transfection efficiency in correlation to degradation are endososmal/vacuolar DNases. Lysosomal DNases of higher eukaryotes are known to decrease transfection efficiency (Howell et al, 2003). There are at least three DNases known to be located to lysosomes in higher eukaryotes. One of these is the conserved lysosomal DNaseII (DNaseII-α) which is ubiquitously distributed over all tissues (Evans and Aquilera, 2003) and is predominantly important during apoptosis. Lysosomal DNASE2B (DLAD or DNaseII-β) is expressed predominantly in the salivary gland and lung tissue (Shiokawa and Tanuma, 1999; Shiokawa and Tanuma, 2001). Muscle specific DNASE1L1 (XIB or DNaseX) (Malferrari et al, 1999) is highly similar to DNaseI, but in contrast to DNaseI DNASE1L1 can be found in muscular lysosomes. However, there are no vacuolar DNases in *Saccharomyces cerevisiae*. Protein sequences of human lysosomal DNases DNaseII, DNASE2B and DNASE1L1 were used in BLAST searches of the *Saccharomyces cerecisiae* proteome using WU-BLAST2 (http://seq.yeastgenome.org/cgi-bin/blast-sgd.pl) with standard adjustments, but no homologies were detected (data not shown).

There are, however, two predicted nucleases Ngl1p and Ngl3p in yeast. The biological process Ngl1p and Ngl3p are involved in, and the intracellular localization, is unknown. It has been known since July 2006 that Ngl1p can be found in mitochondria (Reinders et al, 2006) and both putative nucleases have similarities to Ngl2p, a RNase involved in 5.8S rRNA processing (Faber et al, 2002). Mutations in genes *NGL1*, *NGL2* and *NGL3* did not significantly affect transfection efficiency in correlation to the wild type (data not shown). Lysosomal DNases in mammalian cells do affect transfection efficiency and due to the observation that Ngl1p and Ngl3p do not do this, it can be assumed that they are no vacuolar DNases.

As it is highly improbable that there is no DNase activity in yeasts vacuoles, specific DNases have to be identified. A possible impact on transfection of DNases imported to the vacuole via autophagy is reported on later in this discussion.

5.2.2 Endocytic/vacuolar processing proteases

At this stage our aim was to detect an indirect influence by processing enzymes on transfection efficiency, because no vacuolar DNases, as a direct impact on transfection, were detected in yeast. Endocytic/vacuolar hydrolases are proteolytically processed in most cases. Proteolytic processing has been described in detail for CPY, PrA and PrB as model hydrolases in *S. cerevisiae*, (Jones, 2002; Jones et al, 1982; Zubenko et al, 1983; Kato et al, 2006). It was therefore assumed that a potential yeast vacuolar DNase also has to be processed by a protease to be activated, as is also known for human lysosomal DNaseII-α (MacLea et al, 2003). Therefore, many known proteases of the yeast endosomal/vacuolar system were tested in this thesis for their influence on transfection efficiency. Deletion mutants lacking Pep4p, Prb1p, Ape3p, Cps1p, Dap2p, Lap4p, and Prc1p, respectively, were examined for the influence on transfection efficiency, but no significant effects were detected. This indicates that proteases are not involved in processing a potential yeast vacuolar DNase. These results did not encourage the search for further DNases or processing proteases, and due to this the focus was turned towards mutations which might help avoid contact between endocytosed DNA and degrading conditions further on.

5.2.3 Transport of hydrolases

The first choice to avoid contact of hydrolases and endocytosed DNA is to interrupt endocytosis before hydrolases and DNA intersect. The best studied sorting pathway for vacuolar hydrolases extends from the TGN via the PVC/MVB to the vacuole, or generally named the late endosomal vacuolar protein sorting. The endocytic transport is inhibited before DNA enters the PVC/MVB in the mutant deleted for *VPS21*. This reduces the contact of the endocytosed DNA coming from the early endosome with degradation conditions and results in enhanced transfection efficiency (Fig. 5.1 A, B (b)). This confirms the hypothesis that enhanced transfection efficiency is a result of reduced influence of endosomal/vacuolar hydrolases. Many hydrolases such as PrA and others are sorted via the CPY pathway from the TGN, passing the PVC/MVB to the vacuole (Cooper and Stevens, 1996). Contact of endocytosed DNA to hydrolases using the CVT/autophagy pathway and the ALP pathway is also avoided. This interpretation is supported by analogous results in the *vps45* mutant. Vps45p and Vps21p both act in the same protein complex in transport processes from the Golgi to

the endosomes (Burd et al, 1997; Tall et al, 1999). Vps45p is only involved in transport from the TGN to the PVC/MVB and not directly in endocytosis as Vps21p (Bryant et al, 1998).

Slightly enhanced transfection efficiency was observed in *vps17* mutant. Vps17p being part of the retromer complex (Seaman et al, 1998), seems to be involved in transport of hydrolases which are of only minor influence on transfection efficiency, for example the important vacuolar processing protease PrA (Cooper and Stevens, 1996)

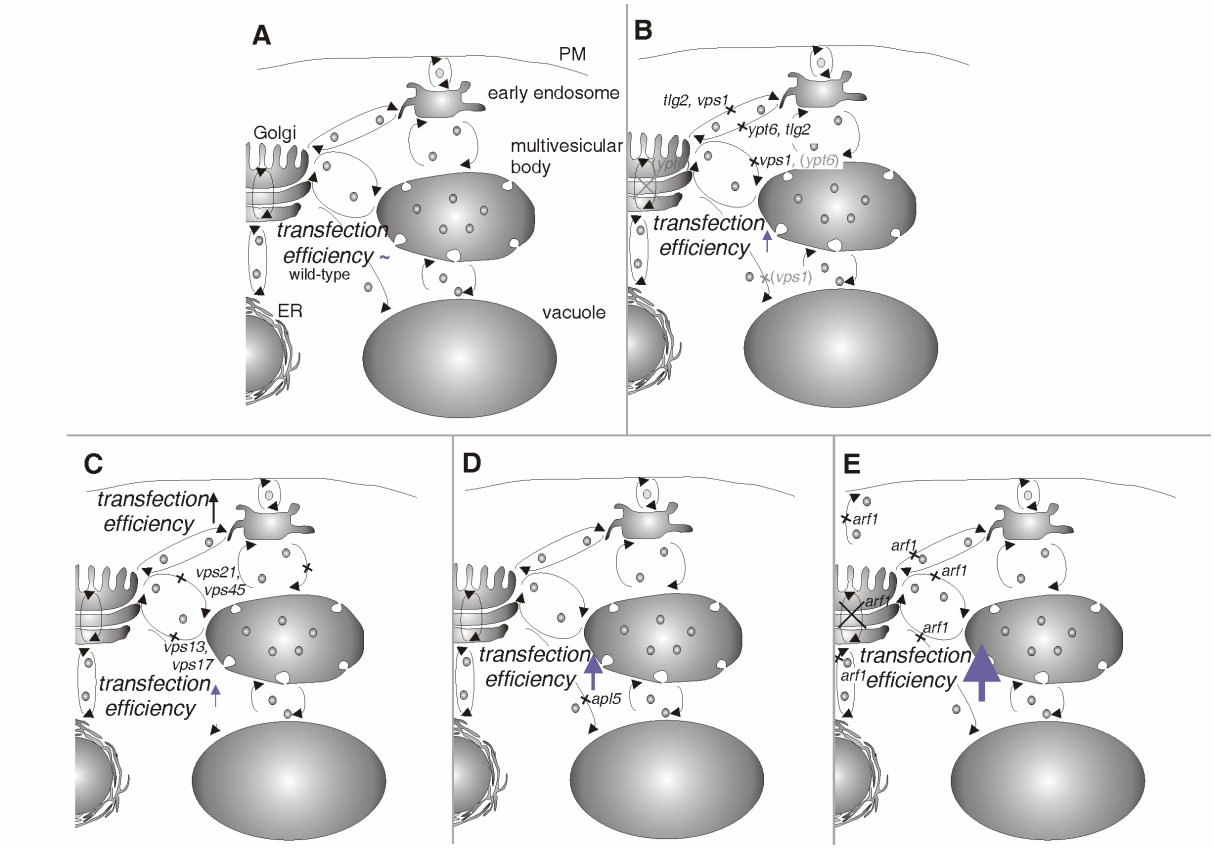

Fig. 5.2: Resulting model concerning transfection efficiency in correlation to transport pathways between the Golgi and the endosomal/vacuolar system. Transport inhibition at the ALP pathway and in deletion mutant BY4741 *arf1* enhances transfection efficiency. Effect on transfection efficiency in BY4741 (A); BY4741 *tlg2*, BY4741 *ypt6*, BY4741 *vps1* (B); BY4741 *vps21*, BY4741 *vps45* (C); BY4741 *apl5* (D) and BY4741 *arf1* (E). PM: plasma membrane.

(Fig. 5.2. A, C). The minor enhancement of transfection efficiency might also be correlated to less pronounced transport inhibition between the TGN and the PVC/MVB in mutant *vps17* in comparison to *vps21* and *vps45* mutants. This would result from the fact that Vps21p and Vps45p are involved in anterograde transport to the PVC/MVB (Burd et al, 1997; Tall et al, 1999), in contrast to Vps17p. In retrograde transport receptors, which are involved in anterograde transport of hydrolases, are sorted back to the TGN. When retrograde transport is interrupted, anterograde

transport is not cut off completely because new receptor molecules are synthetized and transported to the Golgi from the ER.

In this thesis it was observed the first time that endosomal transport inhibition is also present in *vps45* mutant, as previously shown for mutant *vps21*. This might be due to sorting defects for proteins involved in further transport steps at the PVC/MVB. These endosomal transport inhibitions were not observed in the mutant *vps17*.

Data indicate that reducing contact between hydrolases using the CPY pathway and endocytosed DNA reduces the degradation of DNA. This effect is stronger when endocytic transport is inhibited before entering the PVC/MVB.

A negative influence on transfection was observed in mutants *rcy1* and *yil064w*. Endocytic transport is inhibited at a very early stage in these mutants (Wiederkehr et al, 2000) (Fig. 5.1 A, B (a)). A novel observation in this thesis is the effect that mutant *yil064w* has on endocytosis. The negative effect on transfection might be the result of less efficient liberation of DNA during the osmotic shift from these early compartments accumulating endocytosed DNA during the transfection procedure, which might quench positive effects on transfection due to reduced contact to hydrolases. Liberation properties from different endocytic/vacuolar compartments should be different due to differences in membrane and ionic composition, resulting in different osmotic pressures in the compartments and osmotic stabilities of the surrounding membranes.

In mutants which are predominantly defective in transport stages between the Golgi and early endosomes such as *tlg2* and *ypt6* (Siniossoglou and Pelham, 2001; Lewis et al, 2000), transfection efficiency was only weakly enhanced in comparison to *vps21* or *vps45* mutants (Fig. 5.2 A, B, C). Proteins sorted from the Golgi to early endosomes by Tlg2p or Ypt6p do not seem to have a major impact on DNA degradation and/or transport to later compartments. Transfection efficiency in mutant *vps1* was a little bit higher than in mutants *tlg2* and *ypt6,* but also low in comparison to *vps21* or *vps45* mutants. This can be explained by the fact that the level of transfection efficiency in *vps1* mutant is between transfecton efficiencies of *tlg2* and *ypt6* mutants and *vps21* and *vps45* mutants by the fact that dynamine-like GTPase Vps1p is not only involved in transport from the Golgi to early endosomes as Tlg2p and Ypt6p are, but also in transport from the Golgi to late endosomes and hypothetically, also to the vacuole via the ALP pathway (Ekena et al, 1993; Nothwehr et al, 1995; Nothwehr et al, 1996; Yu and Cai, 2004). Further on, the endocytosed

DNA is accumulated in vesicular structures in mutants *vps21* and *vps45*, leading to higher transfection efficiencies than the accumulation in larger structures found in the *vps1* mutant.

No influence on transfection efficiency was observed in mutant *vps13* in comparison to the wild type (Fig. 5.2 A, C). This means that Vps13p is probably not involved in transport steps affecting endocytic DNA delivery or degradation. *VPS13* is the yeast homolog to the human *COH1* gene, known to be involved in human Cohen syndrome (Kolehmainen et al, 2003).

Homotypic vacuolar fusion and fusion of vesicles or late endosomes with vacuolar fragments is inhibited in the *vam6* mutant. This mutant exhibits a fragmented vacuole (Nakamura et al, 1997; Wada et al, 1992) and exhibits enhanced transfection efficiency (Fig. 5.1 A, E). Under these conditions not all of the compartments which accumulate endocytosed DNA have to contain hydrolases in the same distribution as in the wild-type vacuole. It was observed that not all of the vacuolar fragments visible in phase contrast microscopy accumulate LY-CH or FM4-64 in the same way, which supports this hypothesis. Furthermore, not all compartments containing FM4-64 fluorescence also contain the fluorescein labelled DNA fluorescence and the intensities of both dyes were not the same when they do co-localize. Fluorescein fluorescence intensity is dependent on pH-value. This indicates that different pH-conditions are present in the vacuolar fragments which lead to different transport efficiencies to and/or out of some of these fragments. It can be assumed that not all of the compartments carrying accumulated endocytosed DNA exhibit wild type vacuolar conditions. This would in turn result in reduced hydrolase activity, hydrolase transport and maturation. This again would be responsible for the enhanced transfection efficiency observed. It was described earlier that there is a significant delay in processing of CPY and in the accumulation of ALP in *vam6* cells (Nakamura et al, 1997), supporting the interpretation of the results of transfection experiments in this thesis. Inhibition of the ALP pathway using an *apl5* mutant enhances the transfection efficiency as efficieantly as inhibiting vacuolar fusion and import into the vacuole as described for mutant *vam6* (Fig. 5.2 A, D). An additional pH-effect in the compartments accumulating endocytosed DNA cannot be excluded in mutant *vam6*, as non-equal distribution of the V-ATPase in the compartments also has to be assumed and as a consequence, different pH-values might be present. The observations made in the *apl5* and *vam6* mutants are confirmed by the positive effect

on transfection in mutant *arf1* (Fig. 5.2 A, E). Arf1p is also involved in AP3 mediated ALP export from the Golgi, as is Apl5p. However Arf1p is furthermore part of the clathrin and COPI mediated transport processes between ER and Golgi (COPI) and at export steps from the Golgi to the plasma membrane and endosomes (Dell´Angelica et al, 2000; Gall et al, 2002; Gillingham et al, 2004; Ooi et al, 1998; Trautwein et al, 2006; Yahara et al, 2001). Arf1p is involved in exo- and endocytosis and *intra*-Golgi transport (Yahara et al, 2001; Zhdankina et al, 2001). This deletion mutant exhibits more defects than only a defect in the ALP pathway that might influence transfection efficiency. The influence of Arf1p on endocytosis could be demonstrated by LY-CH accumulation and membrane dynamics experiments. This explains why the effect on transfection efficiency is much stronger in mutant *arf1* than in mutants *apl5* and *vam6*.

The observations made, suggest that not only proteins sorted via the CPY-pathway, but also proteins sorted via the ALP-pathway are involved in degradation and maybe also sorting of endocytosed DNA. Furthermore, the occurrence of a fragmented vacuole, as in vps class B deletion mutants (*vam6*), seems to be correlated to efficient liberation of intact endocytosed DNA from these fragments.

However, when vacuolar fragments can no longer be detected, as is the case with vps class C deletion mutant *vps33*, transfection efficiency is not enhanced (Fig. 5.1 A, D). The Sec1/Munc18 protein Vps33p is homolog to human VPS33A and VPS33B (Gissen et al, 2005). The lack of an effect on transfection in *vps33* in comparison to the wild type might be explained by the accumulation of vacuolar proteins in earlier compartments which induces stronger acidification and degradation potential even in these compartments and that results in no positive effect on transfection efficiency. This interpretation is supported by the observation that there is quinacrine backround staining all over the cell in *vps33* cells in contrast to the wild type, possibly representing endocytic vesicles and endosomes. It is known that Vps33p is also involved in vacuolar protein sorting at endosomes (Subramanian et al, 2004; Peterson and Emr, 2001, Banta et al, 1990). Severe problems for the cell due to loss of vacuolar functions in vps class C mutants might be overcome by residual vacuolar potential of earlier compartments realized in this situation.

When a class E compartment is present, such as in a *vps27* or *vps4* mutant, transfection efficiency in the mutant is equal to wild-type mutant transfection efficiency (Fig. 5.1 A, C). Vps27p is associated to the ESCRTI subcomplex of the

ESCRT machinery and Vps4p, a AAA-type ATPase, is associated to the ESCRTIII subcomplex of the ESCRT machinery and both are required for efficient sorting of ubiquitinated membrane proteins into the lumen of the MVB (Bilodeau et al, 2003; Bowers et al, 2004) and for export from the MVB to other organelles (Finken-Eigen et al, 1997; Piper et al, 1995). Class E compartments accumulate plasma membrane, Golgi resident and endocytic markers as well as vacuolar proteins and exhibit quasi vacuolar conditions (Finken-Eigen et al, 1997; Pieper et al, 1995; Raymond et al, 1992; Rieder et al, 1996). These parameters result in near wild-type conditions for the endocytosed DNA and might explain the negligible effect of class E vps mutations on transfection efficiency.

This is also evident from the fluorescence staining which confirms a strong transport inhibition from the class E compartment, and a vacuolar like acidification of these compartments. Simmilar results have been reported earlier under non-transfection conditions (Finken-Eigen et al, 1997; Raymond et al, 1992).

These observations indicate that vacuolar conditions are responsible for near wild-type transfection efficiency and not the compartment per se where the endocytosed DNA accumulates.

Beside API, the most prominent cargo using the cytoplasm to vacuole targeting (CVT) pathway, other hydrolases might enter the vacuole via the CVT/autophagy pathway (Leber et al, 2001; Scott et al, 2001). Transfection efficiency is enhanced in the mutant deleted for *VAC8*, coding for a protein involved in autophagy (Fig. 5.3). Autophagy resulting in the uptake of mitochondria into the vacuole is induced under nitrogen starvation conditions (Onodera and Ohsumi, 2005), as are present during the transfection incubation time of 22 hours in 1 M sucrose. This should result in residual activity of, for example, the nuclear encoded mitochondrial nuclease Nuc1p (Dake et al, 1988; Vincent et al, 1988) in the vacuole before degradation. Also DNases involved in DNA repair mechanisms, such as those from the RMX complex (Mre11p, Rad50p and Xrs2p) (Lewis et al, 2004; Lobachev et al, 2002; Trujillo and Sung, 2001) might enter the vacuole via NVJ mediated PMN which is also induced by nutrient limitation conditions. Moreover, relaxation of supercoiled DNA as mediated by topoisomerases I-III (Chakraverty et al, 2001; Jacquiau et al, 2005; Trigueros and Roca, 2002) might occur and play a role in degradation of endocytosed DNA.

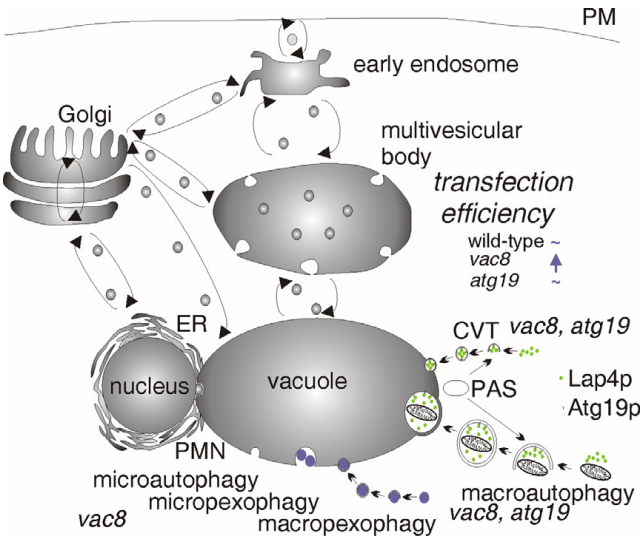

Fig. 5.3: Resulting model concerning transfection efficiency in mutants involved in CVT/autophagy. Defects in autophagy and NVJ (nucleus-vacuole-junctions) mediated PMN (piecemeal microautophagy of the nucleus) is correlated with enhanced transfection efficiency. This seems not to be due to transport defects in Lap4p sorting, because transfection efficiency is not affected in mutants BY4741 *atg19* BY4741 *lap4*. Atg19p is involved in sorting of Lap4p only. PM: plasma membrane PAS: pre-autophagosomal structure

Any of these can be an explanation for the enhanced transfection efficiency of mutant *vac8*. CVT does not seem to be relevant for transfection, as seen from transfection efficiencies of the mutant deleted for *ATG19*. Under starvation conditions, API bound to Atg19p in a CVT–complex is transported to the vacuole via Atg19p mediated binding to the preautophagosomal structure (PAS) followed by autophagocytosis (Shintani et al, 2002; Suzuki et al, 2002).

Finally, this suggests that degradation of endocytosed DNA is mediated by hydrolases sorted via CPY, ALP, and autophagy pathways. Lytic protection and osmotic liberation of endocytosed DNA can be efficiently affected by inhibiting endocytic transport at import steps to the late endosome (*vps21*, *vps45*) or the vacuole (*vam6*). Furthermore, transfection efficiency can efficiently be enhanced by inhibiting transport between Golgi and late endosomes (*vps21*, *vps45*) or between Golgi and the vacuole (*apl5*, *arf1*) or between ER and Golgi (*arf1*) or by inhibiting autophagy (*vac8*).

5.2.4 pH–value and ionic composition of the endocytic/vacuolar compartments

Endocytic/vacuolar membrane transport and protein sorting are regulated by the endo-compartimental pH value (Bowers et al, 2000; Brett et al, 2005; Klionsky et al, 1992). Enzymatic activity and specificity are also influenced by ions, as is known for Kex2p by K^+ ions (Rockwell and Fuller, 2002). Here it could be shown that non wild-

type acidification of the endosomes and/or the vacuole is correlated to enhanced transfection efficiency (summarized in Fig. 5.4).

Defects in endosomal/vacuolar acidification influence transport in deletion mutants under standard conditions (Bowers et al, 2000; Brett et al, 2005; Klionsky et al, 1992). This defect in transport for transfection conditions was confirmed in this thesis. Stv1p is present in the V-ATPase when it is located to the Golgi or the endosomes (Manolson et al, 1994; Perzov et al, 2002). The accumulation of membranes and the reduced accumulation of LY-CH in the mutant deleted for *STV1* result from reduced membrane transport in earlier parts of endocytosis, a defect caused by altered pH in endosomes and Golgi. The activity of proteins involved in endocytic transport will be

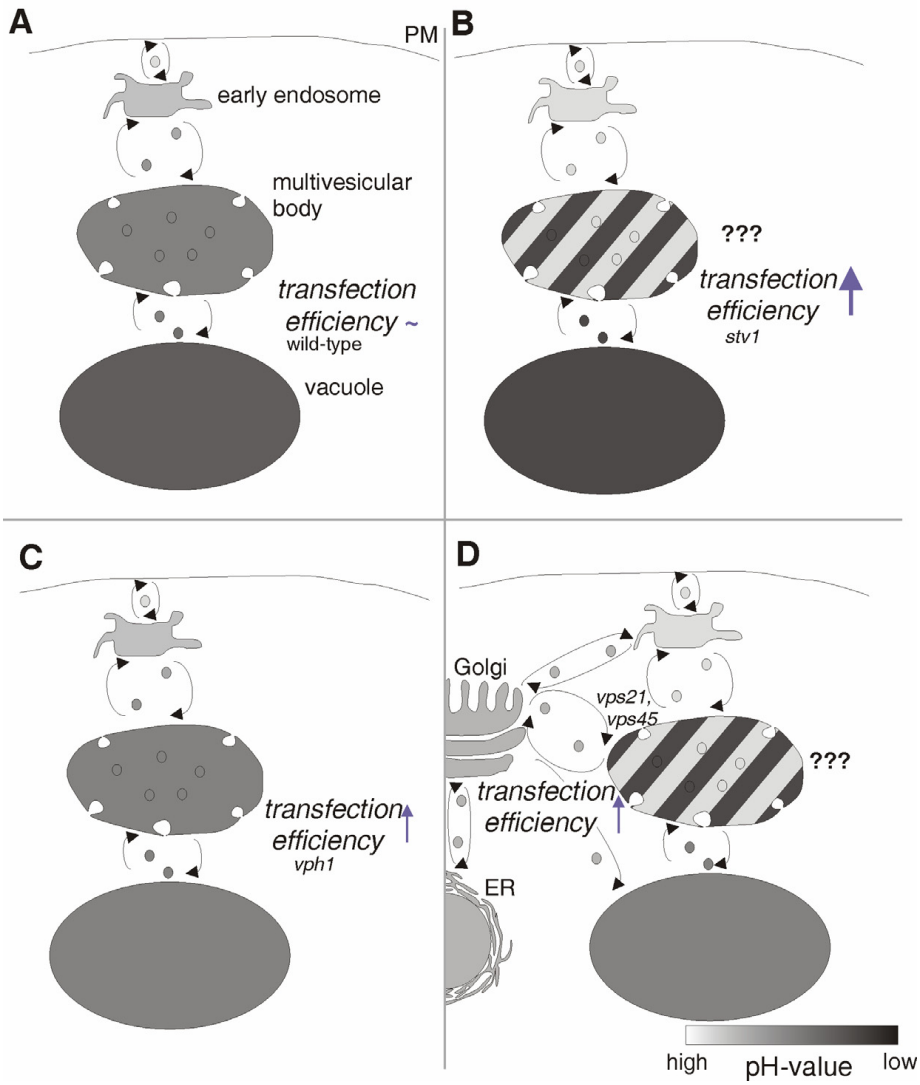

Fig. 5.4: Resulting model concerning transfection efficiency in correlation to intracompartimental pH–value. Non-wild-type endosomal/vacuolar acidification enhances the transfection efficiency. Acidification situations in BY4741 (A); BY4741 *stv1* (B), BY4741 *vph1* (C) BY4741 *vps21* and BY4741 *vps45* (D) mutants. The acidification of the late endosomes in mutant BY4741 *stv1* remains unclear after quinacrine staining, indicated by question marks. Acidified compartments near the vacuole in mutants BY4741 *vps21* and BY4741 *vps45* seem to be MVB/late endosomes. PM: plasma membrane.

reduced under non optimal pH conditions, but also sorting of proteins coming from the Golgi and located to endosomes and the vacuole will be impaired. This, in consequence, will lead to enhanced accumulation of endocytosed DNA in non-vacuolar compartments as, for example, in the *vps21* mutant which exhibits accumulation of membranes similar to the *stv1* mutant (seen in FM4-64 staining). In addition, the transport of hydrolases into endosomes and vacuole and their activity will be reduced due to altered pH in these compartments. This in turn results in a positive effect on transfection efficiency, as endocytosed DNA will have reduced contact with hydrolases in endosomes. This also applies to the *vph1* mutant, but here acidification and transport inhibition is stronger at the vacuole itself, and weaker in early endocytosis in comparison to *stv1* mutant. This is due to the localization of the protein deleted to the V0–subunit of the V-ATPase in the vacuole, while Stv1p is present in the V0–subunit in endosomes and the Golgi (Manolson et al, 1994; Perzov et al, 2002). This is seen as a slightly lower effect of *vph1* phenotype on transfection efficiency.

Reduced vacuolar acidification has been observed in mutants *vps21* and *vps45*, both of which show greatly enhanced transfection efficiency (Fig. 5.4 D). This is probably due to reduced V-ATPase levels caused by the transport defect from the TGN to the PVC/MVB, and results in additional transport inhibitions in the endocytic pathway also in mutant *vps45* which is known not to be directly involved in fusion of vesicles of the early endosome to the PVC/MVB (Bryant et al, 1998). Because of this, altered endosomal/vacuolar pH-values are at least partially responsible for the positive effect on transfection efficiency in both *vps21* and *vps45* mutants.

Nhx1p is involved in the regulation of endosomal and cellular pH–value. A transport defect is observed in the *nhx1* mutant (Brett et al, 2005) - maybe as a result of the effect on pH–value - and a positive effect on transfection efficiency is measured. The K^+-transport activity of Nhx1p might also affect enzymatic activity of endosomal/vacuolar hydrolases, as described for Kex2p (Rockwell and Fuller, 2002).

It can be deduced from this data that non wild-type acidification of endosomal/vacuolar compartments slows down the transport of endocytosed DNA to the vacuole. Furthermore, it can be hypothesised that mutants affected in acidification and endosomal potassium homeostasis exhibit higher transfection efficiency due to reduced degradation of endocytosed DNA.

5.3 Influencing transfection efficiency by regulation of the localization (transport) and degradation of endocytosed DNA

Intracellular transport processes and activities of hydrolases are regulated (Henry et al, 2003; Tahirovic et al, 2005; Bultynck et al, 2006; Böttcher et al, 2006; Chang et al, 2006; Ammerer et al, 1986). These regulatory steps might represent working steps to enhance transfection efficiency.

5.3.1 Golgi protein processing

It is clear from the results discussed in chapter 5.1 that specific proteins sorted to the endocytic system via the Golgi do influence transfection efficiency. Many of these proteins are needed to be processed during their passage through the Golgi to be functional at their final destination compartment, such as Pep4p, for example (Meussdoerffer et al, 1980; Jones, 2002). The two major processing types are proteolytic processing and glycosylation, and have been studied in this thesis.

5.3.1.1 Golgi processing protease Kex2p

Cargo transported to the endocytic/vacuolar system turned out to influence transfection efficiency, as, for example, demonstrated for cargo transported via the ALP pathway (see chapter 5.1). Often this cargo is needed to be processed by proteases to become functionally active. Knowing this, it was promising to find Golgi processing proteases that influence transfection efficiency. The most prominent processing proteases of the Golgi Ste13p, Kex1p, and Kex2p were tested for their effect on transfection efficiency. Deletion of *KEX2* turned out to enhance transfection efficiency when cells were harvested from late logarithmic growth phase. Furthermore, it could be shown that it is highly improbable that cell wall alterations caused by non-wild-type processing of cell wall proteins, known to be Kex2p processed, are the reason for enhanced transfection efficiency in the *kex2* mutant. The effect on transfection in the *kex2* mutant should therefore be due to non-wild-type processing of intracellular Golgi delivered proteins of the Golgi, endosomes or the vacuole.

As known from the literature, Kex2p is sorted between Golgi and endosomes (Fig. 5.5 A) (Tsukada and Gallwitz, 1996; Luo and Chang, 1997; Brickner and Fuller, 1997; Sipos et al, 2004; Chen et al, 2005; Blanchette et al, 2004). Is the effect on

transfection the result of the loss of Kex2p activity at the Golgi, in the early endosome or in the MVB/PVC (Fig. 5.5 A, B)? To answer this, several deletion mutants for proteins involved in Kex2p transport were analysed in comparison to mutant *kex2*. Kex2p is secreted and taken up again via endocytosis and it ends up in the vacuole for degradation in deletion mutants defective for export of Kex2p from the TGN to the early endosome (*ypt6, tgl2)* or for Kex2p retention to the TGN

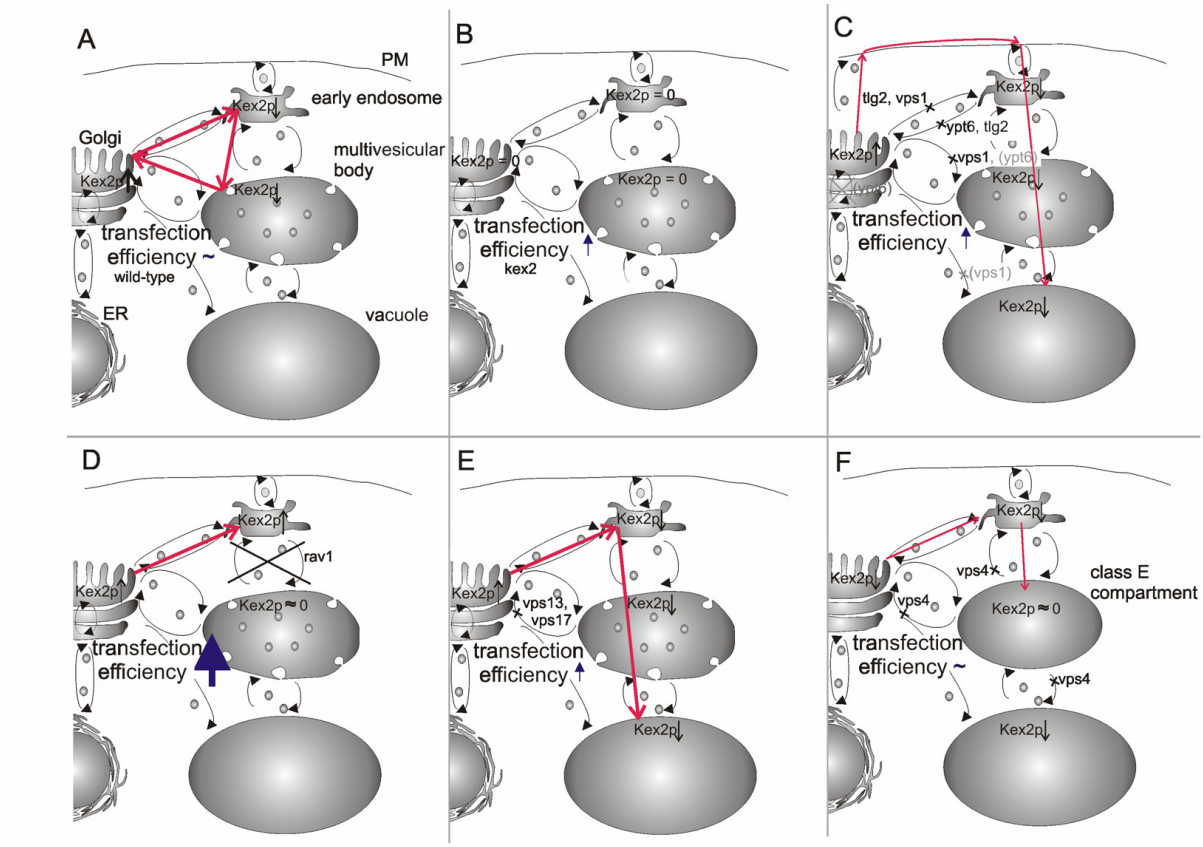

Fig. 5.5: Resulting model concerning the localization of the effect on transfection in mutant BY4741 *kex2*. Kex2p seems to be involved in processing of proteins at the Golgi influencing transfection efficiency resulting in acidification and endosomal transport defects in mutant BY4741 *kex2* (see Fig. 4.18). In the wild-type mutant, Kex2p is sorted from the TGN via the early endosome to the MVB/late endosome and back to the TGN (A). Situation which is present in BY4741 *kex2* mutant (B). A part of Kex2p is transported to the vacuole via the plasma membrane in mutants BY4741 *tlg2*, BY4741 *ypt6* and BY4741 *vps1* (C) and to the vacuole directly via the early endosome in mutants BY4741 *vps17* and BY4741 *vps13* (E). Kex2p accumulates in the early endosome in mutant BY4741 *rav1* (D). In class E vps mutants, the Kex2p amount is reduced by 90% and Kex2p sorted to the class E compartment is degraded there (F). PM: plasma membrane.

and defect in TGN export processes (*vps1*) (Fig. 5.5 C) (Tsukada and Gallwitz, 1996; Panek et al, 2000; Wilsbach and Payne, 1993; Nothwehr et al, 1995). All experiments discussed in this chapter used cells which were in the late logarithmic phase Transfection efficiency is however not enhanced much in mutants *tlg2*, *ypt6* and *vps1*. This means that if the effect on transfection in a *kex2* background is a result of

losing Kex2p activity at the late Golgi, the reduction of Kex2p at the Golgi is not strong enough in mutants *tlg2*, *ypt6* and *vps1* to obtain transfection efficiencies as with the *kex2* mutant. There are no data available to say something concerning activity or amount of Kex2p in endosomes in these mutants.

Rav1p is involved in the transport of Kex2p from the early endosome to the MVB/PVC (Fig. 5.5 D) (Sipos et al, 2004). Anterograde transport is inhibited highly effectively in *rav1* mutant, as seen in LY-CH and FM4-64 staining experiments. It can be assumed that Kex2p transport is also strongly inhibited in this mutant. This will result in Kex2p accumulation in the early endosome. As transfection efficiencies are enhanced in both mutants *kex2* and *rav1*, it is very improbable that losing Kex2p activity at the early endosome is the reason for the effect on transfection efficiency in mutant *kex2*. When the presence of Kex2p in the early endosome is the reason for reduced transfection efficiency, it would mean in consequence that the accumulation of Kex2p there, as seen in mutant *rav1*, would lead to significantly reduced transfection efficiency. This was, however, not observed, and Kex2p in the early endosome can therefore be assumed not to hinder high transfection efficiencies when present.

There is a very efficient transport inhibition for endocytosed DNA out of the early endosome in mutant *rav1*. A transport defect was also detected in mutant *kex2*. Transfection efficiency is enhanced more strongly in mutant *rav1* in comparison to mutant *kex2*. It might be possible that Kex2p is involved in processing of proteins needed for transport between the early and late endosome. If the transport defect in mutant *kex2* is be located between the early and late endosome, a less strong transport inhibition from the early endosome in mutant *kex2*, in comparison to *rav1* mutant, might be an explanation.

In mutant *vps13* which is defective for retrograde transport of Kex2p to the TGN (Fig. 5.5 E) (Brickner and Fuller, 1997), the explanation of the results is comparable to the observations made in mutants *tlg2*, *ypt6* and *vps1*. Transfection efficiency in mutant *vps13* is not much higher than in the wild type. A reduced amount of Kex2p should be found at the Golgi in mutant *vps13* as Kex2p is transported to the vacuole for degradation. This indicates that if the effect on transfection in a *kex2* background is due to the loss of Kex2p activity at the late Golgi, but the reduction of Kex2p at the Golgi is not strong enough in mutant *vps13* to get transfection efficiencies as in *kex2* mutant.

Finally, Kex2p in vps class E mutants, as with other proteins, is sorted to the class E compartment (Fig. 5.5 F) (Cereghino et al, 1995; Panek et al, 2000). This missorting is known to be very efficient. The total amount of Kex2p is reduced till 90% in vps class E mutant *vps28* (65% in *vps27* (Panek et al, 2000)) and Kex2p is known to be degraded in the class E compartment which has vacuole-like properties in these cells (Cereghino et al, 1995). This results in a reduced Kex2p amount at Golgi and endosomes, and Kex2p is not active in the class E compartment due to efficient degradation. Transfection efficiencies in class E mutants are the same as in the wild type. In turn, this indicates that the effect in *kex2* mutant on transfection is not due to loss of Kex2p activity at the MVB/PVC (≡ class E compartment in class E mutants). It further shows that a low amount of Kex2p at the Golgi is sufficient to suppress the effect on tranfection efficiency seen for a complete loss of Kex2p in mutant *kex2*. Additional degradation of endocytosed DNA in the class E compartment in comparison to a MVB/PVC suppressing a possible effect on transfection due to loss of Kex2p activity there, however, cannot be excluded.

Summarizing all these observations, it is most probable that the effect on transfection in mutant *kex2* is due to loss of Kex2p activity at the TGN only. A possible involvement of Kex2p mediated processing of proteins needed for endosomal transport cannot be excuded. This can take place at the early endosomal system or at the Golgi during the delivery of these proteins to their wild type location.

In consequence, it can be predicted that Kex2p processes one or more proteins most probably at the Golgi which thereafter affect transfection efficiency.

5.3.1.2 Golgi N-mannosyltransferase Och1p

The prediction, that Kex2p processes one or more proteins affecting transfection efficiency at the Golgi, is supported by the observation that transfection efficiency is also enhanced in the *och1* mutant. This mutant is deleted for a mannosyltransferase located to the Golgi and involved in protein N-glycosylation (Gaynor et al, 1994; Harris and Waters, 1996). This thesis predicts that Och1p will be cleaved by Kex2p. Apart from proteolytic processing, glycosylation affects the functionality and activity of proteins passing the Golgi. Transfection efficiency is enhanced in the mutant deleted for the mannosyltransferase Och1p which is involved in N-type glycosylation. Many cell wall proteins are predicted to be N-type outer-chain glycosylated (except for Cwp2p) and therefore it was expected that a positive effect on transfection efficiency

in corresponding deletion mutants would be observed. In contrast, the results presented in this thesis indicate that altering the cell wall structure and composition does not enhance transfection efficiency. The cell wall is strongly altered in the mutants tested. Three of the most important genes coding for components of the cell wall were deleted. *EXG1* coding for the major cell wall β-1,3-glucanase was deleted resulting in an altered β-glucan layer of the cell wall, one of the major constituents of the cell wall structure. *CWP2* coding for the major cell wall protein, and the highest expressed protein in the cell, was deleted to significantly alter the composition of and/or amount of cell wall proteins. Finally, *CHS3* coding for the chitin synthase responsible for synthesis of the majority of cell wall chitin was deleted. A weak reduction of transfection efficiency was observed for the deletion mutants *exg1*, *cwp2*, and *chs3*. Additionally, several other mutants deleted for cell wall proteins or proteins altering cell wall structure and charge were tested with the same results in respect to the effect on transfection efficiency. This means that a strong alteration of the cell wall caused by defects in the outer-chain N-glycosylation of cell wall proteins, (Fig. 5.6 A) is not the explanation for the positive effect of *OCH1* deletion on transfection efficiency. A direct alteration of the cell wall by influencing cell wall composition does not seem to significantly positively influence transfection efficiency. Cell wall composition will be altered by defects in protein sorting at the Golgi which is dependent on glycosylation. Indirect alterations to the cell wall in respect to cell wall charge and structure, due to reduced enzymatic activities of cell wall enzymes and structures of cell wall proteins, is indicated not to affect transfection efficiency significantly positive too. However, mutant *och1* does not only affect outer-chain glycosylation, core-type glycosylation of proteins directed to intracellular compartments is also altered (Munro, 2001) (Fig. 5.6 A). There is very little difference between core-type glycosylation structures of the wild type and the mutants *mnn1* and *och1*, but efficiency in transfection experiments is only enhanced in mutant *och1*. To decide if this minor difference in core-type glycosylation can really explain the positive effect on transfection efficiency, deletion mutants defective for membrane proteins predicted or known to be core-type glycosylated were tested. These kind of proteins are located in the Golgi or the endosomal/vacuolar system, and are known to be sorted via the Golgi (Munro, 2001). Candidates which were used to explain the influence of losing Och1p activity on transfection efficiency are mutants *pmr1*, *kex2*, *nhx1*, *stv1* and *vph1*. It is predicted that they are processed by Och1p and show a

positive influence on transfection efficiency. The *och1* mutant can be assumed to have a reduced activity of Pmr1p, Kex2p, Nhx1p and Stv1p (Fig. 5.6 B). Pmr1p is a Golgi Ca^{2+}/Mn^{2+}-importing ATPase (Mandal et al, 2003). Reduced activity of Pmr1p also negatively affects the activity of Kex2p, as Kex2p activity is Ca^{2+}-dependent (Fuller et al, 1989). Furthermore, reduced Nhx1p activity negatively influences Kex2p

A

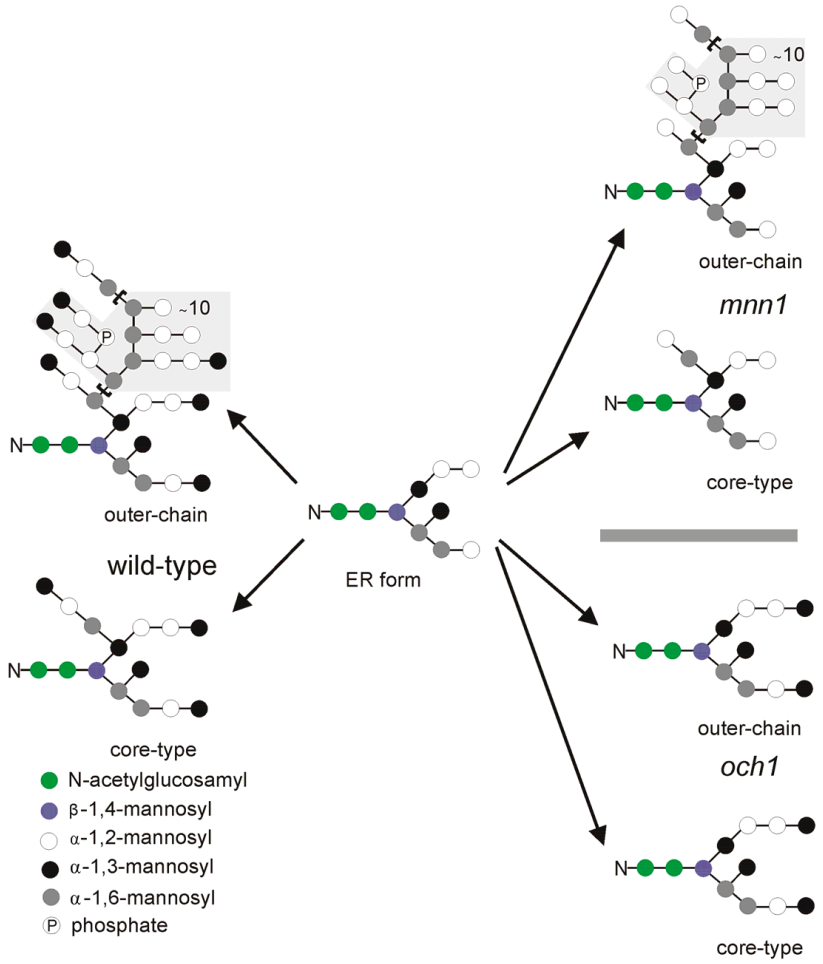

B

strain	N-type glycosylation as in wild-type	N-type glycosylation as in *och1*	activity of Och1p	activity of Pmr1p	activity of Kex2p Golgi/endosomes	activity of Nhx1p	activity of Stv1p/Vph1p	transfection efficiency in [-]
wild-type	X		normal	normal	normal/normal	normal	normal/normal	1
och1		X	0	↓[1]	↓[1]/↓[1]	↓[1]	↓[1,2]/?	$5.25^{\pm 3.35}$
mnn1	(X)		normal	normal?	normal?/normal?	normal?	normal?/normal?	$0.54^{\pm 0.21}$
pmr1		X[3,4]	↓[3,4]	0	↓[1,3,4]/↓[1,3,4]	↓[1,3,4]	↓[1,2,3,4]/?	$36.89^{\pm 6.66}$
kex2		X[3,4]	↓[3,4]	↓[1,3,4]	0/0	↓[1,3,4]	↓[1,2,3,4]/?	$12.34^{\pm 6.60}$
nhx1	X		normal	normal	normal/↓[5]	0	normal/normal	$6.77^{\pm 4.17}$
stv1 or vph1	X		normal	normal	normal/↓[6]	↓[6]	↓[6,8]/↑[7,9]	$16.83^{\pm 2.31}$/$11.62^{\pm 3.47}$

1 due to N-type glycosylation prediction
2 due to strong acidification observed in *och1* and *kex2* mutants - it seems to be a *stv1*-like phenotype present
3 because Och1p is Mn^{2+}dependent and Kex2p is Ca^{2+} dependent
4 Och1p is predicted to be cleaved by Kex2p
5 Kex2p is K^+ dependent
6 in *stv1* mutant; due to reduced H^+ import into endosomes the gradient to import Na^+/K^+ is reduced
7 see results
8 in *vph1* mutant
9 in *stv1* mutant

Fig. 5.6: Resulting model concerning the effect of glycosylation on transfection in mutant BY4741 *och1*. A: Glycosylation of secreted proteins (outer chain) and proteins of the Golgi and the endosomal/vacuolar system, sorted via the secretory pathway, in the wild-type and mutants deleted for *MNN1* or *OCH1*. B: Predicted effect on activities of Och1p, Pmr1p, Kex2p, Nhx1p, Stv1p and Vph1p in mutants deleted for each one of these proteins and the corresponding transfection efficiencies. All these proteins are predicted to be core-type N-glycosylated

activity, as Kex2p activity is K^+-dependent (Rockwell and Fuller, 2002) and Kex2p is sorted to endosomes (Tsukada and Gallwitz, 1996; Luo and Chang, 1997; Brickner and Fuller, 1997; Sipos et al, 2004; Chen et al, 2005; Blanchette et al, 2004) where Nhx1p is present at late endosomal membranes as a $Na^+(K^+)/H^+$-antiporter (Ali et al, 2004; Wells and Rao, 2001). Reduced activity of Stv1p and Vph1p leads to defects in membrane transport as it is a pH-dependent process (Klionsky et al, 1992). Stv1p and Vph1p both have the same function in V-ATPase, but at different locations in the wild type (Manolson et al, 1994; Perzov et al, 2002). This has effects on membrane transport, as seen in the *och1* mutant where intracellular compartments are fragmented. When membrane transport processes are affected, the transport of Kex2p and Nhx1p is also affected, and proper functioning of Kex2p and Nhx1p is suppressed. In addition to fragmented intracellular compartments in mutants *och1* and *stv1*, compartments in *och1* are also acidified more strongly than in the wild type, as seen in mutant *stv1*. This observation might indicate that, contrary to expectation, Vph1p activity is not reduced in the *och1* mutant because a comparable phenotype as seen in *stv1* mutant and not in *vph1* mutant was observed. In *stv* mutant enhanced acidification of the vacuole was interpreted as a result of up-regulation of Vph1p expression as a result of Stv1p loss. These acidification and resulting membrane transport defects might explain the effect on transfection efficiency as described for mutants *stv1* and *vph1* in chapter 5.2.4.

Looking at the results in mutant *pmr1*, comparable connections between the genes in this group can be made to explain the effect of this deletion on transfection efficiency. In *pmr1* mutation background, activities of Kex2p and Och1p are reduced as Ca^{2+} and Mn^{2+} import into the Golgi is defect. As Kex2p is predicted to protolytically process Och1p, the activity of Och1p is further reduced in mutant *pmr1*. This results in the following effects as described in the discussion of the deletion mutant *och1*. The same is true for the deletion mutant *kex2*. Here too the activity of Och1p might be reduced leading to the discussion presented for mutant *och1*. Nhx1p imports K^+-ions into the late endosome which is passed by Kex2p during its sorting, and Kex2p activity is K^+-dependent. This means that the same discussion can be followed for deletion mutant *nhx1* as well.

Finally it can be summarized that it is highly probable that the effect on transfection efficiency in mutant *och1* is a result of core-type N-glycosylation defects which are very specific and cannot be observed in mutant *mnn1* presenting a core-type

glycosylation with only two mannose residues at different positions in comparison to mutant *och1* (Fig 5.6 A). Positive effects on transfection efficiency due to glycosylation defects of specific cell wall proteins in mutant *och1* cannot be excluded but seem to be improbable. All these observations show that there is a network of interacting factors positively affecting transfection efficiency.

5.3.1.3 Kex2p and Och1p relations affecting transfection efficiency

Observations discussed in chapters 5.3.1.1 and 5.3.1.2 lead to a resulting protein interaction model to explain the effect of Golgi localized proteins on transfection efficiency (Fig. 5.7).

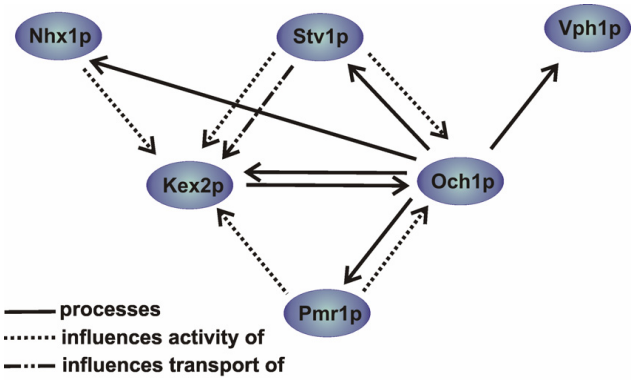

Fig. 5.7: Resulting regulatory model of interaction between important proteins influencing transfection efficiency positively. Pmr1p imports Ca^{2+}- and Mn^{2+}-ions into the Golgi. Och1p activity is Mn^{2+}-dependent. Kex2p activity is Ca^{2+}-dependent. Och1p is predicted to be proteolytically processed by Kex2p. Kex2p, Nhx1p, Stv1p and Vph1p are predicted or known (Kex2p) to be core-type N-glycosylated by Och1p. Nhx1p imports K^{+}-ions into the MVB/late endosome and Kex2p activity, which is sorted between TGN and endosomes, is K^{+}-depemdent. Stv1p as part of the V0 subunit of the vacuolar ATPase at the Golgi and endosomes does influence the pH-value in these compartments also harbouring Kex2p and Och1p.

Pmr1p influences the activity of both Kex2p and Och1p at the Golgi as it imports Ca^{2+}- and Mn^{2+}-ions to the Golgi. Kex2p activity is Ca^{2+}-dependent whereas Och1p activity is Mn^{2+}-dependent (Fuller et al, 1989; Dürr et al, 1998). Nhx1p will influence the activity of Kex2p as it imports K^{+}-ions to the PVC/MVB and the activity of Kex2p depends on K^{+}-ions while it passes the PVC/MVB during its transport between endosomes and Golgi (Tsukada and Gallwitz, 1996; Luo and Chang, 1997; Brickner and Fuller, 1997; Sipos et al, 2004; Chen et al, 2005; Blanchette et al, 2004). Furthermore, Kex2p is predicted to proteolytically process Och1p. Och1p is predicted, and in some cases also known to core-N-glycosylate Pmr1p, Kex2p, Nhx1p, Stv1p and Vph1p. It is highly propable that glycosylation influences the activity of these proteins. Finally, Stv1p influences the activity of Kex2p and Och1p as it is responsible for the wild-type pH-value at the Golgi and endosomes as part of the

V-ATPase at the Golgi. In addition to direct influences on protein activity of Golgi and endosome resident proteins, protein transport is negatively affected as this process is also pH-dependent. This leads to mislocalization, for example, of Kex2p.
In the regulatory network of proteins influencing transfection presented here, it is evident that activities of all other proteins are influenced by deleting or down regulating any protein of the network, except for Vph1p. This always results in changes to the endosomal/vacuolar pH-value and in transport inhibition. This in turn explains the effect on transfection efficiency in every deletion mutant for the proteins discussed here. It is highly probable that this regulatory network is still incomplete as one can observe a much greater effect on transfection efficiency in mutant *pmr1* in comparison to other members of the network. This means that there are probably other Ca^{2+}- or Mn^{2+}-dependent proteins at the Golgi that affect transfection efficiency.

5.3.2 Cytosolic protein processing

Many proteins which are part of complexes involved in intracellular trafficking are cytosolic proteins. These proteins are regulated, for example, as a result of phosphorylation or methylation processes. Protein phosphatase 1 (PP1) is essential for lipid bilayer mixing, the last step of membrane fusion (Peters et al, 1999). The yeast phosphatidylinositol 3-kinase Vps34p phosphorylates PtdIns (phosphatidylinositol) to PtdIns-3P (Schu et al, 1993). As a result, Vps34p regulates membrane transport, for example, from the TGN to the PVC/MVB because PtdIns-3P is recognized by the FYVE domain of Vps27p and regulates its activity (Stahelin et al, 2002; Huijbregts et al, 2000). This means that endocytosis is also regulated by cytosolic protein processing. In this thesis it was observed that mutant *yil064w*, a putative cytosolic methyltransferase, exhibits a phenotype in which endocytosis is inhibited at a very early stage when cells were grown to the late logarithmic growth phase. Transfection efficiency was reduced in comparison to the wild type. This indicates that transfection efficiency is also affected by cytosolic protein processing, but more experiments remain to be done on this area.

Finally the findings presented are promising for the use in optimizing mammalian non-viral transfection in the future.

5.4 Outlook

The results presented in this thesis show the impact of inhibiting specific, particularly endocytic, intracellular transport processes on the efficiency of non-viral transfection. In addition, (i) intra-compartimental pH-value and ion composition of compartments harbouring endocytosed DNA, (ii) proteins affecting relevant transport steps, or (iii) proteins relevant for processing proteins directed to the endosomal/vacuolar system affect transfection efficiency. Deletion of specific genes that code for proteins involved in Golgi processing of proteins directed to the endosomal/vacuolar system also enhance transfection efficiency. It seems very promising to transfer these results to the mammalian system using cell lines such as HepG2, for example, or others to test specific inhibitor substances for proteins tested to enhance non-viral transfection efficiency in its absence in the yeast based non-viral transfection system. It might further be appropriate to use RNA interference (RNAi) in the case a small inhibitor molecule for a mammalian homolog target that can be taken up easily over the plasma membrane is not known. In an RNAi based approach a pre-transfection could be done prior to the main-transfection. siRNA´s or shRNA´s, for example, will be used for pre-transfection, and these constructs are against the mRNA´s of protein targets known to enhance tranfection efficiency in their absence. Maybe chemically modified siRNA´s could be used to enhance the lifetime of the construct.

Observations of transfection enhancing effects made in yeast in this thesis should be combined, for example, in transport inhibition together with a processing inhibition in a single experiment. This could be performed in yeast using multiple deficient mutants or in the mammalian system using multiple inhibitors or RNAi with more than one effector. The results of these experiments would be important to distinguish between synergistic and additive effects of observations made in yeast.

Additionally, the effect of Golgi proteolytic processing and glycosylation on transfection has to be systematically tested doing -omics studies, for example, to verify and extend the interactions between proteins involved in and affected by processing at the Golgi.

6 Summary

Saccharomyces cerevisiae is commonly used as a model system to study endocytosis. Results obtained with yeast can be transferred to the mammalian system in almost all aspects. Here, defined deletion mutants were utilized to identify and locate steps in endocytic transport, endosomal/lysosomal acidification and in intracellular transport of hydrolases, and hydrolases itself which influence DNA delivery in non-viral transfection. Furthermore, Golgi proteins, cell wall constituents and their transport to wild-type locations, and, partially, also the involvement of actin and its corresponding proteins were tested for effects on transfection efficiency in deletion mutants. Transport inhibition in later endocytic steps, such as in the *vps21* mutant, enhances transfection efficiency. By applying transfection conditions in combination with quinacrine staining, it was demonstrated that modifying the pH-value of the endosomal/vacuolar system, for example in the *vph1* and *stv1* mutants, leads to enhanced transfection efficiency. Efficiency is also elevated in specific cases when the ion composition of the endosomal system is affected (*nhx1*). Enhanced transfection efficiency was further observed in mutants which are mutated in the CVT/autophagy pathway or hydrolase transport to the vacuole as in mutant *vac8*. Transfection efficiency can be further enhanced by deleting Golgi processing proteins as with the *kex2* mutant deficient for an important Golgi processing protease, the *och1* mutant deficient for an early Golgi participant in N-glycosylation, or by affecting these proteins' wild-type function by deleting *PMR1* coding for the Golgi Mn^{2+}/Ca^{2+}-importing transporter. The function of Kex2p is dependent on Ca^{2+}–ions and the function of Och1p on Mn^{2+}–ions. Proper function of Kex2p might also be affected by malfunctions in the transport between the *trans*-Golgi network and endosomes. In this study, an interaction network affecting transfection is presented between Kex2p, Och1p, Pmr1p, Stv1p, Vph1p and Nhx1p. Finally, single defects affecting cell wall proteins or proteins involved in actin metabolism seem to be inappropriate to use to enhance transfection efficiency.

In summary, non-viral transfection efficiency can be enhanced by (i) inhibiting the transport of endocytosed material before it meets vacuolar conditions, (ii) inducing a non-natural pH-value of the endosomal/vacuolar system, (iii) slowing down degradative processes by inhibiting vacuolar hydrolases or the transport between Golgi and late endosome/vacuole, or (iv) inhibiting/interrupting Golgi processing.

6 Zusammenfassung

Saccharomyces cerevisiae wird allgemein als Modellsystem zur Untersuchung der Endocytose genutzt. Ergebnisse, die in Hefe gewonnen wurden, können in Bezug auf fast alle Aspekte auf das Säugersystem übertragen werden. Hier wurden definierte Deletionsstämme genutzt, um Schritte im endocytotischen Transport, in der endosomal/lysosomalen Ansäuerung und in dem intrazellulären Transport von Hydrolasen sowie Hydrolasen selbst zu identifizieren und zu lokalisieren, die die DNS Aufnahme und Freisetzung in der nicht-viralen Transfektion beeinflussen. Des Weiteren wurden in entsprechenden Deletionsmutanten Golgi-Proteine, Zellwandbestandteile und deren Transport zu ihren Wildtyp-Lokalisationen und teilweise auch der Einfluss von Aktin und seinen korrespondierenden Proteinen untersucht auf Effekte bezüglich der Transfektionseffizienz. Transportinhibierung in späteren endocytotischen Schritten, wie in der *vps21* Mutante, erhöht die Transfektionseffizienz. Durch Quinacrine-Färbung-Untersuchungen unter Transfektionsbedingungen wurde gezeigt, dass eine Modifizierung des pH-Wertes im endosomal/vakuolären System, wie zum Beispiel in den Mutanten *vph1* und *stv1*, zu einer erhöhten Transfektionseffizienz führt. Die Effizienz ist ebenfalls in spezifischen Fällen erhöht, wenn die Ionenzusammensetzung des endosomalen Systems beeinflusst wird (*nhx1*). Eine erhöhte Transfektionseffizienz wurde außerdem in Mutanten beobachtet, welche in dem CVT/Autophagie Prozess oder dem Transport von Hydrolasen zur Vakuole mutiert sind, wie in der Mutante *vac8*. Die Transfektionseffizienz kann des Weiteren erhöht werden durch Defekte an prozessierenden Proteinen des Golgi, wie in der *kex2* Mutante, die defekt ist für eine wichtige prozessierende Golgi Protease, in der *och1* Mutante, die defekt ist für ein Protein, dass in der frühen N-Glykosylierung des Golgi wichtig ist oder durch Beeinflussung der Wildtyp-Funktion dieser Proteine durch Deletion von *PMR1*, welches für den Golgi Mn^{2+}/Ca^{2+}-Import Transporter kodiert. Die Funktion von Kex2p ist abhängig von Ca^{2+}-Ionen und die Funktion von Och1p von Mn^{2+}-Ionen. Die natürliche Funktion von Kex2p könnte auch beeinflusst werden durch Disfunktionen in seinem Transport zwischen dem *trans*-Golgi-Netzwerk und den Endosomen. In dieser Promotionsarbeit wird ein Interaktionsnetzwerk der transfektions-beeinflussenden Faktoren präsentiert, welches Kex2p, Och1p, Pmr1p, Stv1p, Vph1p und Nhx1p beinhaltet. Zum Schluss kann noch gesagt werden, dass Einzeldefekte

von Zellwandproteinen oder Proteinen, die involviert sind in den Aktin-Metabolismus, scheinbar nicht geeignet sind um die Transfektionseffizienz zu erhöhen.

Zusammenfassend lässt sich sagen, dass die nicht-virale Transfektionseffizienz erhöht werden kann durch (i) die Inhibierung des Transportes endocytierten Materials, bevor es vakuoläre Bedingungen erreicht, (ii) die Erzeugung eines nicht natürlichen pH-Wertes in dem endosomal/vakuolären System, (iii) die Verlangsamung degradativer Prozesse durch Inhibierung vakuolärer Hydrolasen oder des Transports zwischen Golgi und dem späten Endosom/der Vakuole oder (iv) die Inhibierung/Unterbrechung der Prozessierung im Golgi.

7 References

Achstetter T (1989) Regulation of α-factor production in *Saccharomyces cerevisiae*: a-factor pheromone-induced expression of the *MFα1* and *STE13* genes. *Mol Cell Biol* **9**: 4507-4514

Aderem A, Underhill DM (1999) Mechanisms of phagocytosis in macrophages. *Annu Rev Immunol* **17**: 593-623. Review

Aldrich RA, **Steinberg AG**, **Campbell DC** (1954) Pedigree demonstrating a sex-linked recessive condition characterized by draining ears, eczematoid dermatitis and bloody diarrhea. *Pediatrics* **13**: 133-139

Ali R, Brett CL, Mukherjee S, Rao R (2004) Inhibition of sodium/proton exchange by a Rab-GTPase-activating protein regulates endosomal traffic in yeast. *J Biol Chem* **279**: 4498-4506

Ammerer G, Hunter CP, Rothman JH, Saari GC, Valls LA, Stevens TH (1986) *PEP4* gene of *Saccharomyces cerevisiae* encodes proteinase A, a vacuolar enzyme required for processing of vacuolar precursors. *Mol Cell Biol* **6**: 2490-2499

Anderson BL, **Boldogh I**, **Evangelista M**, **Boone C**, **Greene LA**, **Pon LA** (1998) The Src homology domain 3 (SH3) of a yeast type I myosin, Myo5p, binds to verprolin and is required for targeting to sites of actin polarization. *J Cell Biol* **141**: 1357-1370

Anderson RG, **Jacobson K** (2002) A role for lipid shells in targeting proteins to caveolae, rafts, and other lipid domains. *Science* **296**: 1821-1825

Antebi A, Fink GR (1992) The yeast Ca^{2+}-ATPase homologue, *PMR1*, is required for normal Golgi function and localizes in a novel Golgi-like distribution. *Mol Biol Cell* **3**: 633-654

Aridor M, **Hannan LA** (2000) Traffic jam: a compendium of human diseases that affect intracellular transport processes. *Traffic* **1**: 836-851

Aridor M, **Hannan LA** (2002) Traffic jams II: an update of diseases of intracellular transport. *Traffic* **3**: 781-790

Aschenbrenner L, **Naccache SN**, **Hasson T** (2004) Uncoated endocytic vesicles require the unconventional myosin, Myo6, for rapid transport through actin barriers. *Mol Biol Cell* **15**: 2253-2263

Babst M, Sato TK, Banta LM, Emr SD (1997) Endosomal transport function in yeast requires a novel AAA-type ATPase, Vps4p. *EMBO J* **16**: 1820-1831

Baggett JJ, **Wendland B** (2001) Clathrin function in yeast endocytosis. *Traffic* **2**: 297-302. Review

Bagnat M, **Keränen S**, **Shevchenko A**, **Shevchenko A**, **Simons K** (2000) Lipid rafts function in biosynthetic delivery of proteins to the cell surface in yeast. *Proc Natl Acad Sci U S A* **97**:3254-3259

Bankaitis VA, **Aitken JR**, **Cleves AE**, **Dowhan W** (1990) An essential role for a phospholipid transfer protein in yeast Golgi function. *Nature* **347**: 561-562

Banerjea A, **Li MJ**, **Remling L**, **Rossi J**, **Akkina R** (2004) Lentiviral transduction of Tar Decoy and CCR5 ribozyme into CD34+ progenitor cells and derivation of HIV-1 resistant T cells and macrophages. *AIDS Res Ther* **1**:2

Banta LM, Robinson JS, Klionsky DJ, Emr SD (1988) Organelle assembly in yeast: Characterization of yeast mutants defective in vacuolar biogenesis and protein sorting. *J Cell Biol* **107**: 1369-1383

Banta LM, **Vida TA**, **Herman PK**, **Emr SD** (1990) Characterization of yeast Vps33p, a protein required for vacuolar protein sorting and vacuole biogenesis. *Mol Cell Biol* **10**: 4638-4649

Basco RD, Cueva R, Andaluz E, Larriba G (1996) *In vivo* processing of the precursor of the major exoglucanase by *KEX2* endoprotease in the *Saccharomyces cerevisiae* secretory pathway. *Biochim Biophys Acta* **1310**: 110-118

Batard P, **Jordan M**, **Wurm F** (2001) Transfer of high copy number plasmid into mammalian cells by calcium phosphate transfection. *Gene* **270**: 61-68

Beh CT, **Rine J** (2004) A role for yeast oxysterol-binding protein homologs in endocytosis and in the maintenance of intracellular sterol-lipid distribution. *J Cell Sci* **117**: 2983-2996

Benns JM, **Mahato RI**, **Kim SW** (2002) Optimization of factors influencing the transfection efficiency of folate-PEG-folate-graft-polyethylenimine. *J Control Release* **79**: 255-269

Berger AC, **Hanson PK**, **Wylie Nichols J**, **Corbett AH** (2005) A yeast model system for functional analysis of the Niemann-Pick type C protein 1 homolog, Ncr1p. *Traffic* **6**: 907-917

Berger AC, **Vanderford TH**, **Gernert KM**, **Nichols JW**, **Faundez V**, **Corbett AH** (2005[b]) *Saccharomyces cerevisiae* Npc2p is a functionally conserved homologue of the human Niemann-Pick disease type C 2 protein, hNPC2. *Eukaryot Cell* **4**: 1851-1862

Bieber T, **Meissner W**, **Kostin S**, **Niemann A**, **Elsasser HP** (2002) Intracellular route and transcriptional competence of polyethylenimine-DNA complexes. *J Control Release* **82**: 441-454

Bilodeau PS, Winistorfer SC, Kearney WR, Robertson AD, Piper RC (2003) Vps27-Hse1 and ESCRT-I complexes cooperate to increase efficiency of sorting ubiquitinated proteins at the endosome. *J Cell Biol* **163**: 237-243

Blanchette JM, Abazeed ME, Fuller RS (2004) Cell-free reconstitution of transport from the *trans*-G0olgi network to the late endosome/prevacuolar compartment. *J Biol Chem* **279**: 48767-48773

Botstein D, Falco SC, Stewart SE, Brennan M, Scherer S, Stinchcomb DT, Struhl K, Davis RW (1979) Sterile host yeasts (SHY): a eukaryotic system of biological containment for recombinant DNA experiments. *Gene* **8**: 17-24

Böttcher C, Wicky S, Schwarz H, Singer-Krüger B (2006) Sjl2p is specifically involved in early steps of endocytosis intimately linked to actin dynamics via the Ark1p/Prk1p kinases. *FEBS Lett* **580**: 633-641

Boussif O, **Lezoualc'h F**, **Zanta MA**, **Mergny MD**, **Scherman D**, **Demeneix B**, **Behr JP** (1995) A versatile vector for gene and oligonucleotide transfer into cells in culture and *in vivo*: polyethylenimine. *Proc Natl Acad Sci U S A* **92**: 7297-7301

Bowers K, Levi BP, Patel FI, Stevens TH (2000) The sodium/proton exchanger Nhx1p is required for endosomal protein trafficking in the yeast *Saccharomyces cerevisiae*. *Mol Biol Cell* **11**: 4277-4294

Bowers K, Lottridge J, Helliwell SB, Goldthwaite LM, Luzio JP, Stevens TH (2004) Protein-protein interactions of ESCRT complexes in the yeast *Saccharomyces cerevisiae*. *Traffic* **5**: 194-210

Brachmann CB, Davies A, Cost GJ, Caputo E, Li J, Hieter P, Boeke JD (1998) Designer deletion mutants derived from *Saccharomyces cerevisiae* S288C: a useful set of mutants and plasmids for PCR-mediated gene disruption and other applications. *Yeast* **14**: 115-132

Bragonzi A, **Boletta A**, **Biffi A**, **Muggia A**, **Sersale G**, **Cheng SH**, **Bordignon C**, **Assael BM**, **Conese M** (1999) Comparison between cationic polymers and lipids in mediating systemic gene delivery to the lungs. *Gene Ther* **6**: 1995-2004

Bretscher A (2003) Polarized growth and organelle segregation in yeast: the tracks, motors, and receptors. *J Cell Biol* **160**: 811-816. Review

Brett CL, Tukaye DN, Mukherjee S, Rao R (2005) The yeast endosomal $Na^+(K^+)/H^+$ exchanger Nhx1 regulates cellular pH to control vesicle trafficking. *Mol Biol Cell* **16**: 1396-1405

Breunig F, **Wanner C** (2003) Enzyme replacement therapy for Fabry disease: proving the clinical benefit. *Nephrol Dial Transplant* **18**: 7-9. Review

Brickner JH, Fuller RS (1997) *SOI1* encodes a novel, conserved protein that promotes TGN-endosomal cycling of Kex2p and other membrane proteins by modulating the function of two TGN localization signals. *J Cell Biol* **139**: 23-36

Brickner JH, Blanchette JM, Sipos G, Fuller RS (2001) The Tlg SNARE complex is required for TGN homotypic fusion. *J Cell Biol* **155**: 969-978

Bryant NJ, **Piper RC**, **Weisman LS**, **Stevens TH** (1998) Retrograde traffic out of the yeast vacuole to the TGN occurs via the prevacuolar/endosomal compartment. *J Cell Biol* **142**: 651-663

Bryant NJ, Stevens TH (1997) Two separate signals act independently to localize a yeast late Golgi membrane protein through a combination of retrieval and retention. *J Cell Biol* **136**: 287-297

Bryant NJ, Stevens TH (1998) Vacuole biogenesis in *Saccharomyces cerevisiae*: Protein transport pathways to the yeast vacuole. *Microbiol Mol Biol Rev* **62**: 230-247. Review

Bull PC, **Cox DW** (1994) Wilson disease and Menkes disease: new handles on heavy-metal transport. *Trends Genet* **10**: 246-252. Review

Bull PC, **Thomas GR**, **Rommens JM**, **Forbes JR**, **Cox DW** (1993) The Wilson disease gene is a putative copper transporting P-type ATPase similar to the Menkes gene. *Nat Genet* **5**: 327-337

Bultynck G, Heath VL, Majeed AP, Galan JM, Haguenauer-Tsapis R, Cyert MS (2006) Slm1 and slm2 are novel substrates of the calcineurin phosphatase required for heat stress-induced endocytosis of the yeast uracil permease. *Mol Cell Biol* **26**: 4729-4745

Burd CG, Peterson M, Cowles CR, Emr SD (1997) A novel Sec18p/NSF-dependent complex required for Golgi-to-endosome transport in yeast. *Mol Biol Cell* **8**: 1089-1104

Castillo L, Martinez AI, Garcera A, Elorza MV, Valentin E, Sentandreu R (2003) Functional analysis of the cysteine residues and the repetitive sequence of Saccharomyces cerevisiae Pir4/Cis3: the repetitive sequence is needed for binding to the cell wall beta-1,3-glucan. *Yeast* **20**: 973-983

Cereghino JL, Marcusson EG, Emr SD (1995) The cytoplasmic tail domain of the vacuolar protein sorting receptor Vps10p and a subset of VPS gene products regulate receptor stability, function, and localization. *Mol Biol Cell* **6**: 1089-1102

Ceresa BP, Kao AW, Santeler SR, Pessin JE (1998) Inhibition of clathrin-mediated endocytosis selectively attenuates specific insulin receptor signal transduction pathways. *Mol Cell Biol* **18**: 3862-3870

Chakraverty RK, Kearsey JM, Oakley TJ, Grenon M, de La Torre Ruiz MA, Lowndes NF, Hickson ID (2001) Topoisomerase III acts upstream of Rad53p in the S-phase DNA damage checkpoint. *Mol Cell Biol* **21**: 7150-7162

Chang JS, Henry K, Geli MI, Lemmon SK (2006) Cortical recruitment and nuclear-cytoplasmic shuttling of Scd5p, a protein phosphatase-1-targeting protein involved in actin organization and endocytosis. *Mol Biol Cell* **17**: 251-262

Chattopadhyay S, **Roberts PM**, **Pearce DA** (2003) The yeast model for Batten disease: a role for Btn2p in the trafficking of the Golgi-associated vesicular targeting protein, Yif1p. *Biochem Biophys Res Commun* **302**: 534-538

Chelly J, **Tümer Z**, **Tønnesen T**, **Petterson A**, **Ishikawa-Brush Y**, **Tommerup N**, **Horn N**, **Monaco AP** (1993) Isolation of a candidate gene for Menkes disease that encodes a potential heavy metal binding protein. *Nat Genet* **3**: 14-19

Chen CY, **Brodsky FM** (2005) Huntingtin-interacting protein 1 (Hip1) and Hip1-related protein (Hip1R) bind the conserved sequence of clathrin light chains and thereby influence clathrin assembly *in vitro* and actin distribution *in vivo*. *J Biol Chem* **280**: 6109-6117

Chen SH, Chen S, Tokarev AA, Liu F, Jedd G, Segev N (2005) Ypt31/32 GTPases and their novel F-box effector protein Rcy1 regulate protein recycling. *Mol Biol Cell* **16**: 178-192

Chen H, Fre S, Slepnev VI, Capua MR, Takei K, Butler MH, Di Fiore PP, De Camilli P (1998) Epsin is an EH-domain-binding protein implicated in clathrin-mediated endocytosis. *Nature* **394**: 793-797

Chiba Y, **Sakuraba H**, **Kotani M**, **Kase R**, **Kobayashi K**, **Takeuchi M**, **Ogasawara S**, **Maruyama Y**, **Nakajima T**, **Takaoka Y**, **Jigami Y** (2002) Production in yeast of alpha-galactosidase A, a lysosomal enzyme applicable to enzyme replacement therapy for Fabry disease. *Glycobiology* **12**: 821-828

Chu DS, Pishvaee B, Payne GS (1996) The light chain subunit is required for clathrin function in *Saccharomyces cerevisiae*. *J Biol Chem* **271**: 33123-33130

Cid VJ, Duran A, del Rey F, Snyder MP, Nombela C, Sanchez M (1995) Molecular basis of cell integrity and morphogenesis in *Saccharomyces cerevisiae*. *Microbiol Rev* **59**: 345-386. Review

Cobbold C, **Coventry J**, **Ponnambalam S**, **Monaco AP** (2003) The Menkes disease ATPase (ATP7A) is internalized via a Rac1-regulated, clathrin- and caveolae-independent pathway. *Hum Mol Genet* **12**: 1523-1533

Coe JG, Lim AC, Xu J, Hong W (1999) A role for Tlg1p in the transport of proteins within the Golgi apparatus of *Saccharomyces cerevisiae*. *Mol Biol Cell* **10**: 2407-2423

Coll JL, **Chollet P**, **Brambilla E**, **Desplanques D**, **Behr JP**, **Favrot M** (1999) *In vivo* delivery to tumors of DNA complexed with linear polyethylenimine. *Hum Gene Ther* **10**: 1659-1666

Cooper AA, **Stevens TH** (1996) Vps10p cycles between the late-Golgi and prevacuolar compartments in its function as the sorting receptor for multiple yeast vacuolar hydrolases. *J Cell Biol* **133**: 529-541

Cooper A, Bussey H (1989) Characterization of the yeast *KEX1* gene product: a carboxypeptidase involved in processing secreted precursor proteins. *Mol Cell Biol* **9**: 2706-2714

Cooper MD, **Chae HP**, **Lowman JT**, **Krivit W**, **Good RA** (1968) Wiskott-Aldrich syndrome. An immunologic deficiency disease involving the afferent limb of immunity. *Am J Med* **44**: 499-513

Cope MJ, Yang S, Shang C, Drubin DG (1999) Novel protein kinases Ark1p and Prk1p associate with and regulate the cortical actin cytoskeleton in budding yeast. *J Cell Biol* **144**: 1203-1218

Cowles CR, Emr SD, Horazdovsky BF (1994) Mutations in the *VPS45* gene, a *SEC1* homologue, result in vacuolar protein sorting defects and accumulation of membrane vesicles. *J Cell Sci* **107**: 3449-3459

Cunningham KW, Fink GR (1994) Calcineurin-dependent growth control in *Saccharomyces cerevisiae* mutants lacking *PMC1*, a homolog of plasma membrane Ca^{2+} ATPases. *J Cell Biol* **124**: 351-363

Cunningham KW, Fink GR (1996) Calcineurin inhibits *VCX1*-dependent H^{+}/Ca^{2+} exchange and induces Ca^{2+} ATPases in *Saccharomyces cerevisiae*. *Mol Cell Biol* **16**: 2226-2237

Dake E, **Hofmann TJ**, **McIntire S**, **Hudson A**, **Zassenhaus HP** (1988) Purification and properties of the major nuclease from mitochondria of *Saccharomyces cerevisiae*. *J Biol Chem* **263**: 7691-7702

Daro E, **Sheff D**, **Gomez M**, **Kreis T**, **Mellman I** (1997) Inhibition of endosome function in CHO cells bearing a temperature-sensitive defect in the coatomer (COPI) component epsilon-COP. *J Cell Biol* **139**: 1747-1759

Darsow T, Katzmann DJ, Cowles CR, Emr SD (2001) Vps41p function in the alkaline phosphatase pathway requires homo-oligomerization and interaction with AP-3 through two distinct domains. *Mol Biol Cell* **12**: 37-51

De Bruyne C (1897) On a functional adaptation of phagocytosis. *J Anat Physiol* **32**: 92-95

de la Fuente MA, **Sasahara Y**, **Calamito M**, **Antón IM**, **Elkhal A**, **Gallego MD**, **Suresh K**, **Siminovitch K**, **Ochs HD**, **Anderson KC**, **Rosen FS**, **Geha RS**, **Ramesh N** (2007) WIP is a chaperone for Wiskott-Aldrich syndrome protein (WASP). *Proc Natl Acad Sci U S A* **104**: 926-931

Delgado R, **Regueiro BJ** (2005) The future of HIV infection: gene therapy and RNA interference. *Enferm Infecc Microbiol Clin* **23**: 76-83

Dell'Angelica EC, Puertollano R, Mullins C, Aguilar RC, Vargas JD, Hartnell LM, Bonifacino JS (2000) GGAs: a family of ADP ribosylation factor-binding proteins related to adaptors and associated with the Golgi complex. *J Cell Biol* **149**: 81-94

Deloche O, **Schekman RW** (2002) Vps10p cycles between the TGN and the late endosome via the plasma membrane in clathrin mutants. *Mol Biol Cell* **13**: 4296-4307

Dempski RE Jr, Imperiali B (2002) Oligosaccharyl transferase: gatekeeper to the secretory pathway. *Curr Opin Chem Biol* **6**: 844-850. Review

Denis V, Cyert MS (2002) Internal Ca^{2+} release in yeast is triggered by hypertonic shock and mediated by a TRP channel homologue. *J Cell Biol* **156**: 29-34

Dewar H, Warren DT, Gardiner FC, Gourlay CG, Satish N, Richardson MR, Andrews PD, Ayscough KR (2002) Novel proteins linking the actin cytoskeleton to the endocytic machinery in *Saccharomyces cerevisiae*. *Mol Biol Cell* **13**: 3646-3661

Di Guglielmo GM, **Le Roy C**, **Goodfellow AF**, **Wrana JL** (2003) Distinct endocytic pathways regulate TGF-β receptor signalling and turnover. *Nat Cell Biol* **5**: 410-421

Dmochowska A, Dignard D, Henning D, Thomas DY, Bussey H (1987) Yeast *KEX1* gene encodes a putative protease with a carboxypeptidase B-like function involved in killer toxin and α-factor precursor processing. *Cell* **50**: 573-584

Duckert P, Brunak S, Blom N (2004) Prediction of proprotein convertase cleavage sites. *Protein Eng Des Sel* **17**: 107-112

Dulic V, Egerton M, Elguindi I, Raths S, Singer B, Riezman H (1991) Yeast endocytosis assays. *Methods Enzymol* **194**: 697-710

Dupré S, **Haguenauer-Tsapis R** (2003) Raft partitioning of the yeast uracil permease during trafficking along the endocytic pathway. *Traffic* **4**: 83-96

Dürr G, Strayle J, Plemper R, Elbs S, Klee SK, Catty P, Wolf DH, Rudolph HK (1998) The medial-Golgi ion pump Pmr1 supplies the yeast secretory pathway with Ca^{2+} and Mn^{2+} required for glycosylation, sorting, and endoplasmic reticulum-associated protein degradation. *Mol Biol Cell* **9**: 1149-1162

Duyao M, Ambrose C, Myers R, Novelletto A, Persichetti F, Frontali M, Folstein S, Ross C, Franz M, Abbott M, Gray J, Conneally P, Young A, Penney J, Hollingsworth Z, Shoulson I, Lazzarini A, Falek A, Koroshetz W, Sax D, Bird E, Vonsattel J, Bonilla E, Alvir J, Bickham Conde J, Cha JH, Dure L, Gomez F, Ramos M, Sanchez-Ramos J, Snodgrass S, de Young M, Wexler N, Moscowitz C, Penchaszadeh G, MacFarlane H, Anderson M, Jenkins B, Srinidhi J, Barnes G, Gusella J, MacDonald M (1993) Trinucleotide repeat length instability and age of onset in Huntington's disease. *Nat Genet* **4**: 387-392

Ege T, **Reisbig RR**, **Rogne S** (1984) Enhancement of DNA-mediated gene transfer by inhibitors of autophagic-lysosomal function. *Exp Cell Res* **155**: 9-16

Ekena K, Vater CA, Raymond CK, Stevens TH (1993) The *VPS1* protein is a dynamin-like GTPase required for sorting proteins to the yeast vacuole. *Ciba Found Symp* **176**: 198-214

Engqvist-Goldstein AE, Drubin DG (2003) Actin assembly and endocytosis: from yeast to mammals. *Annu Rev Cell Dev Biol* **19**: 287-332. Review

Engqvist-Goldstein AE, Kessels MM, Chopra VS, Hayden MR, Drubin DG (1999) An actin-binding protein of the Sla2/Huntingtin interacting protein 1 family is a novel component of clathrin-coated pits and vesicles. *J Cell Biol* **147**: 1503-1518

Erbacher P, **Remy JS**, **Behr JP** (1999) Gene transfer with synthetic virus-like particles via the integrin-mediated endocytosis pathway. *Gene Ther* **6**: 138-145

Evans CJ, Aguilera RJ (2003) DNase II: genes, enzymes and function. *Gene* **322**: 1-15

Faber AW, Van Dijk M, Raue HA, Vos JC (2002) Ngl2p is a Ccr4p-like RNA nuclease essential for the final step in 3'-end processing of 5.8S rRNA in *Saccharomyces cerevisiae*. *RNA* **8**: 1095-1101

Finbow ME, Harrison MA (1997) The vacuolar H^+-ATPase: a universal proton pump of eukaryotes. *Biochem J* **324**: 697-712. Review

Finken-Eigen M, Röhricht RA, Köhrer K (1997) The *VPS4* gene is involved in protein transport out of a yeast pre-vacuolar endosome-like compartment. *Curr Genet* **31**: 469-480

Frattini A, **Orchard PJ**, **Sobacchi C**, **Giliani S**, **Abinun M**, **Mattsson JP**, **Keeling DJ**, **Andersson AK**, **Wallbrandt P**, **Zecca L**, **Notarangelo LD**, **Vezzoni P**, **Villa A** (2000) Defects in TCIRG1 subunit of the vacuolar proton pump are responsible for a subset of human autosomal recessive osteopetrosis. *Nat Genet* **25**: 343-346

Fu D, **Beeler TJ**, **Dunn TM** (1995) Sequence, mapping and disruption of *CCC2*, a gene that cross-complements the Ca^{2+}-sensitive phenotype of *csg1* mutants and encodes a P-type ATPase belonging to the Cu^{2+}-ATPase subfamily. *Yeast* **11**: 283-292

Fuller RS, Brake A, Thorner J (1989) Yeast prohormone processing enzyme (*KEX2* gene product) is a Ca^{2+}-dependent serine protease. *Proc Natl Acad Sci* **86**: 1434-1438

Gabriely G, **Kama R**, **Gerst JE** (2007) Involvement of specific COPI subunits in protein sorting from the late endosome to the vacuole in yeast. *Mol Cell Biol* **27**: 526-540

Gaigg B, **Timischl B**, **Corbino L**, **Schneiter R** (2005) Synthesis of sphingolipids with very long chain fatty acids but not ergosterol is required for routing of newly synthesized plasma membrane ATPase to the cell surface of yeast. *J Biol Chem* **280**: 22515-22522

Gaigg B, **Toulmay A**, **Schneiter R** (2006) Very long-chain fatty acid-containing lipids rather than sphingolipids per se are required for raft association and stable surface transport of newly synthesized plasma membrane ATPase in yeast. *J Biol Chem* **281**: 34135-34145

Galan JM, Haguenauer-Tsapis R (1997) Ubiquitin lys63 is involved in ubiquitination of a yeast plasma membrane protein. *EMBO J* **16**: 5847-5854

Galan JM, Moreau V, Andre B, Volland C, Haguenauer-Tsapis R (1996) Ubiquitination mediated by the Npi1p/Rsp5p ubiquitin-protein ligase is required for endocytosis of the yeast uracil permease. *J Biol Chem* **271**: 10946-10952

Gallego MD, **Santamaría M**, **Peña J**, **Molina IJ** (1997) Defective actin reorganization and polymerization of Wiskott-Aldrich T cells in response to CD3-mediated stimulation. *Blood* **90**: 3089-3097

Gall WE, Geething NC, Hua Z, Ingram MF, Liu K, Chen SI, Graham TR (2002) Drs2p-dependent formation of exocytic clathrin-coated vesicles *in vivo*. *Curr Biol* **12**: 1623-1627

Gammie AE, Kurihara LJ, Vallee RB, Rose MD (1995) *DNM1*, a dynamin-related gene, participates in endosomal trafficking in yeast. *J Cell Biol* **130**: 553-566

Gao XD, **Wang J**, **Keppler-Ross S**, **Dean N** (2005) *ERS1* encodes a functional homologue of the human lysosomal cystine transporter. *FEBS J* **272**: 2497-2511

Gaynor EC, te Heesen S, Graham TR, Aebi M, Emr SD (1994) Signal-mediated retrieval of a membrane protein from the Golgi to the ER in yeast. *J Cell Biol* **127**: 653-665

Geli MI, Riezman H (1996) Role of type I myosins in receptor-mediated endocytosis in yeast. *Science* **272**: 533-535

Gerrard SR, Bryant NJ, Stevens TH (2000[b]) *VPS21* controls entry of endocytosed and biosynthetic proteins into the yeast prevacuolar compartment. *Mol Biol Cell* **11**: 613-626

Gerrard SR, **Levi BP**, **Stevens TH** (2000) Pep12p is a multifunctional yeast syntaxin that controls entry of biosynthetic, endocytic and retrograde traffic into the prevacuolar compartment. *Traffic* **1**: 259-269

Gillingham AK, Tong AH, Boone C, Munro S (2004) The GTPase Arf1p and the ER to Golgi cargo receptor Erv14p cooperate to recruit the golgin Rud3p to the *cis*-Golgi. *J Cell Biol* **167**: 281-292

Girrbach V, Strahl S (2003) Members of the evolutionarily conserved PMT family of protein *O*-mannosyltransferases form distinct protein complexes among themselves. *J Biol Chem* **278**: 12554-12562

Gissen P, **Johnson CA**, **Gentle D**, **Hurst LD**, **Doherty AJ**, **O'Kane CJ**, **Kelly DA**, **Maher ER** (2005) Comparative evolutionary analysis of VPS33 homologues: genetic and functional insights. *Hum Mol Genet* **14**: 1261-1270

Glebov OO, **Bright NA**, **Nichols BJ** (2006) Flotillin-1 defines a clathrin-independent endocytic pathway in mammalian cells. *Nat Cell Biol* **8**: 46-54

Godbey WT, **Barry MA**, **Saggau P**, **Wu KK**, **Mikos AG** (2000) Poly(ethylenimine)-mediated transfection: a new paradigm for gene delivery. *J Biomed Mater Res* **51**: 321-328

Gourlay CW, Dewar H, Warren DT, Costa R, Satish N, Ayscough KR (2003) An interaction between Sla1p and Sla2p plays a role in regulating actin dynamics and endocytosis in budding yeast. *J Cell Sci* **116**: 2551-2564

Gozuacik D, Kimchi A (2007) Autophagy and cell death. *Curr Top Dev Biol* **78**: 217-245. Review

Graham TR, Seeger M, Payne GS, MacKay VL, Emr SD (1994) Clathrin-dependent localization of α-1,3-mannosyltransferase to the Golgi complex of *Saccharomyces cerevisiae*. *J Cell Biol* **127**: 667-678

Gu F, **Aniento F**, **Parton RG**, **Gruenberg J** (1997) Functional dissection of COP-I subunits in the biogenesis of multivesicular endosomes. *J Cell Biol* **139**: 1183-1195

Günther W, **Lüchow A**, **Cluzeaud F**, **Vandewalle A**, **Jentsch TJ** (1998) ClC-5, the chloride channel mutated in Dent's disease, colocalizes with the proton pump in endocytotically active kidney cells. *Proc Natl Acad Sci U S A* **95**: 8075-8080

Haas C, **Hung AY**, **Citron M**, **Teplow DB**, **Selkoe DJ** (1995) β-Amyloid, protein processing and Alzheimer's disease. *Arzneimittelforschung* **45**: 398-402

Haass C, **Selkoe DJ** (1993) Cellular processing of β-amyloid precursor protein and the genesis of amyloid β-peptide. *Cell* **75**: 1039-1042

Hacein-Bey-Abina S, **Von Kalle C**, **Schmidt M**, **McCormack MP**, **Wulffraat N**, **Leboulch P**, **Lim A**, **Osborne CS**, **Pawliuk R**, **Morillon E**, **Sorensen R**, **Forster A**, **Fraser P**, **Cohen JI**, **de Saint Basile G**, **Alexander I**, **Wintergerst U**, **Frebourg T**, **Aurias A**, **Stoppa-Lyonnet D**, **Romana S**, **Radford-Weiss I**, **Gross F**, **Valensi F**, **Delabesse E**, **Macintyre E**, **Sigaux F**, **Soulier J**, **Leiva LE**, **Wissler M**, **Prinz C**, **Rabbitts TH**, **Le Deist F**, **Fischer A**, **Cavazzana-Calvo M** (2003) LMO2-associated clonal T cell proliferation in two patients after gene therapy for SCID-X1. *Science* **302**: 415-419

Han So , **Mahato RI**, **Kim SW** (2001) Water-soluble lipopolymer for gene delivery. *Bioconjug Chem* **12**: 337-345

Harashima H, **Shinohara Y**, **Kiwada H** (2001) Intracellular control of gene trafficking using liposomes as drug carriers. *Eur J Pharm Sci* **13**: 85-89. Review

Harder T, **Simons K** (1997) Caveolae, DIGs, and the dynamics of sphingolipid-cholesterol microdomains. *Curr Opin Cell Biol* **9**: 534-542. Review

Harris SL, Waters MG (1996) Localization of a yeast early Golgi mannosyltransferase, Och1p, involves retrograde transport. *J Cell Biol* **132**: 985-998

Haviernik P, **Bunting KD** (2004) Safety concerns related to hematopoietic stem cell gene transfer using retroviral vectors. *Curr Gene Ther* **4**: 263-276. Review

Hearn JD, **Lester RL**, **Dickson RC** (2003) The uracil transporter Fur4p associates with lipid rafts. *J Biol Chem* **278**: 3679-3686

Heese-Peck A, **Pichler H**, **Zanolari B**, **Watanabe R**, **Daum G**, **Riezman H** (2002) Multiple functions of sterols in yeast endocytosis. *Mol Biol Cell* **13**: 2664-2680

Helenius A, Aebi M (2004) Roles of N-linked glycans in the endoplasmic reticulum. *Annu Rev Biochem* **73**: 1019-1049. Review

Henkel MK, Pott G, Henkel AW, Juliano L, Kam C-M, Powers JC, Franzusoff A (1999) Endocytic delivery of intramolecularly quenched substrates and inhibitors to the intracellular yeast Kex2 protease. *Biochem J* **341**: 445-452

Henley JR, Krueger EW, Oswald BJ, McNiven MA (1998) Dynamin-mediated internalization of caveolae. *J Cell Biol* **141**: 85-99

Henry KR, D'Hondt K, Chang JS, Nix DA, Cope MJ, Chan CS, Drubin DG, Lemmon SK (2003) The actin-regulating kinase Prk1p negatively regulates Scd5p, a suppressor of clathrin deficiency, in actin organization and endocytosis. *Curr Biol* **13**: 1564-1569

Herscovics A, Orlean P (1993) Glycoprotein biosynthesis in yeast. *FASEB J* **7**: 540-550. Review

Hicke L, Riezman H (1996) Ubiquitination of a yeast plasma membrane receptor signals its ligand-stimulated endocytosis. *Cell* **84**: 277-287

Hilliard CM, **Fletcher S**, **Yeoh GC** (1996) Calcium phosphate transfection and cell-specific expression of heterologous genes in primary fetal rat hepatocytes. *Int J Biochem Cell Biol* **28**: 639-650

Hinshaw JE, Schmid SL (1995) Dynamin self-assembles into rings suggesting a mechanism for coated vesicle budding. *Nature* **374**: 190-192. Review

Hochstrasser M, Johnson PR, Arendt CS, Amerik AYu , Swaminathan S, Swanson R, Li SJ, Laney J, Pals-Rylaarsdam R, Nowak J, Connerly PL (1999) The *Saccharomyces cerevisiae* ubiquitin-proteasome system. *Philos Trans R Soc Lond B Biol Sci* **354**: 1513-1522

Horazdovsky BF, Busch GR, Emr SD (1994) *VPS21* encodes a rab5-like GTP binding protein that is required for the sorting of yeast vacuolar proteins. *EMBO J* **13**: 1297-1309

Horazdovsky BF, Cowles CR, Mustol P, Holmes M, Emr SD (1996) A novel RING finger protein, Vps8p, functionally interacts with the small GTPase, Vps21p, to facilitate soluble vacuolar protein localization. *J Biol Chem* **271**: 33607-33615

Horazdovsky BF, Davies BA, Seaman MN, McLaughlin SA, Yoon S, Emr SD (1997) A sorting nexin-1 homologue, Vps5p, forms a complex with Vps17p and is required for recycling the vacuolar protein-sorting receptor. *Mol Biol Cell* **8**: 1529-1541

Howard JP, Hutton JL, Olson JM, Payne GS (2002) Sla1p serves as the targeting signal recognition factor for NPFX(1,2)D-mediated endocytosis. *J Cell Biol* **157**: 315-326

Howell DP, Krieser RJ, Eastman A, Barry MA (2003) Deoxyribonuclease II is a lysosomal barrier to transfection. *Mol Ther* **8**: 957-963

Huang KM, Gullberg L, Nelson KK, Stefan CJ, Blumer K, Lemmon SK (1997) Novel functions of clathrin light chains: clathrin heavy chain trimerization is defective in light chain-deficient yeast. *J Cell Sci* **110**: 899-910

Huijbregts RP, Topalof L, Bankaitis VA (2000) Lipid metabolism and regulation of membrane trafficking. *Traffic* **1**: 195-202. Review

Hui SW, **Langner M**, **Zhao YL**, **Ross P**, **Hurley E**, **Chan K** (1996) The role of helper lipids in cationic liposome-mediated gene transfer. *Biophys J* **71**: 590-599

Hunziker W, Fumey C (1994) A di-leucine motif mediates endocytosis and basolateral sorting of macrophage IgG Fc receptors in MDCK cells. *EMBO J* **13**: 2963-2969

Idrissi FZ, Wolf BL, Geli MI (2002) Cofilin, but not profilin, is required for myosin-I-induced actin polymerization and the endocytic uptake in yeast. *Mol Biol Cell* **13**: 4074-4087

Innis MA, Gelfand DH (1990) Optimization of PCRs. In *PCR Protocols - A guide to methods and applications* (ed. MA Innis, DH Gelfand, JJ Sninsky, TJ White), pp. 3-12. San Diego: Academic Press Inc.

Jacquiau HR, **van Waardenburg RC**, **Reid RJ**, **Woo MH**, **Guo H**, **Johnson ES**, **Bjornsti MA** (2005) Defects in SUMO (small ubiquitin-related modifier) conjugation and deconjugation alter cell sensitivity to DNA topoisomerase I-induced DNA damage. *J Biol Chem* **280**: 23566-23575

Jenco JM, **Rawlingson A**, **Daniels B**, **Morris AJ** (1998) Regulation of phospholipase D2: selective inhibition of mammalian phospholipase D isoenzymes by α- and β-synucleins. *Biochemistry* **37**: 4901-4909

Johnson AL, **Jurcisek JA**, **Trask OJ**, **Au JL** (1999) A method to monitor DNA transfer during transfection. *AAPS PharmSci* **1**: E6

Jones EW (2002) Vacuolar proteases and proteolytic artifacts in *Saccharomyces cerevisiae*. *Methods Enzymol* **351**: 127-150. Review

Jones EW, Zubenko GS, Parker RR (1982) *PEP4* gene function is required for expression of several vacuolar hydrolases in *Saccharomyces cerevisiae*. *Genetics* **102**: 665-677

Jones SW, **Christison R**, **Bundell K**, **Voyce CJ**, **Brockbank SM**, **Newham P**, **Lindsay MA** (2005) Characterisation of cell-penetrating peptide-mediated peptide delivery. *Br J Pharmacol* **145**: 1093-1102

Jonsdottir GA, Li R (2004) Dynamics of yeast Myosin I: evidence for a possible role in scission of endocytic vesicles. *Curr Biol* **14**: 1604-1609

Julius D, Blair L, Brake A, Sprague G, Thorner J (1983) Yeast α-factor is processed from a larger precursor polypeptide: the essential role of a membrane-bound dipeptidyl aminopeptidase. *Cell* **32**: 839-852

Julius D, Brake A, Blair L, Kunisawa R, Thorner J (1984) Isolation of the putative structural gene for the lysine-arginine-cleaving endopeptidase required for processing of yeast prepro-α-factor. *Cell* **37**: 1075-1089

Jung US, Lewin DE (1999) Genome-wide analysis of gene expression regulated by the yeast cell wall integrity signalling pathway. *Mol Microbiol* **34**: 1049-1057

Kaksonen M, Sun Y, Drubin DG (2003) A pathway for association of receptors, adaptors, and actin during endocytic internalization. *Cell* **115**: 475-487

Kaksonen M, Toret CP, Drubin DG (2005) A modular design for the clathrin- and actin-mediated endocytosis machinery. *Cell* **123**: 305-320

Kalatzis V, **Antignac C** (2002) Cystinosis: from gene to disease. *Nephrol Dial Transplant* **17**: 1883-1886. Review

Kalatzis V, **Cherqui S**, **Antignac C**, **Gasnier B** (2001) Cystinosin, the protein defective in cystinosis, is a H^+-driven lysosomal cystine transporter. *EMBO J* **20**: 5940-5949

Kapteyn JC, Van Egmond P, Sievi E, Van Den Ende H, Makarow M, Klis FM (1999) The contribution of the *O*-glycosylated protein Pir2p/Hsp150 to the construction of the yeast cell wall in wild-type cells and beta 1,6-glucan-deficient mutants. *Mol Microbiol* **31**: 1835-1844

Karin M, Mintz B (1981) Receptor-mediated endocytosis of transferrin in developmentally totipotent mouse teratocarcinoma stem cells. *J Biol Chem* **256**: 3245-3252

Kato M, Kuzuhara Y, Maeda H, Shiraga S, Ueda M (2006) Analysis of a processing system for proteases using yeast cell surface engineering: conversion of precursor of proteinase A to active proteinase A. *Appl Microbiol Biotechnol* **72**: 1229-1237

Katz JE, Dlakic M, Clarke S (2003) Automated identification of putative methyltransferases from genomic open reading frames. *Mol Cell Proteomics* **2**: 525-540

Kawaura C, **Noguchi A**, **Furuno T**, **Nakanishi M** (1998) Atomic force microscopy for studying gene transfection mediated by cationic liposomes with a cationic cholesterol derivative. *FEBS Lett* **421**: 69-72

Kim Y, **Chattopadhyay S**, **Locke S**, **Pearce DA** (2005) Interaction among Btn1p, Btn2p, and Ist2p reveals potential interplay among the vacuole, amino acid levels, and ion homeostasis in the yeast *Saccharomyces cerevisiae*. *Eukaryot Cell* **4**: 281-288

Kim Y, **Ramirez-Montealegre D**, **Pearce DA** (2003) A role in vacuolar arginine transport for yeast Btn1p and for human CLN3, the protein defective in Batten disease. *Proc Natl Acad Sci U S A* **100**: 15458-15462

Kirkham M, **Fujita A**, **Chadda R**, **Nixon SJ**, **Kurzchalia TV**, **Sharma DK**, **Pagano RE**, **Hancock JF**, **Mayor S**, **Parton RG** (2005) Ultrastructural identification of uncoated caveolin-independent early endocytic vehicles. *J Cell Biol* **168**: 465-476

Klionsky DJ, Herman PK, Emr SD (1990) The fungal vacuole: Composition, function, and biogenesis. *Microbiol Rev* **54**: 266-292. Review

Klionsky DJ, Nelson H, Nelson N (1992) Compartment acidification is required for efficient sorting of proteins to the vacuole in *Saccharomyces cerevisiae*. *J Biol Chem* **267**: 3416-3422

Klis FM, Boorsma A, De Groot PW (2006) Cell wall construction in *Saccharomyces cerevisiae*. *Yeast* **23**: 185-202

Knauer R, Lehle L (1999) The oligosaccharyltransferase complex from yeast. *Biochim Biophys Acta* **1426**: 259-273

Köhrer K, Emr SD (1993) The yeast *VPS17* gene encodes a membrane-associated protein required for the sorting of soluble vacuolar hydrolases. *J Biol Chem* **268**: 559-569

Kolehmainen J, **Black GC**, **Saarinen A**, **Chandler K**, **Clayton-Smith J**, **Träskelin AL**, **Perveen R**, **Kivitie-Kallio S**, **Norio R**, **Warburg M**, **Fryns JP**, **de la Chapelle A**, **Lehesjoki AE** (2003) Cohen syndrome is caused by mutations in a novel gene, COH1, encoding a transmembrane protein with a presumed role in vesicle-mediated sorting and intracellular protein transport. *Am J Hum Genet* **72**: 1359-1369

Krsmanović T, Pawelec A, Sydor T, Kölling R (2005) Control of Ste6 recycling by ubiquitination in the early endocytic pathway in yeast. *Mol Biol Cell* **16**: 2809-2821

Kübler E, Riezman H (1993) Actin and fimbrin are required for the internalization step of endocytosis in yeast. *EMBO J* **12**: 2855-2862

Kübler E, Schimmöller F, Riezman H (1994) Calcium-independent calmodulin requirement for endocytosis in yeast. *EMBO J* **13**: 5539-5546

Kukuruzinska MA, Bergh ML, Jackson BJ (1987) Protein glycosylation in yeast. *Annu Rev Biochem* **56**: 915-944

Kunath K, **Merdan T**, **Hegener O**, **Häberlein H**, **Kissel T** (2003) Integrin targeting using RGD-PEI conjugates for *in vitro* gene transfer. *J Gene Med* **5**: 588-599

Kursa M, **Walker GF**, **Roessler V**, **Ogris M**, **Roedl W**, **Kircheis R**, **Wagner E** (2003) Novel shielded transferrin-polyethylene glycol-polyethylenimine/DNA complexes for systemic tumor-targeted gene transfer. *Bioconjug Chem* **14**: 222-231

Kurzchalia TV, Parton RG (1999) Membrane microdomains and caveolae. *Curr Opin Cell Biol* **11**: 424-431

Lamaze C, Dujeancourt A, Baba T, Lo CG, Benmerah A, Dautry-Varsat A (2001) Interleukin 2 receptors and detergent-resistant membrane domains define a clathrin-independent endocytic pathway. *Mol Cell* **7**: 661-671

Lang C, Looman AC (1995) Efficient expression and secretion of *Aspergillus niger* RH5344 polygalacturonase in *Saccharomyces cerevisiae*. *Appl Microbiol Biotechnol* **44**: 147-156

Larriba G, Basco RD, Andaluz E, Luna-Arias JP (1993) Yeast exoglucanases. Where redundancy implies necessity. *Arch Med Res* **24**: 293-299. Review

Leber R, Silles E, Sandoval IV, Mazon MJ (2001) Yol082p, a novel CVT protein involved in the selective targeting of aminopeptidase I to the yeast vacuole. *J Biol Chem* **276**: 29210-29217

Lee MC, **Hamamoto S**, **Schekman R** (2002) Ceramide biosynthesis is required for the formation of the oligomeric H^+-ATPase Pma1p in the yeast endoplasmic reticulum. *J Biol Chem* **277**: 22395-22401

Legendre-Guillemin V, **Metzler M**, **Lemaire JF**, **Philie J**, **Gan L**, **Hayden MR**, **McPherson PS** (2005) Huntingtin interacting protein 1 (HIP1) regulates clathrin assembly through direct binding to the regulatory region of the clathrin light chain. *J Biol Chem* **280**: 6101-6108

Lewis MJ, Nichols BJ, Prescianotto-Baschong C, Riezman H, Pelham HR (2000) Specific retrieval of the exocytic SNARE Snc1p from early yeast endosomes. *Mol Biol Cell* **11**: 23-38

Lewis LK, **Storici F**, **Van Komen S**, **Calero S**, **Sung P**, **Resnick MA** (2004) Role of the nuclease activity of *Saccharomyces cerevisiae* Mre11 in repair of DNA double-strand breaks in mitotic cells. *Genetics* **166**: 1701-1713

Liang KW, **Hoffman EP**, **Huang L** (2000) Targeted delivery of plasmid DNA to myogenic cells via transferrin-conjugated peptide nucleic acid. *Mol Ther* **1**: 236-243

Liscum L, **Ruggiero RM**, **Faust JR** (1989) The intracellular transport of low density lipoprotein-derived cholesterol is defective in Niemann-Pick type C fibroblasts. *J Cell Biol* **108**: 1625-1636

Liu J, **Deyoung SM**, **Zhang M**, **Dold LH**, **Saltiel AR** (2005) The stomatin/prohibitin/flotillin/HflK/C domain of flotillin-1 contains distinct sequences that direct plasma membrane localization and protein interactions in 3T3-L1 adipocytes. *J Biol Chem* **280**: 16125-16134

Li Y, **Chin LS**, **Levey AI**, **Li L** (2002) Huntingtin-associated protein 1 interacts with hepatocyte growth factor-regulated tyrosine kinase substrate and functions in endosomal trafficking. *J Biol Chem* **277**: 28212-28221

Lloyd SE, **Pearce SH**, **Fisher SE**, **Steinmeyer K**, **Schwappach B**, **Scheinman SJ**, **Harding B**, **Bolino A**, **Devoto M**, **Goodyer P**, **Rigden SP**, **Wrong O**, **Jentsch TJ**, **Craig IW**, **Thakker RV** (1996) A common molecular basis for three inherited kidney stone diseases. *Nature* **379**: 445-449

Lobachev KS, **Gordenin DA**, **Resnick MA** (2002) The Mre11 complex is required for repair of hairpin-capped double-strand breaks and prevention of chromosome rearrangements. *Cell* **108**: 183-193

Lücking CB, **Brice A** (2000) α-synuclein and Parkinson's disease. *Cell Mol Life Sci* **57**: 1894-1908. Review

Luo W, Chang A (1997) Novel genes involved in endosomal traffic in yeast revealed by suppression of a targeting-defective plasma membrane ATPase mutant. *J Cell Biol* **138**: 731-746

Luo Z, Gallwitz D (2003) Biochemical and genetic evidence for the involvement of yeast Ypt6-GTPase in protein retrieval to different Golgi compartments. *J Biol Chem* **278**: 791-799

Lussier M, Gentzsch M, Sdicu AM, Bussey H, Tanner W (1995) Protein *O*-glycosylation in yeast. The *PMT2* gene specifies a second protein *O*-mannosyltransferase that functions in addition to the *PMT1*-encoded activity. *J Biol Chem* **270**: 2770-2775

Machesky LM, **Insall RH** (1998) Scar1 and the related Wiskott-Aldrich syndrome protein, WASP, regulate the actin cytoskeleton through the Arp2/3 complex. *Curr Biol* **8**: 1347-1356

Mack CA, **Song WR**, **Carpenter H**, **Wickham TJ**, **Kovesdi I**, **Harvey BG**, **Magovern CJ**, **Isom OW**, **Rosengart T**, **Falck-Pedersen E**, **Hackett NR**, **Crystal RG**, **Mastrangeli A** (1997) Circumvention of anti-adenovirus neutralizing immunity by administration of an adenoviral vector of an alternate serotype. *Hum Gene Ther* **8**: 99-109

Mack KD, **Wei R**, **Elbagarri A**, **Abbey N**, **McGrath MS** (1998) A novel method for DEAE-dextran mediated transfection of adherent primary cultured human macrophages. *J Immunol Methods* **211**: 79-86

MacLea KS, Krieser RJ, Eastman A (2003) Structural requirements of human DNase II alpha for formation of the active enzyme: the role of the signal peptide, N-glycosylation, and disulphide bridging. *Biochem J* **371**: 867-876

Madania A, **Dumoulin P**, **Grava S**, **Kitamoto H**, **Schärer-Brodbeck C**, **Soulard A**, **Moreau V**, **Winsor B** (1999) The *Saccharomyces cerevisiae* homologue of human Wiskott-Aldrich syndrome protein Las17p interacts with the Arp2/3 complex. *Mol Biol Cell* **10**: 3521-3538

Malathi K, **Higaki K**, **Tinkelenberg AH**, **Balderes DA**, **Almanzar-Paramio D**, **Wilcox LJ**, **Erdeniz N**, **Redican F**, **Padamsee M**, **Liu Y**, **Khan S**, **Alcantara F**, **Carstea ED**, **Morris JA**, **Sturley SL** (2004) Mutagenesis of the putative sterol-sensing domain of yeast Niemann Pick C-related protein reveals a primordial role in subcellular sphingolipid distribution. *J Cell Biol* **164**: 547-556

Malferrari G, Mazza U, Tresoldi C, Rovida E, Nissim M, Mirabella M, Servidei S, Biunno I (1999) Molecular characterization of a novel endonuclease (Xib) and possible involvement in lysosomal glycogen storage disorders. *Exp Mol Pathol* **66**: 123-130

Mandal D, Rulli SJ, Rao R (2003) Packing interactions between transmembrane helices alter ion selectivity of the yeast Golgi Ca^{2+}/Mn^{2+}-ATPase *PMR1*. *J Biol Chem* **278**: 35292-35298

Manolson MF, Wu B, Proteau D, Taillon BE, Roberts BT, Hoyt MA, Jones EW (1994) *STV1* gene encodes functional homologue of 95-kDa yeast vacuolar H^+-ATPase subunit Vph1p. *J Biol Chem* **269**: 14064-14074

Marone G, **Albini F**, **di Martino L**, **Quattrin S**, **Poto S**, **Condorelli M** (1986) The Wiskott-Aldrich syndrome: studies of platelets, basophils and polymorphonuclear leucocytes. *Br J Haematol* **62**: 737-745

Maxfield FR, Schlessinger J, Shechter Y, Pastan I, Willingham MC (1978) Collection of insulin, EGF and α2-macroglobulin in the same patches on the surface of cultured fibroblasts and common internalization. *Cell* **14**: 805-810

McMahon HT, **Mills IG** (2004) COP and clathrin-coated vesicle budding: different pathways, common approaches. *Curr Opin Cell Biol* **16**: 379-391. Review

Medzon EL, Gedies A (1971) Substitution of 4-(2-hydroxyethyl)-1-piperazineethane sulfonic acid (HEPES) for bicarbonate in protein-free animal cell culture medium: application to vaccinia virus quantitation and fluorogenic acetylesterase assay in living LM cells. *Can J Microbiol* **17**: 651-653

Mercer JF, **Livingston J**, **Hall B**, **Paynter JA**, **Begy C**, **Chandrasekharappa S**, **Lockhart P**, **Grimes A**, **Bhave M**, **Siemieniak D**, **Glover TW** (1993) Isolation of a partial candidate gene for Menkes disease by positional cloning. *Nat Genet* **3**: 20-25

Meussdoerffer F, Tortora P, Holzer H (1980) Purification and properties of proteinase A from yeast. *J Biol Chem* **255**: 12087-12093

Midoux P, **Mendes C**, **Legrand A**, **Raimond J**, **Mayer R**, **Monsigny M**, **Roche AC** (1993) Specific gene transfer mediated by lactosylated poly-L-lysine into hepatoma cells. *Nucleic Acids Res* **21**: 871-878

Minshall RD, **Tiruppathi C**, **Vogel SM**, **Niles WD**, **Gilchrist A**, **Hamm HE**, **Malik AB** (2000) Endothelial cell-surface gp60 activates vesicle formation and trafficking via G(i)-coupled Src kinase signaling pathway. *J Cell Biol* **150**: 1057-1070

Miseta A, Kellermayer R, Aiello DP, Fu L, Bedwell DM (1999) The vacuolar Ca^{2+}/H^+ exchanger Vcx1p/Hum1p tightly controls cytosolic Ca^{2+} levels in *S. cerevisiae*. *FEBS Lett* **451**: 132-136

Mizushima N, Ohsumi Y, Yoshimori T (2002) Autophagosome formation in mammalian cells. *Cell Struct Funct* **27**: 421-429. Review

Mochida J, **Yamamoto T**, **Fujimura-Kamada K**, **Tanaka K** (2002) The novel adaptor protein, Mti1p, and Vrp1p, a homolog of Wiskott-Aldrich syndrome protein-interacting protein (WIP), may antagonistically regulate type I myosins in *Saccharomyces cerevisiae*. *Genetics* **160**: 923-934

Moehle CM, Aynardi MW, Kolodny MR, Park FJ, Jones EW (1987) Protease B of *Saccharomyces cerevisiae*: isolation and regulation of the *PRB1* structural gene. *Genetics* **115**: 255-263

Moehle CM, Tizard R, Lemmon SK, Smart J, Jones EW (1987) Protease B of the lysosomelike vacuole of the yeast *Saccharomyces cerevisiae* is homologous to the subtilisin family of serine proteases. *Mol Cell Biol* **7**: 4390-4399

Moreau V, Galan JM, Devilliers G, Haguenauer-Tsapis R, Winsor B (1997) The yeast actin-related protein Arp2p is required for the internalization step of endocytosis. *Mol Biol Cell* **8**: 1361-1375

Moukadiri I, Jaafar L, Zueco J (1999) Identification of two mannoproteins released from cell walls of a *Saccharomyces cerevisiae mnn1 mnn9* double mutant by reducing agents. *J Bacteriol* **181**: 4741-4745

Moukadiri I, Zueco J (2001) Evidence for the attachment of *Hsp150*/*Pir2* to the cell wall of *Saccharomyces cerevisiae* through disulfide bridges. *FEMS Yeast Res* **1**: 241-245

Moukadiri I, Zueco J (2001) *YJL159w* does encode *Pir2*/*Hsp150*. *Yeast* **18**: 323-324

Mrsă V, Seidl T, Gentzsch M, Tanner W (1997) Specific labelling of cell wall proteins by biotinylation. Identification of four covalently linked O-mannosylated proteins of *Saccharomyces cerevisiae*. *Yeast* **13**: 1145-1154

Mrsă V, Tanner W (1999) Role of NaOH-extractable cell wall proteins Ccw5p, Ccw6p, Ccw7p and Ccw8p (members of the Pir protein family) in stability of the *Saccharomyces cerevisiae* cell wall. *Yeast* **15**: 813-820

Mueller SC, Branton D (1984) Identification of coated vesicles in *Saccharomyces cerevisiae*. *J Cell Biol* **98**: 341-346

Mukherjee S, Kallay L, Brett CL, Rao R (2006) Mutational analysis of the intramembranous H10 loop of yeast *Nhx1* reveals a critical role in ion homeostasis and vesicle trafficking. *Biochem J* **398**: 97-105

Mulholland J, Preuss D, Moon A, Wong A, Drubin D, Botstein D (1994) Ultrastructure of the yeast actin cytoskeleton and its association with the plasma membrane. *J Cell Biol* **125**: 381-391

Munn AL, **Heese-Peck A**, **Stevenson BJ**, **Pichler H**, **Riezman H** (1999) Specific sterols required for the internalization step of endocytosis in yeast. *Mol Biol Cell* **10**: 3943-3957

Munro S (2001) What can yeast tell us about N-linked glycosylation in the Golgi apparatus? *FEBS Lett* **498**: 223-227. Review

Murata M, **Peränen J**, **Schreiner R**, **Wieland F**, **Kurzchalia TV**, **Simons K** (1995) VIP21/caveolin is a cholesterol-binding protein. *Proc Natl Acad Sci U S A* **92**: 10339-10343

Nair U, Klionsky DJ (2005) Molecular mechanisms and regulation of specific and nonspecific autophagy pathways in yeast. *J Biol Chem* **280**: 41785-41788. Minireview.

Nakamura N, Hirata A, Ohsumi Y, Wada Y (1997) Vam2/Vps41p and Vam6/Vps39p are components of a protein complex on the vacuolar membranes and involved in the vacuolar assembly in the yeast *Saccharomyces cerevisiae*. *J Biol Chem* **272**: 11344-11349

Nakanishi M, **Noguchi A** (2001) Confocal and probe microscopy to study gene transfection mediated by cationic liposomes with a cationic cholesterol derivative. *Adv Drug Deliv Rev* **52**: 197-207. Review

Nakayama K, Nagasu T, Shimma Y, Kuromitsu J, Jigami Y (1992) *OCH1* encodes a novel membrane bound mannosyltransferase: outer chain elongation of asparagine-linked oligosaccharides. *EMBO J* **11**: 2511-2519

Naqvi SN, **Zahn R**, **Mitchell DA**, **Stevenson BJ**, **Munn AL** (1998) The WASp homologue Las17p functions with the WIP homologue End5p/verprolin and is essential for endocytosis in yeast. *Curr Biol* **8**: 959-962

Nass R, Cunningham KW, Rao R (1997) Intracellular sequestration of sodium by a novel Na^+/H^+ exchanger in yeast is enhanced by mutations in the plasma membrane H^+-ATPase. Insights into mechanisms of sodium tolerance. *J Biol Chem* **272**: 26145-26152

Nebreda AR, Villa TG, Villanueva JR, del Rey F (1986) Cloning of genes related to exo-β-glucanase production in *Saccharomyces cerevisiae*: characterization of an exo-β-glucanase structural gene. *Gene* **47**: 245-259

Neukamm B, Stahl U, Lang C (2002) Endocytosis is involved in DNA uptake in yeast. *Biochim Biophys Acta* **1572**: 67-76

Neukamm B, **Weimann A**, **Wu S**, **Danevad M**, **Lang C**, **Gessner R** (2006) Novel two-stage screening procedure leads to the identification of a new class of transfection enhancers. *J Gene Med* **8**: 745-753

Newpher TM, Idrissi FZ, Geli MI, Lemmon SK (2006) Novel function of clathrin light chain in promoting endocytic vesicle formation. *Mol Biol Cell* **17**: 4343-4352

Newpher TM, Lemmon SK (2006) Clathrin is important for normal actin dynamics and progression of Sla2p-containing patches during endocytosis in yeast. *Traffic* **7**: 574-588

Newpher TM, Smith RP, Lemmon V, Lemmon SK (2005) *In vivo* dynamics of clathrin and its adaptor-dependent recruitment to the actin-based endocytic machinery in yeast. *Dev Cell* **9**: 87-98

Nichols BJ, **Lippincott-Schwartz J** (2001) Endocytosis without clathrin coats. *Trends Cell Biol* **11**: 406-412. Review

Nohe A, Keating E, Underhill TM, Knaus P, Petersen NO (2005) Dynamics and interaction of caveolin-1 isoforms with BMP-receptors. *J Cell Sci* **118**: 643-650

Norkin LC (1999) Simian virus 40 infection via MHC class I molecules and caveolae. *Immunol Rev* **168**: 13-22. Review

Nothwehr SF, Bryant NJ, Stevens TH (1996) The newly identified yeast GRD genes are required for retention of late-Golgi membrane proteins. *Mol Cell Biol* **16**: 2700-2707

Nothwehr SF, Conibear E, Stevens TH (1995) Golgi and vacuolar membrane proteins reach the vacuole in *vps1* mutant yeast cells via the plasma membrane. *J Cell Biol* **129**: 35-46

Nothwehr SF, Roberts CJ, Stevens TH (1993) Membrane protein retention in the yeast Golgi apparatus: dipeptidyl aminopeptidase A is retained by a cytoplasmic signal containing aromatic residues. *J Cell Biol* **121**: 1197-1209

Ochs HD, **Slichter SJ**, **Harker LA**, **Von Behrens WE**, **Clark RA**, **Wedgwood RJ** (1980) The Wiskott-Aldrich syndrome: studies of lymphocytes, granulocytes, and platelets. *Blood* **55**: 243-252

Odorizzi G, **Babst M**, **Emr SD** (1998) Fab1p PtdIns(3)P 5-kinase function essential for protein sorting in the multivesicular body. *Cell* **95**: 847-858

Odorizzi G, **Katzmann DJ**, **Babst M**, **Audhya A**, **Emr SD** (2003) Bro1 is an endosome-associated protein that functions in the MVB pathway in *Saccharomyces cerevisiae*. *J Cell Sci* **116**: 1893-1903

Ohno H, Stewart J, Fournier MC, Bosshart H, Rhee I, Miyatake S, Saito T, Gallusser A, Kirchhausen T, Bonifacino JS (1995) Interaction of tyrosine-based sorting signals with clathrin-associated proteins. *Science* **269**: 1872-1875

Oh P, McIntosh DP, Schnitzer JE (1998) Dynamin at the neck of caveolae mediates their budding to form transport vesicles by GTP-driven fission from the plasma membrane of endothelium. *J Cell Biol* **141**: 101-114

Okada CY, Rechsteiner M (1982) Introduction of macromolecules into cultured mammalian cells by osmotic lysis of pinocytic vesicles. *Cell* **29**: 33-41

Onodera J, Ohsumi Y (2005) Autophagy is required for maintenance of amino acid levels and protein synthesis under nitrogen starvation. *J Biol Chem* **280**: 31582-31586

Ooi CE, Dell'Angelica EC, Bonifacino JS (1998) ADP-Ribosylation factor 1 (*ARF1*) regulates recruitment of the AP-3 adaptor complex to membranes. *J Cell Biol* **142**: 391-402

Ooms LM, **McColl BK**, **Wiradjaja F**, **Wijayaratnam AP**, **Gleeson P**, **Gething MJ**, **Sambrook J**, **Mitchell CA** (2000) The yeast inositol polyphosphate 5-phosphatases Inp52p and Inp53p translocate to actin patches following hyperosmotic stress: mechanism for regulating phosphatidylinositol 4,5-bisphosphate at plasma membrane invaginations. *Mol Cell Biol* **20**: 9376-9390

Orlandi PA, **Fishman PH** (1998) Filipin-dependent inhibition of cholera toxin: evidence for toxin internalization and activation through caveolae-like domains. *J Cell Biol* **141**: 905-915

Outeiro TF, **Lindquist S** (2003) Yeast cells provide insight into α-synuclein biology and pathobiology. *Science* **302**: 1772-1775

Palmer CP, Zhou XL, Lin J, Loukin SH, Kung C, Saimi Y (2001) A TRP homolog in *Saccharomyces cerevisiae* forms an intracellular Ca^{2+}-permeable channel in the yeast vacuolar membrane. *Proc Natl Acad Sci U S A* **98**: 7801-7805

Pammer M, Briza P, Ellinger A, Schuster T, Stucka R, Feldmann H, Breitenbach M (1992) *DIT101* (*CSD2*, *CAL1*), a cell cycle-regulated yeast gene required for synthesis of chitin in cell walls and chitosan in spore walls. *Yeast* **8**: 1089-1099

Panek HR, Conibear E, Bryan JD, Colvin RT, Goshorn CD, Robinson LC (2000) Identification of Rgp1p, a novel Golgi recycling factor, as a protein required for efficient localization of yeast casein kinase 1 to the plasma membrane. *J Cell Sci* **113**: 4545-4555

Panek HR, Stepp JD, Engle HM, Marks KM, Tan PK, Lemmon SK, Robinson LC (1997) Suppressors of YCK-encoded yeast casein kinase 1 deficiency define the four subunits of a novel clathrin AP-like complex. *EMBO J* **16**: 4194-4204

Pan X, Roberts P, Chen Y, Kvam E, Shulga N, Huang K, Lemmon S, Goldfarb DS (2000) Nucleus-vacuole junctions in *Saccharomyces cerevisiae* are formed through the direct interaction of Vac8p with Nvj1p. *Mol Biol Cell* **11**: 2445-2457

Parton RG, **Joggerst B**, **Simons K** (1994) Regulated internalization of caveolae. *J Cell Biol* **127**: 1199-1215

Parton RG (1994) Ultrastructural localization of gangliosides; GM1 is concentrated in caveolae. *J Histochem Cytochem* **42**: 155-166

Payne GS, **Hasson TB**, **Hasson MS**, **Schekman R** (1987) Genetic and biochemical characterization of clathrin-deficient *Saccharomyces cerevisiae*. *Mol Cell Biol* **7**: 3888-3898

Pearse BM (1976) Clathrin: a unique protein associated with intracellular transfer of membrane by coated vesicles. *Proc Natl Acad Sci U S A* **73**: 1255-1259

Pelkmans L, **Kartenbeck J**, **Helenius A** (2001) Caveolar endocytosis of simian virus 40 reveals a new two-step vesicular-transport pathway to the ER. *Nat Cell Biol* **3**: 473-483

Perrone GG, **Grant CM**, **Dawes IW** (2005) Genetic and environmental factors influencing glutathione homeostasis in *Saccharomyces cerevisiae*. *Mol Biol Cell* **16**: 218-230

Perzov N, Padler-Karavani V, Nelson H, Nelson N (2002) Characterization of yeast V-ATPase mutants lacking Vph1p or Stv1p and the effect on endocytosis. *J Exp Biol* **205**: 1209-1219

Peters C, Andrews PD, Stark MJ, Cesaro-Tadic S, Glatz A, Podtelejnikov A, Mann M, Mayer A (1999) Control of the terminal step of intracellular membrane fusion by protein phosphatase 1. *Science* **285**: 1084-1087

Peterson MR, Emr SD (2001) The class C Vps complex functions at multiple stages of the vacuolar transport pathway. *Traffic* **2**: 476-486

Petrukhin K, Fischer SG, Pirastu M, Tanzi RE, Chernov I, Devoto M, Brzustowicz LM, Cayanis E, Vitale E, Russo JJ, Matseoane D, Boukhgalter B, Wasco W, Figus AL, Loudianos J, Cao A, Sternlieb I, Evgrafov O, Parano E, Pavone L, Warburton D, Ott J, Penchaszadeh GK, Scheinberg IH, Gilliam TC (1993) Mapping, cloning and genetic characterization of the region containing the Wilson disease gene. *Nat Genet* **5**: 338-343

Pichler H, **Riezman H** (2004) Where sterols are required for endocytosis. *Biochim Biophys Acta* **1666**: 51-61. Review

Pike LJ (2004) Lipid rafts: heterogeneity on the high seas. *Biochem J* **378**: 281-292. Review

Piper RC, Cooper AA, Yang H, Stevens TH (1995) *VPS27* controls vacuolar and endocytic traffic through a prevacuolar compartment in *Saccharomyces cerevisiae*. *J Cell Biol* **131**: 603-617

Pishvaee B, **Costaguta G**, **Yeung BG**, **Ryazantsev S**, **Greener T**, **Greene LE**, **Eisenberg E**, **McCaffery JM**, **Payne GS** (2000) A yeast DNA J protein required for uncoating of clathrin-coated vesicles *in vivo*. *Nat Cell Biol* **2**: 958-963

Polo S, Sigismund S, Faretta M, Guidi M, Capua MR, Bossi G, Chen H, De Camilli P, Di Fiore PP (2002) A single motif responsible for ubiquitin recognition and monoubiquitination in endocytic proteins. *Nature* **416**: 451-455

Pond L, Kuhn LA, Teyton L, Schutze MP, Tainer JA, Jackson MR, Peterson PA (1995) A role for acidic residues in di-leucine motif-based targeting to the endocytic pathway. *J Biol Chem* **270**: 19989-19997

Pozos TC, Sekler I, Cyert MS (1996) The product of *HUM1*, a novel yeast gene, is required for vacuolar Ca^{2+}/H^{+} exchange and is related to mammalian Na^{+}/Ca^{2+} exchangers. *Mol Cell Biol* **16**: 3730-3741

Pralle A, **Keller P**, **Florin EL**, **Simons K**, **Hörber JK** (2000) Sphingolipid-cholesterol rafts diffuse as small entities in the plasma membrane of mammalian cells. *J Cell Biol* **148**: 997-1008

Prins HW, **Van den Hamer CJ** (1979) Primary biochemical defect in copper metabolism in mice with a recessive X-linked mutation analogous to Menkes' disease in man. *J Inorg Biochem* **10**: 19-27

Qaddoumi MG, **Gukasyan HJ**, **Davda J**, **Labhasetwar V**, **Kim KJ**, **Lee VH** (2003) Clathrin and caveolin-1 expression in primary pigmented rabbit conjunctival epithelial cells: role in PLGA nanoparticle endocytosis. *Mol Vis* **9**: 559-568

Qian ZM, Li H, Sun H, Ho K (2002) Targeted drug delivery via the transferrin receptor-mediated endocytosis pathway. *Pharmacol Rev* **54**: 561-587. Review

Raymond CK, Howald-Stevenson I, Vater CA, Stevens TH (1992) Morphological classification of the yeast vacuolar protein sorting mutants: Evidence for a prevacuolar compartment in class E vps mutants. *Mol Biol Cell* **3**: 1389-1402

Razani B, **Zhang XL**, **Bitzer M**, **von Gersdorff G**, **Böttinger EP**, **Lisanti MP** (2001) Caveolin-1 regulates transforming growth factor (TGF)-β/SMAD signaling through an interaction with the TGF-β type I receptor. *J Biol Chem* **276**: 6727-6738

Redding K, Brickner JH, Marschall LG, Nichols JW, Fuller RS (1996) Allele-specific suppression of a defective *trans*-Golgi network (TGN) localization signal in Kex2p identifies three genes involved in localization of TGN transmembrane proteins. *Mol Cell Biol* **16**: 6208-6217

Reinders J, Zahedi RP, Pfanner N, Meisinger C, Sickmann A (2006) Toward the complete yeast mitochondrial proteome: multidimensional separation techniques for mitochondrial proteomics. *J Proteome Res* **5**: 1543-1554

Rejman J, **Oberle V**, **Zuhorn IS**, **Hoekstra D** (2004) Size-dependent internalization of particles via the pathways of clathrin- and caveolae-mediated endocytosis. *Biochem J* **377**: 159-169

Reneke JE, Blumer KJ, Courchesne WE, Thorner J (1988) The carboxy-terminal segment of the yeast α-factor receptor is a regulatory domain. *Cell* **55**: 221-234

Richard JP, **Melikov K**, **Brooks H**, **Prevot P**, **Lebleu B**, **Chernomordik LV** (2005) Cellular uptake of unconjugated TAT peptide involves clathrin-dependent endocytosis and heparan sulfate receptors. *J Biol Chem* **280**: 15300-15306

Richard JP, **Melikov K**, **Vives E**, **Ramos C**, **Verbeure B**, **Gait MJ**, **Chernomordik LV**, **Lebleu B** (2003) Cell-penetrating peptides. A reevaluation of the mechanism of cellular uptake. *J Biol Chem* **278**: 585-590

Rieder SE, **Banta LM**, **Köhrer K**, **McCaffery JM**, **Emr SD** (1996) Multilamellar endosome-like compartment accumulates in the yeast *vps28* vacuolar protein sorting mutant. *Mol Biol Cell* **7**: 985-999

Rieder SE, Emr SD (1997) A novel RING finger protein complex essential for a late step in protein transport to the yeast vacuole. *Mol Biol Cell* **8**: 2307-2327

Rivera-Milla E, **Stuermer CA**, **Málaga-Trillo E** (2006) Ancient origin of reggie (flotillin), reggie-like, and other lipid-raft proteins: convergent evolution of the SPFH domain. *Cell Mol Life Sci* **63**: 343-357

Robbins PD, **Ghivizzani SC** (1998) Viral vectors for gene therapy. *Pharmacol Ther* **80**: 35-47. Review
Roberts P, Moshitch-Moshkovitz S, Kvam E, O'Toole E, Winey M, Goldfarb DS (2003) Piecemeal microautophagy of nucleus in *Saccharomyces cerevisiae*. *Mol Biol Cell* **14**: 129-141

Robinson M, Poon PP, Schindler C, Murray LE, Kama R, Gabriely G, Singer RA, Spang A, Johnston GC, Gerst JE (2006) The Gcs1 Arf-GAP mediates Snc1,2 v-SNARE retrieval to the Golgi in yeast. *Mol Biol Cell* **17**: 1845-1858

Rockwell NC, Fuller RS (2002) Specific modulation of Kex2/furin family proteases by potassium. *J Biol Chem* **277**: 17531-17537

Rodal SK, **Skretting G**, **Garred O**, **Vilhardt F**, **van Deurs B**, **Sandvig K** (1999) Extraction of cholesterol with methyl-β-cyclodextrin perturbs formation of clathrin-coated endocytic vesicles. *Mol Biol Cell* **10**: 961-974

Rohrer J, Bénédetti H, Zanolari B, Riezman H (1993) Identification of a novel sequence mediating regulated endocytosis of the G protein-coupled α-pheromone receptor in yeast. *Mol Biol Cell* **4**: 511-521

Rothberg KG, Heuser JE, Donzell WC, Ying YS, Glenney JR, Anderson RG (1992) Caveolin, a protein component of caveolae membrane coats. *Cell* **68**: 673-682

Royle SJ, Lagnado L (2003) Endocytosis at the synaptic terminal. *J Physiol* **553**: 345-355. Review

Rupp S, Wolf DH (1995) Biogenesis of the yeast vacuole (lysosome). The use of active-site mutants of proteinase *yscA* to determine the necessity of the enzyme for vacuolar proteinase maturation and proteinase *yscB* stability. *Eur J Biochem* **231**: 115-125

Russo P, Kalkkinen N, Sareneva H, Paakkola J, Makarow M (1992) A heat shock gene from *Saccharomyces cerevisiae* encoding a secretory glycoprotein. *Proc Natl Acad Sci U S A* **89**: 3671-3675 Erratum in: *Proc Natl Acad Sci U S A* **89**: 8857

Russo P, Simonen M, Uimari A, Teesalu T, Makarow M (1993) Dual regulation by heat and nutrient stress of the yeast *HSP150* gene encoding a secretory glycoprotein. *Mol Gen Genet* **239**: 273-280

Säälik P, **Elmquist A**, **Hansen M**, **Padari K**, **Saar K**, **Viht K**, **Langel U**, **Pooga M** (2004) Protein cargo delivery properties of cell-penetrating peptides. A comparative study. *Bioconjug Chem* **15**: 1246-1253

Sabah JR, Schultz BD, Brown ZW, Nguyen AT, Reddan J, Takemoto LJ (2007) Transcytotic passage of albumin through lens epithelial cells. *Invest Ophthalmol Vis Sci* **48**: 1237-1244

Sabharanjak S, **Sharma P**, **Parton RG**, **Mayor S** (2002) GPI-anchored proteins are delivered to recycling endosomes via a distinct cdc42-regulated, clathrin-independent pinocytic pathway. *Dev Cell* **2**: 411-423

Sakuma R, **Noser JA**, **Ohmine S**, **Ikeda Y** (2007) Inhibition of HIV-1 replication by simian restriction factors, TRIM5alpha and APOBEC3G. *Gene Ther* **14**: 185-189

Salaün C, **James DJ**, **Chamberlain LH** (2004) Lipid rafts and the regulation of exocytosis. *Traffic* **5**: 255-264. Review

Scherer PE, Okamoto T, Chun M, Nishimoto I, Lodish HF, Lisanti MP (1996) Identification, sequence, and expression of caveolin-2 defines a caveolin gene family. *Proc Natl Acad Sci U S A* **93**: 131-135

Schlegel A, Pestell RG, Lisanti MP (2000) Caveolins in cholesterol trafficking and signal transduction: implications for human disease. *Front Biosci* **5**: D929-D937

Schuck S, **Honsho M**, **Ekroos K**, **Shevchenko A**, **Simons K** (2003) Resistance of cell membranes to different detergents. *Proc Natl Acad Sci U S A* **100**: 5795-5800

Schulz JB, **Lindenau J**, **Seyfried J**, **Dichgans J** (2000) Glutathione, oxidative stress and neurodegeneration. *Eur J Biochem* **267**: 4904-4911. Review

Schu PV, Takegawa K, Fry MJ, Stack JH, Waterfield MD, Emr SD (1993) Phosphatidylinositol 3-kinase encoded by yeast *VPS34* gene essential for protein sorting. *Science* **260**: 88-91

Scott SV, Guan J, Hutchins MU, Kim J, Klionsky DJ (2001) Cvt19 is a receptor for the cytoplasm-to-vacuole targeting pathway. *Mol Cell* **7**: 1131-1141

Seals DF, Eitzen G, Margolis N, Wickner WT, Price A (2000) A Ypt/Rab effector complex containing the Sec1 homolog Vps33p is required for homotypic vacuole fusion. *Proc Natl Acad Sci U S A* **97**: 9402-9407

Seaman MN, **McCaffery JM**, **Emr SD** (1998) A membrane coat complex essential for endosome-to-Golgi retrograde transport in yeast. *J Cell Biol* **142**: 665-681

Seol JH, Shevchenko A, Shevchenko A, Deshaies RJ (2001) Skp1 forms multiple protein complexes, including RAVE, a regulator of V-ATPase assembly. *Nat Cell Biol* **3**: 384-391

Sesaki H, Jensen RE (1999) Division versus fusion: Dnm1p and Fzo1p antagonistically regulate mitochondrial shape. *J Cell Biol* **147**: 699-706

Shaw JD, Cummings KB, Huyer G, Michaelis S, Wendland B (2001) Yeast as a model system for studying endocytosis. *Exp Cell Res* **271**: 1-9

Shintani T, Huang WP, Stromhaug PE, Klionsky DJ (2002) Mechanism of cargo selection in the cytoplasm to vacuole targeting pathway. *Dev Cell* **3**: 825-837

Shiokawa D, Tanuma S (1999) DLAD, a novel mammalian divalent cation-independent endonuclease with homology to DNase II. *Nucleic Acids Res* **27**: 4083-4089

Shiokawa D, Tanuma SI (2001) Isolation and characterization of the DLAD/Dlad genes, which lie head-to-head with the genes for urate oxidase. *Biochem Biophys Res Commun* **288**: 1119-1128

Siddiqui SS, Siddiqui ZK, Malik AB (2004) Albumin endocytosis in endothelial cells induces TGF-β receptor II signaling. *Am J Physiol Lung Cell Mol Physiol* **286**: L1016-L1026

Singer-Krüger B, **Stenmark H**, **Zerial M** (1995) Yeast Ypt51p and mammalian Rab5: counterparts with similar function in the early endocytic pathway. *J Cell Sci* **108**: 3509-3521

Silberstein S, Gilmore R (1996) Biochemistry, molecular biology, and genetics of the oligosaccharyltransferase. *FASEB J* **10**: 849-858

Silver S, **Nucifora G**, **Phung LT** (1993) Human Menkes X-chromosome disease and the staphylococcal cadmium-resistance ATPase: a remarkable similarity in protein sequences. *Mol Microbiol* **10**: 7-12. Review

Simons K, **Ikonen E** (1997) Functional rafts in cell membranes. *Nature* **387**: 569-572. Review

Singer-Krüger B, Stenmark H, Zerial M (1995) Yeast Ypt51p and mammalian Rab5: counterparts with similar function in the early endocytic pathway. *J Cell Sci* **108**: 3509-3521

Siniossoglou S, Pelham HR (2001) An effector of Ypt6p binds the SNARE Tlg1p and mediates selective fusion of vesicles with late Golgi membranes. *EMBO J* **20**: 5991-5998

Sipos G, Brickner JH, Brace EJ, Chen L, Rambourg A, Kepes F, Fuller RS (2004) Soi3p/Rav1p functions at the early endosome to regulate endocytic trafficking to the vacuole and localization of *trans*-Golgi network transmembrane proteins. *Mol Biol Cell* **15**: 3196-3209

Skrzypek M, Lester RL, Dickson RC (1997) Suppressor gene analysis reveals an essential role for sphingolipids in transport of glycosylphosphatidylinositol-anchored proteins in *Saccharomyces cerevisiae*. *J Bacteriol* **179**: 1513-1520

Smardon AM, Tarsio M, Kane PM (2002) The RAVE complex is essential for stable assembly of the yeast V-ATPase. *J Biol Chem* **277**: 13831-13839

Smits GJ, van den Ende H, Klis FM (2001) Differential regulation of cell wall biogenesis during growth and development in yeast. *Microbiology* **147**: 781-794. Review

Sobacchi C, **Frattini A**, **Orchard P**, **Porras O**, **Tezcan I**, **Andolina M**, **Babul-Hirji R**, **Baric I**, **Canham N**, **Chitayat D**, **Dupuis-Girod S**, **Ellis I**, **Etzioni A**, **Fasth A**, **Fisher A**, **Gerritsen B**, **Gulino V**, **Horwitz E**, **Klamroth V**, **Lanino E**, **Mirolo M**, **Musio A**, **Matthijs G**, **Nonomaya S**, **Notarangelo LD**, **Ochs HD**, **Superti Furga A**, **Valiaho J**, **van Hove JL**, **Vihinen M**, **Vujic D**, **Vezzoni P**, **Villa A** (2001) The mutational spectrum of human malignant autosomal recessive osteopetrosis. *Hum Mol Genet* **10**: 1767-1773

Stahelin RV, Long F, Diraviyam K, Bruzik KS, Murray D, Cho W (2002) Phosphatidylinositol 3-phosphate induces the membrane penetration of the FYVE domains of Vps27p and Hrs. *J Biol Chem* **277**: 26379-26388

Steinman RM, Mellman IS, Muller WA, Cohn ZA (1983) Endocytosis and the recycling of plasma membrane. *J Cell Biol* **96**: 1-27. Review

Stoltze HJ, Lui NS, Anderson OR, Roels OA (1969) The influence of the mode of nutrition on the digestive system of *Ochromonas malhamensis*. *J Cell Biol* **43**: 396-409

Strahl-Bolsinger S, Gentzsch M, Tanner W (1999) Protein O-mannosylation. *Biochim Biophys Acta* **1426**: 297-307. Review

Strauss BE, **Costanzi-Strauss E** (2007) Combating oncogene activation associated with retrovirus-mediated gene therapy of X-linked severe combined immunodeficiency. *Braz J Med Biol Res* **40**: 601-613

Strous GJ, van Kerkhof P, Govers R, Ciechanover A, Schwartz AL (1996) The ubiquitin conjugation system is required for ligand-induced endocytosis and degradation of the growth hormone receptor. *EMBO J* **15**: 3806-3812

Sturley SL, **Patterson MC**, **Balch W**, **Liscum L** (2004) The pathophysiology and mechanisms of NP-C disease. *Biochim Biophys Acta* **1685**: 83-87. Review

Subramanian S, Woolford CA, Jones EW (2004) The Sec1/Munc18 protein, Vps33p, functions at the endosome and the vacuole of *Saccharomyces cerevisiae*. *Mol Biol Cell* **15**: 2593-2605

Subtil A, **Gaidarov I**, **Kobylarz K**, **Lampson MA**, **Keen JH**, **McGraw TE** (1999) Acute cholesterol depletion inhibits clathrin-coated pit budding. *Proc Natl Acad Sci U S A* **96**: 6775-6780

Sun X, **Marks DL**, **Park WD**, **Wheatley CL**, **Puri V**, **O'Brien JF**, **Kraft DL**, **Lundquist PA**, **Patterson MC**, **Pagano RE**, **Snow K** (2001) Niemann-Pick C variant detection by altered sphingolipid trafficking and correlation with mutations within a specific domain of NPC1. *Am J Hum Genet* **68**: 1361-1372

Su X, Lodhi IJ, Saltiel AR, Stahl PD (2006) Insulin-stimulated interaction between insulin receptor substrate 1 and p85α and activation of protein kinase B/Akt require Rab5. *J Biol Chem* **281**: 27982-27990

Suzuki K, Kamada Y, Ohsumi Y (2002) Studies of cargo delivery to the vacuole mediated by autophagosomes in *Saccharomyces cerevisiae*. *Dev Cell* **3**: 815-824

Szafer E, Pick E, Rotman M, Zuck S, Huber I, Cassel D (2000) Role of coatomer and phospholipids in GTPase-activating protein-dependent hydrolysis of GTP by ADP-ribosylation factor-1. *J Biol Chem* **275**: 23615-23619

Tachibana R, **Harashima H**, **Shono M**, **Azumano M**, **Niwa M**, **Futaki S**, **Kiwada H** (1998) Intracellular regulation of macromolecules using pH-sensitive liposomes and nuclear localization signal: qualitative and quantitative evaluation of intracellular trafficking. *Biochem Biophys Res Commun* **251**: 538-544

Tahirovic S, Schorr M, Mayinger P (2005) Regulation of intracellular phosphatidylinositol-4-phosphate by the Sac1 lipid phosphatase. *Traffic* **6**: 116-130

Tall GG, Hama H, DeWald DB, Horazdovsky BF (1999) The phosphatidylinositol 3-phosphate binding protein Vac1p interacts with a Rab GTPase and a Sec1p homologue to facilitate vesicle-mediated vacuolar protein sorting. *Mol Biol Cell* **10**: 1873-1889

Tang Z, Scherer PE, Okamoto T, Song K, Chu C, Kohtz DS, Nishimoto I, Lodish HF, Lisanti MP (1996) Molecular cloning of caveolin-3, a novel member of the caveolin gene family expressed predominantly in muscle. *J Biol Chem* **271**: 2255-2261

Tan PK, Davis NG, Sprague GF, Payne GS (1993) Clathrin facilitates the internalization of seven transmembrane segment receptors for mating pheromones in yeast. *J Cell Biol* **123**: 1707-1716

Tan PK, Howard JP, Payne GS (1996) The sequence NPFXD defines a new class of endocytosis signal in *Saccharomyces cerevisiae*. *J Cell Biol* **135**: 1789-1800

Tanzi RE, Petrukhin K, Chernov I, Pellequer JL, Wasco W, Ross B, Romano DM, Parano E, Pavone L, Brzustowicz LM, Devoto M, Peppercorn J, Bush AI, Sternlieb I, Pirastu M, Gusella JF, Evgrafov O, Penchaszadeh GK, Honig B, Edelman IS, Soares MB, Scheinberg IH, Gilliam TC (1993) The Wilson disease gene is a copper transporting ATPase with homology to the Menkes disease gene. *Nat Genet* **5**: 344-350

Tellam JT, James DE, Stevens TH, Piper RC (1997) Identification of a mammalian Golgi Sec1p-like protein, mVps45. *J Biol Chem* **272**: 6187-6193

Teichert U, Mechler B, Muller H, Wolf DH (1989) Lysosomal (vacuolar) proteinases of yeast are essential catalysts for protein degradation, differentiation, and cell survival. *J Biol Chem* **264**: 16037-16045

Teichler Zallen D (2000) US gene therapy in crisis. *Trends Genet* **16**: 272-275

Thomsen P, **Roepstorff K**, **Stahlhut M**, **van Deurs B** (2002) Caveolae are highly immobile plasma membrane microdomains, which are not involved in constitutive endocytic trafficking. *Mol Biol Cell* **13**: 238-250

Tiberghien P (1994) Use of suicide genes in gene therapy. *J Leukoc Biol* **56**: 203-209. Review

Toshima JY, Toshima J, Kaksonen M, Martin AC, King DS, Drubin DG (2006) Spatial dynamics of receptor-mediated endocytic trafficking in budding yeast revealed by using fluorescent α-factor derivatives. *Proc Natl Acad Sci U S A* **103**: 5793-5798

Tran D, **Carpentier JL**, **Sawano F**, **Gorden P**, **Orci L** (1987) Ligands internalized through coated or noncoated invaginations follow a common intracellular pathway. *Proc Natl Acad Sci U S A* **84**: 7957-7961

Trautwein M, Schindler C, Gauss R, Dengjel J, Hartmann E, Spang A (2006) Arf1p, Chs5p and the ChAPs are required for export of specialized cargo from the Golgi. *EMBO J* **25**: 943-954

Trigueros S, **Roca J** (2002) Failure to relax negative supercoiling of DNA is a primary cause of mitotic hyper-recombination in topoisomerase-deficient yeast cells. *J Biol Chem* **277**: 37207-37211

Trujillo KM, **Sung P** (2001) DNA structure-specific nuclease activities in the *Saccharomyces cerevisiae* Rad50*Mre11 complex. *J Biol Chem* **276**: 35458-35464

Tseng W, Purvis N, Haselton FR, Giorgio TD (1996) Cationic liposomal delivery of plasmid to endothelial cells measured by quantitative flow cytometry. *Biotech Bioeng* **50**: 548-554

Tsukada M, Gallwitz D (1996) Isolation and characterization of *SYS* genes from yeast, multicopy suppressors of the functional loss of the transport GTPase Ypt6p. *J Cell Sci* **109**: 2471-2481

Tsukada M, Will E, Gallwitz D (1999) Structural and functional analysis of a novel coiled-coil protein involved in Ypt6 GTPase-regulated protein transport in yeast. *Mol Biol Cell* **10**: 63-75

Ungermann C, Price A, Wickner W (2000) A new role for a SNARE protein as a regulator of the Ypt7/Rab-dependent stage of docking. *Proc Natl Acad Sci U S A* **97**: 8889-8891

Valdivia RH, Schekman R (2003) The yeasts Rho1p and Pkc1p regulate the transport of chitin synthase III (Chs3p) from internal stores to the plasma membrane. *Proc Natl Acad Sci U S A* **100**: 10287-10292

van Delft S, Schumacher C, Hage W, Verkleij AJ, van Bergen en Henegouwen PM (1997) Association and colocalization of Eps15 with adaptor protein-2 and clathrin. *J Cell Biol* **136**: 811-821

van den Hazel HB, Kielland-Brandt MC, Winther JR (1996) Review: biosynthesis and function of yeast vacuolar proteases. *Yeast* **12**: 1-16

van der Vaart JM, Caro LHP, Chapman JW, Klis FM, Verrips CT (1995) Identification of three mannoproteins in the cell wall of *Saccharomyces cerevisiae*. *J Bacteriol* **177**: 3104-3110

Varadan R, Assfalg M, Haririnia A, Raasi S, Pickart C, Fushman D (2004) Solution conformation of Lys63-linked di-ubiquitin chain provides clues to functional diversity of polyubiquitin signaling. *J Biol Chem* **279**: 7055-7063

Varma R, **Mayor S** (1998) GPI-anchored proteins are organized in submicron domains at the cell surface. *Nature* **394**: 798-801

Vashist S, Frank CG, Jakob CA, Ng DT (2002) Two distinctly localized p-type ATPases collaborate to maintain organelle homeostasis required for glycoprotein processing and quality control. *Mol Biol Cell* **13**: 3955-3966

Vida TA, Emr SD (1995) A new vital stain for visualizing vacuolar membrane dynamics and endocytosis in yeast. *J Cell Biol* **128**: 779-792

Vincent RD, **Hofmann TJ**, **Zassenhaus HP** (1988) Sequence and expression of *NUC1*, the gene encoding the mitochondrial nuclease in *Saccharomyces cerevisiae*. *Nucleic Acids Res* **16**: 3297-3312

Vinogradov E, Petersen BO, Duus JO (2000) Isolation and characterization of non-labeled and 13C-labeled mannans from *Pichia pastoris* yeast. *Carbohydr Res* **325**: 216-221

Vives E (2003) Cellular uptake [correction of utake] of the Tat peptide: an endocytosis mechanism following ionic interactions. *J Mol Recognit* **16**: 265-271. Review

Voskoboinik I, Mar J, Strausak D, Camakaris J (2001) The regulation of catalytic activity of the menkes copper-translocating P-type ATPase. Role of high affinity copper-binding sites. *J Biol Chem* **276**: 28620-28627

Vowels JJ, Payne GS (1998) A dileucine-like sorting signal directs transport into an AP-3-dependent, clathrin-independent pathway to the yeast vacuole. *EMBO J* **17**: 2482-2493

Vulpe C, **Levinson B**, **Whitney S**, **Packman S**, **Gitschier J** (1993) Isolation of a candidate gene for Menkes disease and evidence that it encodes a copper-transporting ATPase. *Nat Genet* **3**: 7-13

Vulpe CD, **Packman S** (1995) Cellular copper transport. *Annu Rev Nutr* **15**: 293-322. Review

Wada Y, Ohsumi Y, Anraku Y (1992) Genes for directing vacuolar morphogenesis in *Saccharomyces cerevisiae*. I. Isolation and characterization of two classes of vam mutants. *J Biol Chem* **267**: 18665-18670

Walther TC, Brickner JH, Aguilar PS, Bernales S, Pantoja C, Walter P (2006) Eisosomes mark static sites of endocytosis. *Nature* **439**: 998-1003

Wang DA, **Narang AS**, **Kotb M**, **Gaber AO**, **Miller DD**, **Kim SW**, **Mahato RI** (2002) Novel branched poly(ethylenimine)-cholesterol water-soluble lipopolymers for gene delivery. *Biomacromolecules* **3**: 1197-1207

Wang Q, **Chang A** (2002) Sphingoid base synthesis is required for oligomerization and cell surface stability of the yeast plasma membrane ATPase, Pma1. *Proc Natl Acad Sci U S A* **99**: 12853-12858

Wang Y, **Thiele C**, **Huttner WB** (2000) Cholesterol is required for the formation of regulated and constitutive secretory vesicles from the *trans*-Golgi network. *Traffic* **1**: 952-962

Wang YX, Catlett NL, Weisman LS (1998) Vac8p, a vacuolar protein with armadillo repeats, functions in both vacuole inheritance and protein targeting from the cytoplasm to vacuole. *J Cell Biol* **140**: 1063-1074

Wang YX, Kauffman EJ, Duex JE, Weisman LS (2001) Fusion of docked membranes requires the armadillo repeat protein Vac8p. *J Biol Chem* **276**: 35133-35140

Wang YX, Zhao H, Harding TM, Gomes de Mesquita DS, Woldringh CL, Klionsky DJ, Munn AL, Weisman LS (1996) Multiple classes of yeast mutants are defective in vacuole partitioning yet target vacuole proteins correctly. *Mol Biol Cell* **7**: 1375-1389

Warren DT, Andrews PD, Gourlay CW, Ayscough KR (2002) Sla1p couples the yeast endocytic machinery to proteins regulating actin dynamics. *J Cell Sci* **115**: 1703-1715

Welch MD (1999) The world according to Arp: regulation of actin nucleation by the Arp2/3 complex. *Trends Cell Biol* **9**: 423-427. Review

Wells KM, Rao R (2001) The yeast Na^+/H^+ exchanger Nhx1 is an N-linked glycoprotein. Topological implications. *J Biol Chem* **276**: 3401-3407

Welply JK, Shenbagamurthi P, Lennarz WJ, Naider F (1983) Substrate recognition by oligosaccharyltransferase. Studies on glycosylation of modified Asn-X-Thr/Ser tripeptides. *J Biol Chem* **258**: 11856-11863

Wendland B, Emr SD (1998) Pan1p, yeast eps15, functions as a multivalent adaptor that coordinates protein-protein interactions essential for endocytosis. *J Cell Biol* **141**: 71-84

Wendland B, Steece KE, Emr SD (1999) Yeast epsins contain an essential N-terminal ENTH domain, bind clathrin and are required for endocytosis. *EMBO J* **18**: 4383-4393

Whitney JA, **Gomez M**, **Sheff D**, **Kreis TE**, **Mellman I** (1995) Cytoplasmic coat proteins involved in endosome function. *Cell* **83**: 703-713

Wiederkehr A, Avaro S, Prescianotto-Baschong C, Haguenauer-Tsapis R, Riezman H (2000) The F-box protein Rcy1p is involved in endocytic membrane traffic and recycling out of an early endosome in *Saccharomyces cerevisiae*. *J Cell Biol* **149**: 397-410

Wilcox CA, Redding K, Wright R, Fuller RS (1992) Mutation of a tyrosine localization signal in the cytosolic tail of yeast Kex2 protease disrupts Golgi retention and results in default transport to the vacuole. *Mol Biol Cell* **3**: 1353-1371

Wilsbach K, Payne GS (1993) Vps1p, a member of the dynamin GTPase family, is necessary for Golgi membrane protein retention in *Saccharomyces cerevisiae*. *EMBO J* **12**: 3049-3059

Wilson SP, **Liu F**, **Wilson RE**, **Housley PR** (1995) Optimization of calcium phosphate transfection for bovine chromaffin cells: relationship to calcium phosphate precipitate formation. *Anal Biochem* **226**: 212-220

Winzeler EA, **Shoemaker DD**, **Astromoff A**, **Liang H**, **Anderson K**, **Andre B**, **Bangham R**, **Benito R**, **Boeke JD**, **Bussey H**, **Chu AM**, **Connelly C**, **Davis K**, **Dietrich F**, **Dow SW**, **El Bakkoury M**, **Foury F**, **Friend SH**, **Gentalen E**, **Giaever G**, **Hegemann JH**, **Jones T**, **Laub M**, **Liao H**, **Liebundguth N**, **Lockhart DJ**, **Lucau-Danila A**, **Lussier M**, **M'Rabet N**, **Menard P**, **Mittmann M**, **Pai C**, **Rebischung C**, **Revuelta JL**, **Riles L**, **Roberts CJ**, **Ross-MacDonald P**, **Scherens B**, **Snyder M**, **Sookhai-Mahadeo S**, **Storms RK**, **Véronneau S**, **Voet M**, **Volckaert G**, **Ward TR**, **Wysocki R**, **Yen GS**, **Yu K**, **Zimmermann K**, **Philippsen P**, **Johnston M**, **Davis RW** (1999) Functional characterization of the *S. cerevisiae* genome by gene deletion and parallel analysis. *Science* **285**: 901-906

Wisneiwski KE, **Kida E**, **Patxot OF**, **Connell F** (1992) Variability in the clinical and pathological findings in the neuronal ceroid lipofuscinoses: review of data and observations. *Am J Med Genet* **42**: 525-532. Review

Wolff AM, Din N, Petersen JGL (1996) Vacuolar and extracellular maturation of *Saccharomyces cerevisiae* proteinase A. *Yeast* **12**: 823-832

Woolford CA, Daniels LB, Park FJ, Jones EW, van Arsdell JN, Innis MA (1986) The *PEP4* gene encodes an aspartyl protease implicated in the posttranslational regulation of *Saccharomyces cerevisiae* vacuolar hydrolases. *Mol Cell Biol* **6**: 2500-2510

Wrobel I, **Collins D** (1995) Fusion of cationic liposomes with mammalian cells occurs after endocytosis. *Biochim Biophys Acta* **1235**: 296-304

Wrong OM, **Norden AG**, **Feest TG** (1994) Dent's disease; a familial proximal renal tubular syndrome with low-molecular-weight proteinuria, hypercalciuria, nephrocalcinosis, metabolic bone disease, progressive renal failure and a marked male predominance. *QJM* **87**: 473-493

Yahara N, Ueda T, Sato K, Nakano A (2001) Multiple roles of Arf1 GTPase in the yeast exocytic and endocytic pathways. *Mol Biol Cell* **12**: 221-238

Yan A, Lennarz WJ (2005) Unraveling the mechanism of protein N-glycosylation. *J Biol Chem* **280**: 3121-3124. Review

Yang Y, **Xiang Z**, **Ertl HC**, **Wilson JM** (1995) Upregulation of class I major histocompatibility complex antigens by interferon gamma is necessary for T-cell-mediated elimination of recombinant adenovirus-infected hepatocytes *in vivo*. *Proc Natl Acad Sci U S A* **92**: 7257-7261

Yanisch-Perron C, Vieira J, Messing, J (1985) Improved M13 phage cloning vectors and host mutants: nucleotide sequences of the M13mp18 and pUC19 vectors. *Gene* **33**: 103-119

Yarar D, **Waterman-Storer CM**, **Schmid SL** (2005) A dynamic actin cytoskeleton functions at multiple stages of clathrin-mediated endocytosis. *Mol Biol Cell* **16**: 964-975

Yuan DS, **Dancis A**, **Klausner RD** (1997) Restriction of copper export in *Saccharomyces cerevisiae* to a late Golgi or post-Golgi compartment in the secretory pathway. *J Biol Chem* **272**: 25787-25793

Yuan DS, **Stearman R**, **Dancis A**, **Dunn T**, **Beeler T**, **Klausner RD** (1995) The Menkes/Wilson disease gene homologue in yeast provides copper to a ceruloplasmin-like oxidase required for iron uptake. *Proc Natl Acad Sci U S A* **92**: 2632-2636

Yu X, Cai M (2004) The yeast dynamin-related GTPase Vps1p functions in the organization of the actin cytoskeleton via interaction with Sla1p. *J Cell Sci* **117**: 3839-3853

Zacharias DA, **Violin JD**, **Newton AC**, **Tsien RY** (2002) Partitioning of lipid-modified monomeric GFPs into membrane microdomains of live cells. *Science* **296**: 913-916

Zanolari B, **Friant S**, **Funato K**, **Sütterlin C**, **Stevenson BJ**, **Riezman H** (2000) Sphingoid base synthesis requirement for endocytosis in *Saccharomyces cerevisiae*. *EMBO J* **19**: 2824-2833

Zeng G, Yu X, Cai M (2001) Regulation of yeast actin cytoskeleton-regulatory complex Pan1p/Sla1p/End3p by serine/threonine kinase Prk1p. *Mol Biol Cell* **12**: 3759-3772

Zhang H, **Komano H**, **Fuller RS**, **Gandy SE**, **Frail DE** (1994) Proteolytic processing and secretion of human β-amyloid precursor protein in yeast. Evidence for a yeast secretase activity. *J Biol Chem* **269**: 27799-27802

Zhang S, **Ren J**, **Li H**, **Zhang Q**, **Armstrong JS**, **Munn AL**, **Yang H** (2004) Ncr1p, the yeast ortholog of mammalian Niemann Pick C1 protein, is dispensable for endocytic transport. *Traffic* **5**: 1017-1030

Zhang W, **Espinoza D**, **Hines V**, **Innis M**, **Mehta P**, **Miller DL** (1997) Characterization of β-amyloid peptide precursor processing by the yeast Yap3 and Mkc7 proteases. *Biochim Biophys Acta* **1359**: 110-122

Zhdankina O, Strand NL, Redmond JM, Boman AL (2001) Yeast GGA proteins interact with GTP-bound Arf and facilitate transport through the Golgi. *Yeast* **18**: 1-18

Ziman M, Chuang JS, Schekman RW (1996) Chs1p and Chs3p, two proteins involved in chitin synthesis, populate a compartment of the *Saccharomyces cerevisiae* endocytic pathway. *Mol Biol Cell* **7**: 1909-1919

Ziman M, Chuang JS, Tsung M, Hamamoto S, Schekman R (1998) Chs6p-dependent anterograde transport of Chs3p from the chitosome to the plasma membrane in *Saccharomyces cerevisiae*. *Mol Biol Cell* **9**: 1565-1576

Zubenko GS, Park FJ, Jones EW (1983) Mutations in *PEP4* locus of *Saccharomyces cerevisiae* block final step in maturation of two vacuolar hydrolases. *Proc Natl Acad Sci U S A* **80**: 510-514

Zuhorn IS, **Kalicharan R**, **Hoekstra D** (2002) Lipoplex-mediated transfection of mammalian cells occurs through the cholesterol-dependent clathrin-mediated pathway of endocytosis. *J Biol Chem* **277**: 18021-18028

Own publications:

Riechers SP, Stahl U, Lang C (2007) Endocytic/lysosomal acidification and specific sorting pathways are relevant for non-viral transfection efficiency. (submitted)

Hornbogen T, **Riechers SP**, **Prinz B**, **Schultchen J**, **Lang C**, **Schmidt S**, **Mügge C**, **Turkanovic S**, **Süssmuth RD**, **Tauberger E**, **Zocher R** (2007) Functional characterization of the recombinant N-methyltransferase domain from the multienzyme Enniatin synthetase. *Chembiochem* **8**: 1048-1054

Riechers SP, Stahl U, Lang C A genetic network for DNA transfection – Yeast as a model. 2006 Yeast Genetics and Molecular Biology Meeting, Princeton, NJ, USA, 2006

Riechers SP, Stahl U, Lang C Using a set of yeast deletion mutants to optimize non-viral transfection. GBM Annual Fall Meeting, Berlin, Germany, 2005

Riechers SP, Stahl U, Lang C Using a set of yeast deletion mutants to optimize non-viral transfection. BioPerspectives 2005, Wiesbaden, Germany, 2005

Hornbogen T, Tauberger E, Zocher R, Prinz B, Schultchen J, Riechers SP, Lang C Functional Expression of the *N*-Methyltransferase Domain of Enniatin Synthetase in *Saccharomyces cerevisiae*. BioPerspectives 2005, Wiesbaden, Germany, 2005

Riechers SP, Stahl U, Lang C Improving eukariotic transfection using deletion mutants of the model system *Saccharomyces cerevisiae*. BioPerspectives 2004, Wiesbaden, Germany, 2004

Riechers SP, Lang C, Geßner R Optimierung eines nicht-viralen, endocytosebasierten zellulären Aufnahmesystems für die Gentherapie. RiNA RNA-Network Meeting, Berlin, Germany, 2004

Grants:

Travel support of the Deutsche Forschungsgemeinschaft for participation with the “2006 Yeast Genetics and Molecular Biology Meeting”

Travel Award of the Genetics Society of America for participation with the “2006 Yeast Genetics and Molecular Biology Meeting”